

# **Investigating Anti-Inflammatory Effects of Common Dietary Phenolic Acids and Their Structurally Related Synthetic Analogues in Immune Cells**

**Nursabah Atli**

A Thesis Presented for the Degree of Doctor of Philosophy  
from the School of Pharmacy at the University of East Anglia,  
Norwich, UK

March 2022

*© This copy of the thesis has been supplied on condition that anyone who consults it is understood to recognise that its copyright rests with the author and that use of any information derived there from must be in accordance with current UK Copyright Law. In addition, any quotation or extract must include full attribution.*

# **Acknowledgments**

## **Dedicated to my Mom and my love, Ross**

This thesis mainly has been written during 3<sup>rd</sup> lockdown of COVID-19 pandemic, cast away from friends and family. The final year of my PhD has been a tremendously challenging year and the most difficult period of my PhD journey and my life. So, I want to express my greatest gratitude to everyone, especially to those supporting me during this period of time.

But first of all, I would like to thank my supervisory team. Maria, Colin, Richard, & Arno, Mark, and Anja for their guidance and council throughout my PhD.

A special thanks goes to my primary supervisor Maria, who was a big support, guidance and help throughout writing this thesis. Maria, we were not always on the same page, but I have learned from you to work hard and build up trust and bridges and learn how to be patient and resilient. Your encouragement to go to conferences and broaden my knowledge was among the highlights of my PhD journey. Mark and Anja thank you both for your invaluable input in my formal meetings to keep me on track and push me to focus on what matters the most. Anja thank you for your help and advice on chemotaxis and MCP-1 assay and providing me with controls for those assays. Colin thank you for your help and sharing your endless knowledge about flavonoids whenever I needed. Great brainstorming on skype meetings and great comments on my reports and for answering all my oblivious questions about flavonoids. I would like to thank the research team at Unilever, Vlaardingen that made my stay as great and efficient as possible: Those were, Richard, Alex, Joung, Paul, Clemons, Veronique, Pieter, and all those I forget to mention. Among those, a special thanks to Alex for training me for transendothelial migration assay and introducing me to flow cytometry, and a big thank to Richard to make my stay as efficient as possible and spoiling me with maximum support.

I also want to thank the Norwich NRP-DTP team for the amazing training opportunity and to enhancing my knowledge about other fields.

Secondly, I would like to thank all people in PHA department for their support and help throughout my PhD. A special thanks goes to O'Connell's lab members: Saurabh, Emily and Gabrielle. Another big thanks goes to Andrew, for his help with synthetic flavonoids and method section, and all other stuff that I needed from Searcey's lab; James for providing the synthetic esters and not hesitating to answer any question, Marco for his practical help with any chemistry question or compound/ chemicals, Griselda for her endless patience helping me with cytospin and staining; Noelia thank for providing me with PCR controls and primers; and Gabrielle, for starting up and helping me with BV2 IL-6 assay and westerns; Julie for lending me DMEM:F12 media after 1<sup>st</sup> lockdown when most consumables were scarce; Anastasia for her efficient and invaluable input in HL60-differentiated neutrophils and Leanne for providing BV2 cells and controls for PCR, westernblot and flow cytometry when my experiments were not working, but most of all thank you for being so easy and accessible for any troubleshooting. You were one of my role model scientist in the department.

A big thanks goes to all my office mates, Sherly, Hui, Gerald, Isabel, Enana, Winnie, Noelia and Ali for their friendship and to make me not feeling lonely in the lab. Especially, Gerald, thanks for your help with Calcium flux and chemotaxis assay. And, Enana, thank you for cheering me up, introducing me to climbing, and together with Isabel driving me crazy with your unexhausted clicking sounds (wound healing!? What about my head wounding?). And Ali, thank you for being such an awesome colleagues and friend. I could not imagine a better office with someone looking after plants, snacks & sweets to boost the mood and make the live bearable in big stress times. And for great conversations about existential crisis in science. Note to mention sharing your enthusiasm and great tips what to do alone in Japan.

Also, a huge gratitude to UEA yoga society to keeping me sane and zen! Especially, Pema for her inspirational Thursday's zoom yoga during 2<sup>nd</sup> and 3<sup>rd</sup> lockdown.

Thirdly, I want to thank all my fun friends for making my life colour-and-flavourful in Norwich and making me love the City. People makes the places memorable and Norwich will be remembered with the "Norwich survival group members" (everyone knows who you are, forgive me not mentioning more than 30 names)! And a big thank to my other friends, my Spanish-gang+Carmen the Writer & Chloe the Chef: Maui, Maria, Nuria, & Ferran for adopting me and making me love Spanish speaking more than I ever realised. I'll keep learning good words 😊. Maria, I will miss your amazing summer BBQ parties (pre-lockdown) and meeting all the interesting outsiders. And off course "Chloe the Chef", that "Sunday Roast" was everything I should be tasting from a Sunday-roast and absolutely you changed my mind about Sunday-roast! I also want to thank my friend and house-mates Ely and Essra for sharing the love of food accompanied with great all-round length-conversations especially those feminist one!; Ely and Ross you guys made the 1<sup>st</sup> lockdown bearable and taught me that house-sharing could be harmonious, exciting, and fun even in a lock-down. Never enjoyed so much cooking and developed a big love to cook! I know my sourdough breads and yoghurt experiments will be forever missed.

And my dear family, do not expect me to thank you for daily 150 WhatsApp messages that made me to turn my phone all time in silence mode. But I'll thank you for your moral support and sharing your casual live experiences daily dosage of pictures to make me feel like I am still at home and never left. You all have a special place in my heart and that is all that matter.

And Ross, my lover, much-loved boyfriend and favourite person on the planet= my anchor and my rock. Your dedicated love and care were the most important pillar during this period of writing the thesis and during turbulent times. I'll remember all the coffee & tea (and occasionally beers)

you bring me when burried in my PC screen. You always come and find me when I forget the time, saying, "take one at a time!". But most of all thank you for being an incredible person and being in my life.

And mom there will be never a single word to express my gratitude toward you. At least thank you for all your love, wisdom and selfless labour and endeavour to make our live as easy as possible. You are so sweet and so strong!

## **Abstract**

A diet rich in flavonoids and phenolic acids (PAs) is inversely correlated with chronic age-related disorders including cardiovascular disease (CVD) and neurological disorders. A central underlying cause of these disorders is chronic inflammation, orchestrated by a wide array of pro-inflammatory mediators including adhesion molecules, cytokines, and chemokines. In CVD, atherosclerosis develops, which is characterised in the early stage by endothelial activation and transendothelial migration of monocytes and macrophages. In neurological disorders, microglial activation takes the centre stage. Flavonoids and PAs are thought to exert their health effects by downregulating pro-inflammatory biomarkers and/or upregulating anti-inflammatory mediators. Flavonoids have been extensively studied for their effects on pro- and anti-inflammatory mediators at supraphysiological concentrations. However, they are poorly absorbed in their native form and instead are metabolised into PAs in the body. These PA metabolites are more bioavailable and stay longer in the circulation. This study investigated the anti-inflammatory effects of common PAs and related synthetic analogues at physiological concentrations (1-10  $\mu\text{M}$ ) on different type of immune cells, including monocytes, macrophages, neutrophils, and microglial cells as well as their effect on monocyte and neutrophil transendothelial migration.

Seven common diet-derived PA (ferulic acid (FA), isoferulic acid (IFA), caffeic acid (CA), protocatechuic acid (PCA), vanillic acid (VA), isovanillic acid (IVA) and 4-hydroxybenzoic acid (4HBA)), and 33 related non-dietary derived analogues, including 7 glycinated analogues, 12 alkyl esters and 14 structurally related, non-natural PAs were investigated for their effects on LPS-induced TNF- $\alpha$  in THP-1 monocytes. None of the diet-derived or glycinated phenolic acids had any effect on TNF- $\alpha$  secretion. FA-hexyl ester (FA-Hex-Es) and FA-propyl ester (FA-Pro-Es) dose-dependently inhibited LPS-induced TNF- $\alpha$  secretion but did not affect TNF- $\alpha$  mRNA levels suggesting involvement of a post-translational mechanism. FA-Hex-Es and

FA-Pro-Es upregulated haem oxygenase-1 and NADPH quinone oxidoreductase-1 expression, potentially via the Nrf2 pathway.

In microglial cells, three diet-derived PAs (FA, IFA and PCA) and their synthetic esters were studied for their effects on LPS-induced TNF- $\alpha$  and IL-6 secretion. None of the diet-derived PA affected secretion of either cytokine. In contrast, FA-Hex-Es and IFA ethyl ester (IFA-Et-Es) showed a trend in reducing TNF- $\alpha$  and suppressed IL-6 protein and gene expression, most likely through inhibition of the NF- $\kappa$ B signalling pathway.

In a transendothelial migration assay, the 7 diet-derived PA and 14 related analogues were screened at 1  $\mu$ M for their effects on neutrophil and monocyte migration in response to fMLP. None of the PA inhibited neutrophil migration. However, PCA and 3-iodobenzoic acid (3IBA) significantly inhibited monocyte migration. The mechanism of action was then investigated. PA did not inhibit MCP-1 secretion from HL60-differentiated neutrophils but 2IBA and 3IBA had a moderate inhibitory effect on MCP-1 mediated THP-1 monocyte chemotaxis, although this did not reach statistical significance. Higher concentrations of PA could possibly have resulted in significant effects.

These studies suggest that diet-derived PA and their related non-esterified analogues may have poor absorption or uptake by immune cells. Higher concentrations may help to reveal their mechanisms of action. Synthetic esters of FA and IFA with longer alkyl groups exert anti-inflammatory properties in monocytes and microglial cells and could be used as potential therapeutics or nutraceuticals with anti-inflammatory properties. Ultimately, these findings could help future study design of new analogues of metabolites with enhanced uptake and more immunomodulatory effects *in vitro* and *in vivo*.

## **Access Condition and Agreement**

Each deposit in UEA Digital Repository is protected by copyright and other intellectual property rights, and duplication or sale of all or part of any of the Data Collections is not permitted, except that material may be duplicated by you for your research use or for educational purposes in electronic or print form. You must obtain permission from the copyright holder, usually the author, for any other use. Exceptions only apply where a deposit may be explicitly provided under a stated licence, such as a Creative Commons licence or Open Government licence.

Electronic or print copies may not be offered, whether for sale or otherwise to anyone, unless explicitly stated under a Creative Commons or Open Government license. Unauthorised reproduction, editing or reformatting for resale purposes is explicitly prohibited (except where approved by the copyright holder themselves) and UEA reserves the right to take immediate 'take down' action on behalf of the copyright and/or rights holder if this Access condition of the UEA Digital Repository is breached. Any material in this database has been supplied on the understanding that it is copyright material and that no quotation from the material may be published without proper acknowledgement.



# Table of Contents

<b><i>Investigating Anti-Inflammatory Effects of Common Dietary Phenolic Acids and Their Structurally Related Synthetic Analogues in Immune Cells.....</i></b>	<b>1</b>
<b><i>Acknowledgments .....</i></b>	<b>2</b>
<b><i>Abstract.....</i></b>	<b>6</b>
<b><i>List of Tables.....</i></b>	<b>14</b>
<b><i>List of Figures.....</i></b>	<b>15</b>
<b><i>List of Abbreviations.....</i></b>	<b>20</b>
<b><i>Chapter 1. General Introduction.....</i></b>	<b>28</b>
<b>1.1 Introduction .....</b>	<b>29</b>
<b>1.2 (Poly)phenols.....</b>	<b>32</b>
1.2.1 Chemistry and functions of flavonoids .....	34
1.2.2 Chemistry and function of phenolic acids.....	36
<b>1.3 Dietary sources and intake of flavonoids and phenolic acids .....</b>	<b>38</b>
<b>1.4 Metabolism and absorption .....</b>	<b>42</b>
<b>1.5 Bioavailability .....</b>	<b>45</b>
<b>1.6 Bioactivity .....</b>	<b>49</b>
<b>1.7 Flavonoid intake and vascular diseases .....</b>	<b>50</b>
1.7.1 Cardiovascular diseases .....	50
1.7.2 Flavonoid and phenolic acid intake and CVD .....	50
1.7.3 Inflammation and CVD .....	56
1.7.4 Atherosclerosis initiation and progression .....	56
<b>1.8 Flavonoid intake and neurological disorders .....</b>	<b>60</b>
1.8.1 Neuroinflammation and microglial cell activation .....	65
<b>1.9 Mechanism of chronic inflammation and inflammatory biomarkers</b>	
<b>69</b>	
1.9.1 NF- $\kappa$ B .....	69

1.9.2 TNF- $\alpha$ .....	72
1.9.3 TNF- $\alpha$ receptor TNFR1 & TNFR2 .....	75
1.9.4 The IL-1 and TLR4 signalling pathways .....	78
1.9.5 IL-6 .....	80
1.9.6 MCP-1 .....	84
<b>1.10 Oxidative stress and anti-oxidative biomarkers .....</b>	<b>89</b>
1.10.1 Nrf2.....	89
1.10.2 HO-1.....	92
1.10.3 NQO1 .....	95
<b>1.11 Concluding remarks and aims .....</b>	<b>98</b>
<b>1.12 Aims of the study .....</b>	<b>100</b>
<b><i>Chapter 2. Materials &amp; Methods.....</i></b>	<b>101</b>
<b>2.1 Consumables and Chemicals .....</b>	<b>102</b>
2.1.1 General Consumables .....	102
2.1.2 General Chemicals & Reagents .....	102
2.1.3 Phenolic Metabolites, Related Compounds and Synthetic Analogues .....	103
<b>2.2 Cell Culture .....</b>	<b>107</b>
2.2.1 Cells and Reagents .....	107
2.2.2 Cell Culture conditions .....	108
2.2.3 Cryopreservation .....	109
2.2.4 Thawing Cells.....	110
2.2.5 Cell Counting.....	110
<b>2.3 Treatment Solutions of Phenolic acids &amp; Synthetic Analogues .....</b>	<b>111</b>
<b>2.4 Cell Proliferation (MTS) Assay.....</b>	<b>112</b>
<b>2.5 ELISA.....</b>	<b>113</b>
2.5.1 Reagents .....	113
2.5.2 TNF- $\alpha$ ELISA.....	113
2.5.3 IL-6 ELISA.....	117
2.5.4 MCP-1 ELISA .....	119
2.5.5 HO-1 ELISA.....	120
<b>2.6 NQO1 Enzyme Activity Assay.....</b>	<b>123</b>
2.6.1 Reagents .....	123
2.6.2 Cell Stimulation and Sample Preparation .....	123
2.6.3 NQO1 Assay Procedure.....	123

<b>2.7 Real Time-QPCR</b> .....	<b>125</b>
2.7.1 Reagents .....	125
2.7.2 Cell stimulation and Sample collection .....	126
2.7.3 RNA Extraction .....	127
2.7.4 RNA Quantification & Reverse Transcription .....	128
2.7.5 RT-qPCR Procedure .....	129
<b>2.8 Western Blotting</b> .....	<b>130</b>
2.8.1 Reagents .....	130
2.8.2 Cell Stimulation and Sample Preparation .....	130
2.8.3 Cell Lysate Preparation .....	131
2.8.4 Gel Electrophoresis .....	132
2.8.5 Transfer .....	132
2.8.6 Immunoblotting .....	133
2.8.7 Re-Probing .....	135
2.8.8 Densitometry .....	135
<b>2.9 Transendothelial Migration Assay</b> .....	<b>136</b>
2.9.1 Reagents .....	136
2.9.2 Seeding HMEC-1 .....	136
2.9.3 PBMC Isolation from Whole blood .....	137
2.9.4 Seeding PBMCs & Adding Treatment and Fixing Migrated Cells .....	137
2.9.5 Flow Cytometry .....	138
<b>2.10 Chemotaxis and Calcium Flux</b> .....	<b>142</b>
2.10.1 Reagents .....	142
2.10.2 Chemotaxis Assay.....	142
2.10.3 Calcium Release Assay .....	143
<b>2.11 Cytospin</b> .....	<b>145</b>
2.11.1 Reagents .....	145
2.11.2 Cytospinning and staining .....	145
<b>2.12 General Flow Cytometry</b> .....	<b>146</b>
2.12.1 Reagents .....	146
2.12.2 Differentiated HL-60 Flow Cytometry .....	146
2.12.3 mTNF- $\alpha$ Flow Cytometry .....	147
<b>2.13 Fluorescent Microscopy</b> .....	<b>148</b>
<b>2.14 Statistical Analysis</b> .....	<b>150</b>

**Chapter 3. Effect of Phenolic Metabolites and Their Synthetic Conjugates on Inflammatory and Oxidative Stress Biomarkers in THP-1 monocytes..... 151**

**3.1 Introduction ..... 152**

**3.2 Aims and objectives ..... 155**

**3.3 Results..... 158**

3.3.1 Effect of flavonoid metabolites, related phenolic acids, and synthetic analogues on LPS-induced TNF- $\alpha$  secretion in THP-1 cells ..... 158

3.3.2 Combined effect of flavonoid metabolites with  $\Omega$ -3 fatty acids on LPS-Induced TNF- $\alpha$  secretion in THP-1 monocytes and macrophages ..... 163

3.3.3 Effects of glycine-conjugated phenolic acids on LPS-induced TNF- $\alpha$  secretion in THP-1 monocytes ..... 171

3.3.4 Effect of esterified phenolic acids on LPS-induced TNF- $\alpha$  secretion in THP-1 cells ..... 174

3.3.5 FA-Hex-Es and FA-Pro-Es do not affect LPS-induced TNF- $\alpha$  mRNA expression in THP-1 cells..... 177

3.3.6 Post translational mechanisms of action of FA-Hex-Es and FA-Pro-Es ..... 179

3.3.7 FA esters activate HO-1 expression and NQO1 activity in THP-1 cells ..... 186

3.3.8 Effect of FA esters on HO-1 and NQO1 mRNA expression in THP-1 cells.. 190

3.3.9 Effect of FA and FA esters on Nrf2 protein expression in THP-1 cells ..... 191

**3. 4 Discussion ..... 193**

**Chapter 4. Anti-Inflammatory Effects of Flavonoid Metabolites and Their Esters in Microglial Cells ..... 203**

**4.1 Introduction ..... 204**

**4.2 Aim ..... 206**

**4.3 Results ..... 207**

4.3.1 Effect of phenolic acids and ester analogues on BV2 microglial cell viability ..... 207

4.3.2 Kinetics of LPS-induced TNF- $\alpha$  secretion in BV2 cells ..... 209

4.3.3 Phenolic acids and ester analogues do not significantly inhibit TNF- $\alpha$  Secretion in BV2 cells ..... 210

4.3.4 LPS-induced IL-6 secretion in BV2 cells ..... 211

4.3.5 FA-Hex-Es suppresses LPS-induced IL-6 secretion in BV2 cells..... 212

4.3.6 FA-Hex-Es significantly reduces LPS-induced IL-6 secretion in a dose-dependent manner in BV2 cells .....	213
4.3.7 LPS-induced IL-6 mRNA expression in BV2 cells .....	214
4.3.8 Effect of FA-Hex-Es, FA-Pro-Es and FA on IL-6 mRNA expression in BV2 cells .....	215
4.3.9 Effect of FA-Hex-Es on upstream regulators of IL-6 gene expression .....	216
4.3.10 Optimisation of LPS-induced JNK protein phosphorylation in BV2 Cells ...	216
4.3.11 Effect of FA-Hex-Es, IFA-Et-Es and FA on JNK phosphorylation in BV2 cells .....	217
4.3.12 Kinetics of LPS-induced c-Jun and c-Fos phosphorylation in BV2 cells.....	220
4.3.13 Effect of FA-Hex-Es, FA-Pro-Es and FA on c-Jun and c-Fos phosphorylation in BV2 Cells .....	221
4.3.14 FA-Hex-Es inhibits p65 NF- $\kappa$ B phosphorylation in BV2 cells.....	223
<b>4.4 Discussion .....</b>	<b>225</b>
<b><i>Chapter 5. Effect of Phenolic Metabolites and Related Phenolic Acids on Transendothelial Migration of Neutrophils and Monocytes.....</i></b>	<b>231</b>
<b>5.1 Introduction .....</b>	<b>232</b>
<b>5.2 Aims .....</b>	<b>234</b>
<b>5.3 Results .....</b>	<b>236</b>
5.3.1 Transendothelial migration assay optimisation .....	236
5.3.2 Effect of phenolic metabolites of dietary flavonoids and related phenolic acids on neutrophil and monocyte transendothelial migration .....	240
5.3.3 Optimisation and validation of differentiated HL-60s as a model for neutrophils .....	244
5.3.4 Effect of Phenolic acids on MCP-1 secretion from HL60-differentiated neutrophils.....	250
5.3.6 Effect of Phenolic acids on Monocyte Migration .....	254
5.3.7 Phenolic acids at 1 $\mu$ M do not significantly reduce MCP-1 induced monocyte chemotaxis .....	255
<b>5.4 Discussion .....</b>	<b>257</b>
<b><i>Chapter 6. General Discussion &amp; Future Perspectives.....</i></b>	<b>263</b>
<b><i>Chapter 7 References .....</i></b>	<b>273</b>

<b>Chapter 8. Appendices .....</b>	<b>315</b>
<b>Appendix I: Buffers &amp; Reagent Recipes .....</b>	<b>316</b>
10X Phosphate-Buffered Saline (PBS) (1L) .....	316
ELISA Assays Buffers .....	316
NQO1 Enzymatic Activity Assay Buffers .....	320
Real Time-QPCR .....	321
Western Blotting .....	322
Immunoblotting .....	323
Transendothelial Migration Assay Buffers and Solutions .....	324
Chemotaxis and Calcium Flux Assay Buffers .....	325
General Flow Cytometry Buffers .....	326
<b>Appendix II: Cell Viability Assay .....</b>	<b>327</b>
THP-1 cell viability in response to naturally occurring phenolic acids and their synthetic analogues .....	327
<b>Appendix III: Method Optimization .....</b>	<b>333</b>
8.3.1 Optimization for Chapter 3 .....	333
8.3.2 Optimization for Chapter 4 .....	343
8.3.3 Optimization for Chapter 5 .....	350
8.3.3.5 Chemotaxis Effect of Halogenated and Non-halogenated Compounds on THP-1 .....	356

## List of Tables

<b>Table 1. 1</b> Food classes with examples of food stuffs containing flavonoids and phenolic acids.....	38
<b>Table 1. 2</b> Main dietary food sources with high content of phenolic acids and flavonoids.....	39
<b>Table 1. 3</b> Dietary sources and main content of flavonoids.....	41
<b>Table 2. 1</b> List of screened phenolic acids.....	104
<b>Table 2. 2</b> Primer sequences for RT-qPCR.....	125
<b>Table 2. 3</b> Primary and Secondary antibodies used in Western blotting assays. ....	134
<b>Table 2. 4</b> Cell surface markers for flow cytometry analysis.....	140
<b>Table 2.5</b> Antibodies and controls used in General Flow Cytometry & Fluorescent Microscopy.....	149
<b>Table 3. 1</b> List of common parental/flavonoid metabolites and analogues used in this study.....	156
<b>Table 3. 2</b> Effects of 1 and 10 $\mu$ M glycine-conjugated phenolic acids on LPS-induced TNF- $\alpha$ secretion in THP-1 cells. ....	172
<b>Table 3. 3</b> Effect of phenolic acid esters on LPS-induced TNF- $\alpha$ secretion.....	175
<b>Table 5. 1</b> List of screened phenolic acids.....	235
<b>Table 8.1</b> Treatment effect of halogenated and non-halogenated phenolic acids at 1 $\mu$ M on THP-1 chemotaxis in response to MCP-1 (0.3 nM).....	356
<b>Table 8.2</b> List of PA used in transendothelial migration model with LogP values.....	357

# List of Figures

<b>Figure 1. 1</b> Six classes of (poly)phenols with examples and six major sub-classes of flavonoids.....	32
<b>Figure 1. 2</b> Common structure of flavonoids based on chrome rings (A +C) and aromatic ring (B).....	34
<b>Figure 1. 3</b> Major sub-classes of flavonoids with common structures.....	35
<b>Figure 1. 4</b> Common structures of benzoic and cinnamic acid derivatives.....	37
<b>Figure 1. 5</b> Mechanisms of flavonoid absorption.....	43
<b>Figure 1. 6</b> The major cell types in the CNS. ....	66
<b>Figure 1. 7</b> Schematic overview of microglial activation.....	67
<b>Figure 1. 8</b> The NF- $\kappa$ B signalling pathway.....	71
<b>Figure 1. 9</b> The TNF- $\alpha$ signalling pathway.....	76
<b>Figure 1. 10</b> Overview of IL-6 signalling.....	81
<b>Figure 1. 11</b> The human IL-6 gene promoter with approximate binding sites for transcription regulator elements and trans-regulatory factors.....	83
<b>Figure 1. 12</b> Overview of the MCP-1/CCR2 signalling pathways in monocyte migration. ....	87
<b>Figure 1. 13</b> Overview of the Nrf2 signalling pathway.....	90
<b>Figure 1. 14</b> Overview of the role of HO-1 in oxidative stress.....	93
<b>Figure 1. 15</b> An overview of NQO1 cellular functions.....	95
<b>Figure 2. 1</b> Schematic overview of the transendothelial migration assay.....	138
<b>Figure 2. 2</b> Schematic Workflow of Flow Cytometry.....	141
<b>Figure 3. 1</b> Flow chart of method optimisation for measuring LPS-induced TNF- $\alpha$ secretion in THP-1 cells.....	159
<b>Figure 3. 2</b> Optimisation of LPS concentration and positive control for TNF- $\alpha$ secretion in THP-1 cells.....	160
<b>Figure 3. 3</b> Flavonoid metabolites and related phenolic acids do not reduce LPS-induced TNF- $\alpha$ secretion in THP-1.....	162



<b>Figure 3. 4</b> Flow chart of method optimisation for effects of combined omega-3 fatty acids and flavonoid metabolites in THP-1 macrophages.....	164
<b>Figure 3. 5</b> PMA differentiation of THP-1 monocytes.....	165
<b>Figure 3. 6</b> Pre-incubation of DHA, EPA and EPA+DHA reduces LPS-stimulated TNF- $\alpha$ secretion in THP-1 monocytes and macrophages.....	167
<b>Figure 3. 7</b> Combined effects of 10 $\mu$ M phenolic acids with 50 $\mu$ M DHA on LPS-induced TNF- $\alpha$ secretion in THP-1 monocytes.....	169
<b>Figure 3. 8</b> Combined effects of 10 $\mu$ M phenolic acids with 50 $\mu$ M DHA on LPS-induced TNF- $\alpha$ secretion in THP-1 macrophages.....	170
<b>Figure 3. 9</b> Concentration-dependent effects of glycine-conjugated phenolic acids on LPS-induced TNF- $\alpha$ secretion in THP-1.....	173
<b>Figure 3. 10</b> FA-Hex-Es and FA-Pro-Es significantly and dose-dependently reduce LPS-stimulated TNF- $\alpha$ secretion in THP-1.....	176
<b>Figure 3. 11</b> FA, FA-Pro-Es and FA-Hex-Es do not affect LPS-induced TNF- $\alpha$ mRNA expression in THP-1.....	178
<b>Figure 3. 12</b> Kinetics of LPS induced p38 phosphorylation in THP-1.....	180
<b>Figure 3. 13</b> FA and its propyl and hexyl esters do not modulate LPS-induced p38 MAPK phosphorylation in THP-1.....	181
<b>Figure 3. 14</b> LPS-induced membrane-bound TNF- $\alpha$ expression in THP-1.....	183
<b>Figure 3. 15</b> Membrane-bound TNF- $\alpha$ expression in THP-1 cells by flow cytometry.....	185
<b>Figure 3. 16</b> FA-Hex-Es and FA-Pro-Es significantly increase HO-1 protein expression in THP-1.....	187
<b>Figure 3. 17</b> FA-Hex-Es dose-dependently increases HO-1 protein expression in THP-1.....	188
<b>Figure 3. 18</b> Flow chart of method optimisation for NQO1 enzymatic assay in THP-1 monocytes.....	189
<b>Figure 3. 19</b> FA-Hex-Es and FA-Pro-Es significantly increase NQO1 enzyme activity in THP-1.....	189

<b>Figure 3. 20</b> Treatment effect FA-Hex-Es on HO-1 and NQO1 gene expression in THP-1.....	190
<b>Figure 3. 21</b> Nrf2 protein expression is not modulated by FA and its esters in THP-1.....	192
<b>Figure 4. 1</b> Effect of phenolic acids esters on murine BV2 microglial cell viability measured by MTS assay.....	208
<b>Figure 4. 2</b> LPS-induced TNF- $\alpha$ secretion in BV2.....	209
<b>Figure 4. 3</b> Effect of FA, IFA, PCA and their esters on LPS-induced TNF- $\alpha$ secretion in BV2.. ..	210
<b>Figure 4. 4</b> LPS-induced IL6 secretion in BV2.....	211
<b>Figure 4. 5</b> Effect of 10 $\mu$ M flavonoid metabolites and their esters on LPS-induced IL-6 protein secretion in BV2.....	212
<b>Figure 4. 6</b> FA-Hex-Es dose dependently inhibits LPS-induced IL-6 secretion in BV2.....	213
<b>Figure 4. 7</b> Kinetics of LPS-induced IL-6 mRNA expression in BV2.....	214
<b>Figure 4. 8</b> Effects of FA, FA-Hex-Es and IFA-Et-Es on LPS-induced IL-6 mRNA expression in BV2.....	215
<b>Figure 4. 9</b> Kinetics of LPS-induced JNK protein phosphorylation in BV2.....	217
<b>Figure 4. 10</b> LPS-stimulated JNK phosphorylation is not affected by treatment with FA, FA-Hex-Es or IFA-Et-Es in BV2.....	218-219
<b>Figure 4. 11</b> Kinetics of c-Jun and c-Fos protein phosphorylation and expression in response to LPS stimulation in BV2.. ..	221
<b>Figure 4. 12</b> FA, FA-Hex and IFA-Et do not significantly reduce LPS-induced c-Fos/c-Jun phosphorylation in BV2.....	222
<b>Figure 4. 13</b> FA-Hex-Es reduces LPS-induced p65 NF- $\kappa$ B phosphorylation in BV2.....	224
<b>Figure 4. 14</b> Hypothetical model of the FA-Hex-Es-mediated anti-inflammatory effect via NF- $\kappa$ B pathway inhibition, with subsequent downregulation of IL-6 in BV2 microglial cells.....	230
<b>Figure 5. 1</b> HMEC-1 cells express PECAM-1 (CD31).....	237

<b>Figure 5. 2</b> Transendothelial migration of neutrophils and monocytes in response to fMLP, MCP-1 and CX3CL1.....	238
<b>Figure 5. 3</b> Kinetics of granulocytes (neutrophil) and monocyte migration in response to fMLP in the TEM model.....	239
<b>Figure 5. 4</b> Treatment effect of phenolic acids on neutrophils and monocytes TEM.....	241
<b>Figure 5. 5</b> Structures of PAs used in the TEM assay. ....	242
<b>Figure 5. 6</b> Treatment effect of non-natural phenolic acids on neutrophils and monocytes TEM.....	243
<b>Figure 5. 7</b> Inhibition of cell HL60 cell growth by DMSO and ATRA.....	245
<b>Figure 5. 8</b> Nuclear morphology of HL60-differentiated cells.....	247
<b>Figure 5. 9</b> HL-60 cells differentiated with DMSO or ATRA express CD11b....	248
<b>Figure 5. 10</b> Spontaneous and fMLP and CXCL12-induced chemotaxis of DMSO- and ATRA-differentiated HL60.....	250
<b>Figure 5. 11</b> fMLP induced MCP-1 secretion in neutrophils.....	251
<b>Figure 5. 12</b> Phenolic acids do not inhibit MCP-1 secretion from neutrophils..	253
<b>Figure 5. 13</b> Effects of fMLP and MCP-1 on THP-1 chemotaxis.....	255
<b>Figure 5. 14</b> Effects of 1 $\mu$ M PCA, FA or related phenolic acids on MCP-1 induced THP-1 chemotaxis.....	256
<b>Figure 6. 1</b> Schematic overview of overall experiments conducted in chapter 3, 4 and 5.....	265
<b>Figure 8. 1</b> Effect of phenolic acids, flavonoid metabolites on THP-1 cell viability measured by MTS assay.....	328
<b>Figure 8. 2</b> Effect of non-natural phenolic acids on THP-1 cell viability measured with MTS Assay.....	329
<b>Figure 8. 3</b> Effect of phenolic acids glycine conjugates on THP-1 cell viability measured with MTS Assay.....	330
<b>Figure 8. 4</b> Effect of Halogenated compounds on THP-1 Cell Viability measured with MTS Assay.....	331

<b>Figure 8. 5</b> Effect of 20 $\mu$ M treatment on THP-1 Cell Viability measured with MTS Assay.....	332
<b>Figure 8. 6</b> Effect of cell volume and density on LPS-induced TNF $\alpha$ secretion in THP-1 cells.....	334
<b>Figure 8. 7</b> LPS kinetic of THP-1 macrophages.....	335
<b>Figure 8. 8</b> in RPMI complete media co-incubation of LPS with DHA, EPA and EPA&DHA did not inhibit TNF- $\alpha$ secretion from THP-1 macrophages.....	336
<b>Figure 8. 9</b> The optimal buffer for immunoblot antibody staining.....	337
<b>Figure 8. 10</b> Optimisation of standard curve, kinetic of standard curve, and cell density of NQO-1 enzymatic activity assay for THP-1 cells.....	339
<b>Figure 8. 11</b> Optimal time point of HO-1 and NQO-1 messenger RNA in THP-1 cells for the positive control DMF and Quercetin (Nrf2 inducer) and FA-Hex-Es.....	341
<b>Figure 8. 12</b> Validation of specificity of qPCR amplification for human A) GAPDH, B) TNF- $\alpha$ , C) HO-1, D) NQO1.....	342
<b>Figure 8. 13</b> Kinetics of IL-6 gene expression. BV2 cells (1x10 <sup>5</sup> cells/well) in 2 mL o/n incubated.....	343
<b>Figure 8. 14</b> Melting temperature (T <sub>m</sub> ) of BV2 cDNA with three different template concentrations.....	346
<b>Figure 8. 15</b> Melting Temperature of Murine GAPDH and IL-6 template and primer pairs.. ..	347
<b>Figure 8. 16</b> Serum starvation did not alter the effect of LPS on non-phospho c-Jun and c-Fos.....	349
<b>Figure 8. 17</b> Overview of TEM flow cytometry gating strategy.....	351
<b>Figure 8. 18</b> HL-60 growth and differentiation by DMSO and ATRA versus control.....	353-354

## List of Abbreviations

<b>24DHBA</b>	2,4-Dihydroxybenzoic acid ( $\beta$ -Resorcylic acid)
<b>24DMBA</b>	2,4-Dimethoxybenzoic acid
<b>2IBA</b>	2-Iodobenzoic acid
<b>35DABA</b>	3,5-Diaminobenzoic acid
<b>3ABA</b>	3-Aminobenzoic acid
<b>3C4MBA</b>	3-Chloro-4-methoxybenzoic acid (3-Chloro-p-anisic acid)
<b>3CBA</b>	3-Chlorobenzoic acid
<b>3H4MCA</b>	isoferulic acid (3-Hydroxy-4-methoxycinnamic acid)
<b>3HBA</b>	3-Hydroxybenzoic acid
<b>3IBA</b>	3-Iodobenzoic acid
<b>4ABA</b>	4-Aminobenzoic acid (Para-aminobenzoic acid)
<b>4BBA</b>	4-Bromobenzoic acid
<b>4HBA</b>	4-Hydroxybenzoic acid
<b>4NBA</b>	4-Nitrobenzoic acid
<b>4'MEC7G</b>	4'-O-methyl-EC-7- $\beta$ -D-glucuronide
<b>4'MEC</b>	4'-O-methyl-epcatechin
<b>5C2MBA</b>	5-Chloro-2-methoxybenzoic acid (5-Chloro-o-anisic acid)
<b>A<math>\beta</math></b>	amyloid-beta
<b>AC</b>	adenyl cyclase
<b>ADME</b>	absorption, distribution, metabolism, and excretion
<b>AD</b>	Alzheimer's disease
<b>ARE/EpRE</b>	antioxidant response element/electrophile response element
<b>ATRA</b>	all-trans retinoic acid
<b>BA</b>	Benzoic acid
<b>BDNF</b>	plasma-brain-derived neurotrophic factors
<b>BP</b>	blood pressure

<b>BV2</b>	murine microglial cell line
<b>C3Arab</b>	C-3-arababinoside
<b>C3G</b>	cyanidin-3-glucoside
<b>C3Gal</b>	C-3-galactoside
<b>C<math>\beta</math>G</b>	cytosolic- $\beta$ -glucosides
<b>CCL22</b>	C-C motif chemokine ligand 2
<b>CD40L</b>	Cluster of differentiation 40 ligand
<b>CFA</b>	complete Freund's Adjuvant
<b>CFX</b>	calcium flux
<b>CGJ</b>	Concord grape juice
<b>cGMP</b>	Cyclic guanosine monophosphate
<b>CHD</b>	coronary heart disease
<b>CI</b>	confidence interval
<b>C<sub>MAX</sub></b>	Maximum concentration
<b>CNS</b>	central nervous system
<b>CO</b>	Carbon monoxide
<b>COMT</b>	Catechol-O-methyltransferase
<b>COX-2</b>	cyclooxygenase type 2
<b>CREB</b>	cyclic AMP-responsive element
<b>CVD</b>	Cardiovascular disease
<b>D3G</b>	delphinidin 3-O-glucoside
<b>DC</b>	Dendritic cells
<b>DHA</b>	<i>cis</i> -4,7,10,13,16,19-docosahexaenoic acid
<b>DMEM</b>	Dulbecco's Modified Eagle Medium
<b>DMF</b>	dimethyl fumarate
<b>DMSO</b>	Dimethylsulfoxide
<b>DPB</b>	diastolic blood pressure

<b>DPBS</b>	Dulbecco's Phosphate Buffered Saline
<b>DSS</b>	dextran sulfate sodium
<b>EAE</b>	Experimental autoimmune encephalomyelitis
<b>EC</b>	(-)-epicatechin
<b>EC4'S</b>	EC-4'-sulfate
<b>EC7G</b>	EC-7- $\beta$ -D-glucuronide
<b>EF</b>	Executive function
<b>EGC</b>	epigallocatechin
<b>EGCG</b>	epigallocatechin gallate
<b>EMA</b>	European Medicines Agency
<b>EPA</b>	<i>cis</i> -5,8,11,14,17-eicosapentaenoic acid
<b>ERK</b>	extracellular signal-related kinase
<b>ET-1</b>	endothelin-1
<b>FA</b>	ferulic acid (trans-4-Hydroxy-3-methoxycinnamic acid)
<b>FBS</b>	fetal bovine serum
<b>FDA</b>	Food and Drug Administration
<b>FMD</b>	flow mediated dilation
<b>FTH</b>	Ferritin heavy
<b>FTL</b>	Ferritin light
<b>GA</b>	gallic acid
<b>GCL</b>	glutamate cysteine ligase
<b>Gly</b>	glycine
<b>GPCR</b>	G-coupled protein receptor
<b>Gp130</b>	cell surface glycoprotein 130
<b>GPX2</b>	glutathione peroxidase 2
<b>GRE</b>	glucocorticoid responsive elements
<b>GSH</b>	Glutathione

<b>GSR</b>	glutathione reductase
<b>GT</b>	glucuronosyltransferase
<b>HA</b>	hippuric acid
<b>HFD</b>	high-fat diet
<b>HK-2</b>	Human kidney cells
<b>HMEC-1</b>	The human dermal microvascular endothelial cell – 1
<b>HO-1</b>	heme oxygenase-1 (HMOX1)
<b>HR</b>	hazard ratio
<b>HUVEC</b>	human umbilical vein endothelial cells
<b>IBD</b>	inflammatory bowel disease
<b>ICAMs</b>	intercellular adhesion molecules
<b>IFA</b>	isoferulic acid (3-Hydroxy-4-methoxycinnamic acid)
<b>IFA-GI</b>	isoferulic acid-glycine
<b>IFN</b>	interferons
<b>IL</b>	interleukins
<b>IL-17A</b>	interleukin-17A
<b>IL-6</b>	interleukin-6
<b>iNOS</b>	inducible nitric oxide synthase
<b>IS</b>	Inflammation score
<b>IRAKs</b>	IL-1 receptor-associated kinase 1
<b>IVA</b>	isovanillic acid
<b>IVA3G</b>	IVA-3-glucoside
<b>JAK</b>	Janus kinase
<b>JNK</b>	C-Jun N-terminal kinases
<b>LBP</b>	LPS binding protein
<b>LPH</b>	Lactase phloridzin hydrolase
<b>LPS</b>	Lipopolysaccharide



<b>M-CSF</b>	macrophage colony-stimulating factor
<b>MCP-1</b>	monocyte chemoattractant protein 1
<b>MD2</b>	myeloid differentiation protein 2
<b>MetS</b>	metabolic-syndrome
<b>MMPs</b>	matrix metalloproteases
<b>MOG</b>	myelin oligodendrocyte glycoprotein
<b>MOA</b>	mechanism of action
<b>MRP</b>	multidrug resistance protein
<b>MS</b>	Multiple sclerosis
<b>MTS</b>	3-(4,5-dimethylthiazol-2-yl)-5-(3-carboxymethoxyphenyl)-2-(4-sulfophenyl)-2H-tetrazolium
<b>MyD88</b>	myeloid differentiation primary response gene 88
<b>NADP+</b>	nicotinamide adenine dinucleotide phosphate
<b>NADPH</b>	nicotinamide adenine dinucleotide phosphate hydrate
<b>NF-IL6</b>	nuclear factor for interleukins 6 transcription factor
<b>NF-κB</b>	nuclear factor kappa-light-chain-enhancer of activated B cells
<b>NK</b>	Natural killer
<b>Nrf2</b>	nuclear factor erythroid 2-related factor 2
<b>NTC</b>	non-template control
<b>NO</b>	Nitric oxide
<b>NS</b>	normal saline
<b>NQO1</b>	(NAD(P)H quinone acceptor oxidoreductase
<b>P3G</b>	peonidin 3-O-glucoside
<b>PAMPs</b>	pathogen associated molecular patterns
<b>PBMC</b>	peripheral blood mononuclear cells
<b>PBS</b>	phosphate buffered saline
<b>PCA</b>	protocatechuic acid

<b>PCA3S</b>	PCA -3- O-sulphate
<b>PCA4S</b>	PCA-4- O-sulphate
<b>PCA-Et-Es</b>	Protocatechuic acid (3,4-Dihydroxybenzoic acid)-Ethyl ester
<b>PCA-GI</b>	protocatechuic acid-glycine
<b>PCA-Met-Es</b>	Protocatechuic acid (3,4-Dihydroxybenzoic acid)-Methyl ester
<b>PCA-Pro-Es</b>	Protocatechuic acid (3,4-Dihydroxybenzoic acid)-Propyl ester
<b>PCA-iProp-Es</b>	protocatechuic acid-isopropyl ester
<b>PD</b>	Parkinson's disease
<b>PDGF</b>	platelet derived growth factor
<b>PECAM</b>	platelet endothelial cellular adhesion molecules
<b>PGA</b>	phloroglucinaldehyde
<b>PI3K</b>	phosphoinositide 3-kinase
<b>PLA<sub>2</sub></b>	phospholipase A type 2
<b>PLC</b>	phospholipase C
<b>PMA</b>	phorbol-12-myristate-13-acetate
<b>PMNC</b>	polymorphonuclear cells
<b>PMS</b>	phenazine methosulfate
<b>PT</b>	pertussis toxin
<b>PUFA</b>	polyunsaturated fatty acids
<b>PWV</b>	pulse wave velocity
<b>QUE</b>	quercetin
<b>RA</b>	rheumatoid arthritis
<b>RBC</b>	red blood cell
<b>RCE</b>	retinoblastoma control element
<b>RCT</b>	randomized control trials
<b>RD</b>	Reagent Diluent

<b>ROS</b>	reactive oxygen species
<b>RPMI</b>	Roswell Park Memorial Institute
<b>SAR</b>	structure-activity relationships
<b>SB203580</b>	p38 MAP kinase inhibitor
<b>SBP</b>	systolic blood pressure
<b>SEL</b>	selectins
<b>SGLT1</b>	Sodium dependent glucose transporter 1
<b>SHP1/2</b>	Src homology domain 2-containing tyrosine phosphatase-1/2
<b>SRE</b>	serum-responsive element
<b>STAT 1-6</b>	Signal Transducer and Activator of Transcription
<b>T2D</b>	Type 2 diabetes
<b>TAB1/3</b>	transforming growth factor beta (TFG $\beta$ )-activated kinase 1/3
<b>TACE</b>	TNF- $\alpha$ converting enzyme (also known as ADAM-17)
<b>TAK1</b>	TFG $\beta$ -activated kinase 1
<b>TF</b>	transcription factors
<b>THP-1</b>	the human monocytic cell line derived from an acute monocytic leukemia patient
<b>TIR</b>	Toll IL-1 receptor
<b>T<sub>MAX</sub></b>	Time at highest concentration
<b>TNF-<math>\alpha</math></b>	tumor necrosis factor- $\alpha$
<b>TRAF6</b>	TNF-receptor associated factor 6
<b>TXN</b>	thioredoxin
<b>TXNRD1</b>	thioredoxin reductase 1
<b>UC</b>	ulcerative colitis
<b>UV</b>	Ultraviolet
<b>VA</b>	Vanillic acid (4-Hydroxy-3-methoxybenzoic acid)
<b>VCAM-1</b>	vascular cell adhesion molecule-1

<b>VC</b>	Vehicle control
<b>vD3</b>	1 $\alpha$ , 25-dihydroxyvitamin D3
<b>WBB</b>	Wild blueberry

# **Chapter 1. General Introduction**

## 1.1 Introduction

Flavonoids (from the Latin word, *flavus*, meaning yellow, their colour) and phenolic acids are the two largest classes of plant-derived (poly)phenols and have diverse chemical structures. In the plant kingdom they are widely distributed and found naturally in fruits, vegetables, grains, seeds, nuts, roots, stems, barks and flowers <sup>1,2</sup>. They are plant secondary metabolites and are considered to be non-essential for growth and development. Nonetheless they play an important role in plant defence and survival and fulfil many biological functions. Such functions include attracting pollinators with their vibrant colours (yellow, red/blue)<sup>3</sup>, regulating the symbiotic interaction between plants and microorganisms (e.g. rhizobium bacteria) <sup>4,5</sup>, maintaining redox state in the cells as antioxidants and participating in plant defence against abiotic (ultraviolet radiation, heat) and biotic (herbivores and pathogens) stresses <sup>6,7</sup>.

Flavonoids and phenolic acids are found in numerous plant-derived foods in the diet including spices and herbs, nuts, seeds, olives, fruits such as berries and citrus fruit, vegetables including onions and garlic, cocoa products, tea, wine and other plant-derived beverages <sup>8,9</sup>. A large body of evidence suggests that flavonoids contribute beneficially to human health as they exert antibacterial <sup>10-12</sup>, antifungal <sup>13,14</sup>, antiviral <sup>15-17</sup> and anti-inflammatory <sup>18-20</sup> effects. Furthermore, a surge of evidence from epidemiological studies suggests that chronic intakes of flavonoid-rich foods may be beneficial in delaying ageing and/or reducing the risk of various chronic age-related disorders, including neurological disorders and cardiovascular diseases (CVD) <sup>21-26</sup>. CVD is the leading cause of death globally <sup>27</sup> and neurological disorders affects hundreds of millions of people worldwide <sup>28</sup>. The strain of these diseases is not just a health issue for the individual but the burden for their families, the wider society, health systems and the economy is tremendous <sup>29,30</sup>. Preventing and or reducing the risk of chronic disorders by flavonoid-rich diets could be considered as a sustained investment to human health and the economy to reduce the increasing

health costs and burden to millions of people in the UK and worldwide. A better understanding of the mechanisms of action of dietary flavonoids is therefore of utmost interest to the medical and nutritional fields.

The mechanisms by which flavonoids may prevent development of chronic disease is an ongoing debate. The general assumption is that flavonoids exert their effect by interacting with cell signalling pathways that regulate inflammation and oxidative stress, which play key roles in the pathogenesis of CVD and neurological disorders <sup>21,31–35</sup>. Inflammation is regulated by the nuclear factor kappa-light-chain-enhancer of activated B cells (NF-κB) signalling pathway while another transcription factor, nuclear factor erythroid 2-related factor 2 (Nrf2), co-ordinates cell responses to oxidative stress. NF-κB activation leads to pro-inflammatory signalling molecules while Nrf2 inhibits oxidative stress and indirectly down regulates inflammation by upregulating anti-oxidant enzymes and cytoprotective proteins, which interfere with the NF-κB signalling pathway and indirectly reduce pro-inflammatory mediator expression <sup>36</sup>.

Decades of research has been focused on the health effects of parent flavonoids (the native form from plants and present in foods) in *in vivo* and *in vitro* studies using supra-physiological concentrations. However, although flavonoids are plentiful in vegetables and fruits, their bioavailability as parent compounds has been scrutinised by the wider scientific community. In addition, advances in research techniques e.g. meta-omics approaches, have illuminated the role of gut microbiota in changing the fate of flavonoids consumed <sup>37</sup>. Gut microbes metabolise parent flavonoids, giving rise to small compounds which are absorbed by intestinal enterocytes and further metabolised by phase II enzymes in the liver <sup>38–40</sup>.

Recent research suggests that flavonoid metabolites are more bioavailable and more bioactive than their parent compounds at physiologically achievable concentrations <sup>18–20,41–53</sup>. As flavonoids are modified in the body, their metabolites are more abundant and more bioactive. Strikingly the most common flavonoid metabolites identified in circulation are the simple

phenolic acids such as protocatechuic acid (PCA), vanillic acid (VA), caffeic acid (CA) and ferulic acid (FA) which are either taken as free form from food as well as originating from the colon (colonic metabolites) as degradation products of various major dietary flavonoids such as quercetin and epicatechin. Together the magnitude of simple phenolic acid found in circulation may reach far greater bioavailability. Moreover, recent evidence suggesting that these simple phenolic acids are able to pass the blood brain barrier (BBB) indicating the protective effect of flavonoids on preventing neuroinflammation might be due to these simple phenolic acids <sup>54,55</sup>.

Nevertheless, it is unclear which metabolites or phenolic acids are involved in specific health effects, for example reducing the risk of developing CVD and neurological disorders, and several questions remain.

Which compounds are more bioactive for observed health effects? What is the mechanism of bioactivity? Can we classify metabolites based on their structure activity relationships? This study set out to answer those questions by investigating the potential effects of some of the most bioavailable phenolic acids from the common diet to help determine their role in combating inflammation. Furthermore, as flavonoids and phenolic acids are diverse and so are their metabolites, we intended to explore the chemical space occupied by the compounds, investigating their structure activity relationships and mechanisms of action as potential nutraceuticals or pharmaceuticals. For this purpose, we screened a large numbers of structurally related and non-natural, commercially available phenolic acids as well as ester analogues of these common phenolic acids to understand if the anti-inflammatory bioactivity of naturally occurring phenolic acids can enhance their pharmacological properties for therapeutic use.



## 1.2 (Poly)phenols

(Poly)phenols are the major ubiquitous phytochemical group in nature, found predominantly in plants as secondary metabolites as well as in mushrooms (fungi), slime molds and bacteria <sup>56–58</sup>. They are characterised by the presence of at least one phenolic ring coupled to one or several hydroxyl groups (**Figure 1. 16**). Furthermore, these compounds can have several moieties attached, for example sugars, known as glycosides, in addition to a range of different groups, including hydroxyl, methoxyl, methyl, benzyl and isoprene resulting in tremendously diverse shapes and structures <sup>29, 30</sup>. Based on their origin (synthesis pathway), chemical structure and biological function, (poly)phenols are currently divided into six classes and further split into numerous sub-classes <sup>60–62</sup>. The current classification includes phenolic acids, lignans, stilbenes, non-phenolic metabolites, other (poly)phenols and flavonoids according to the Phenol-Explorer database <sup>60,61</sup> (**Figure 1. 16**). Phenol-explorer is the most complete online database of (poly)phenols and to date, containing food composition of more than 500 (poly)phenols (classified in 6 classes and 31 sub-classes) in 459 foods <sup>60</sup>.

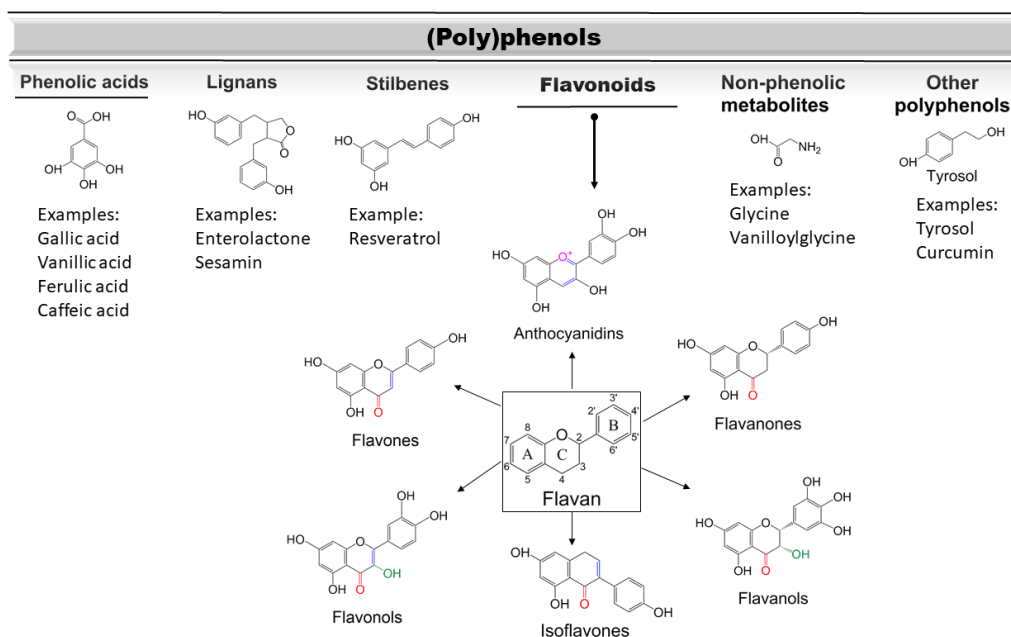


Figure 1. 16 Six classes of (poly)phenols with examples and six major sub-classes of flavonoids. Adapted from Moosavi et al., 2015.

Important to note that in the scientific, regulatory, and popular literature, the term “polyphenols” is widely and interchangeably used to refer to the whole family of phenolic compounds including those with less than one ring or no ring. This term in a recent review has been scrutinized and the proposed correct nomenclature should be (poly)phenols when referring to ‘a mixture containing, or combination of phenolics and polyphenols’ to emphasize that phenolic compounds with one or more rings and the term “polyphenol” when referring to ‘a compound containing 2 or more phenolic rings in its chemical structure’<sup>63</sup>.

To our current knowledge, dietary flavonoids are the most abundant class of (poly)phenols (60%), followed by phenolic acids (30%)<sup>59</sup>. At the time of writing this thesis, an estimation of 15000 flavonoid structures have already been characterised<sup>64</sup> and divided into nine subclasses: chalcones, dihydrochalcones, dihydroflavonols, isoflavonoids, flavanones, flavanols, flavones, flavonols and anthocyanins<sup>60,65</sup>. The first three sub-classes are less abundant in the common diet and therefore only the remaining six subclasses will be further discussed (**Figure 1. 16**). On the contrary, phenolic acids encompass five subclasses: hydroxybenzoic acids, hydroxycinnamic acids, hydroxyphenylacetic acids, hydroxyphenylpropanoic acids and hydroxyphenylpentanoic acids<sup>60,65,66</sup>. The first two classes are prevalent<sup>66</sup> and therefore these will mainly be addressed henceforth.

### 1.2.1 Chemistry and functions of flavonoids

The prevalent structure of flavonoids arises from the shikimate (C6-C3) and acetate (C6) biosynthetic pathway<sup>67</sup> and is composed of a 2-phenyl-benzopyran (flavan) backbone. The flavan core is a tricyclic (C6-C3-C6), a C<sub>15</sub> framework (**Figure 1. 17**), which consists of a heterocyclic benzopyran ring (ring C) that merge two benzene rings (A ring and B ring), the aromatic and phenyl constituents respectively<sup>59</sup>.

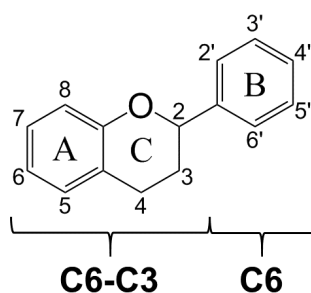


Figure 1. 17 Common structure of flavonoids based on chrome rings (A +C) and aromatic ring (B).

The sub-classification of flavonoids is based on the differences in the presence of a double bond in the C ring (at C2-C3 position) as well as the oxidation level (**Figure 1. 18**). The variation within a sub-class is based on the number and/or substitution (usually hydroxyl and methoxy group) of the B-ring (**Figure 1. 18**) or C-ring functional groups as well as the variation in glycosylation arrangements on both the A and B rings<sup>68-70</sup>.

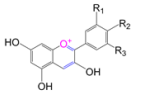
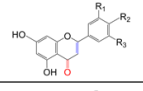
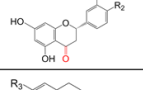
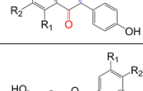
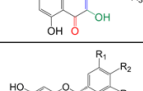
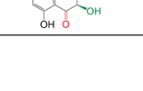
Sub-class	Common structure	Prominent dietary flavonoids	B-ring functional groups*		
			R <sub>1</sub>	R <sub>2</sub>	R <sub>3</sub>
Anthocyanidins		Cyanidin	OH	OH	H
		Delphinidin	OCH <sub>3</sub>	OH	H
Flavones		Apigenin	H	OH	H
		Luteolin	OH	OH	H
Flavanones		Naringenin	H	OH	H
		Hesperetin	OH	OCH <sub>3</sub>	H
Isoflavones		Daidzein	OH	H	H
		Genistein	OH	H	OH
Flavonols		Myricetin	OH	OH	OH
		Quercetin	OH	OH	H
Flavan-3-ols (Flavanols)		(+)-Catechin	OH	OH	H
		(+)-Gallocatechin	OH	OH	OH

Figure 1. 18 Major sub-classes of flavonoids with common structures. Figure adapted from Manach et al, 2004. \* with exception of Isoflavones (poses a C-ring functional group).

The existence of a double bond in the flavonoid core structure, combined with a carbonyl group (C=O) stabilises electron delocalisation. Those, combined with multiple hydrogen atoms of the aromatic groups behave as scavenger of reactive oxygen species (ROS) and therefore function as potent antioxidants in plants <sup>70</sup>. The core structure of flavonoids is an aromatic chromophore (structures with selective light absorption), which can absorb different region of visible ultraviolet (UV) light <sup>71</sup>. Hence, the emitted light is responsible for the distinct colour of flowers and fruits. Those colours play an important role in plant reproduction i.e. pollination by insects and seed dispersal by animals (in general by birds and mammals) <sup>72</sup>. Moreover, flavonoids play a central role in a range of vital biological activities in plants. Such functions are important in early plant development, acting as chemical messengers (e.g. in symbiosis and auxin regulation) <sup>4,73</sup>, defence mechanisms against a range of abiotic (excessive light irradiation, temperature and heavy metal tolerance) <sup>7,71,74-76</sup> and biotic stresses (herbivores and pathogens) <sup>77,78</sup>.

The role of flavonoids combating diseases in humans and animals is widely investigated<sup>10–20,79</sup>. Despite well-documented *in vitro* antioxidant activities of flavonoids<sup>80–84</sup>, a vast body of evidence suggests that in animals and humans their potential for being antioxidants and free radical scavengers is limited to the gastrointestinal tract because of their inadequate bioavailability and metabolism<sup>85–92</sup>. A widely approved alternative assumption is that *in vivo*, flavonoids implement their health effects through modulation of proteins and enzymes in the cell signalling pathways by their metabolites<sup>72,89,93–95</sup>. This research will be focused on flavonoid metabolites, in particular phenolic acids and their mechanisms of action *in vivo*.

### **1.2.2 Chemistry and function of phenolic acids**

Dietary phenolic acids, also known as phenolcarboxylic acids, are the second largest (poly)phenolic compounds found in the habitual diet<sup>60,65,66</sup> and are synthesised through the shikimate pathway via phenylalanine and tyrosine<sup>96</sup>. The most prevalent sub-classes of phenolic acids are hydroxybenzoic and hydroxycinnamic acid (**Figure 1. 19**). Hydroxybenzoic acids are derivatives of benzoic acid and bear a seven carbon atom framework of C6-C1 structure<sup>8,97,98</sup>. The structural differences between distinct compounds are based on the modification of the phenyl ring with one or more hydroxyl or methoxy substitutes (listed in **Figure 1. 19**). Hence, the most prevalent structures in the common diet include protocatechuic acid, vanillic acid, 4-hydroxybenzoic acid (also known as *p*-hydroxybenzoic acid), salicylic acid, ellagic acid, syringic acid and gallic acid<sup>60,66,97–100</sup>.

In contrast, the derivatives of hydroxycinnamic acids have the framework of C6-C3 structure<sup>8,98</sup> and arise from cinnamic acid. As in hydroxybenzoic acids, differences between structures of this subclass are based on modification of the aromatic ring.

Function group	Benzoic acid derivatives	Cinnamic acid derivatives
$R^3=R^4=OH$	Protocatechuic acid	Caffeic acid
$R^2=OCH_3, R^3=OH$	Vanillic acid	Ferulic acid
$R^2=OH, R^3=OCH_3$	Isovanillic acid	Isoferulic acid
$R^3=OH$	<i>p</i> -Hydroxybenzoic acid	<i>p</i> -Coumaric acid
$R^2=R^3=R^4=OH$	Gallic acid	-
$R^1=R^4=OH$	Gentisic acid	-
$R^2=R^4=OCH_3, R^3=OH$	Syringic acid	Sinapinic acid

Figure 1. 19 Common structures of benzoic and cinnamic acid derivatives. Figure adapted from Barros et al., 2009 and Heleno et al., 2015.

The most common structures from habitual human diet include caffeic acid, ferulic acid, isoferulic acid, cinnamic acid, sinapinic acid, *p*-coumaric acid and *p*-hydroxycinnamic acid<sup>66,97–99</sup>. Both hydroxybenzoic acids and hydroxycinnamic acids are usually present in bound form such as glycosides, amides and esters<sup>8,97,99,101–103</sup>. Moreover, in addition to existing free or bound structures from the diet, phenolic acids can also be produced through metabolism of flavonoids by gut microbiota<sup>52,100,104–107</sup>. Thus, they are present in higher quantities in the circulation.

Similarly to flavonoids, phenolic acids are not essential in plant growth and development but nevertheless play an important role in plant immunity and defence against biotic and abiotic stressors<sup>97,108–110</sup>. Moreover, certain plant species use phenolic acids such as ferulic, caffeic and *p*-hydroxybenzoic acid to suppress the growth of other plant competitors (allopathy) thereby contributing to plant colonisation and survival<sup>111,112</sup>.

## 1.3 Dietary sources and intake of flavonoids and phenolic acids

Dietary flavonoids and phenolic acids are the most abundant (poly)phenolic compounds from almost any product of plant origin, including fruits and fruit products, vegetables, seeds, cereals and cereal products, seasonings, oils, coffee, and cocoa (Table 1. 4).<sup>1,2,9,61,69,113,114</sup> . Moreover, plant derived beverages including alcoholic (e.g. wine, beer, cider, liquor) and non-alcoholic (tea and herb infusions, fruit juices, cocoa, and coffee beverages) are also rich sources of phenolic acids and flavonoids<sup>114</sup>.

Table 1. 4 Food classes with examples of food stuffs containing flavonoids and phenolic acids. Data retrieved from Phenol-Explorer database, version 3.6.

Food Classes	Example food stuff
Fruits and fruit products	berries, citrus, drupes (cherry, nectarine, apricot, plum and peach), melons, apple and pears, tropical fruits (banana, kiwi, mango, pineapple), dried fruits, jams and purees
Vegetables	Potatoes, onions, shoot (asparagus, fennel, globe artichoke), stalk (celery), root (carrot, radish, beetroot), peas and beans, cabbages, gourds (e.g. cucumber, pumpkin, squash), fruit vegetables (pepper, tomato, eggplant, olive and avocado)
Cocoa	Chocolates and cocoa powder
Cereals and cereal products	Wheat, buckwheat, rye, sorghum, rice, maize, pasta, bread and breakfast cereals
Seeds	nuts (e.g. almond, peanut, walnut), flaxseed, sesame seed, poppy seed, pulses (beans, lentils, peas), soy
Oils	Olive oil, corn oil, peanut butter, rape seed, sesame seed, sunflower seed, soy
Seasonings	Herbs, spices, spice blends (i.e. curry powder), soy sauce, vinegar
Alcoholic beverages	Wines, beers, ciders, liquors, spirits
Non-alcoholic beverages	Coffee beverage, cocoa beverage, tea infusions, herb infusions, fruit juices, vegetable juices, soy drinks

Among all foodstuffs, cocoa, tea, wine, and berries are exceptionally high in phenolic acids and flavonoids, exemplified in Table 1. 5. Flavanols are abundant in cocoa and green tea while berries, plums and grapes (red wine) are rich in anthocyanins<sup>8,41</sup>. Flavonols are found abundantly in seasonings and vegetables such as cloves and onions and flavanones are primarily in citrus fruits, while isoflavones are found almost exclusively in soy and soy products<sup>115</sup>.

Table 1. 5 Main dietary food sources with high content of phenolic acids and flavonoids. Information derived from Phenol-Explorer, version 3. and Martín et al., 2017.

Food sources	Total (poly)phenol content (per 100 g or mL)	Major composition flavonoids / phenolic acids	Prominent compound
Cocoa powder	5624 mg	Flavanols (>500 mg) hydroxybenzoic acids (>45 mg) hydroxycinnamic acid (>35 mg)	(-)-Epicatechin (158 mg) Protocatechuic acid (40 mg) caffeoylaspartic acid (37 mg)
Dark chocolate	1860 mg	Flavanols (>230 mg) hydroxycinnamic acid (>20 mg)	(-)-Epicatechin (70 mg) Ferulic acid (24 mg)
Black chokeberry	1752 mg	Anthocyanins (>870 mg) Flavonols (>40) hydroxycinnamic acid (>140 mg)	Cyanidin 3-O-galactoside (558 mg) Quercetin 3-O-galactoside (46 mg) Caffeic acid (141 mg)
Strawberry	289 mg	Anthocyanins (>70 mg) Flavanols (> 8 mg) hydroxybenzoic acids (> 5 mg)	Pelargonidin 3-O-glucoside (47 mg) (+)-Catechin (6 mg) 4-Hydroxybenzoic acid (7 mg)
Orange (blonde)	279 mg	Flavanones (> 40 mg)	Hesperetin (34 mg) Naringenin (11 mg)
Coffee (filter)	266 mg	hydroxycinnamic acid (> 210 mg)	Caffeic acid (87 mg) 5-Caffeoylquinic acid (70 mg)
Red wine	215 mg	Anthocyanins (>20 mg) Flavanols (>40) hydroxybenzoic acids (> 5 mg) hydroxycinnamic acid (7 mg)	Malvidin 3-O-glucoside (10 mg) Procyanidin dimer B3 (9 mg) Gallic acid (4 mg) Caffeoyltartaric acid (3 mg)
Tea black (infusion)	104 mg	Flavanols (> 65 mg) hydroxybenzoic acids (> 16 mg)	(+)-Gallocatechin (14 mg) 5-O-Galloylquinic acid (11 mg)

Among all food stuffs, coffee, tea, and fruits (**Table 1. 5**) are the most important sources of total (poly)phenols in the European and UK diet<sup>116</sup>. Overall, the main (poly)phenol contributors are phenolic acids and flavonoids<sup>117</sup>. In the UK diet, flavonoids account for nearly half of total (poly)phenol intake. The average intake of flavonoids in Europe has been estimated to be 428 mg/d in adults (18-64 years) which is based on food consumption data from the European Food Safety Authority (EFSA) and



FLAVIOLA Food Consumption Database <sup>118</sup>. Among fourteen investigated countries, Ireland, UK, and the Netherlands were the highest flavonoid-consuming countries with an average of 851, 655 and 643 mg/d respectively. In the UK diet, the main flavonoid compounds are gallated compounds (110 mg/d), followed by epicatechin (30 mg/d), flavonols (28 mg/d) and anthocyanidins (16 mg/d).

Non-alcoholic beverages, especially tea and coffee, are the main sources of dietary phenolic acids and flavonoids for European populations. The average UK daily intake of total flavonoids from tea has been estimated to be approximately 157 mg/d <sup>118</sup>, which is more than ¼ of total flavonoid intake. Furthermore, the average UK diet contains 43 mg/day of flavanol catechins, the highest concentration of all flavonoids found in the diet <sup>118</sup>. The most important sources of catechins include apple, cocoa and cocoa products and tea <sup>66</sup>. Moreover, tea is thought to be the most popular drink after water worldwide and contains approximately 62 and 104 mg/100 mL (poly)phenols (green tea and black tea respectively) and the majority of these flavonoids are flavan-3-ols (flavanols), followed by flavonols and phenolic acids acids (**Table 1. 6**). Based on consumption of a cup of tea (200 mL cup, 1% tea leaves w/v), the estimated intake of total catechins is approximately 30 and 135 mg from black tea and green tea respectively <sup>119</sup>. The relative concentrations of major flavanols from tea are catechins with (-)-epigallocatechin 3-O-gallate the most prevalent (27 mg/100 ml) <sup>115</sup> and the average daily intake is approximately 157 mg/d in the UK alone.

Table 1. 6 Dietary sources and main content of flavonoids. Derived from Phenol-Explorer, version 3.

Dietary sources	Total polyphenol content (per 100 g)	Major flavonoid sub-classes	Major content
Green tea	62 mg	Flavanols, Flavonols	(-)-Epigallocatechin 3-O-gallate (27 mg), (-)-Epigallocatechin (20 mg), (-)-Epicatechin (8 mg)
Black tea	104 mg		(-)-Epigallocatechin 3-O-gallate (9 mg), (-)-Epicatechin 3-O-gallate (7 mg), (-)-Epigallocatechin (7 mg)
Apple [Cider], peeled	251 mg	Flavanols	(-)-Epicatechin (29 mg), Procyanidin dimer B2 (20 mg), (+)-Catechin (20 mg)
Cocoa powder	5624 mg		(-)-Epicatechin (158 mg), Procyanidin dimer B1 (112 mg), (+)-Catechin (108 mg)
Dark chocolate	1860 mg	Flavanols	(-)-Epicatechin (70 mg), quercetin (25 mg), (+)-Catechin (20 mg)
Peach	107 mg		Procyanidin dimer B1 (25.77 mg), (-)-Epicatechin (7.97 mg), (+)-Catechin (5.47 mg),
Banana	155 mg	Flavanones, Flavones	(+)-Catechin (1.34 mg), (-)-Epicatechin (0.11 mg)
Orange	279 mg		Hesperetin (33.60 mg), Naringenin (11.22 mg),
Lemon	60 mg	Anthocyanins, Flavonols, Flavonols	Eriodictyol (17.60 mg), Hesperetin (17.10 mg), Luteolin (1.27 mg)
Strawberry	289 mg		Pelargonidin 3-O-glucoside, Kaempferol 3-O-glucoside, Pelargonidin 3-O-(6"-succinyl-glucoside), (+)-Catechin

Coffee is the major source of the phenolic acids, hydroxycinnamates including caffeic acid, ferulic acid, *p*-coumaric acid and sinapinic acid, <sup>8,120</sup>. These are mostly found as conjugates e.g. with tartaric or quinic acid and referred to as chlorogenic acids <sup>121,122</sup>. Hence, high consumption of coffee may exceed the average daily intake of phenolic acids and so is the major dietary (poly)phenol intake for many people in UK and around the globe <sup>116,123</sup>.

Other sources of flavonoids in the UK diet include fruit and fruit products (57 mg/d), grain and grain-based products (20 mg/d), alcoholic beverages (19 mg/d) and legumes, nuts, and oilseeds (15 mg/d). The main content of flavonoids is found on the outer layers (such as skins) of fruits, seeds and cereals and intake of the whole food is associated with a healthy diet. Finally, it should be noted that the content of flavonoids and phenolic acids in food sources varies hugely depending on plant variety, ripeness, storage time, food treatment/processing, drying, heat treatment and biotic and abiotic stress to which the plants have been exposed <sup>39</sup>.

## 1.4 Metabolism and absorption

It is now well established that flavonoids are extensively metabolised upon intake <sup>69,124–129</sup>. In nature, the majority of flavonoids usually occur conjugated to sugar moieties (with the exception of flavanols) as  $\beta$ -glycosides or glycones. It was therefore speculated that their absorption is limited to aglycone forms <sup>130</sup>, underestimating their metabolism by the gut microbiota. Upon consumption, flavonoids are metabolised through various mechanisms depending on their structure and composition <sup>127</sup> and a wide range of metabolites arise from both gut and phase II metabolism. For this reason, a better understanding of flavonoid metabolism is a key step toward understanding the mechanisms of action of dietary flavonoids.

Metabolism occurs in the enterocytes lining the gastrointestinal tract, in the lower gastrointestinal tract by the gut microbiota and further in the liver <sup>11,12,131</sup>. Flavonoids are first metabolised in the small intestinal tract (**Figure 1. 20**). Here, flavonoid aglycones are directly absorbed by intestinal enterocytes, while the sugar moiety of glycones are cleaved by lactase phloridzin hydrolase (LPH), located on the brush border, leaving the aglycone to be directly absorbed into enterocytes <sup>132, 133</sup>. Alternatively, glycones may be actively transported to enterocytes via the sodium-dependent glucose transporter (SGLT1) <sup>133, 134</sup>. Upon absorption into enterocytes, aglycones passively diffuse into the hepatic portal vein, while the glycones may be targeted by cytosolic- $\beta$ -glucosidases (C $\beta$ G), to cleave off the sugar moiety, releasing aglycones <sup>135</sup>. Moreover, within enterocytes, the aglycones can be further conjugated to methyl, sulphate or glucuronide groups by phase II enzymes, UDP-catechol-O-methyltransferase (COMT), sulfotransferase (ST) or glucuronosyltransferase (GT). These conjugated flavonoids are rapidly targeted by the multidrug resistance protein (MRP) and expelled back to the intestinal lumen or into the hepatic portal vein <sup>132, 136, 127</sup>.

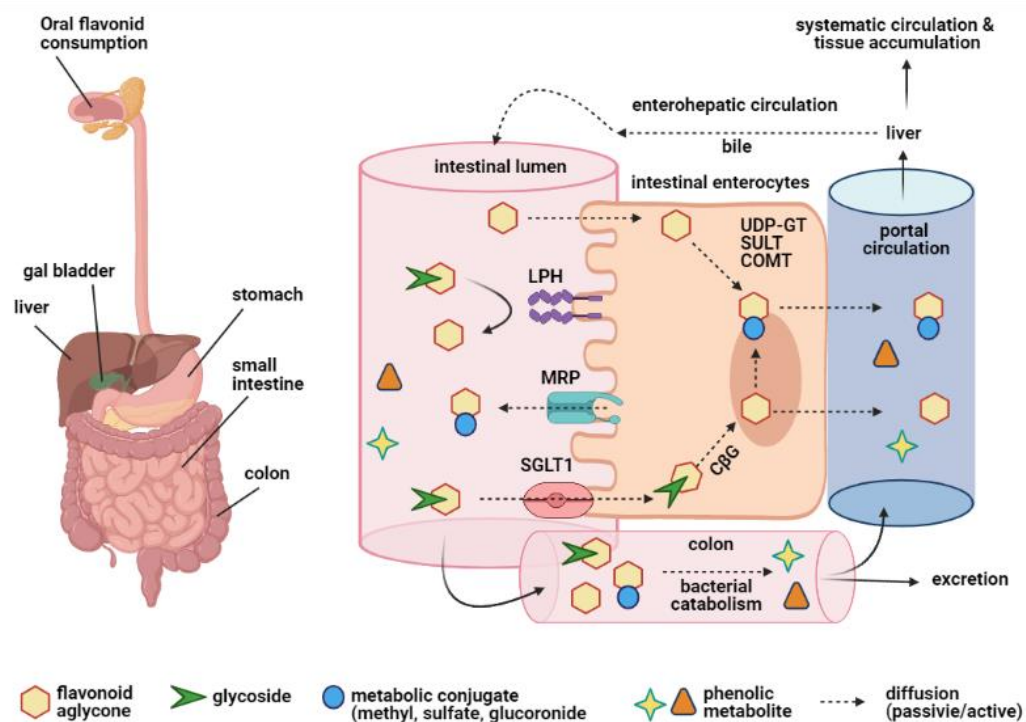


Figure 1. 20 Mechanisms of flavonoid absorption. LPH, lactase phloridzin hydrolase; MRP, multidrug resistance protein; SGLT1, sodium-dependant glucose transporter; UDP-GT, UDP-glucuronosyltransferase; SULT, sulfotransferase; COMT, catechol-O-methyltransferase; C $\beta$ G, cytosolic- $\beta$ -glucosidase. Adapted from Warner, 2016 137 and created in BioRender.com.

All metabolites that reach the hepatic portal vein are transported to the liver where they may further undergo methylation, sulfation and/or glucuronidation <sup>19, 56</sup>. After this, they may be released into systemic circulation, followed by distribution to tissues and/or targeted for rapid excretion by the kidneys and/or through bile to re-enter the small intestinal lumen <sup>92</sup>.

All flavonoids that are unabsorbed or returned to the small intestine are passed to the colon. Throughout the passage to the colon, anthocyanidin compounds spontaneously degrade, while other flavonoids are targeted by gut microbiota, which possess certain metabolic enzymes including glucosidases, demethylases, decarboxylases, hydroxylases and esterases and these give rise to small compounds upon metabolism <sup>20, 58</sup>. In the early

70s Griffiths and co-workers <sup>140</sup> first highlighted the importance of the gut microbiota in flavonoid metabolism by feeding flavonoids to antibiotic-treated or germ-free animals. Treatment with antibiotics decreased or completely suppressed the formation of metabolites in germ-free subjects. Three decades later, Bowey and co-workers (2003) showed that transplanting faecal flora from healthy human subjects to germ-free rats resulted in metabolism of flavonoids, emphasizing the importance of the gut flora in metabolism<sup>141</sup>. The products of catabolism are further excreted in faeces, and/or absorbed and transferred to the liver via the hepatic portal vein where they are further processed and/or distributed to various tissues and/or excreted as mentioned above.

One of the key steps in catabolism is thought to be the A-ring fission and carbon loss from C5 to C8, released as oxaloacetate which is converted to CO<sub>2</sub> and exhaled through the lungs <sup>24, 50</sup>. However, a large proportion of flavonoid metabolites found in the circulation have been shown to originate from B-ring fission as phenolic metabolites <sup>143</sup>. These metabolites include procatechuic acid, cinnamic acid, vanillic acid, phenylpropionic acids, phenylacetic acid, benzoic acid and caffeic acid. Other important metabolites found in the circulation include valerolactones and glycine conjugates <sup>22, 60–62</sup>. Moreover, the majority of flavonoid metabolites found in the circulation and urine are methylated, sulphated, glucuronidated and glycosylated conjugates <sup>19, 24, 27, 61</sup>.

Based on the above evidence it has been theorised that the health effects of flavonoids are more likely the result of their metabolites that are abundant in circulation rather than their parental flavonoids, which are poorly found in the circulation <sup>146, 92, 41</sup>. Subsequently, more recent studies, including work from our lab, have focused on the bioactivity of phenolic metabolites in comparison with their parental flavonoids and demonstrate that metabolites are more bioactive than their parent compounds. <sup>147, 19, 44, 47, 46</sup>.

## 1.5 Bioavailability

The health effects of flavonoids and phenolic acids depends on the amount consumed and their bioavailability. Bioavailability is defined as the fraction of all compounds (including nutrient /drugs or xenobiotics), relative to dose which is absorbed into the systemic circulation for a certain physiological function or storage <sup>148,149</sup>. The usual biometrics used for bioavailability assessments are blood/plasma and urine <sup>150</sup>. Several methods are used to measure the bioavailability of nutrients, including tracer methods (e.g. isotopes) or serum concentrations <sup>151</sup>. Measuring serum concentration is one of the widely used methods and considered as analogous to the traditional pharmacokinetic measures used for drugs, such as measuring the area under the curve (AUC) <sup>152</sup>. AUC is a measure of the extent of a given compound absorbed and its persistence in circulation. For measuring plasma concentration, usually two parameters,  $C_{max}$  and  $T_{max}$  are used, the maximum concentration of a given compound in plasma ( $C_{max}$ ) and the time at which this concentration is highest ( $T_{max}$ ).

The maximal concentration ( $C_{max}$ ) of flavonoid metabolites found in human plasma range between 0.09 – 0.32  $\mu\text{M}$  with a median time to reach a maximum concentration ( $T_{max}$ ) ranging between 0.5 - 7h <sup>32, 66</sup>. Rothwell et al. (2016) hypothesized that the maximum concentration of flavonoid metabolites in human circulation (although theoretically possible) cannot exceed 10  $\mu\text{M}$  from diet. However, Czank et al., (2013) <sup>106</sup>, reported that the serum concentration of metabolites from anthocyanin range between 0.1 - 42.2  $\mu\text{M}$  within 0.5 – 48 h which is 42-fold higher than previously suggested. In this study, the research group investigated the absorption, distribution, metabolism, and excretion (ADME) of a <sup>13</sup>C5-labeled anthocyanin in humans where they found that the  $C_{max}$  and the  $T_{max}$  of anthocyanin metabolites varies greatly, suggesting a much higher bioavailability of metabolites than previously suggested.

Ottaviani et al investigated the ADME of isotope labelled [2-<sup>14</sup>C](–)-epicatechin in humans and reported a 95% absorption of (–)-epicatechin

(EC) with the total 0–48 h. <sup>154,155</sup>. In this study 8 healthy middle-aged males (31 ± 3y, 75 ± 11 kg) subjects were given 50 mL drinks containing 60 mg (207 µM) of EC, with 300 µCi of radioactivity. Post-consumption, two peaks were observed in both blood and plasma at 1 h and at 6 h with ( $C_{max}$ ) of 699 ± 65 nM and 516 ± 93 nM for blood and, 1209 ± 104 nM and 952 ± 168 nM for serum, respectively. Detection in blood and plasma lasted up to 36h and 72h respectively. The elimination of radioactivity was 82 ± 5% in urine after 24h and 12 ± 3% in faeces, accounting for 95% bioavailability of total <sup>14</sup>C][(-)-epicatechin ingested. More interestingly, EC was converted into more than 20 structurally related metabolites with the majority being gamma-valerolactones accounting for 42% and 28% were hippuric and phenolic acids. Moreover, the level of unmetabolised EC in this study was below the detection limit suggesting the bioactivity of EC must be exclusively due to metabolites. This is an important point for designing intervention studies and in *ex vivo* studies in order to be able to use relevant metabolites and their physiological concentrations.

An important aspect of bioavailability is the huge inter-individual variability between human subjects. Several studies have reported a huge variability in plasma metabolite concentration of study participants <sup>50,155</sup>. This variability has been attributed to several factors such as genetic variation <sup>100</sup>, age and metabolotypes <sup>156</sup> of subjects, and variations in their gut microbiome <sup>53</sup> as well as the general food matrix <sup>155</sup> or, most likely, a combination of all these factors. The gut microbiome has emerged as one of the most critical factors of (poly)phenol bioavailability as well as bioactivity <sup>157</sup>. Two-way interaction between gut microbiota and (poly)phenols occur i.e. (poly)phenols may modify composition of microbial population (“prebiotic-like effect”) <sup>158</sup> of gut microbiota through their microbial catabolites, by acting as antimicrobial agents for specific bacterial groups and contributing to the growth and modifying the composition of commensal gut microbiota <sup>79, 80</sup> such as bifidobacterial and lactobacilli <sup>158</sup>. In return, the beneficial microbiome can metabolise (poly)phenols into smaller molecules, metabolites which are more bioavailable. Flavonoids,

together with the composition of beneficial gut microbiota has been shown to exert a protective effect on obesity-associated pathologies through modulation of inflammatory-related cellular events in the intestine <sup>12, 44, 81</sup>.

Furthermore, intake of flavonoids can be enhanced by presence of the food matrix. For instance, consumption of tea (flavan-3-ols) with milk, ascorbic acid or citrus juice (lemon, lime, orange and grapefruit) can enhance parent flavonoid bioavailability <sup>161</sup>. This assumption is also valid for anthocyanins e.g. anthocyanin bioavailability from common foodstuffs or from pure compounds has been suggested to range between <0.1-2%, in contrast to 5% from wine, suggesting that other compounds from wine possibly enhance the bioavailability of anthocyanins <sup>92</sup>.

Other factors that affect bioavailability are different concentrations of administered compounds, additive/synergistic effects, intake with fat and/or fibre, micro and macronutrients, solubilisation and miscellarization, use of antibiotics and physical activity <sup>8,39,70,107,162–164</sup>. The concentration of tissue and plasma protein bound phenolic metabolites may be higher than plasma concentrations, contradicting previous views that storage in tissue is low <sup>8, 79</sup>. This is another important point to consider when designing experiments with metabolites. However, in our lab three studies have demonstrated that the majority of bioactive metabolites exhibit their effects at 1-10  $\mu\text{M}$  and their effects can be seen as non-linear U-shaped <sup>19,47</sup> which suggests that these concentrations can be achieved via normal dietary consumption.

Frequently reported metabolites found in human and animal fluids following dietary consumption include those from four flavonoid sub-classes: anthocyanins (cyanidin, delphinidin, and peonidin glucosides, usually originated from different berries and berries extracts) <sup>41,43,89,165 22, 59, 71</sup>; flavanones (hesperetin and naringenin glucuronides, usually originated from citrus fruits) <sup>41,128</sup>; flavonol (quercetin) <sup>41,166</sup> and flavanol ((-)-epicatechin) <sup>41,167</sup>. Furthermore, the most frequently identified metabolites that are derived from a range of different (poly)phenols are: protocatechuic acid, ferulic acid, caffeic acid, 4-hydroxybenzoic acid, 4-hydroxyphenylacetic acid, gallic acid, isovanillic acid, isoferulic acid,



hippuric acid and their sulfate, glucuronide conjugates as well as 5C-ring fission metabolites such as 5-(hydroxyphenyl)- $\gamma$ -valerolactones<sup>41,52,53,65,89,155,165</sup>.

A growing body of evidence suggests that metabolites are more bioavailable and active than their parental flavonoids at physiological concentrations<sup>18–20,44,45,47,49,51,55,168</sup>. For instance, our lab previously investigated the effect of the peak signature of cyanidin-3-glucoside (C3G) metabolites on soluble vascular adhesion molecule-1 (VCAM-1) and interleukin-6 (IL-6) in human endothelial cells<sup>20</sup> and showed that the metabolites reduced soluble VCAM-1 and IL-6 secretion contrasting their parental compounds which did not shown any effect at the same concentrations. This suggests that metabolites are bioactive at physiological levels and physiological concentrations could be utilised in *in vitro* studies.

## 1.6 Bioactivity

It has long been understood that a diet rich in (poly)phenols is associated with a reduced incidence of all-cause mortality <sup>21,169</sup> and a lower risk of developing various chronic diseases <sup>31,170</sup>, including various types of cancer <sup>23,150,171–175</sup>, Type 2 diabetes (T2D) <sup>11, 12, 78</sup>, cardiovascular diseases (CVD) <sup>31,35,150,177–182</sup>, neurological disorders (depression, Alzheimer, Parkinson, stroke) <sup>150,177,183–188</sup> and improved cognitive function <sup>26,189,190</sup>. Flavonoids and phenolic acids have been particularly postulated to be responsible for these health effects, with stronger evidence for beneficial effects in CVD and neurological disorders <sup>180</sup>. This review will focus on the impact of flavonoids and phenolic acids on CVD and neurological disorders and the underlying mechanisms and major signalling pathways involved.

## **1.7 Flavonoid intake and vascular diseases**

### **1.7.1 Cardiovascular diseases**

Cardiovascular disease is an umbrella term used to describe several conditions that affect the heart and blood vessels, including coronary heart disease (CHD) or ischemic heart disease, rheumatic heart disease, aortic diseases, peripheral arterial disease and cerebrovascular disease <sup>27,191</sup>. CVD is the leading cause of death worldwide, taking an estimated 17.9 million lives per year <sup>27</sup>. In a wider context, the burden of CVD is also an economic challenge. Public Health England estimated the annual costs of CVD to NHS (£ 4.7 billion, 6% of total NHS budget) and the wider economy (£ 15.8 billion) <sup>29</sup>. With increased life expectancy, the cost of CVD-related disorders is expected to grow exponentially <sup>192</sup>.

The specific cause of CVD is not clear, nevertheless developing CVD depends on several factors including high blood pressure, cholesterol, diabetes, obesity, smoking, high alcohol consumption, physical inactivity, and genetic susceptibility <sup>191,193</sup>. CVD can be largely prevented by leading a healthy lifestyle <sup>194</sup> and adopting a diet rich in fruits and vegetables. The benefit of a healthy diet may be due to numerous factors including vitamins, minerals, fibre, and (poly)phenols. Furthermore, eating more fruits and vegetables might reduce consumption of less healthy food stuffs, such as red meat and calorie rich foods, contributing to a reduced risk of developing CVD.

### **1.7.2 Flavonoid and phenolic acid intake and CVD**

Over the last few decades, researchers have attempted to link the observed health effect of a diet rich in fruits and vegetables with consumption of (poly)phenols, particularly flavonoids and phenolic acids. This assumption is broadly supported by a large body of evidence from epidemiological

studies <sup>21,23,31</sup>; randomized control trials (RCTs) <sup>32–35</sup> and meta-analysis studies <sup>195</sup>.

In a prospective 16 year follow up study, 34,489 postmenopausal women (the Iowa Women's Health study) were recruited to evaluate an association between flavonoid intake and CVD mortality. Consumption of anthocyanidins, flavanones and certain foods rich in flavonoids was associated with a reduced risk of mortality from coronary heart disease (CHD), CVD and all other causes <sup>196</sup>. Moreover, Cassidy et al (2011) examined the association between habitual flavonoid intake and hypertension incidence in a prospective study in both men and women. Flavonoid consumption intake was assessed every four years over a 14-year period in 156,957 subjects. The findings suggest an association between reduced risk of hypertension and the highest intake of anthocyanins, and some specific flavone and flavanol compounds <sup>197</sup>. Another prospective cohort study with 56,048 participants followed for 23 years noted that a moderate habitual intake of flavonoids reduced the risk of all causes of CVD mortality and a strong association plateaued at approximately 0.5 g/day intake <sup>23</sup>.

More recently, high intake of isoflavones was associated with a moderately lower risk of developing CHD in healthy participants from three prospective cohort studies (NHS (Nurses' Health Study); with 74,241 women, between 1984–2012) and NHSII (94,233 women, between 1991–2013), and Health Professionals Follow-Up Study (42,226 men, between 1986–2012) who were free of CVD and cancer at baseline <sup>22</sup>.

Cassidy and co-workers (2015) implemented another approach to examine the associations of intake of different flavonoid classes with twelve inflammatory biomarkers by using an inflammation score (IS) <sup>198</sup>. They studied a cross-sectional analysis of 2375 participants from the Framingham Heart Study Offspring Cohort for their total flavonoid intake and different classes (anthocyanins, flavonols, flavan-3-ols, flavanones, flavones, and their polymers) by quantifying the intake from validated food questionnaires. They found an inverse association between high intake of

anthocyanins and flavonol and IS, where higher intakes of anthocyanins were associated with a reduction in all selected biomarkers and flavonols with lower cytokine and oxidative stress biomarker concentrations. In addition, higher intakes of flavan-3-ols and their polymers were inversely associated with lower oxidative stress biomarkers. Other studies have investigated specific flavonoids that could be responsible for CVD prevention. In a prospective cohort study, Knekt et al (2002), collected the total dietary intake histories of 10,054 Finnish females and males for one year. After 28 years, a follow up suggested that higher intake of the flavonols quercetin and kaempferol, and the flavanones hesperetin and naringenin were associated with a lower mortality from ischaemic heart disease (or CHD) and CVD <sup>31</sup>.

Furthermore, tea and cocoa are rich in catechins and phenolic acids and have been postulated to be responsible for the beneficial effects of these food products in CVD. A meta-analysis of the data from 16 RCTs on systolic blood pressure (SBP) and 15 RCTs on diastolic blood pressure (DBP) with 391 subjects demonstrated that blood pressure reduction linked to consumption of cocoa depends on the dose of ingested catechin <sup>199</sup>. Previously, Arts et al (2001) also assessed the effect of catechins on fatal heart disease risk in 806 men aged 65-84 years over 16 years. High consumption of catechins (mainly from chocolate, black tea and apples) was inversely correlated with deaths from ischemic heart disease <sup>200</sup>. Moreover, the effect of tea derived flavonoids on risk of myocardial infarction was assessed in 4,807 Dutch men and women aged  $\geq 55$  y over a period of 5.6 years. The relative risk of myocardial infarction was lower in tea drinkers with a daily intake  $>375$  ml compared with non-tea drinkers <sup>201</sup>. Another meta-analysis based on seven prospective cohorts of 68,860 men and 36,877 women including a total of 2087 fatal CHD event also concluded an association between a reduced risk of CVD and high intake of flavonols from tea, red wine and other fruits and vegetables <sup>202</sup>. In another meta-analysis, 22 prospective cohort studies were examined and an inverse

correlation found between incremental intake of flavonoids (100 mg/day) and decreased risk of all-cause (6%) and CVD (4%) mortality <sup>169</sup>.

In contrast, other studies have found low or no associations between CVD risk and these flavonoids. For example, a study of 38,445 women, extended over 6.9 years, found only a weak association between CVD and a high consumption of flavonoids from tea, apples and broccoli <sup>203</sup>. A systematic review and dose-response meta-analysis, including 27 cohort studies reported a low inverse association between chocolate intake and CHD and stroke <sup>204</sup>. In another meta-analysis of nine population cohorts with 216,908 participants, including over 5249 CHD cases, there was no significant association between CHD and the highest flavonol intake <sup>205</sup>. Furthermore, another prospective cohort study, Vogiatzoglou et al 2015 <sup>206</sup> the Norfolk arm of the European Prospective Investigation into Cancer and Nutrition (EPIC-Norfolk) investigated the associations between flavan-3-ol intake and CVD risk and mortality rate. The flavan-3-ol intake was assessed using 7-day food diaries of 24,885 (11,252 men; 13,633 women) participants followed between 1993-1997. There was no consistent relationship between high intake and overall reduced risk or mortality rate of CVD.

Epidemiological studies, based on food questionnaires have their own limitations and are prone to many confounding factors including accuracy of dietary intake measurements, for example errors in food frequency questionnaires, recall methods and in dietary histories and large variation in dietary sources of flavonoids between different countries <sup>207</sup>. In addition, food processing, storage methods and varying environmental stress to the plant depending on geographical location varies greatly and all of those factors can collectively influence the (poly)phenol content of food stuffs. In addition, a lack of suitable biomarkers <sup>208</sup>, bioavailability (composition of gut microbiome and food matrix), interindividual variability <sup>209</sup>, (e.g. age, sex, ethnicity, pathophysiological statuses and medication <sup>210</sup>), life style, physical activity and socioeconomical statuses <sup>116</sup> can also hugely affect variation between participants and studies.

To bypass certain obstacles, well controlled intervention trials with pure compounds or supplements have been undertaken to examine the health effect of flavonoids <sup>211–213</sup>. For example, Grassi et al. (2015) <sup>211</sup>, examined the effect of different doses of cocoa flavonoids on several CVD biomarkers in 20 healthy subjects aged 18-70 years, for five 1-week periods. In this study, participants received five 1-week periods of 10 g cocoa (0, 80, 200, 500, 800 mg cocoa flavonoids/day) according to a randomised controlled, double-blind, cross-over design. Cocoa dose-dependently improved flow mediated dilation (FMD) and decreased pulse wave velocity (PWV) and endothelin-1 (ET-1) also by ameliorating office- and monitored- blood pressure (BP) <sup>211</sup>. Another study investigated the effect of black tea on blood pressure in a randomised placebo-controlled double-blind 6-month parallel trial on men and women aged 35 to 75 y, who were regular tea drinkers where they found that long-term regular consumption of black tea resulted in significantly lower BPs in individuals with normal to high-normal range BPs <sup>212</sup>. Moreover, Dower et al. (2015) <sup>213</sup>, examined the effect of pure epicatechin and quercetin supplementation on cardiometabolic health and vascular function in healthy men and women aged 40–80 years in a randomised, double placebo-controlled, crossover trial in a four week intervention. Quercetin-3-glucoside supplementation did not affect CVD risk factors and had no effect on insulin, while epicatechin improved fasting plasma insulin and insulin resistance, but did not significantly affect flow-mediated dilation. They concluded that epicatechin but not quercetin might be responsible for the cardioprotective effects of cocoa and tea by improving insulin resistance.

In a double-blind RCT study, long-term blueberry consumption improved cardiometabolic biomarkers in participants with high risk CVD by 12-15% <sup>32</sup>. During a 6-month intervention, 115 overweight or obese (BMI  $\geq$  25 kg/m<sup>2</sup>) participants, aged 50-75 y with  $\geq$  3 metabolic-syndrome (MetS) components (incl. hypertension, hypertriglyceridemia, impaired fasting glucose, low levels of HDL cholesterol or central adiposity) were randomly assigned (n=37, 39, 39) to consume a product equivalent to a daily 1 cup

or ½ cup of blueberries (freeze-dried) or placebo treatment, containing 879, 439, and 0 mg phenolic acids and 364, 182 or 0 mg of anthocyanins respectively. A dose-dependent significant increase in total concentration of anthocyanin-derived phenolic acid metabolites in serum and 24 h-urine was observed. A daily intake of 1 cup blueberry significantly improved and sustained endothelial function, systemic arterial stiffness, lipid statuses, and underlying NO bioactivity, and lowered cGMP levels.

In another double-crossover RCT, wild blueberries (150 mg) and purified anthocyanins (160 mg) dose-dependently improved endothelial function (as FMD and SBP) in comparison to control drinks with vitamins, minerals or fibre in 60 healthy humans <sup>52</sup>. Furthermore, 63 plasma anthocyanin metabolites were quantified with a majority of cinnamic and benzoic acid derivatives. Of these plasma metabolites, 14 and 21 correlated with acute and chronic flow-mediated dilation improvements, respectively and intracardiac injection of these metabolites also improved flow-mediated dilation in mice. Moreover, daily blueberry intake led to differential expression of 608 genes involved in cell differentiation, immune response, cell adhesion and migration, suggesting that anthocyanin metabolites are major mediators of vascular bioactivity via changes in cellular and gene response <sup>46</sup>.

However, although exact dietary intake can be better quantified, these trials also have limitations, and the results are not consistent with findings from epidemiological studies. Several factors can affect intervention trials with supplements, including the food matrix, inter-individual variability and additive/synergistic effects of other bioactives from diet <sup>39, 214</sup>. Furthermore, the health state of participants may be an important contributor to the outcome, i.e. the effect of phenolic acids or flavonoids on overall cardiovascular health might be more visible in individuals at higher risk (e.g. smokers and high alcohol consumers) of CVD <sup>21,23,32,195,215</sup>. In conclusion, the relationship between CVD and high intake of flavonoids is still not fully convincing and more robust studies are needed which may aspire to include



more accurate flavonoid content of different type of foods and sufficient standardised materials and well-matched controls used in RCTs <sup>35</sup>.

In addition, an alternative approach to investigate the relationship between CVD and flavonoids is to focus on the molecular level and study the mechanisms of action of dietary bioactives in relation to the underlying mechanisms of CVD.

### **1.7.3 Inflammation and CVD**

Inflammation is the primary defence mechanism of the body against damage caused by internal and external factors. In general, it triggers a cascade of mediators resulting in cell, tissue, and systemic responses to eliminate pathogens or injurious agents and remove the damaged tissue to allow the body to heal. Chronic inflammation occurs when the inflammation is unresolved and leads to long-term damage. Inflammation is a central underlying component in the pathogenesis of several chronic age-related diseases, including atherosclerosis <sup>216</sup>, which is thought to be the single most important contributor to CVD development <sup>217</sup>.

### **1.7.4 Atherosclerosis initiation and progression**

Atherosclerosis is defined as a progressive disease characterised by the accumulation of lipids and fibrous debris in the large arteries ultimately leading to thrombotic complications at the end stage <sup>216</sup>. The normal process of atherosclerosis starts with activation of endothelial cells in response to multiple factors, including infectious agents, circulating inflammatory cytokines (for example, tumor necrosis factor- $\alpha$  (TNF- $\alpha$ ), interleukin-6 (IL-6), monocyte chemoattractant protein-1 (MCP-1), reactive oxygen species (ROS), autoantibodies and traditional risk factors e.g. high plasma cholesterol, high glucose and smoking particles <sup>217–223</sup>. All of these factors directly or indirectly activate the endothelium resulting in impaired

vascular relaxation, increased leukocyte adhesion, increased endothelial permeability and formation of pro-thrombotic state <sup>220</sup>.

Upon activation, endothelial cells express various selective adhesion molecules on their surface to bind various types of leukocytes. These include L-, P- and E-selectins (SEL), intercellular adhesion molecules (ICAMs), platelet endothelial cellular adhesion molecules (PECAMs) and vascular cell adhesion molecule-1 (VCAM-1) <sup>224</sup>, which is one of the key molecules that mediates monocyte adhesion to the endothelial cells. VCAM-1 and ICAM-1 can also be cleaved from the cell surface by proteolytic enzymes (e.g. matrix metalloproteases (MMPs)) and released into the circulation as soluble forms (e.g. sVCAM-1, sICAM-1, sSEL) where they mediate recruitment of lymphocytes, monocytes and neutrophils to the activated endothelial cells <sup>224-226</sup>. ICAM-1 deficiency reduces atherosclerotic lesions in double-knockout mice (ApoE(-/-)/ICAM-1(-/-)) <sup>227</sup>, emphasising the importance of regulation of adhesion molecules. Collectively, sSEL, sICAM-1 and sVCAM-1 are important plasma biomarkers for endothelial dysfunction to predict future death from CVD and have been extensively investigated as target molecules of flavonoids <sup>105, 106</sup>.

In the last decade, evidence suggests that some flavonoids and metabolites exert potential health effects in CVD by decreasing the expression of SEL, ICAM-1 and VCAM-1 and their soluble forms <sup>66, 107, 108</sup>. Our lab has previously demonstrated that commonly consumed parent flavonoids inhibit VCAM-1 secretion in CD40L-stimulated HUVECs (human umbilical vein endothelial cells). In this study, 0.1-10  $\mu$ M cyanidin-3-glucoside (C3G) reduced VCAM-1 protein expression <sup>18</sup>. Furthermore, orientin and isoorientin (40  $\mu$ M) down-regulate ICAM-1, VCAM-1 and E-selectin mRNA and protein expression in LPS-induced HUVECs <sup>232</sup>. Apigenin (25  $\mu$ M) down-regulated ICAM1 and VCAM1 gene expression in LPS-stimulated mouse J774A.1 macrophages <sup>231</sup>.

Moreover, flavonoids and their gut metabolites decrease ICAM and VCAM expression and the adhesion of monocytes to HUVECs. Previous research from our lab has used physiologically achievable concentrations of six

parent flavonoids and fourteen conjugated metabolites/unconjugated phenolic acid metabolites to investigate the effect on protein and mRNA expression of ICAM-1 and VCAM-1 in HUVECs in response to TNF- $\alpha$ . Of all 20 compounds, protocatechuic acid (PCA) (1-100  $\mu$ M), PCA -3-O-sulphate (PCA3S) and isovanillic acid (IVA) (10-100  $\mu$ M), PCA-4-O-sulphate (PCA4S) and IVA-3-glucoside (IVA3G) (100  $\mu$ M) reduced sVCAM-1 protein expression and no significant effect on VCAM-1 mRNA expression was observed <sup>47</sup>. These results were consistent with previous findings from our lab where PCA, PCA-4-O-sulfate (PCA4S), phloroglucinaldehyde (PGA), IVA, ferulic acid (FA) and vanillic acid (VA) at 0.1-10  $\mu$ M reduced VCAM-1 secretion in CD40L-stimulated HUVECs <sup>18</sup>. Furthermore, PCA has been reported to inhibit monocyte adhesion to MAECs (mouse aortic endothelial cells) at 20-40  $\mu$ M and attenuate TNF- $\alpha$ -stimulated VCAM-1 and ICAM-1 expression <sup>233</sup>.

Others have reported that flavonoid (-)-epicatechin (EC) and its metabolites (EC-4'-sulfate (EC4'S), 4'-O-methyl-EC (4'MEC), EC-7- $\beta$ -D-glucuronide (EC7G), 4'-O-methyl-EC-7- $\beta$ -D-glucuronide (4'MEC7G)) at physiological concentrations (0.2-2  $\mu$ M) significantly reduced U937 monocyte (U937) adhesion to HUVECs <sup>51</sup>. Furthermore, the anthocyanins C3G, C-3-galactoside (C3Gal), C-3-arababinoside (C3Arab), delphinidin 3-O-glucoside (D3G), peonidin 3-O-glucoside (P3G) and their metabolites PCA, VA, FA and hippuric acid (HA) at physiologically-relevant concentrations (0.1-2  $\mu$ M) decreased the adhesion of monocytes (THP-1) to HUVECs. A trend toward decreased ICAM-1 VCAM-1 and SEL expression was observed <sup>46</sup>. There was no change in gene expression with these metabolites. Hence, these anthocyanins and their metabolites may have other cellular targets to reduce monocyte adhesion to endothelial cells.

In conclusion both conjugated and unconjugated metabolites at physiologically relevant concentrations reduce the adhesion of monocytes and the secretion of sSEL, sICAM-1 and sVCAM-1 in endothelial cells. Since there was no significant effect on mRNA expression at physiological concentrations, this indicates that the mechanism of action is likely to be

post-transcriptional. One of the post-translational regulators of ICAM-1 and VCAM-1 is MMP-9, which cleaves these molecules from the cell surface, releasing them into the circulation <sup>234</sup>.

In all stages of atherosclerosis, inflammation plays a key role and is orchestrated by a range of pro-inflammatory mediators including cytokines which are divided into several classes e.g. interleukins (IL), chemokines and interferons (IFN) and TNF- $\alpha$  <sup>222</sup>.

All cytokines and adhesion molecules are tightly controlled by various intracellular signalling proteins. One of the major regulators of pro-inflammatory cytokine and adhesion molecule expression is the transcription factor NF- $\kappa$ B (nuclear factor kappa-light-chain-enhancer of activated B cells), Section 1.9.1 describes in more detail the key regulators in vascular inflammation and summarises the impact of flavonoids on these regulators. NF- $\kappa$ B activity is counter regulated by Nrf2 (nuclear factor erythroid 2-related factor 2), a central transcription factor upregulating anti-inflammatory and detoxifying enzymes. Nrf2 is described in more detail in section 1.10.1.

## **1.8 Flavonoid intake and neurological disorders**

Neurological disorders encompass a broad range of diseases affecting the central and peripheral nervous systems including depression, Alzheimer's disease (AD) and other dementias, Parkinson's disease (PD), multiple sclerosis (MS) and cerebrovascular diseases (stroke, brain ischemia, migraine, and other headache disorders).

Worldwide, hundreds of millions of people are affected by neurological disorders <sup>28</sup> and the sum of burden to the individual, their families and carers, the wider society, health systems and the economy are tremendous. People with these conditions have the lowest health-related quality of life of any chronic disorders and an increased trend in deaths accounting 39% compared to 6% decrease in all-cause of deaths since 2001 <sup>30</sup>. Moreover, 35% deaths associated with neurological disorder are premature.

The causes of many neurological disorders are largely unknown but the neurological symptoms occur as a result of injury, infection or an immune response <sup>28</sup>.

Consumption of flavonoid-rich food, especially berries, tea, and chocolate has been linked to a reduced risk of cerebrovascular diseases i.e. stroke and ischemia, AD, depression, and improved cognitive functions. This assumption is greatly supported by evidence from epidemiological studies, RTCs and meta-data analyses.

### **Cerebrovascular disease**

Knekt (2002) <sup>31</sup> investigated the total dietary intake of flavonoids of 10,054 Danish men and women by assessing their dietary history. A lower incidence of cerebrovascular disease was associated with higher kaempferol, naringenin, and hesperetin intakes <sup>31</sup>. Dark chocolate is rich in cocoa flavonoids and a systematic review and dose-response meta-analysis revealed a small inverse association of increasing dose of

chocolate consumption (10 g/day daily increase) with reduced risk of stroke<sup>204</sup>. In a prospective cohort of Swedish men, high dark chocolate consumption was associated with lower risk of stroke<sup>235</sup>. Chocolate consumption of 37,103 participants was assessed based on a food-frequency questionnaire. Over 10.2 years, 1,995 total stroke incidents were recorded. The relative risk of stroke comparing the highest chocolate intake (median 62.9 g/wk) with the lowest quartile (median 0 g/wk) was 0.83 (95 % confidence interval [CI] 0.70–0.99). Furthermore, they conducted a meta-analysis of five studies, with 4,260 stroke cases and the overall relative risk of stroke for highest vs lowest category of chocolate intake was 0.81 (95 % CI 0.73–0.90) suggesting that moderate flavonoid-rich chocolate consumption may lower the risk of stroke. In another large prospective cohort study of Japanese men (38,182) and women (46,415), aged 44-76 y, a strong inverse association between chocolate consumption and risk of developing stroke was found only in women<sup>236</sup>.

### **Neurodegenerative disorders - AD & PD**

In the Framingham Offspring Cohort study, long-term flavonoid intake was associated with lower risk of developing AD and related dementias in US adults<sup>24</sup>. In this study 2801 participants (mean baseline age = 59.1 y; 52% females) were followed. Over 19 years, 193 AD-related dementias (ADRD) occurred of which 158 AD were registered. Participants with the highest (>60<sup>th</sup> percentile) intake of anthocyanins, flavonols, and flavonoid polymers had a lower risk of ADRD relative to lower intake (<15<sup>th</sup> percentile). In particular, higher intake of anthocyanins and flavonols was associated with lower risk of AD.

Habitual intake of specific flavonoids has also been linked to a reduced risk of developing PD<sup>237</sup>. In a study of combining cohorts of 80,336 women from the NHS and 49,218 men in the Health Professional Follow-up Study, the association of high intake of flavonoids from tea, berries, apples, red wine, and oranges/orange juice with the PD risk was examined. During 20-22 years of follow-up 805 (438 men and 367 women) participants developed

PD. No significant association was found in women while in men, participants in the highest quintile of total flavonoids had a 40% lower PD risk than those in the lowest quintile (hazard ratio [HR] = 0.60; 95% CI 0.43, 0.83;  $p = 0.001$ ). Further analysis showed a significant association of anthocyanin and berry intake with lower risk of PD.

### **Cognitive function**

Several human intervention studies have attempted to link a flavonoid-rich diet, especially berries, to improved cognitive function <sup>26,189,190,238</sup>. A crossover RCT study evaluated the effects of a mixture of berries on cognitive function during a 5-wk intervention. 40 healthy subjects between 50–70 years old (10 males, 30 females) were given daily either a mixed berry beverage (150 g blueberries, 50 g strawberry, 50 g elderberry, 50 g lingonberries, 50 g blackcurrant and 100 g tomatoes) or a control beverage and were subjected to cognitive tests including selective attention, psychomotor reaction time, and working memory capacity <sup>190</sup>. High intake of the berry mixture, rich in (poly)phenols, enhanced working memory relative to the control supplement but no effect was observed on selective attention or psychomotor reaction.

Dodd et al. <sup>26</sup> also examined the acute effect of blueberry consumption on the cognitive function of healthy older adults. In this RCT study, 18 healthy participants (8 men, 10 women), aged 60-75 years were randomly assigned to drink either a flavonoid-rich blueberry beverage (579 mg antho- and pro-cyanidins) or a placebo drink (a sugar matched control) on one visit and vice versa. Cognitive function was measured at baseline, 2 and 5 h post-consumption as well as blood pressure (BP), arterial stiffness and plasma-brain-derived neurotrophic factors (BDNF), measured at baseline and at 1-hour post-consumption. Relative to placebo, the blueberry drink significantly improved cognitive function at both post-intervention time-points and lowered systolic BP and decreased BDNF plasma concentration, suggesting that a single dose of flavonoid rich blueberry drink may improve

cerebrovascular function and positive interactions with cell signalling molecules involved in cognitive processes.

More evidence comes from a 12-wk intervention study (a randomised, placebo-controlled cross-over trial) where concord grape juice (CGJ) (containing 777 mg total (poly)phenols) improved cognitive function in 25 healthy mothers (aged 40-50 y) of preteen children. At baseline of 6-12 wk, mood, attention, executive function, and verbal and spatial memory were assessed. Relative to placebo, CGJ intake resulted in significant improvements in immediate and spatial memory and driving performance of participants, suggesting that long-term consumption of flavonoid-rich grape juice is not beneficial exclusively to adults with impaired mild cognitive function <sup>189</sup>.

## **Depression**

The relationship between flavonoid intake and depression is unclear. However, a limited number of studies have investigated the association between berry intake and depression in the young and adults <sup>185,186</sup>. A prospective cohort study followed 82,643 women without a previous history of depression at baseline from the NHS (aged 53–80 y) and the NHSII (aged 36–55 y) cohorts and calculated their total intake of flavonoids and subclasses (anthocyanin, procyanidins, flavonols, flavan-3-ols, flavones, flavanones and polymeric flavonoids) from food-frequency questionnaires, collected every 2-4 y. Physician- or clinician-diagnosed depression or antidepressant use was self-reported in response to periodic questionnaires and taken as criteria of depression. In total 10,752 depression incidences occurred during follow-up. An inverse association was observed between depression and flavonol, flavone and flavanone intake. In the NHS cohort, a 9-12% lower depression risk was observed with total flavonoids, proanthocyanidin and polymers intakes. Older women ( $\geq 65$ ) with higher intake of all flavonoid subclasses (except flavan-3-ol) had a significant lower risk of depression and strongest associations were observed with flavones



and procyanidins <sup>185</sup>. These findings suggest that higher flavonoid intakes may be inversely associated with lower risk of depression, especially in older women.

In a double-blind, placebo-controlled RCT with two parallel studies, acute wild blueberry (WBB) consumption was positively associated with mood in young children and young adults <sup>186</sup>. This study looked at the effect of blueberry drink 2h post consumption on impaired executive function (EF), which is linked to cognitive processes (e.g., rumination) that maintain low mood and depression. In one study 21 young adults (aged 18-21) consumed a blueberry drink (30 g freeze-dried WBB containing 253 mg anthocyanins dissolved in 30 mL orange squash and 220 mL water) or a matched placebo drink in a counterbalanced cross-over design. In another parallel study, 50 children (aged 7-10) were randomly assigned to a blueberry drink or a matched placebo. Mood was assessed using the Positive and Negative Affect Schedule at baseline and 2 h post-consumption of the drinks. In both studies, relative to placebo control, the blueberry intervention increased positive effects on mood.

From these studies, the plant compounds responsible for these improved effects on neurological function are unclear but likely are at least partly due to flavonoids and their metabolites since the foods chosen for these studies were rich in flavonoids and curcumin, quercetin, kaempferol, cyanidin, luteolin, catechin, epicatechin (EC), epigallocatechin (EGC) and epigallocatechin gallate (EGCG) and gallic acid (GA) have been reported to be beneficial in prevention of AD, PD, and depression <sup>239</sup>. Since neuroinflammation plays a major role in the pathogenesis of these disorders and flavonoids inhibit inflammation, the mechanism of action of flavonoids in these disorders is likely due to their interaction with signalling molecules that regulate inflammation.

### **1.8.1 Neuroinflammation and microglial cell activation**

Neuroinflammation is characterised as the inflammatory response within the brain or spinal cord and is mediated by reactive oxygen species (ROS), secondary messengers, cytokines and chemokines <sup>240</sup>. The neuroinflammatory response consequently affects biochemical, psychological, immune, and physiological response of the brain and body. However, there are different degrees of neuroinflammation with positive and negative aspects. Transient low-level inflammation has positive effects on neurological tissue including tissue repair, neuroprotection, enhanced plasticity, and reorganisation of host priorities. However, high-transient, and chronic low-to high-inflammation has negative effects including neuronal damage, cognitive impairment, reduced plasticity, anxiety, and depression.

The central nervous system (CNS) comprises several different types of cells including neurons, oligodendrocytes (communicating between neurons), pericytes (surrounding endothelial cells), astrocytes (communicating between neurons and blood vessels) and microglial cells (**Figure 1. 21**). Astrocytes and microglial cells are mainly involved in maintaining homeostasis of the CNS and in repairing brain injury <sup>241</sup>. Neuroinflammation is a major contributor to both age-related <sup>242,243</sup> and age-independent neurological disorders. The neuroinflammatory mediators are mainly produced by the microglial cells, astrocytes, endothelial cells, and peripherally derived immune cells in the CNS.

In age-dependent AD and PD <sup>243-245</sup> and in age-independent diseases such as stroke <sup>246</sup>, neuroinflammation plays a central role and is initiated by chronic microglial activation.

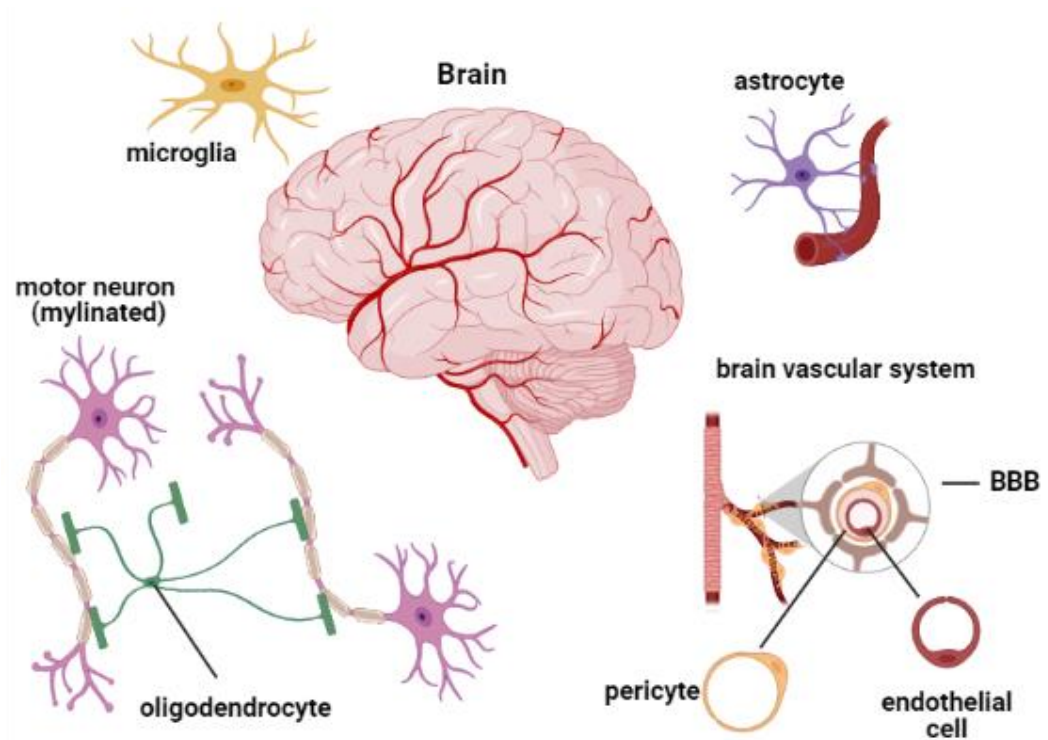


Figure 1. 21 The major cell types in the CNS. Microglial cells (resident macrophage-like cells, constantly monitoring microenvironment for damage to repair), oligodendrocytes (communicating between neurons), pericytes (surrounding endothelial cells), astrocytes (communicating between neurons and endothelia cells). BBB, blood brain barrier. Created in BioRender.com.

Microglial cells are myeloid lineage cells <sup>247</sup>, arising from the yolk sac during development <sup>247,248</sup> and act as residential macrophage-like immune cells in the CNS, representing 10% of the adult brain cell population. In contrast to other brain cells (neurons, astrocytes, oligodendrocytes), microglial cells are capable of rapid regeneration and repopulation from residual microglia after acute depletion <sup>249</sup>. They are involved in early brain development and later acquire a key role in the regulation of neuroinflammation and play a central role in neurological dysfunction and disease <sup>250</sup>.

Resting microglial cells constantly survey the brain environment and become activated upon signals from surrounding cells (**Figure 1. 22**). Depending on the signal, they either become pro-inflammatory (classical-activation, or M1 state) or anti-inflammatory (non-classical activation, or M2

state). Microglial cells acquire the M1 phenotype in response to IFN- $\gamma$ , GM-CSF or LPS, and M2 phenotype by IL-4 and IL-10 <sup>245</sup>. Classical activation leads to activation of transcription factors (TF) such as NF- $\kappa$ B, AP1, STAT1 and STAT5 leading to secretion of pro-inflammatory cytokines (TNF- $\alpha$ , IL-1 $\beta$ , IL-6, IL-12) and chemokines CCL2 and CXCL10 <sup>245</sup>. In turn, alternative activation leads to Nrf2, STAT3 and STAT6 TF activation and subsequent upregulation of several genes including IL-10 and TGF- $\beta$  <sup>245</sup>.

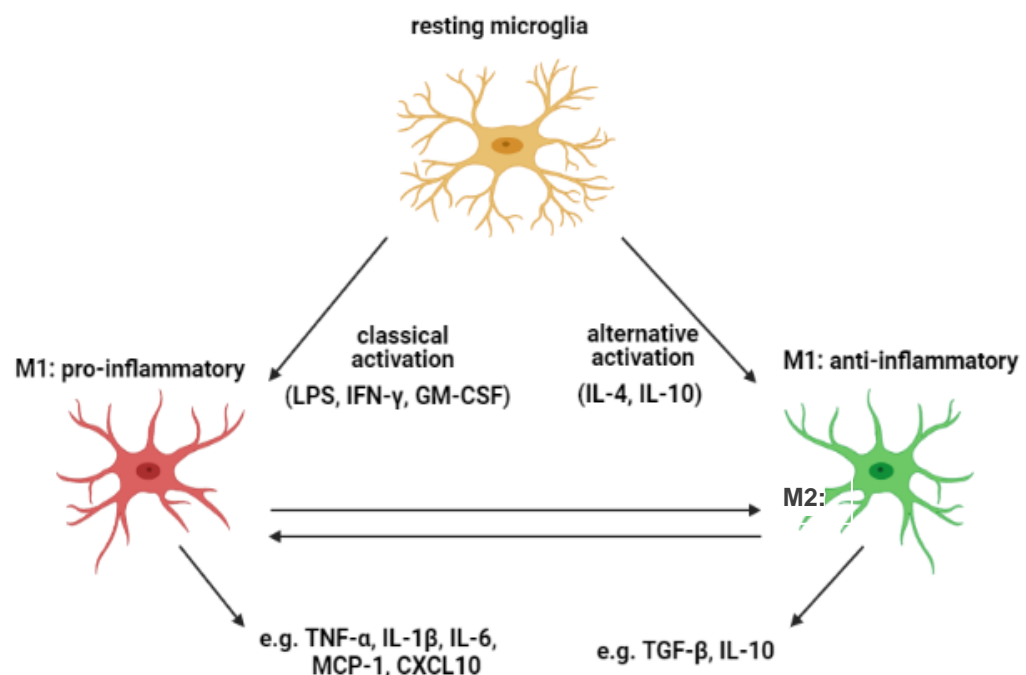


Figure 1. 22 Schematic overview of microglial activation. Resting microglial cells become activated by LPS, IFN- $\gamma$ , GM-CSF (classical activation) or by IL-4, IL-10 (alternative activation), resulting in M1 (pro-inflammatory) or M2 state (anti-inflammatory) respectively. Adapted from Subramaniam et al., 2017 and created in BioRender.com.

The role of microglial cells in neuroinflammation <sup>250</sup> and neurodegenerative diseases has become increasingly evident <sup>243,244,250</sup>. Although classically activated microglia are essential for primary immune responses in the brain, when the response becomes chronic, the resulting neuroinflammation damages the CNS tissue. Hence, diet derived natural compounds (nutraceuticals) with the potential to affect microglial activation are

promising candidates for promoting anti-inflammatory responses or inhibiting neuroinflammation and neurodegenerative conditions. Although high intake of flavonoids has been linked to a reduced risk of developing neurological disorders, their uptake and role in the brain remains elusive. Cell based assays are promising methods to discover the cellular mechanisms of flavonoids on microglial cells.

## **1.9 Mechanism of chronic inflammation and inflammatory biomarkers**

As previously discussed, chronic low-grade inflammation is the main underlying mechanism of cardio- and cerebro-vascular diseases and is orchestrated by a range of pro-inflammatory signalling molecules. Here, some of the main inflammatory biomarkers including TNF- $\alpha$ , IL-6, MCP-1 and their master regulator, the transcription factor NF- $\kappa$ B will be discussed.

### **1.9.1 NF- $\kappa$ B**

NF- $\kappa$ B is a master regulator of inflammation, controlling the transcription of more than 200 genes that are involved in cellular survival (e.g., cFLIP, BclXL, SOD) <sup>251</sup> and inflammation <sup>252</sup> (e.g. adhesion molecules, cytokines, chemokines, and matrix metalloproteinases). Hence, the activation of NF- $\kappa$ B has been associated with many chronic inflammatory diseases such as atherosclerosis <sup>216</sup>, rheumatoid arthritis (RA) <sup>253</sup>, inflammatory bowel disease (IBD) <sup>254</sup> and cerebrovascular diseases <sup>255</sup>.

NF- $\kappa$ B is activated in response to various stimuli through either a classical (canonical) pathway or an alternative pathway <sup>256</sup> (**Figure 1. 23** ) In the classical pathway, it is activated by cytokines (e.g. TNF- $\alpha$  or IL-1) or LPS (lipopolysaccharide) that binds to TLRs (toll like receptors), the antigen receptors TCR/BCR, RANK (receptor activator NF- $\kappa$ B) or lymphocyte coreceptors, CD30/CD40 <sup>257</sup>. Activation of the alternative pathway occurs through activation of certain TNF receptors e.g. CD40, L $\beta$ R (lymphotoxin  $\beta$  receptor) and the BAFF receptor <sup>257</sup>. NF- $\kappa$ B is a family with five members, p65 (RelA), RelB, p50, p52 and c-Rel, which exist as dimers <sup>252,258</sup>, and their activation depends on either the canonical or non-canonical pathway. For example, the canonical pathway induced by TNF- $\alpha$  or IL-1 usually activates RelA (p65)-containing dimers, whereas the non-canonical pathway usually activates RelB. which then translocate into nucleus <sup>259</sup>. NF- $\kappa$ B is

sequestered in the cytosol by I $\kappa$ B (inhibitor of kappa-B). This complex is phosphorylated by its upstream kinase, IKK (I $\kappa$ B kinase).

The IKK kinase complex, known as the core regulatory element of the NF- $\kappa$ B signalling pathway, can be activated by various upstream kinases thus plays a central role in the activation of NF- $\kappa$ B. The IKK kinase complex consists of two regulatory kinases, IKK $\alpha$  and  $\beta$ , and a modulatory subunit, IKK $\gamma$ /NEMO (NF- $\kappa$ B essential modulator) (**Figure 1. 23**). The IKK $\beta$  subunit regulates the activation of the I $\kappa$ B complex in the canonical pathway while the IKK $\alpha$ -subunit activates the alternative NF- $\kappa$ B pathway <sup>259</sup>. Upon phosphorylation I $\kappa$ B is ubiquitinated and targeted for proteasomal degradation, thereby releasing the NF- $\kappa$ B heterodimer to enter the nucleus <sup>259</sup> where it initiates transcription of numerous genes including adhesion molecules (ICAM, VCAM, selectins), cytokines (TNF- $\alpha$ , IL-1  $\alpha/\beta$ , IL-6) and chemokines (MCP-1, MIP-1, CXCL12) <sup>252</sup>.

Numerous flavonoids and their metabolites have been reported to inhibit NF- $\kappa$ B activation either directly or via upstream kinases. Wu et al. (2009) reported that rutin, luteolin, catechin, EGCG (epigallocatechin 3-O-gallate) and quercetin (20  $\mu$ M) stabilised I $\kappa$ B degradation in high glucose-induced THP-1 cells and consequently prevented NF- $\kappa$ B p65 translocation to the nucleus <sup>260</sup>. In addition, quercetin (15-60  $\mu$ M) and apigenin (6.25-25  $\mu$ M) both inhibited NF- $\kappa$ B binding to DNA in LPS-induced macrophages <sup>231,261</sup>. Moreover, C3G (cyanidin 3-O-glucoside) prevented NF- $\kappa$ B-p65 nuclear translocation by inhibiting I $\kappa$ B- $\alpha$  phosphorylation in LPS-induced RAW264.7 cells at 25  $\mu$ M <sup>262</sup>. Mounting evidence also suggests that phenolic acids, including protocatechuic acid <sup>110, 130</sup>, vanillic acid <sup>263</sup>, ferulic acid <sup>132, 151–153</sup>, caffeic acid and chlorogenic acid <sup>268</sup> prevent NF- $\kappa$ B activation thereby reducing the pro-inflammatory mediators TNF- $\alpha$ , IL-1 $\beta$ , ICAM-1 and VCAM-1 in RAW264 macrophages, RASMC, intestinal epithelial cells and HUVECs.

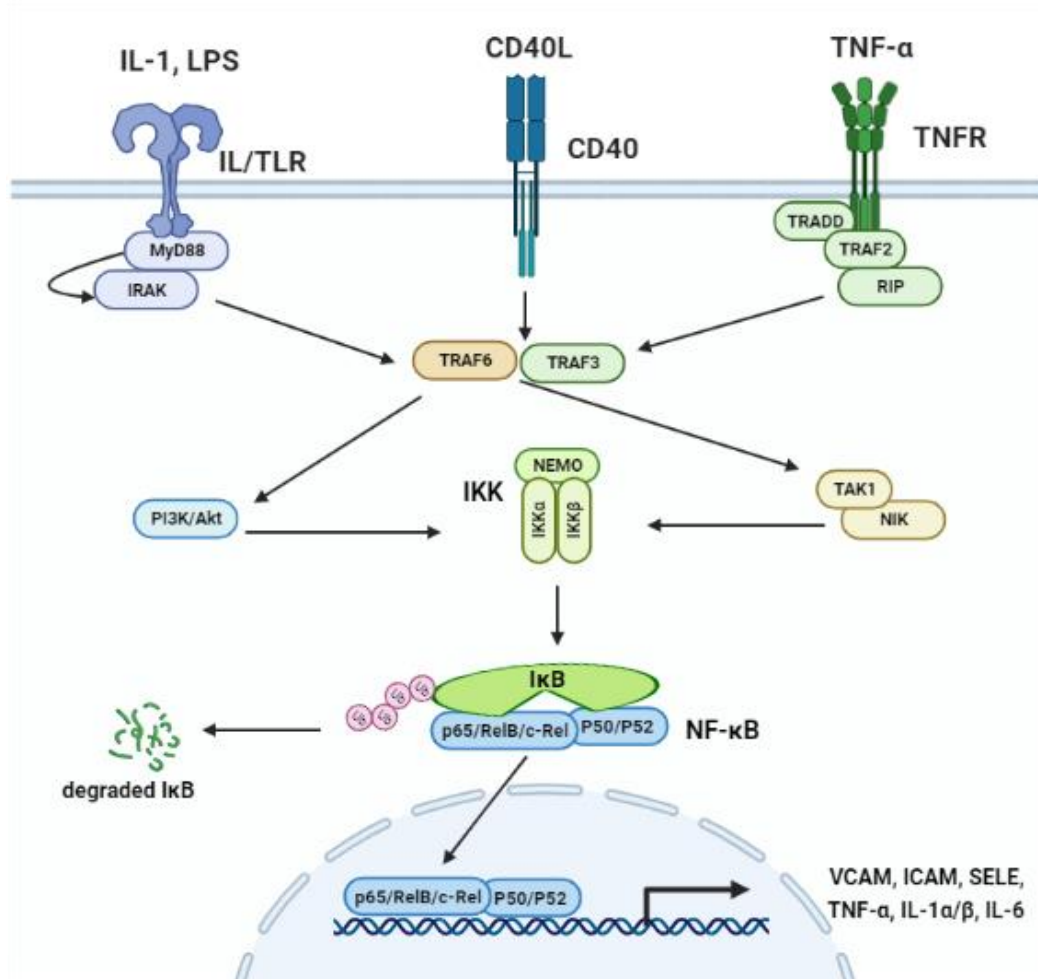


Figure 1. 23 The NF- $\kappa$ B signalling pathway. IL, Interleukin-1; LPS, lipopolysaccharide; TLR, Toll-like receptor; CD40L, Cluster of differentiation ligand 40; TNFR, TNF- $\alpha$  receptor; MyD88, Myeloid differentiation primary response gene 88; IRAK, Interleukin-1 receptor-associated kinase; TRADD, TNFR associated death domain; RIP1, receptor interacting protein 1; TRAF2, 3, 6, TNFR associated factor 2/3/6; TAK1, TFG $\beta$ -activated kinase 1; NIK, NF- $\kappa$ B-inducing kinase; PI3K, phosphoinositide 3-kinase; IKK, I $\kappa$ B kinase; I $\kappa$ B, inhibitor of kappa B; NF- $\kappa$ B, nuclear factor kappa-light-chain-enhancer of activated B cells. Created in BioRender.com.

However, not all studies have shown an inhibitory effect on the NF- $\kappa$ B signalling pathway. Recent studies from our lab and by others have provided evidence for post-translational regulation of cytokines and adhesion molecules by metabolites <sup>19,46,47</sup>. For example, quercetin at physiological concentration (10  $\mu$ M), does not inhibit LPS-induced NF- $\kappa$ B activation in THP-1 cells <sup>19</sup>. In some studies, metabolites of flavonoids have increased NF- $\kappa$ B activation. For example, 20-40  $\mu$ M C3G increased NF- $\kappa$ B nuclear translocation in TNF- $\alpha$ -induced HUVECs <sup>269</sup>. In addition,



epicatechin increased NF- $\kappa$ B (p65) nuclear translocation in HepG2 cells at a physiological concentration of 10  $\mu$ M, suggesting that flavonoids may have different mechanisms of action in different cell types and at different concentrations and further studies are required with physiologically achievable levels of metabolites.

### **1.9.2 TNF- $\alpha$**

TNF- $\alpha$  plays a central role in innate and adaptive immunity, cell proliferation, differentiation, migration, apoptosis, and survival<sup>251,270,271</sup>. In response to infection or in chronic inflammatory disorders, TNF- $\alpha$  is the primary cytokine to be released and a potent activator of the subsequent cascade of cytokines, chemokines, and proteases. Hence, control and regulation of TNF- $\alpha$  is highly important from a therapeutic viewpoint and has been widely investigated as a potential therapeutic target<sup>259,272</sup>. Currently on the market, there are 25 approved TNF- $\alpha$  blockers that inhibit or modulate the effects of TNF- $\alpha$ <sup>273</sup>. Five of these blockers are recombinant monoclonal antibodies including infliximab, adalimumab, golimumab, certolizumab and etanercept that neutralise the TNF- $\alpha$  activity. These blockers are approved by the European Medicines Agency (EMA) and Food and Drug Administration (FDA) for the treatment of RA, Ankylosing spondylitis, psoriasis, psoriatic arthritis, juvenile idiopathic arthritis, ulcerative colitis and Crohn's disease<sup>273</sup>. However, these drugs have several limitations, including loss of response in 30-50% of patients or various side effects, including an increased risk of serious infections<sup>273,274</sup>.

TNF- $\alpha$  is produced by a wide range of cells including immune cells such as monocytes, macrophages, resident macrophages including microglial cells<sup>268</sup>, mast cells<sup>275</sup>, T and B lymphocytes<sup>276</sup> and natural killer cells (NK)<sup>277</sup> and non-immune cells (fibroblasts and osteoclasts, smooth and cardiac muscle cells and endothelial cells)<sup>272,276</sup> in response to various stimuli e.g. LPS, ILs, CD40L, TNF- $\alpha$  itself, ox-LDL, macrophage colony-stimulating

factor (M-CSF) and granulocyte-monocyte colony-stimulating factor (GM-CSF) <sup>252,275,277,278</sup>.

TNF- $\alpha$  is tightly regulated by various mechanisms that operate at different stages i.e. gene transcription, mRNA turnover, translation and secretion <sup>253,279</sup>. At the transcriptional level, TNF- $\alpha$  gene expression is controlled by chromatin modification, co-regulators, and a network of various transcription factors including NF- $\kappa$ B, Egr-1, AP-1 and NFAT (nuclear factor of activated T cells) <sup>252,280</sup>.

At the post-translational level TNF- $\alpha$  mRNA is regulated by several mechanisms, including ARE-binding proteins <sup>281,282</sup>, micro RNA (miRNA) <sup>253</sup>, and p38 MAPK <sup>282,283</sup>. The first control checkpoint is ARE (Adenosine and Uridine-rich element) <sup>281,282</sup>, a destabilisation element is located at the 3' untranslated region of transcripts <sup>284</sup>, controlling TNF- $\alpha$  mRNA for its stability, transport (from nucleus to cytoplasm) and mediating initiation of its translation <sup>285</sup>. Thus, mRNAs with this element are not stable and have a short life. Another important mechanism at the post-transcriptional level is the regulation by micro RNA (miRNA) which can either trigger translational activation or suppression of mRNA <sup>283</sup>. For TNF- $\alpha$  mRNA inhibition, a few miRNA have been identified e.g. miR-369-3p, miR-16, miR-125b and miR-155 <sup>253</sup>. miR-125b directly targets TNF- $\alpha$  mRNA and decreases its transcription. In contrast, miR-155 enhances TNF- $\alpha$  translation by directly interfering with the transcripts of several upstream proteins, including FADD, IKK $\epsilon$ , and RIPK1 that are involved in LPS signalling pathways <sup>286</sup>. Interestingly, neutrophil microvesicles have recently been reported to mediate atherosclerosis by delivering miR-155 to atheroprone endothelial cells <sup>287</sup>.

Following post-transcriptional modification, TNF- $\alpha$  is translated into a 26 kDa pro-TNF- $\alpha$  and transported to the cell membrane. The extracellular part of TNF- $\alpha$  can be cleaved by numerous proteases such as MMPs (1-3, 7, 9, 12, 14, and 17, ADAM17). A disintegrin and metalloprotease 17 (ADAM-17), also called TNF- $\alpha$  converting enzyme (TACE) is a well-known TNF- $\alpha$  sheddase. TACE cleaves the membrane-bound TNF- $\alpha$  in response to

stimulation with various molecules e.g. reactive oxygen species (ROS) <sup>253</sup>. Cleavage by TACE produces a 17 kDa soluble form, which circulates in the serum. TACE has a broad range of substrates including the adhesion molecules L-SEL, ICAM-1, VCAM-1 and the receptors IL-6R, EPCR and TNFR <sup>288,289</sup>. Cleavage of the TNF- $\alpha$  and IL-6 receptors results in their soluble forms, which can act as decoy receptors to neutralise the bioactivity of these pro-inflammatory cytokines.

As a master regulator of chronic inflammation, TNF- $\alpha$  has been frequently investigated in flavonoid and phenolic acid studies. Chang et al., (2013) <sup>261</sup> reported that quercetin (30  $\mu$ M) inhibits LPS (100 ng/mL)-induced TNF- $\alpha$  and IL-1 $\beta$  gene and protein expression via IKK, Akt and JNK signalling pathways in murine macrophages (RAW264.7). In high-glucose-induced THP-1 cells, quercetin, catechin, rutin, luteolin and EGCG at 20  $\mu$ M inhibit TNF- $\alpha$  secretion via p65 NF- $\kappa$ B pathway by I $\kappa$ B $\alpha$  stabilisation <sup>260</sup>. EGCG has also been reported by others to attenuate TNF- $\alpha$  expression at 25-100  $\mu$ M but has no effect at 6.25-12.5  $\mu$ M in LPS-(250 ng/mL)-induced HREC (Human Retinal Endothelial cells) <sup>290</sup>.

Although at supraphysiological concentrations these flavonoids have been shown to be active, they show either no or a low effect at physiological levels (0.2-10  $\mu$ M). For instance, orientin reduced TNF- $\alpha$  levels moderately at 5-10  $\mu$ M and at 20-40  $\mu$ M together with isoorientin dose-dependently markedly reduced levels <sup>232</sup>. Our lab has previously investigated the effects of anthocyanins and their metabolites at 1  $\mu$ M on TNF- $\alpha$ , IL-1 $\beta$  and IL-10 secretion in LPS-stimulated THP-1 cells. Metabolites showed more bioactivity at physiological concentrations than their parent compounds <sup>19</sup>, however the effect was protein specific. No effect on TNF- $\alpha$  mRNA levels was seen, suggesting that the regulatory mechanism of action might be post-translational, possibly involving TACE <sup>19</sup>. Moreover, the flavonoids rutin, orientin, and isoorientin have been reported to inhibit TACE expression and activity <sup>232,291</sup>.

### 1.9.3 TNF- $\alpha$ receptor TNFR1 & TNFR2

Under physiological conditions, both the soluble form and membrane-bound TNF- $\alpha$  assemble as homo-trimers and bind to the extracellular domain of either of two types of TNF- $\alpha$  receptors (TNFR1 and TNFR2)<sup>292</sup>, followed by trimerisation of the receptor (**Figure 1. 24**). The membrane-bound form activates both TNFR1 and TNFR2. Conversely, the soluble form almost exclusively activates TNFR1<sup>293</sup> and is assumed to be the most active form<sup>253,294</sup> suggesting that controlling the soluble ligand is important for controlling its role in inflammation. Various cell types ubiquitously express TNFR1, which is mainly involved in pro-inflammatory and apoptotic pathways that are associated with tissue injury<sup>271</sup>. In contrast, TNFR2 has been shown to be involved in cell signalling that promotes angiogenesis and tissue repair<sup>253</sup> and is expressed at low levels and only on specific cell types, including immune cells, endothelial cells, cardiac myocytes, and selective subtypes of neurons (microglia, astrocytes, oligodendrocytes)<sup>259,293,295</sup>. Although both receptors play different roles, there is cross-talk between them, facilitated by TRAF2, allowing the two receptors to interact and modulate each other's signalling pathways<sup>295</sup>, therefore it is important to understand the signalling pathways of both receptors.

Upon TNF- $\alpha$  reception, TNFR1 is activated and via its intracellular death domain (DD) recruits the core adaptor protein TRADD (TNFR associated death domain), which assembles with RIP1 (receptor interacting protein 1), TRAF-2 (TNFR associated factor 2), cIAP1 and cIAP2 (inhibitor of apoptosis protein 1 and 2) to form complex I (**Figure 1. 24**)<sup>259</sup>. This initial complex transduces the signal further to activate several pathways including NF- $\kappa$ B and several kinase pathways including JNK, p38, ERK (extracellular signal-related kinase) and PI3K (phosphoinositide 3-kinase) pathways, leading to pro-inflammatory gene transcription<sup>292,296</sup>.

In contrast to TNFR1, TNFR2 does not include a death domain and is only activated by membrane-bound TNF- $\alpha$ <sup>259</sup>. Activation of TNFR2 leads to recruitment of TRAF2 which recruits TRAF1 and cIAP1/2. This complex activates NF- $\kappa$ B by at least three different pathways, either through direct

activation of the IKK complex, TRAF3/NIK-mediated IKK $\alpha$  phosphorylation and activation of the PI3K/Akt (Akt also known as PKB, Protein kinase B) signalling pathway. Furthermore, this complex can activate non-apoptotic signalling through p38 MAPK and the MEKK1/JNKK1/JNK signalling pathways <sup>259</sup>.

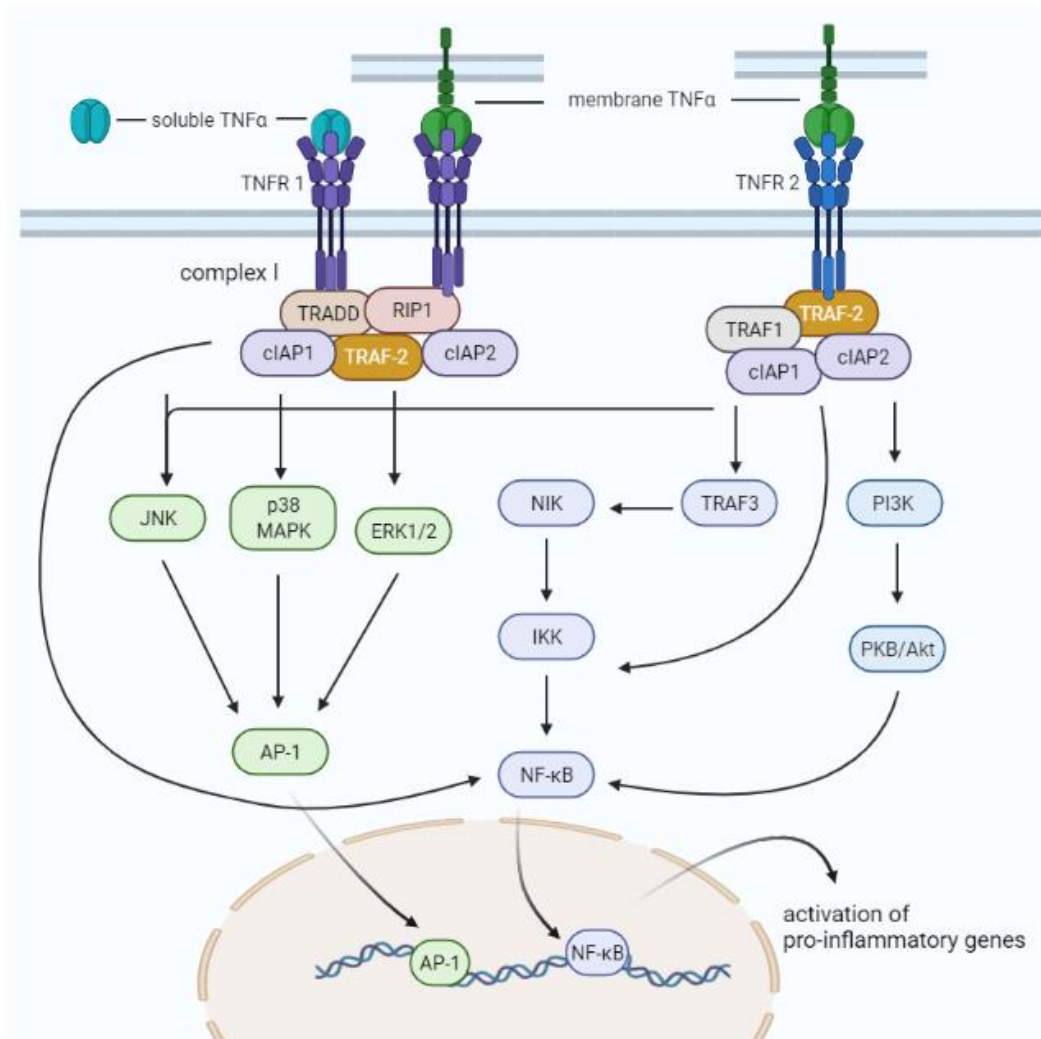


Figure 1. 24 The TNF- $\alpha$  signalling pathway. TNFR1/TNFR2, TNF- $\alpha$  receptor 1/2; NIK, NF- $\kappa$ B-inducing kinase; TRADD, TNFR associated death domain; RIP1, receptor interacting protein 1; TRAF1,2, 3, TNFR associated factor 1/2/3; PI3K, phosphoinositide 3-kinase; JNK, c-Jun N-terminal kinases; ERK, extracellular signal-related kinase; IKK, I $\kappa$ B kinase; I $\kappa$ B, inhibitor of kappa B; NF- $\kappa$ B, nuclear factor kappa-light-chain-enhancer of activated B cells; AP1, Activator protein 1. Created in BioRender.com.

Flavonoids may affect TNF- $\alpha$  activity via a largely unknown pathway. Therefore, TNF- $\alpha$  and its upstream regulators are the most widely studied molecules as targets for flavonoids. The majority of investigated flavonoids and their metabolites reduce TNF- $\alpha$  secretion in response to various stimuli, including LPS, high glucose and PMA (Phorbol 12-myristate 13-acetate) <sup>19,231,260–263,265,266,291</sup>.

Reports on the mechanisms by which flavonoids inhibit TNF- $\alpha$  secretion are conflicting. For example Wu et al. (2009), demonstrated that 20  $\mu$ M quercetin reduced the secretion of TNF- $\alpha$  and IL-1 $\beta$  in high glucose-stimulated THP-1 cells <sup>260</sup> and a concomitant inhibition of p65 NF- $\kappa$ B nuclear translocation through stabilised I $\kappa$ B degradation and inhibition of PKC, p38 and ERK1/2 MAP kinases. However, Chang et al. (2013) reported that quercetin (at 15-60  $\mu$ M) decreased TNF- $\alpha$  and IL-1 $\beta$  protein and gene expression through suppression of Akt/JNK and NF- $\kappa$ B activation, rather than p38 and ERK, in LPS-induced RAW264.7 macrophages <sup>261</sup>.

In studies of flavonoid metabolites, Min et al., (2010) demonstrated that 25  $\mu$ M C3G and its metabolite, PCA, inhibited IL-1 $\beta$  and TNF- $\alpha$  secretion through attenuation of p65 NF- $\kappa$ B nuclear translocation by inhibition of I $\kappa$ B $\alpha$ , and inhibition of p38, ERK and JNK MAP kinases in LPS-induced RAW264.7 cells <sup>262</sup>. Moreover, Kim et al (2011) reported that vanillic acid at 10-100  $\mu$ M reduced TNF- $\alpha$  and IL-6 secretion and inhibited NF- $\kappa$ B activation via I $\kappa$ B- $\alpha$  degradation, and caspase-1 activation in LPS-stimulated macrophages <sup>263</sup>. To conclude, flavonoids or their metabolites may have different mechanisms of action in different cell types and/or under different conditions (LPS vs high glucose). Further research is needed to investigate physiological concentrations of metabolites in relevant cell types such as human immune and endothelial cells.

### 1.9.4 The IL-1 and TLR4 signalling pathways

The IL (Interleukin) cytokine family plays a central role in inflammation and innate immunity. This family has 11 members including IL-1 $\alpha/\beta$ , IL-2, IL-6, IL-12, IL-15, IL-17, IL-18, and IL-33, among which the IL-1 $\beta$  and IL-18 ligands and the IL-1RI receptor are well characterised. IL-1 $\beta$  stimulates multiple genes involved in inflammation, vasodilation and hypotension e.g. cytokines, COX-2 (cyclooxygenase type 2), PLA<sub>2</sub> (phospholipase A type 2), and iNOS (inducible nitric oxide synthase) involved in NO (nitric oxide) production <sup>297</sup>. Moreover, IL-1 $\beta$  also stimulates ICAM-1 and VCAM-1 secretion.

Usually, IL-1 $\beta$  secretion can be auto-activated through the IL-1RI and IL-1RAcP heterodimer that possess TIR (Toll IL-1 receptor) domains. Receptor dimerisation recruits MyD88 (myeloid differentiation primary response gene 88) followed by a kinase signalling cascade and gene transcription (**Figure 1. 23**). The IL-1 $\beta$  precursor is translated in the cytosol and further transferred into secretory lysosomes where it is cleaved by activated caspase-1 and released into the extracellular matrix. Caspase-1 also cleaves IL-18 and IL-33 <sup>297</sup>. IL-18 is an essential co-activator of IL-2, IL-12, and IL-15, inducing IFN- $\gamma$  activation, which plays a role in viral and microbial infection <sup>298</sup>. In contrast, IL-33 has both pro-and anti-inflammatory effects in atherosclerosis <sup>299</sup>. IL-17A (interleukin-17A) is a key cytokine of T helper 17 (TH17) cells that are involved in tissue inflammatory response. The binding of IL-17A to its receptor IL-17RA leads to activation of NF- $\kappa$ B <sup>300</sup>.

Interleukin members share a highly homologous cytoplasmic domain with TLRs (toll like receptors) <sup>297</sup>. TLRs are expressed on various immune cells and are an integral part of the innate immune system by recognising microorganism derived pathogen associated molecular patterns (PAMPs) <sup>301</sup>. However, in the absence of infections they are involved in the response to endogenous stimuli during tissue injury and chronic inflammation <sup>256</sup>. TLR4 is one of these receptors that plays an important role in inflammation and is classically stimulated by the gram-negative bacterial cell wall

component, LPS. This leads to upregulation of pro-inflammatory mediators such as TNF- $\alpha$ , IL-1 $\alpha/\beta$ , IL-6 (**Figure 1. 23**)<sup>302</sup>.

In general, TLR4 activation is facilitated by LBP (LPS binding protein), CD14, a cell surface molecule, and MD2 (myeloid differentiation protein 2), an adapter protein. LBP is a soluble shuttle protein that is ubiquitously present in the serum at low levels and binds to LPS<sup>303</sup>. Upon exposure to bacteria, the level of LBP acutely increases in response to pro-inflammatory cytokines such as IL-1, IL-6 and TNF- $\alpha$  to enhance the inflammatory response<sup>304</sup>. LBP facilitates LPS assembly with CD14, which further facilitates the transfer of LPS to the TLR4 and MD2 receptor complex. This complex transfers the signal either through a MyD88-dependent or independent pathway<sup>302</sup>. The MyD88-dependent pathway involves recruitment of TRAF6 (TNF-receptor associated factor 6) and IRAKs (IL-1 receptor-associated kinases) (**Figure 1. 23**). This recruitment leads to TRAF6 self-ubiquitination and oligomerisation. Ubiquitination of TRAF6 leads to recruitment of TAB1, TAB3 (transforming growth factor beta (TFG $\beta$ )-activated kinase 1 and 3) and TAK1 (TFG $\beta$ )-activated kinase 1) to the complex, leading to TAK1 activation which in turn initiates phosphorylation of the IKK complex and ultimately activation of NF- $\kappa$ B.

TLR4 and its downstream signalling molecules have been widely investigated as promising therapeutic targets due to their role in sepsis and other inflammatory-mediated disorders such as ischemia/reperfusion injury and rheumatoid arthritis<sup>305</sup>. Hence, several drugs have been introduced to inhibit TLR4 and its associated molecule MD2<sup>146,147</sup>. Moreover, some small molecules with a phenolic ring have been shown to inhibit the TLR4 signalling pathway. For example, resatorvid (TAK-242), a small molecule with two phenolic rings, selectively binds to extracellular domain of TLR4 and interferes with interactions between TLR4 and its adaptor molecule<sup>307</sup>.

It seems reasonable to think that since flavonoids and their metabolites are small molecules with phenolic rings, they may be promising anti-inflammatory therapeutic agents. To our knowledge, only a few studies have reported that flavonoids exert their anti-inflammatory effects by



inhibiting pro-inflammatory receptors. The flavones orientin and isoorientin inhibited LPS-induced TLR4 expression in HUVECs at 40  $\mu\text{M}$  <sup>232</sup>. More recently, cyanidin inhibited IL-17A and alleviated inflammation in vivo <sup>308</sup>. In this study, Liu et al (2017) used a structure-based search through computer-aided, docking-based virtual screening for small molecules that inhibit IL-17A. Cyanidin specifically recognized an IL-17A binding site in the IL-17A receptor subunit and inhibited the IL-17A/IL-17RA interaction, perhaps competing with pro-inflammatory receptor ligands or directly blocking receptors by flavonoids and their metabolites. This process deserves more attention and needs to be further investigated.

### **1.9.5 IL-6**

IL-6 is another major cytokine with a unique pleiotropic function, being both pro- and anti-inflammatory. It is involved in a variety of physiological events including cell proliferation, differentiation, survival, and apoptosis <sup>309</sup>. Moreover, IL-6 plays key roles in the immune and haematopoietic system, cardiovascular and nervous system, the placenta and endocrine system and liver and bone metabolism <sup>309–312</sup>.

Dysregulation of IL-6 underlies the pathology of numerous diseases including IBD <sup>313</sup>, RA and Castleman's disease <sup>314</sup>, renal diseases <sup>315</sup>, CVD <sup>311,316</sup> and neuroinflammation <sup>310,317,318</sup>. IL-6 was originally identified as B-cell differentiation factor that matures B-cells into antibody-producing cells in the mid-80s <sup>319</sup>. Since then, IL-6 has been intently studied. IL-6 is produced in a wide variety of tissues and cells, including immune cells (T- and B-cells, monocytes/macrophages, and microglia), endothelial cells and vascular smooth muscle cells, fibroblasts, liver, muscle adipocytes, neurons, and astrocytes <sup>309–311,318</sup>. IL-6 is induced in response to different stimuli including TNF- $\alpha$ , IFN $\gamma$ , IL-1 $\beta$ , CD40L, oxLDL, platelet derived growth factor (PDGF), PAMPS such as LPS, and viral infection <sup>309,310,316,320,321</sup>.

## IL-6 Receptor and signal transduction

In contrast to the IL-6 protein, its receptor IL-6 (IL-6R) is only expressed on certain cells including epithelial cells and hepatocytes<sup>322</sup> and some immune cells (microglia<sup>323,324</sup>, monocytes/macrophages, neutrophils and some lymphocytes) but not on endothelial cells<sup>325</sup> or on other neuroglial cells<sup>318</sup>. In addition, IL-6R can exist as a soluble form either by alternative splicing<sup>326</sup> or, as previously mentioned, by enzymatic cleave of TACE<sup>288</sup>.

IL-6 signalling is transduced either via a classical pathway or trans-signalling pathway<sup>327,328</sup>. Classical signalling occurs through membrane bound IL-6R which upregulates pro-inflammatory gene (such as ICAM, VCAM) transcription via several pathways and is involved in acute immune responses against pathogens. In contrast, trans-signalling only occurs by sIL-6R that acts on cells lacking IL-6R (illustrated in **Figure 1. 25**).

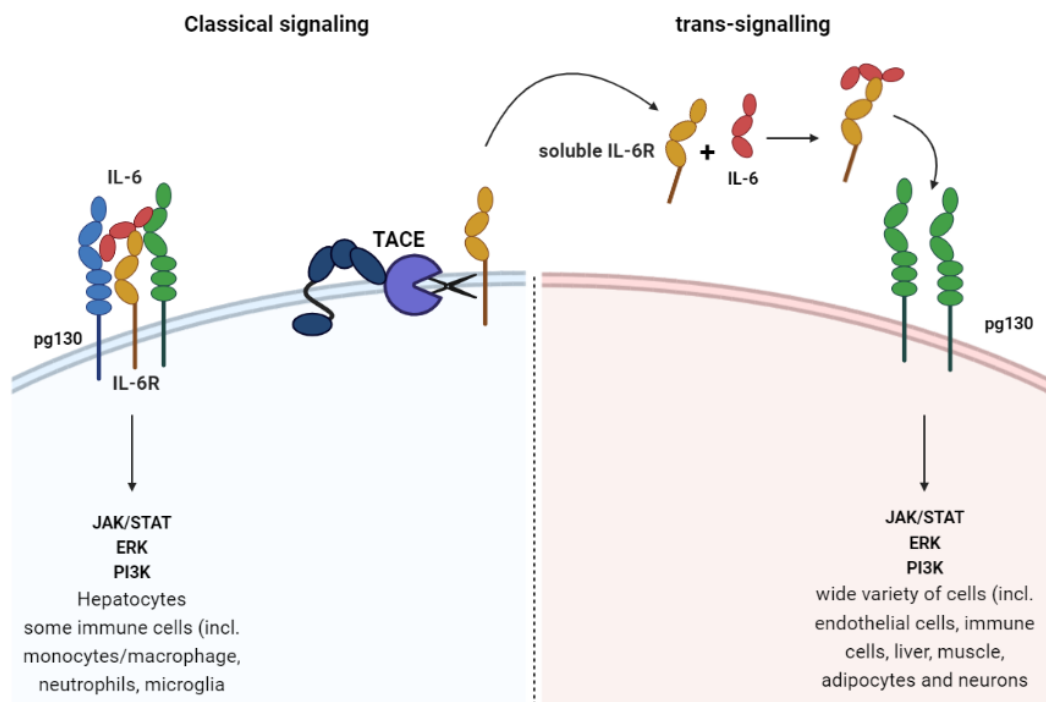


Figure 1. 25 Overview of IL-6 signalling. In classical signalling binding of IL-6 to IL-6 receptor (IL-6) activates gp130 which transduce down-stream signalling via JAK/STAT signalling in restricted cell types. Cleavage by TACE liberates IL-6R which can bind to IL-6 and activates distal cells that lacking IL-6R. Adapted from Rothaug et al., 2016 and created in BioRender.com.

Trans-signalling has been reported to amplify pro-inflammatory cytokines including MCP-1, IL-6, IL-8, and PAI-1 production in endothelial cells <sup>325</sup>. The sIL-6R can be detected in various bodily fluids and at sites of inflammation. Hence trans-signalling is postulated to promote transition from acute to chronic inflammation, and therefore plays an important role in inflammatory disorders.

The signal transduction of both the classical and alternative pathway is mediated by the cell surface glycoprotein 130 (gp130) <sup>314</sup> which interacts with homodimers of IL-6R and IL-6, forming hexamers (2 of each of these molecules).

The intracellular domain of gp130 has a binding site for Janus kinase (JAK), Src homology domain 2-containing tyrosine phosphatase 1-2 (SHP1/2) and STAT1-6 (Signal Transducer and Activator of Transcription 1-6) <sup>309,314</sup>. JAK kinases are constitutively associated with gp130 while STAT and SHP is recruited to the activated gp130 <sup>309</sup>.

Activation of the hexamer complex leads to transcription of inflammatory genes via several downstream signalling pathways, including JAK/STAT3, JAK/Akt/STAT3, JAK/PI3K/NF- $\kappa$ B, SHP2/MAPK/NF- $\kappa$ B, SHP1/ERK TF, and PI3K pathway, leading to the activation of inflammatory target genes. Alternatively, IL-6 signalling can also occur via the SHP2/ERK pathway <sup>310</sup>.

IL-6 signalling via JAK/STAT3 <sup>325</sup> is predominantly anti-inflammatory <sup>316</sup> and is involved in growth arrest and differentiation <sup>309</sup>. In contrast, signalling via SHP2/MAPK/NF- $\kappa$ B <sup>309,321</sup> or JAK/STAT1 <sup>316</sup> is pro-inflammatory leading to transcription of chemokines and adhesion molecules. Moreover, STAT1 crosstalk with the STAT3 pathway via SOCs suppresses STAT3 <sup>316</sup>, hence STAT1 plays an important role in IL-6-induced inflammation.

## IL-6 protein production is under several TFs

The human IL-6 gene promoter includes an AP-1 site, an NF- $\kappa$ B site, and a multiple response element, c-fos serum-responsive element (SRE) homolog which includes the c-fos retinoblastoma control element (RCE) and cyclic AMP-responsive element (CREB) together with a nuclear factor for IL-6 expression (NF-IL6, aka the CCAAT/enhancer binding protein binding site (CEBP $\beta$ ), flanked by two glucocorticoid responsive elements (GRE) and two TATA boxes (**Figure 1. 26**)<sup>309,329</sup>.

As described above, NF- $\kappa$ B is involved in transcription of pro-inflammatory genes, especially TNF- $\alpha$ , MCP-1 and IL-6. Likewise, AP-1 is a dimeric transcription factor consisting of c-fos and c-jun which can form homodimers or heterodimers. Both AP-1 and SRE share a high degree of sequence similarity and c-jun:c-jun or c-jun:c-Fos can bind to both sites<sup>330</sup>.

NF-IL6 activation is regulated in several ways through its phosphorylation at different sites. More importantly, NF-IL6 co-operates with NF- $\kappa$ B and AP-1, playing a synergistic role in IL-6 gene expression<sup>329</sup>. Interestingly, NF-IL6 also has an affinity to bind to the regulatory regions of several other cytokine genes such as TNF- $\alpha$ , and IL-8<sup>331</sup>, implying that NF-IL6 has a wider role in the inflammatory response.

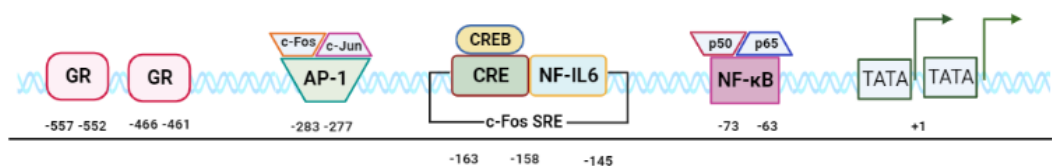


Figure 1. 26 The human IL-6 gene promoter with approximate binding sites for transcription regulator elements and trans-regulatory factors. Adapted from Luo et al., 2016 and created in BioRender.com.

Several negative regulators suppress IL-6 gene expression. For example, steroid hormones suppress gene expression via binding to GREs, suppressing AP-1 and NF- $\kappa$ B activity <sup>329</sup>, while the tumor suppressors p53 and retinoblastoma proteins suppress IL-6 promoter activity at the region of -221 to +13 bp <sup>309</sup>.

High plasma levels of soluble IL-6 are associated with an increased CVD risk and atherosclerosis <sup>311</sup> and high expression levels are also associated with neuroinflammation <sup>310</sup>. Early studies reported that anthocyanins protect vascular endothelial cells from ox-LDL-induced oxidative stress injury <sup>332</sup> and inhibited CD40L-induced secretion of IL-6, IL-8 and MCP-1 via TRAF2-NF- $\kappa$ B <sup>333</sup>. Furthermore, anthocyanins and their metabolites including phenolic acids inhibit IL-6 expression induced by CD40L <sup>334</sup> and oxLDL <sup>18</sup> at physiologically relevant concentrations of 0.01-10  $\mu$ M in endothelial cells. It is important to note that phenolic acids were more bioactive at lower concentrations compared to their parent anthocyanins. Moreover, IL-6 expression was inhibited by apigenin in LPS-induced THP-1-derived and murine macrophages via ERK1/2 <sup>231</sup> and by orientin and isoorientin in LPS-induced human endothelial cells via ERK1/2-NF- $\kappa$ B <sup>232</sup>. Furthermore, PCA suppressed expression of LPS-induced IL-6 via activating PPAR- $\gamma$  pathway and suppressing NF- $\kappa$ B in human gingival fibroblasts <sup>335</sup>. A synthetic hybrid of ferulic-acid-caffeic acid also inhibited LPS-induced IL-6 expression via NF- $\kappa$ B in murine microglial cells <sup>336</sup>.

### **1.9.6 MCP-1**

Chemokines are a large family of chemoattractant small cytokines. They are divided into four subfamilies based on the number and spacing of their conserved cysteine (C) residues in the N-terminus of the protein and named C, CC, CXC and CX<sub>3</sub>C <sup>337</sup>. Collectively, chemokines are the main players in selective recruitment of immune cells to the site of inflammation that is induced either by an injury or infection.

The C-C motif chemokine ligand 2 (CCL2) also known as monocyte chemoattractant protein 1 (MCP-1) is a potent inflammatory mediator by triggering firm adhesion of monocytes to endothelial cells contributing to early atherosclerotic lesions<sup>338</sup>. MCP-1 is found in human atheroma<sup>339</sup> and mice lacking MCP-1 receptor (CCR2)<sup>340,341</sup> have fewer monocytes in vascular lesions and are less susceptible to atherosclerosis<sup>341</sup>. Blocking MCP-1 release from myeloid cells abolishes leukocyte adhesion to atherosclerotic lesions<sup>221</sup>. In addition, MCP-1 also regulates migration and infiltration of natural killer (NKs), dendritic cells (DCs) and memory T cells to the site of inflammation<sup>337,342,343</sup>, thus playing a broader and key role in innate and adaptive immunity.

MCP-1 is secreted by various cells including immune cells (peripheral blood mononuclear cells (PBMCs), polymorphonuclear cells (PMNCs) and microglia, astrocytes, fibroblasts, smooth muscle, mesangial, epithelial, and endothelial cells<sup>337,340,343,344</sup>. It is secreted in response to a variety of stimuli, including cytokines (TNF- $\alpha$ , IFN $\gamma$ , IL-1, IL-4 and IL-6), growth factors, complement factors (C3a, C5a), viral<sup>345</sup> and bacterial particles (LPS, fMLP)<sup>343</sup>, a high fat diet<sup>344</sup>, or high glucose<sup>346</sup>. Besides being a potent chemokine for monocytes, MCP-1 may increase cytotoxic activity of lymphocytes and NK cells and may alter the phenotypes of vascular smooth muscle cells and activate MAPKs in endothelial cells<sup>347</sup>.

MCP-1 gene transcription is regulated by three transcription factors: NF- $\kappa$ B, AP-1 and SP1<sup>348-350</sup>. NF- $\kappa$ B (three binding sites) and AP-1 (two binding sites) are the two main regulators, while SP1 (one binding site) is only essential for basal transcription activity of MCP-1<sup>345,348</sup>. As in the case of many pro-inflammatory cytokines, MCP-1 gene expression is regulated mainly by MAPKs/AP-1 (c-jun/c-fos) or NF- $\kappa$ B signalling pathways<sup>345,346,351</sup>.

The role of the NF- $\kappa$ B signalling pathway has been discussed above. The mitogen-activated protein kinases (MAPKs) are an evolutionary-conserved family of serine/threonine kinases enzymes. Upon stimulation by mitogens and pro-inflammatory mediators, they co-ordinate cellular responses by protein phosphorylation and signal transduction in three main signalling

cascades. These pathways are named after their terminal kinase: the extracellular signal-regulated kinases 1/2 (ERK1/2), C-Jun N-terminal kinases (JNKs), and p38 MAPKs <sup>352</sup>. ERK-induced c-fos and JNK-induced c-Fos are re-joined in the formation of the dimeric transcription factor AP-1. ERK1/2 are typically activated by growth factors and mitogenic stimuli and regulate transcription factors (c-fos) involved in cell division, proliferation, and differentiation. Both p38 and JNK are mainly activated by oxidative stress and inflammatory cytokines and are often called stress-activated protein kinases and are involved in inflammation, growth/cell cycle arrest, and cell differentiation <sup>352</sup>.

MCP-1 secretion is stimuli- and cell type-dependent <sup>348</sup>. For instance, in murine microglia cells, LPS-induced MCP-1 secretion is regulated via c-jun/JNK under normal glucose conditions, while under high glucose conditions is regulated via STAT/ERK/c-jun/JNK <sup>346</sup>. In human primary monocytes, serine protease plasmin-induced expression of MCP-1 occurs via activation of the p38 MAPK and (JAK)/STAT signalling pathway <sup>353</sup>.

MCP-1 (CCL2) induces chemotactic effects by binding to its receptor CCR2 (**Figure 1. 27**). Like all chemokine receptors, CCR2 is a G-coupled protein receptor (GPCR), composed of a short extracellular N-terminus, seven hydrophobic transmembrane domains each connected by three extracellular and three intracellular loops, and a C-terminal intracellular region <sup>337</sup>. CCR2 expression is not exclusive to monocytes but is also expressed on NKs <sup>354</sup>, T lymphocytes <sup>355</sup>, B-lymphocytes, memory CD4+ T-cells <sup>337</sup>, aortic smooth muscle cells <sup>356</sup> and neutrophils under specific conditions <sup>342,343</sup>.

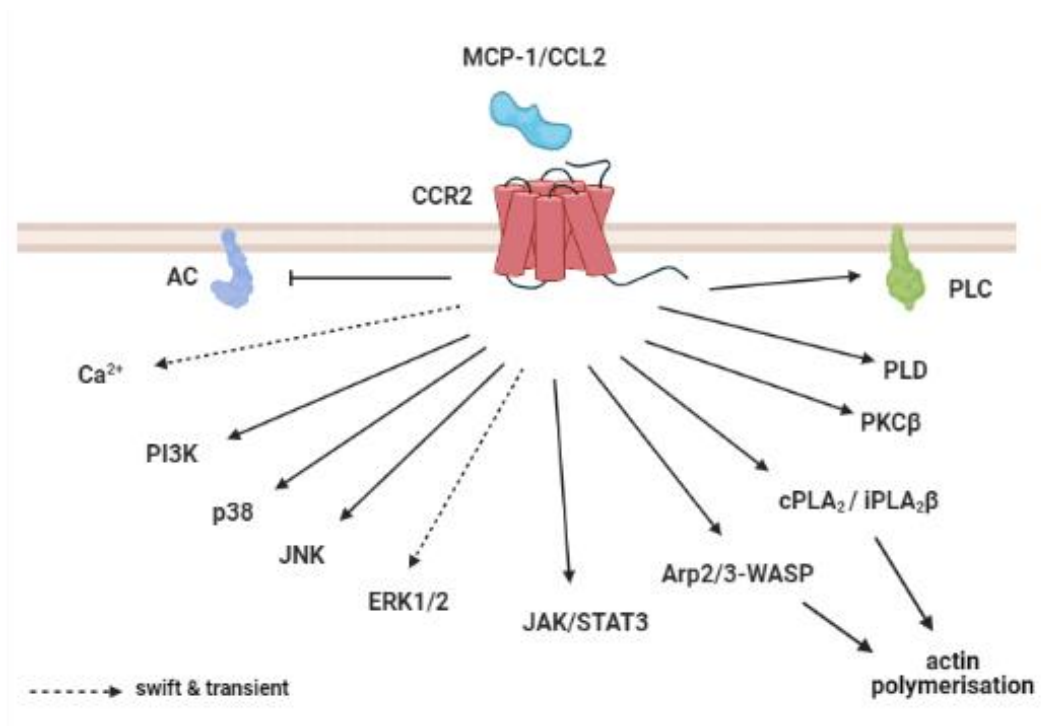


Figure 1. 27 Overview of the MCP-1/CCR2 signalling pathways in monocyte migration. Created in BioRender.com.

Although the exact mechanism of MCP-1 mediated monocyte migration in atherosclerosis is not fully understood, a few signalling pathways have been described<sup>343</sup>. These include: a pertussis toxin (PT) sensitive intracellular calcium ion (Ca<sup>2+</sup>) rise<sup>357,358</sup>, inhibition of adenylyl cyclase (AC)<sup>358</sup>, activation of phospholipase C (PLC)<sup>359</sup>, upregulation of ERK1/2<sup>360</sup>, JNK and p38<sup>361</sup> stimulation of PI3K<sup>362</sup>, and triggering of the JAK2/STAT3 pathway activation in a PTX-independent manner<sup>363</sup>. However, intracellular Ca<sup>2+</sup> rise and ERK activation have been shown to be swift and transient<sup>358,361</sup>, while activation of JNK and p38 was delayed and more sustained<sup>361</sup> suggesting a co-ordinated and involvement of multiple mechanisms in monocyte migration. For a more directional MCP-1-mediated monocyte migration some other mechanisms have been associated with directing cellular compass actin polymerisation. Arp2/3 and WASP<sup>364</sup> were



associated with stimulating actin polymerisation, while activation and recruitment of iPLA<sub>2</sub>β and cPLA<sub>2</sub> to membrane pseudopods and ER respectively (in a Ca<sup>2+</sup>-independent way) were associated with actin polymerisation and directing cellular movement <sup>365</sup>.

MCP-1 plays a role in the pathogenesis of various inflammatory-related disorders including atherosclerosis, RA, congenital heart failure and various types of cancer <sup>343</sup>. Several flavonoids have been shown to inhibit MCP-1 secretion including EGCG, apigenin, C3G and quercetin. EGCG (25-100 μM) reduced LPS-induced MCP-1 secretion from human retinal endothelial cells (HRECs) <sup>290</sup> and at 30, 50 μM inhibited TNF-α-mediated MCP-1 secretion in HUVECs <sup>366</sup>. Also, C3G (50 μM) reduced MCP-1 secretion in high glucose-induced HK2 cells <sup>367</sup>. Apigenin (10, 30 μM) inhibited LPS-induced MCP-1 secretion from J774.2 macrophages <sup>368</sup>. However, at physiological concentrations (0.3-3 μM) no effect was observed and mRNA expression was only apparent at 30 μM. Quercetin (2 and 10 μM) attenuated MCP-1 mRNA and protein expression in TNF-α simulated human umbilical artery smooth muscle cells (HUASMC) <sup>369</sup>.

## **1.10 Oxidative stress and anti-oxidative biomarkers**

Oxidative stress is a key underlying factor in ageing, cancer, diabetes, and various chronic age-related disorders including CVD and neurological disorders. Oxidative stress is defined as the imbalance between oxidants and antioxidants in favour of oxidants, leading to a disruption of redox signalling and control and/or molecular damage to the host <sup>370</sup>. Oxidants are reactive oxygen species (ROS) and reactive nitrogen species (RNS). ROS include free radicals, such as superoxide radicals ( $O_2^{\bullet-}$ ) and hydroxyl radicals ( $HO^{\bullet}$ ) as well as non-free radicals e.g. hydrogen peroxide ( $H_2O_2$ ) and singlet oxygen ( $^1O_2$ ). Under normal conditions, oxidative stress is regulated through redox homeostasis to ensure normal cellular function and cell survival. Usually, the cellular redox status is balanced by ROS inducers and scavengers. Inducers include hypoxia, metabolic defects, oncogenes and endoplasmic reticulum (ER) stress and inhibitors include NADPH, glutathione, tumor suppressors, dietary antioxidants and the transcription factor Nrf2 <sup>371</sup>.

### **1.10.1 Nrf2**

Nrf2 (nuclear factor erythroid 2-related factor 2) plays a critical role in maintaining oxidative homeostasis by regulating the transcription of genes that have a detoxifying or antioxidant function within the cell <sup>372</sup>. Moreover, Nrf2 also controls genes that play a role in xenobiotic metabolism and drug transport <sup>373</sup>. Under normal conditions, like the transcription factor NF- $\kappa$ B, Nrf2 is also kept in the cytosol preventing it from entering the nucleus (**Figure 1. 28**). Nrf2 has a short half-life and is continually made and degraded. It is sequestered in the cytosol and continually targeted for proteasomal degradation by the Keap1-CUL3-E3 ligase complex (Kelch-like ECH-associated protein 1, and Cullin 3) <sup>373</sup>. In response to stress, the Nrf2/Keap1 interaction is disrupted, resulting in accumulation and nuclear

translocation of Nrf2. In the nucleus, Nrf2 heterodimerises with small Maf proteins and binds to the ARE/EpRE (antioxidant response element/electrophile response element). Consequently, Nrf2 promotes the transcription of over 250 genes involved in cytoprotection. Many products of these genes are either directly involved in ROS detoxification or indirectly help to modify and balance intra-cellular ROS levels.

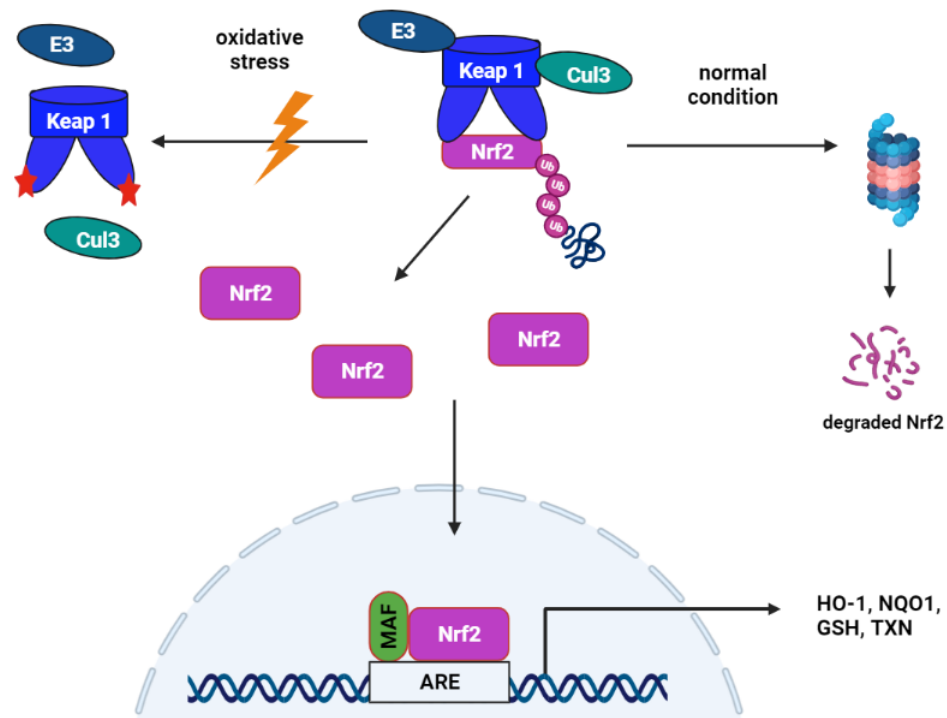


Figure 1. 28 Overview of the Nrf2 signalling pathway. Nrf2 under normal condition sequestered in the cytoplasm by Keap1, Cul3, E3 ligase, aiding ubiquitination and targeting Nrf2 to proteasomal degradation. Upon stress stimuli, the Keap1 is degraded resulting complex disassociation and Nrf2 release that translocate into nucleus where together with MAF bind to promotor region of genes with ARE sequence, upregulation gene transcription. Created in BioRender.com.

Nrf2 directly controls the transcription of key components of the glutathione (GSH) and thioredoxin (TXN) antioxidant system by upregulating those enzymes or enzymatic components that regulate their reduced state <sup>374</sup>. These include glutathione reductase (GSR), glutathione peroxidase 2

(GPX2), several glutathione-S-transferases (GSTA1-5, GSTM1-3)<sup>371</sup>, and thioredoxin reductase 1 (TXNRD1)<sup>371</sup>. Moreover, NADPH is used by these reductases and S-transferases for electron donor and Nrf2 directly regulates NADPH-generating enzymes as well<sup>374</sup>, linking NADPH production to GSH and TXN detoxifying system<sup>371</sup>.

Indirect antioxidant gene targets include phase II detoxification enzymes such as NAD(P)H:quinone oxidoreductase 1 (NQO1)<sup>375</sup> and enzymes regulating sequestration, such as heme oxygenase (HO-1 or HMOX1)<sup>376</sup>, ferritin heavy- (FTH) and light-chain (FTL)<sup>371</sup>.

Nrf2-mediated gene expression depends on the intensity of oxidative stress<sup>377</sup>. For example, under strong oxidative stress ( $\geq 50 \mu\text{M H}_2\text{O}_2$ ) a gene called Kruppel-like factor 9 (Klf9) is expressed, resulting in further Klf9-dependent increases in ROS and sub-sequent cell death<sup>378</sup>, while some other genes including HO-1 and NQO1 are upregulated in response low dose (25  $\mu\text{M}$ )  $\text{H}_2\text{O}_2$ , thus maintaining redox balance.

In the last two decades, substantial research has focused on the effect of flavonoids on the Nrf2 signalling pathway. Various flavonoids are recognised as Nrf2 activators, such as quercetin<sup>379–382</sup>, naringenin<sup>383</sup>, hesperidin<sup>384,385</sup>, EGCG<sup>386</sup>, EGC<sup>387</sup>, EG<sup>388</sup>, C3G<sup>266,269</sup>, PCA<sup>389–391</sup> and ferulic acid<sup>264,266</sup>. Among these flavonoids, quercetin is the most widely investigated compound with various effects in monocytes, endothelial cells and neurons.

Pharmacological activation of Nrf2 negatively regulates VCAM-1 expression in human endothelial cells and mice atherosusceptible sites<sup>392</sup>. Quercetin dose dependently (5-20  $\mu\text{M}$ ) inhibited LPS-induced adhesion molecules ICAM-1 and E-SEL expression in human aortic endothelial cells (HAEC) via p38-mediated Nrf2 activation and upregulation of HO-1, NQO1 and glutamate cysteine ligase (GCL)<sup>381</sup>. Isoquercetin has been found to be neuroprotective against cerebral ischemic stroke by reducing oxidative

stress and neuronal apoptosis via Nrf2-mediated downregulation of the NOX4/ROS/NF- $\kappa$ B signalling pathway in ischemic/reperfusion-induced injury in murine neuronal cells and in rats <sup>393</sup>. In addition, naringenin prevented hydroxydopamine (6-OHDA)-induced neurotoxicity in SH-SY5Y human neuroblastoma cells and in mice via p38/JNK/Nrf2 axis by increasing Nrf2 protein expression and its target genes HO-1, GSH and GCL <sup>383</sup>. Nrf2 knockdown of SH-SY5Y cells resulted in decreased HO-1, GSH, GCL and p38/JNK phosphorylation. Hypobaric hypoxia-induced apoptosis and retinal impairment in rats was also down regulated by hesperidin intake by upregulation of Nrf2/HO-1<sup>385</sup> and our lab has previously shown that in THP-1 monocytes, curcumin and EGC activated Nrf2/HO-1 via upregulation of PKC $\delta$  <sup>387,394</sup>.

### **1.10.2 HO-1**

HO-1 is a major regulator of immune homeostasis by mediating cross talk between the innate and adaptive immune systems. Heme oxygenase (HO) is a ubiquitous enzyme with three isozymes; the inducible HO-1, the constitutive HO-2 and HO-3 <sup>395</sup> which is a pseudogene <sup>376,396</sup>. While HO-2 is constitutively expressed, HO-1 is expressed at low levels under normal conditions but can be induced by various stimuli under stress conditions or highly expressed during pregnancy in the placenta <sup>396</sup>. HO-1 has been hypothesized to be one of the most critical cytoprotective mechanisms activated under cellular stress conditions such as hypoxia, hyperoxia, thermia, radiation and inflammation and induced by variety of stimuli including by its own substrate heme, heavy metals, heat shock, prostaglandins, endotoxins and inflammatory cytokines <sup>396,397</sup>.

HO-1 catalyses the first and rate-limiting step in heme degradation, which produces ferrous iron (Fe<sup>2+</sup>), carbon monoxide (CO), and biliverdin which is further reduced to bilirubin by biliverdin reductase <sup>396</sup> (**Figure 1. 29**).

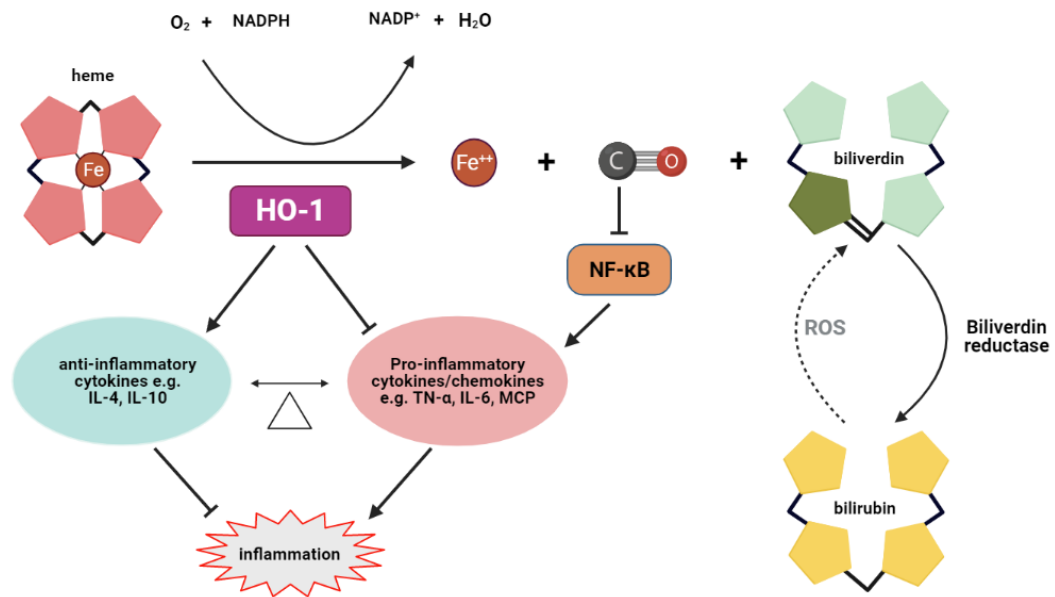


Figure 1. 29 Overview of the role of HO-1 in oxidative stress. HO-1 convert heme into CO, ferrous iron ( $\text{Fe}^{2+}$ ) and biliverdin. Biliverdin further catalysed by biliverdin reductase and may be re-oxidized by reducing ROS. CO supresses NF- $\kappa$ B activation and downstream pro-inflammatory genes. Adapted from Ahmed et al., 2017 and Weaver et al., 2018. Created in BioRender.com.

Heme is a complex of protoporphyrin IX with a central iron, an essential molecule for the function of all living aerobic organisms and plays a fundamental role in various biological processes including oxygen transport, respiration, signal transduction, and drug detoxification<sup>398</sup>. Free heme operates as a pro-inflammatory molecule and plays a role in the pathology of various conditions affecting the CNS, cardiac tissue, liver, and kidneys<sup>399</sup>. Free heme is a highly cytotoxic molecule with lipophilic properties, which can intercalate and damage membranes and organelles (mitochondria and nuclei) by impairing lipid bilayers and destabilising the cytoskeleton. Moreover, heme can catalyse the formation of cytotoxic lipid peroxide via lipid peroxidation as well as oxidation, covalent cross-linking and aggregate formation of proteins and damages DNA through oxidative stress<sup>399</sup>.

The HO-1 catalytic products, bilirubin and CO are anti-inflammatory molecules that play major roles in maintaining the protective effects of HO-1<sup>400,401</sup>. For instance, elevated serum levels of bilirubin are inversely

associated with atherosclerosis and metabolic syndrome <sup>402,403</sup>. Several mechanisms have been described for the anti-inflammatory effects of bilirubin and biliverdin. Biliverdin has been reported to activate PI3K/Akt-IL-10 axis and inhibit TLR4 via direct binding and inhibit of IL-6 and MCP-1 <sup>404</sup>. Bilirubin is a potent antioxidant that prevents lipid oxidation and activation of PPAR- $\alpha$ , a transcription factor regulating lipid metabolism <sup>401</sup> and inhibits TNF- $\alpha$  and IL-1 $\beta$  <sup>401</sup>. Moreover, bilirubin may be recycled back to biliverdin by reducing ROS <sup>401</sup>.

On the other hand, the HO-1 catalytic activity by-product ferrous iron ( $\text{Fe}^{2+}$ ) involves in the conversion of  $\text{H}_2\text{O}_2$  into highly unstable hydroxyl radicals ( $\text{HO}^\bullet$ ), known as the Fenton reaction. However, as discussed above, Nrf2 activation also induces the expression of FTH and FTL, the components of the ferritin complex which oxidizes  $\text{Fe}^{2+}$  into  $\text{Fe}^{3+}$  and incorporates it within its structure making it unavailable for the Fenton reaction <sup>374</sup>.

HO-1 induction is associated with protective effects against endothelial dysfunction and atherosclerosis <sup>405</sup> and against inflammation, oxidative damage and cell death in neurons and astrocytes <sup>406</sup>. Various flavonoids have been reported to down-regulate inflammation and oxidative stress via the HO-1/Nrf2 pathway, quercetin being the most frequently reported. In ApoE<sup>-/-</sup> mice fed a high-fat diet, quercetin administration upregulated HO-1 protecting them from atherosclerosis <sup>405</sup>. Quercetin was further reported to attenuate  $\text{H}_2\text{O}_2$ -induced cell damage in endothelial cells by upregulation of HO-1 <sup>407</sup>. Quercetin also reduced LPS-induced inflammatory responses via upregulation of HO-1 in BV2 microglia <sup>382</sup>. Ferulic acid prevented high-glucose induced oxidative damage to cardiomyocytes and hepatocytes by activating Nrf2-HO-1 signalling <sup>264</sup>. Moreover, ferulic acid and its parent compound, C3G, reduced light-induced retinal oxidative stress in pigmented rabbits by upregulating the Nrf2/HO-1 pathway <sup>266</sup>. FA further inhibited light-induced retinal inflammation by downregulating NF- $\kappa$ B activation. Hesperidin upregulated HO-1 expression in tert-butyl

hydroperoxide (t-BuOOH)-induced cytotoxicity in human hepatic cells via ERK1/2-Nrf2 pathway <sup>384</sup>. These studies demonstrate that flavonoids and their metabolites can protect cells and tissues against oxidative stress via HO-1 and most likely the mechanism is via a cross talk between Nrf2/HO-1 and the MAPK and NF-κB signalling pathways.

### 1.10.3 NQO1

NQO1 (NAD(P)H:quinone acceptor oxidoreductase) is another target gene of Nrf2 <sup>408</sup>. It is a highly inducible enzyme that plays multiple roles in cellular adaptation, redox cycling, oxidative stresses and inflammation in response to a variety of stress elements <sup>409,410</sup> (**Figure 1. 30**). NQO1 was originally identified as a flavoenzyme that catalyses two-electron reduction of quinones and their hydroxyquinone derivatives by NADH and NADPH in mammalian systems, protecting cells from oxidative stress, redox cycling and neoplasia <sup>411</sup>.

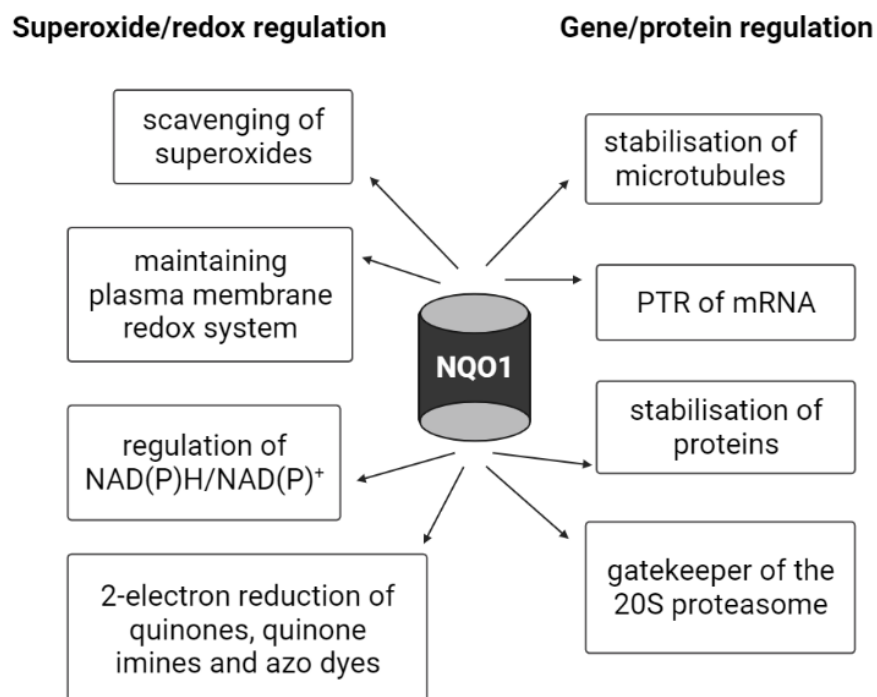


Figure 1. 30 An overview of NQO1 cellular functions.



However, NQO1 is now known as having multiple cytoprotective functions including catalysing two-electron reduction of quinones, quinone imines and azo dyes; modulation of nicotinamide nucleotide ratios (NAD<sup>+</sup> for enzymes PARP and sirtuins); scavenging of superoxides, and maintaining plasma membrane redox state (by generating antioxidant forms of coenzyme CoQ<sub>9</sub>, CoQ<sub>10</sub> and vitamin E); stabilising of microtubules and protecting proteins from the 20S proteasomal degradation <sup>409,412</sup>.

Evidence from genomic and proteomic studies indicates that NQO1 also plays a role in anti-inflammatory gene regulation. A study of the mRNA interactome identified NQO1 as a potential RNA-binding protein that is found in ribonucleoprotein complexes <sup>413</sup>. NQO1 also regulates serine protease inhibitor  $\alpha$ -1-antitrypsin, A1AT (SERPINA1) translation by binding to its 3'-UTR region <sup>414</sup>. SERPINA1 is associated with inflammatory disorders. NQO1 was reported to inhibit TLR-induced IL-6 production via interacting with nuclear protein I $\kappa$ B- $\zeta$  and targeting it for ubiquitination and degradation <sup>375</sup>, suggesting that NQO1 plays a potential role in post-transcriptional and translational regulation of genes and proteins involved in inflammation. Indeed, our group have previously shown that Nrf2-dependent NQO1 downregulates TNF- $\alpha$  expression via an NF- $\kappa$ B-independent alternative pathway as well as via an NF- $\kappa$ B-dependent pathway <sup>408</sup>. This study provided evidence that NQO1 is involved in innate immunity by downregulating LPS-induced expression of pro-inflammatory cytokines in monocytes. LPS induced NQO1 expression while silencing Nrf2 inhibited NQO1 expression and elevated TNF- $\alpha$  and IL-1 $\beta$  secretion. When NQO1 alone, or in combination with HO-1 was silenced, LPS-induced TNF- $\alpha$  and IL-1 $\beta$  levels were markedly raised and when NQO1 and HO-1 was over-expressed, LPS-induced TNF- $\alpha$  and IL-1 $\beta$  expression was inhibited, suggesting a protective role of Nrf2-NQO1-HO-1 in innate immunity by reducing excessive secretion of pro-inflammatory cytokines during an infectious insult. Additionally, Nrf2-dependant HO-1 and NQO1 induction downregulates expression of other pro-inflammatory biomarkers such as MCP-1 <sup>415</sup>, p38 MAPK and VCAM-1 <sup>392</sup>. These results suggest a

crosstalk between Nrf2-dependent NQO1 and HO-1 with pro-inflammatory cell signalling molecules and flavonoids may potentially directly or indirectly target these interactions.

## 1.11 Concluding remarks and aims

Flavonoids and phenolic acids are by far the largest (poly)phenol classes in plant-based diets. A large body of evidence from epidemiological and clinical studies suggest that habitual intake of food rich in flavonoids, especially anthocyanins and phenolic acids is inversely associated with developing CVD and neurological disorders. Chronic inflammation is the hallmark of cardiovascular and cerebrovascular diseases and evidence shows that the beneficial effects of flavonoids are due to their interaction with the cell signalling molecules involved in inflammation.

The most important biomarkers of inflammation are chemokines, cytokines and cell adhesion molecules that are regulated by the transcription factor NF- $\kappa$ B. Flavonoids and their metabolites act on multiple signalling pathways to inhibit MAPKs (p38, ERK1/2, JNK), PI3K/Akt and NF- $\kappa$ B pathway and activate Nrf2<sup>388, 262, 389, 379, 269, 416, 266</sup>. Phenolic acids and their metabolites may reduce chronic inflammation by altering these mediators.

The effects of parent flavonoids have been widely investigated on a wide array of pro-inflammatory biomarkers at concentrations exceeding serum levels despite being extensively metabolised by gut microbiota and further by phase II enzymes with poor bioavailability. The serum concentrations of metabolites and phenolic acids range between 0.1 to <50  $\mu$ M<sup>106</sup> and have been shown to be bioactive at 1-10  $\mu$ M concentrations in contrast to their parent compounds<sup>19,47</sup>. The majority of metabolites from commonly consumed foods are those with low molecular weight including phenolic acids and the most frequently reported phenolic acids are benzoic acid derivatives (including protocatechuic acid, vanillic acid and isovanillic acid) and cinnamic acid derivatives (including ferulic acid, caffeic acid and isoferulic acid),<sup>20,184</sup>. Flavonoids and phenolic acids are diverse and so are their metabolites and so it is important to understand their structure activity relationships and explore the chemical space occupied by these

compounds and investigate their mechanisms of action in order to determine their suitability as nutraceuticals or pharmaceuticals.

## **1.12 Aims of the study**

- To investigate, in monocytic cells, the anti-inflammatory effects of the most common phenolic acids that are found in the diet in free form and produced by the gut microbiota.
- To investigate structure activity relationships of these phenolic acids by studying anti-inflammatory effects of related non-natural, synthetic phenolic acids with nitro, amino or halogen (chloro, bromo, iodo) groups.
- To study the effect of common phenolic acids and their synthetic analogues on trans-endothelial cell migration in response to chemokines.
- To investigate whether anti-inflammatory activity of naturally occurring common phenolic acids can be enhanced by esterification for their therapeutic potential as pharmaceuticals.
- To study the anti-inflammatory mechanisms of action of the most bioactive compounds in immune cells.

## **Chapter 2. Materials & Methods**

## 2.1 Consumables and Chemicals

Contents and recipes of all buffers can be found in **Appendix I**.

### 2.1.1 General Consumables

T25 and T75 culture flasks, 96-well, 24-well and 48 well cell culture plates, falcon tubes (15 mL and 50 mL) and Nunc 96-well black plates were purchased from Thermo Fisher Scientific (Loughborough, UK) or Corning (Amsterdam, The Netherlands). Cryogenic tubes (1.5 mL) were obtained from Nalgene (Rochester, USA). All other consumables and plastics were from Thermo Fisher Scientific unless stated otherwise.

### 2.1.2 General Chemicals & Reagents

Lipopolysaccharide (LPS) (Calbiochem® E. Coli 0111: B4) was purchased from Merck Chemicals Ltd. (Nottingham, UK). Gibco™ Trypan Blue Solution, 0.4% (Cat# 11538886) was from Fisher Scientific (Loughborough, UK). Phorbol 12-myristate 13-acetate (PMA) (Cat# 1201) was obtained from Tocris bio-technique (Bristol, UK), and SB203580 (Cat# S1076) was from Selleckchem (Cambridge, UK). Bay 11-7082 (Cat# B5556), SP600125 (Cat# S5567), PD 98,059 (Cat# P215), dimethyl fumarate (DMF) (Cat# 242926), all-trans-retinoic acid (ATRA) (Cat# R2625), DAPI (Cat# D9542), *cis*-5,8,11,14,17-eicosapentaenoic acid sodium salt (EPA) (Cat# E6627), *cis*-4,7,10,13,16,19-docosahexaenoic acid (DHA), (Cat# D2534) dimethyl sulfoxide (DMSO) and all other reagents and buffer components were from Sigma-Aldrich (Poole, UK), unless stated otherwise and were molecular biology grade. All water utilised was of Milli-Q grade (18.2 MΩ cm<sup>-1</sup>). Water and buffers used for cell culture were sterilised by autoclaving in-house.

### **2.1.3 Phenolic Metabolites, Related Compounds and Synthetic Analogues**

3-chlorobenzoic acid was purchased from Alfa Aesar (Heysham, UK). Benzoic acid, para-aminobenzoic acid, 2- and 3-iodobenzoic acid were obtained from Acros Organics (Geel, Belgium). All other commercially available compounds were purchased from Sigma Aldrich. Seven glycinated conjugates and twelve ester analogues of metabolites (Table 2. 1) were synthesised by the Searcey lab (Dr James Harvey and Dr Andrew Beekman), School of Pharmacy, UEA as follows. Glycine conjugates were prepared following synthetic procedures described by O'Hagan and co-workers<sup>417</sup>. Briefly, once compounds were appropriately protected (phenols and carboxylic acids with the benzyl protecting group) carboxylic acids were treated with HATU (1 eq.), DIPEA (2 eq.) and H-Gly-OMe (1 eq.) in DMF for 4 h at room temperature (RT). Water was added and the solution extracted with EtOAc. The organic solution was concentrated under vacuum and the residue was dissolved in the minimum amount of methanol. 2 M LiOH was added until the solution appeared slightly cloudy, and the mixture was stirred at RT for 16 h. The solution was washed with EtOAc, acidified with NH<sub>4</sub>Cl (aq) and extracted with EtOAc. The organic layer was concentrated to provide the benzyl protected glycine conjugated. Benzyl protection was removed with reduction<sup>417</sup>, and compounds were purified with preparative reverse phase HPLC.

Ester analogues were prepared in a similar manner as described above. Appropriately protected compounds were treated with alkyl alcohols in THF with catalytic H<sub>2</sub>SO<sub>4</sub> at reflux for 16 h. Water was added, and the solution was extracted with EtOAc. After concentration protecting groups were removed with reduction<sup>417</sup>. and compounds were purified with preparative reverse phase



Table 2. 1 List of screened phenolic acids.

<b>IUPAC Name</b>	<b>Common Name</b>	<b>Acronym</b>
<b>4-Hydroxybenzoic acid</b>		4HBA
<b>3,4-Dihydroxybenzoic acid</b>	Protocatechuic acid	PCA
<b>3,4-Dihydroxycinnamic acid</b>	Caffeic acid	CA
<b>3-Hydroxy-4-methoxybenzoic acid</b>	Isovanillic acid	IVA
<b>4-Hydroxy-3-methoxybenzoic acid</b>	Vanillic acid	VA
<b>3-Hydroxy-4-methoxycinnamic acid</b>	Isoferulic acid	IFA
<b>trans-4-Hydroxy-3-methoxycinnamic acid</b>	Ferulic acid	FA
<b>Benzoic acid</b>		BA
<b>2-Iodobenzoic acid</b>		2IBA
<b>3-Iodobenzoic acid</b>		3IBA
<b>3-Chlorobenzoic acid</b>		3CBA
<b>3-Aminobenzoic acid</b>		3ABA
<b>3-Hydroxybenzoic acid</b>		3HBA

<b>4-Aminobenzoic acid</b>	para-aminobenzoic acid	4ABA
<b>4-Nitrobenzoic acid</b>		4NBA
<b>4-Bromobenzoic acid</b>		4BBA
<b>2,4-Dihydroxybenzoic acid</b>	$\beta$ -resorcylic acid	24DHBA
<b>2,4-Dimethoxybenzoic acid</b>		24DMBA
<b>3,5-Diaminobenzoic acid</b>		35DABA
<b>3-Chloro-4-methoxybenzoic acid</b>	3-chloro-p-anisic acid	3C4MBA
<b>5-Chloro-2-methoxybenzoic acid</b>	5-chloro-o-anisic acid	5C2MBA
<b>4-Hydroxybenzoic acid-Glycine</b>	4-hydroxy benzoic acid-glycine	4HBA-Gly
<b>3,4-Dihydroxybenzoic acid-glycine</b>	Protocatechuic acid-glycine	PCA-Gly
<b>3,4-Dihydroxycinnamic acid-Glycine</b>	Caffeic acid-glycine	CA-Gly
<b>3-Hydroxy-4-methoxybenzoic acid-glycine</b>	Isovanillic acid-glycine	IVA-Gly
<b>4-Hydroxy-3-methoxybenzoic acid-glycine</b>	Vanillic acid-glycine	VA-Gly
<b>3-Hydroxy-4-methoxycinnamic acid-glycine</b>	Isoferulic acid-glycine	IFA-Gly
<b>4-Hydroxy-3-methoxycinnamic acid-glycine</b>	Ferulic acid-glycine	FA-Gly

<b>3,4-Dihydroxybenzoic acid-methyl ester</b>	Protocatechuic acid-methyl ester	PCA-Met-Es
<b>3,4-Dihydroxybenzoic acid-ethyl ester</b>	Protocatechuic acid-ethyl ester	PCA-Et-Es
<b>3,4-Dihydroxybenzoic acid-isopropyl ester</b>	Protocatechuic acid-isopropyl ester	PCA-iProp-Es
<b>3,4-Dihydroxybenzoic acid-hexyl ester</b>	Protocatechuic acid-hexyl ester	PCA-Hex-Es
<b>4-Hydroxy-3-methoxybenzoic acid-hexyl ester</b>	Vanillic acid-hexyl ester	VA-Hex-Es
<b>3-hydroxy-4-methoxy cinnamic acid methyl ester</b>	Isoferulic acid-methyl ester	IFA-Met-Es
<b>3-Hydroxy-4-methoxycinnamic acid-ethyl ester</b>	Isoferulic acid-ethyl ester	IFA-Et-Es
<b>3-hydroxy-4-methoxy cinnamic acid hexyl ester</b>	Isoferulic acid-hexyl ester	IFA-Hex-Es
<b>4-Hydroxy-3-methoxycinnamic acid-methyl ester</b>	Ferulic acid-methyl ester	FA-Met-Es
<b>4-Hydroxy-3-methoxycinnamic acid-ethyl ester</b>	Ferulic acid-ethyl ester	FA-Et-Es
<b>4-Hydroxy-3-methoxycinnamic acid-propyl ester</b>	Ferulic acid-propyl ester	FA-Prop-Es
<b>4-Hydroxy-3-methoxycinnamic acid-hexyl ester</b>	Ferulic acid-hexyl ester	FA-Hex-Es

IUPAC: International Union of Pure and Applied Chemistry.

## 2.2 Cell Culture

### 2.2.1 Cells and Reagents

**THP-1** (ECACC 88081201), a human monocytic cell line derived from the peripheral blood of a 1-year-old male with acute monocytic leukaemia <sup>418</sup>, and **HL-60** (ECACC 98070106), a human myeloid cell line obtained from peripheral blood leukocytes of a 36-year-old Caucasian female with acute promyelocytic leukemia <sup>419</sup> were purchased from the European Collection of Authenticated Cell Cultures (ECACC, Salisbury, UK). **BV2**, an immortalized cell line originated from primary neonatal murine microglia by immortalisation with a -raf/v-myc oncogene carrying retrovirus <sup>420</sup> was from American Type Culture Collection (ATCC) (Manassas, Virginia, USA). The human dermal microvascular endothelial cell - 1 (**HMEC-1**) (CDC 98247) obtained by transfection of dermal microvascular endothelial cells (isolated from human foreskins) with pSVT vector containing the coding region for transforming protein SV40 large T antigen <sup>421</sup> was obtained from Centers for Disease Control (Atlanta, GA, USA). **RPMI 1640** medium was obtained from Corning, PAN Biotech (Aidenbach, Germany) or Sigma. Dulbecco's Modified Eagle Medium (**DMEM**) and UltraGlutamine were from Lonza (Benelux B.V., Verviers, Belgium). **DMEM/F-12 (1:1)** and L-Glutamine were from PAA Laboratories (Pasching, Austria) or Gibco Life Technologies (Paisley, UK). Penicillin and Streptomycin and TrypLE™ Express Enzyme phenol red (TEE) were purchased from Gibco Life Technologies. Heat inactivated fetal bovine serum (FBS) (South American origin) was obtained from Gibco or Biowest (Nuaille, France). Dulbecco's PBS (DPBS, without Ca<sup>2+</sup> and Mg<sup>2+</sup>) was purchased from HyClone (Thermo Fisher Scientific).

## **2.2.2 Cell Culture conditions**

### **2.2.2.1 THP-1 Cell Culture**

THP-1 cells were cultured in RPMI 1640 medium supplemented with 10% FBS, 2 mM L-glutamine, 100 U/mL penicillin and 100 µg/mL streptomycin as previously described<sup>408</sup>. This composition will be referred to as RPMI complete medium henceforth. THP-1 cells (passage 8-20) were maintained at 37°C, 5% CO<sub>2</sub> in a humidified atmosphere. The cells were sub-cultured twice weekly, and a density was maintained ideally between 3 – 8 x 10<sup>5</sup> cells/mL in T75 flasks with 10-30 mL medium. Experiments were conducted 2 days after passaging when cells were in exponential phase.

### **2.2.2.2 HL-60 Cell Culture**

HL-60 cells were cultured in RPMI 1640 medium containing 10% FBS, 2 mM L-glutamine, 100 U/mL penicillin and 100 µg/mL streptomycin. The cells (passage 7-56) were maintained at 37°C, 5% CO<sub>2</sub> in a humidified atmosphere. HL-60 were sub-cultured every 2-3 days (1:20) and a density was maintained ideally between 10<sup>5</sup> - 10<sup>6</sup> cells/mL in T75 flasks with 10-20 mL medium. Experiments were conducted 2 days after passaging when cells were in exponential phase.

### **2.2.2.3 BV2 Cell Culture**

Murine microglial BV2 cells were grown in DMEM/F12 medium supplemented with 10% FBS, 2 mM L-glutamine, 100 U/mL penicillin and 100 µg/mL streptomycin (BV2 medium henceforth). BV2 cells (passage 25-40) were maintained at 37°C, 5% CO<sub>2</sub> in a humidified atmosphere and sub-cultured twice weekly at 70-90% confluency in T75 flasks in 10 mL medium. Briefly, the growth medium was removed, and the cells were washed with

10 mL warm Dulbecco's Phosphate Buffered Saline (DPBS) (w/o  $\text{Ca}^{2+}/\text{Mg}^{2+}$ ) prior to adding 2 mL TrypLE Express and incubated for 2-5 min at 37°C to allow the cells to detach. Then 8 mL BV2 medium was added to neutralise the trypsin. Cells were diluted 1 in 20 for maintenance or 1 in 10 for experiments.

#### **2.2.2.4 HMEC-1 Cell Culture**

Human dermal microvascular endothelial cell – 1 (HMEC-1) were cultured in DMEM medium supplemented with 4.5 g/L glucose with UltraGlutamine, 10% FBS and 1% penicillin/streptomycin (HMEC-1 medium henceforth). HMEC-1 cells (passage 5-20) were cultured at 37°C, 5% (v/v)  $\text{CO}_2$  in a humidified atmosphere and sub-cultured every 3-4 days at 70-90% confluency with 1.5 mL 0.1% TEE (1 X) at  $10^4$  cells/cm<sup>2</sup> seeding density in T175 cm<sup>2</sup> flasks, with a total volume of 33 mL.

#### **2.2.3 Cryopreservation**

Two days after passaging, cells were counted to confirm density was between  $5 - 6 \times 10^5$  cells/mL for suspension cells or 80% confluency in a T75 flask for adherent cells. Cells were centrifuged at 1200 x rpm for 5 min. Then, the culture media was removed, and the pellet was re-suspended in 1 mL ice-cold freezing medium (sterile FBS with 10% DMSO) and transferred into a labelled cryovial. The cryovials were placed into a Mr. Frosty™ freezing container (Fisher) with 100% isopropyl alcohol and stored overnight in -80°C to achieve a rate of cooling to -1°C/min. Cells were transferred to liquid nitrogen for long-term storage.

## **2.2.4 Thawing Cells**

A cryovial containing cells was removed from the liquid nitrogen store and thawed rapidly in a 37°C water bath and centrifuged for 5 min at 2000 rpm. The freezing medium was discarded, and the pellet re-suspended in 1 mL pre-warmed complete media. The cell suspension was transferred into a T25 flask containing 7 mL of pre-warmed complete media. Cells were checked under light microscopy for morphology, then placed in an incubator at 37°C, 5% CO<sub>2</sub> under high humidity. The following day, cell viability was examined by diluting cells (1:1) with 0.4% trypan blue (Sigma), where a diazo dye colours dead cells. The cells were transferred to a T75 culture flask when cell density increased.

## **2.2.5 Cell Counting**

### **2.2.5.1 THP-1, HL-60 and BV2 Cells**

Cells were counted in a Malassez haemocytometer under a light microscope. Briefly cells were diluted in 0.4% trypan blue (1:1) and 10 µL of cells was pipetted onto the haemocytometer. The number of cells in a grid of four by five squares was counted 2 x and averaged. The cells per mL was calculated using the following equation:

$$\text{Number of cells per mL} = \text{Number of viable cells counted} \times 10^4$$

### **2.2.5.2 HMEC-1 Cells**

Cell count was determined by using a bright field automated cell counter. Briefly 2 x 20 µL cells were pipetted onto both sides of a Cellometer Disposable Counting Chamber and the slide was inserted into a Cellometer Auto T4 system. Cell concentration was determined automatically following imaging and counting of viable cells and non-viable cells. The average of the viable cell count from both sides of the slide was taken as cells/mL.

## **2.3 Treatment Solutions of Phenolic acids & Synthetic Analogues**

All commercially available and synthesised metabolites were initially solubilised in DMSO at 100 mM final concentration, with the exception of nine synthesized compounds, which were prepared at the following concentrations: 50 mM 4-hydroxy benzoic acid-glycine (4HBA-GI), 34 mM protocatechuic acid-glycine (PCA-GI), 132 mM isovanillic acid-glycine (IVA-GI), 39 mM isoferulic acid-glycine (IFA-GI), 4 mM ferulic acid-glycine (FA-GI), 10 mM protocatechuic acid-methyl ester (PCA-Met-Es), 79 mM protocatechuic acid-ethyl ester (PCA-Et-Es), 92 mM protocatechuic acid-isopropyl ester (PCA-iProp-Es) and 91 mM ferulic acid-methyl ester (FA-Met-Es). All main stocks were stored at -80 °C. From these initial stocks, working stocks were prepared and stored for short term at -20 °C or at -80 °C for longer periods. Prior to the cell treatment, the working stocks were defrosted and vortexed. Final concentrations of DMSO did not exceed 0.1% or 0.03% for transendothelial migration assay treatment. All transendothelial migration assay treatment solutions were prepared in a 96-well plate on the day prior to the experiment and kept at 4 °C overnight.



## 2.4 Cell Proliferation (MTS) Assay

Cell viability was measured using the CellTiter 96® AQueous Non-radioactive Cell Proliferation assay ((MTS/PMS), cat# G5430, Promega (Madison, USA) according to the manufacturer's protocol <sup>422</sup>. Briefly, 100  $\mu$ L of  $1 \times 10^6$  cells/mL THP-1 ( $1 \times 10^5$  cells/well) or 100  $\mu$ L of  $3 \times 10^4$  cells/mL BV2 (3000 cells/well) were seeded in a 96-well plate. Treatments of selected common flavonoid metabolites and their analogues and esters were added in technical triplicates at final concentrations of 1 and 10  $\mu$ M or 20  $\mu$ M for THP-1 and BV2. Each assay had four controls, blank (media only), basal (cell in media only), vehicle control (treatment with 0.1% DMSO) and doxorubicin (1  $\mu$ M) as cell proliferation inhibitor to provide a positive control. The plates with cells were incubated for 24 h at 37°C and 5% CO<sub>2</sub>. Next day, 10  $\mu$ L MTS/PMS reagent was added into each well and returned to the incubator for 3 h for BV2 and for 4 h for THP-1 cells. Following incubation, the absorbance was measured at 492 nm using a POLARstar Optima microplate reader (BMG Labtech; Aylesbury, UK). Cell viability was calculated by normalizing the absorbance of treatment to the absorbance of the basal control (%).

## **2.5 ELISA**

### **2.5.1 Reagents**

The BD OptEIA™ Human TNF- $\alpha$  ELISA Set (Cat# 555212), BD OptEIA™ recombinant human TNF- $\alpha$  lyophilized standard, BD OptEIA™ Human MCP-1 ELISA Set (Cat# 555179) and TMB Substrate Reagent Set (Cat# 555214) were obtained from BD Biosciences (Oxford, UK). The mouse TNF- $\alpha$  Uncoated ELISA (Cat# 88-7324) was obtained from Invitrogen (Thermo Fisher Scientific). The human IL-6 DuoSet ELISA (Cat# DY206), the mouse IL-6 DuoSet® ELISA (Cat# DY406) and Substrate Solution (Color Reagent A [H<sub>2</sub>O<sub>2</sub>] and Color Reagent B [Tetramethylbenzidine] (Cat# DY999), the Human Total HO-1/HMOX1 DuoSet® IC (Cat# DYC3776), and TMB Substrate Reagent Set (Cat# DY999) were obtained from R & D Systems (Biotechne, Abingdon, UK). F96 Maxisorp Nunc-Immuno 96-well plates were from Thermo Fisher Scientific. Leupeptin hemisulfate (1167) and pepstatin A were from Tocris Bio-technie. Lyophilized aprotinin from bovine lung (A1153), phenylmethanesulfonyl fluoride (PMSF) (P7626), Triton™ X-100 (T9284) and sodium azide (NaN<sub>3</sub>) were obtained from Sigma-Aldrich.

### **2.5.2 TNF- $\alpha$ ELISA**

#### **2.5.2.1 Cell Stimulation and Sample Preparation**

**THP-1:** Two days after passaging, THP-1 cells were counted, and the cell density was adjusted to  $1 \times 10^6$  cells/mL. Cells were seeded at  $5 \times 10^5$  cells/well. Then 5  $\mu$ L of working solutions of selected common flavonoid metabolites and their analogues and esters were added into the referred wells to a final concentration of 0.1  $\mu$ M, 1  $\mu$ M, 10  $\mu$ M and 20  $\mu$ M. On every 24-well or 48-well plate 8 wells were left untreated: two with only cells to provide basal control; two to provide an LPS control; two with LPS and 0.1% DMSO (vehicle control) and two wells with 10  $\mu$ M SB203580 to provide a

positive control for reducing TNF- $\alpha$  secretion. The plate was incubated at 37°C, 5% (v/v) CO<sub>2</sub> for 30 min. Pre-incubated cells were then stimulated with 1 ng/mL (5  $\mu$ L 100 ng/mL) LPS, (except for the two basal control wells) for a further 3 h. Cell suspensions were transferred into Eppendorfs and centrifuged at 10,000 x rpm for 1 min or the whole plate was centrifuged at 3000 x g for 5 min. Finally, 100  $\mu$ L supernatant was either immediately used for ELISA and/or 260  $\mu$ L supernatant per sample was transferred into a well of a 96-well plate in order to provide the use of a multichannel pipet for ELISA assay. The plate was sealed and stored at -80°C for further use within one week. Additionally, to provide the TNF- $\alpha$  ELISA assay with an internal control, an internal standard stock was created by stimulating 8 mL  $4 \times 10^5$  cells/mL THP-1 with 1 ng/mL LPS in a T25 flask for 3 h. Cells were pelleted per above mention method and the supernatants were stored at -80 °C in 220  $\mu$ L aliquots until use.

**THP-1 Macrophages:** Two days after passaging, THP-1 cells were counted, and the required volume of cells was spun at 1200 rpm for 5 minutes. Media was removed and cell pellets resuspended in differentiation media (RPMI complete medium with 200 nM PMA) to a cell density of  $2.5 \times 10^5$  cells/mL. Then, 2 mL/well ( $5 \times 10^5$  cells/well) was seeded in 12-well plates and incubated for 3 days at 37°C, 5% (v/v) CO<sub>2</sub> in a humidified atmosphere. After differentiation cells were washed twice with 1 mL warm DPBS to remove any remaining PMA and 1 mL RPMI complete medium was added to the wells. Then, 50  $\mu$ M DHA was added to referred wells and pre-incubator for 2.5 h. Followed by 0.5 h incubation with 10  $\mu$ M flavonoid metabolites alone or to the wells with DHA. On each plate one well was left untreated (basal), one with 10  $\mu$ M SB 203580 as positive control, one with 0.2% DMSO as vehicle control (VC), and one with LPS alone. After total pre-incubation of 3h, then 1ng/mL LPS was added and further incubated for another 3h at 37°C. Supernatants were collected and stored at -80 °C until further analysis.

**BV2:** Two days after passaging, BV2 cells were counted and the cell density was adjusted to  $1 \times 10^5$  cells/mL. Then, 2 mL cells/well were seeded in a 6-well plate ( $2 \times 10^5$  cells/well). The plates were incubated overnight at 37°C, 5% CO<sub>2</sub> and under a humidified atmosphere. Next day, 1 mL media from each well was removed. Then, 10 µM of treatment solutions of selected common flavonoid metabolites and their esters were added into referred wells. For each experiment three wells were left untreated: one with only cells to provide basal control; one with DMSO (0.1%) to provide a vehicle control (VC) and one well with 1 µM BAY 11-7082 (an NF-κB inhibitor) to provide a positive control for reducing cytokine secretion. The treated plates were returned to the incubator for 30 min. After pre-incubation each well (except basal control) was stimulation with 10 ng/mL LPS for 4 h. Following incubation, supernatants were collected and transferred into eppendorf tubes and used immediately for ELISA assay or stored at 80°C and proceeded as described here above.

### **2.5.2.2 TNF-α ELISA Assay Procedure**

The human TNF-α ELISA assay was carried out according to the manufacturer's instructions<sup>423</sup>. Briefly, anti-human TNF-α capture antibody was diluted 1:250 in coating buffer (recipe in **Appendix I**) and 100 µL per well was added to a F96 Maxisorp Nunc-Immuno 96-well plate. The coated plate was sealed and stored at 4°C overnight. Next day the wells were aspirated and washed three times with 275 µL washing buffer (**Appendix I**). The plates were then blocked in assay diluent (**Appendix I**) and incubated at RT for 1 h. Meanwhile, standards were created by diluting known concentrations of TNF-α (0 - 500 pg/mL) in assay diluent. Likewise, samples (except basal control) were diluted in assay diluent at 2-10X. For each assay two aliquots of internal standard controls were used to assess the inter- and intra-assay variability and the reproducibility of the assays. Following blocking, the washing step was repeated and 100 µL of each known standard, sample or internal control in technical duplicates were

added to wells. The plate was sealed and incubated for 2 h at RT. Then, the washing step was repeated for five times before adding 100  $\mu$ L working detector (1:500 detection antibody and 1:250 enzyme reagent in assay diluent) and incubated at RT for 1 h. Next, the plate was washed seven times with washing buffer to remove any unbound detection antibodies and enzyme reagent. Finally, 100  $\mu$ L substrate solution (recipe in **Appendix I**) was added to each well and the plate was incubated at RT for a maximal 10 min in the dark to allow the colour change to light blue. Finally, 50  $\mu$ L stop solution (**Appendix I**) was added to each well to denature the enzyme and stop the reaction. The optical density (OD) of each well was determined at 450 nm and a correction wavelength of 570 nm using a POLARstar Optima microplate reader (BMG Labtech, Aylesbury, UK). Absorbance values were corrected by extracting 570 nm values from 450 nm values. The quantification of TNF- $\alpha$  secretion was calculated by extrapolating from the standard curve plotted between 0-500 pg/mL recombinant TNF- $\alpha$  standard, using a linear or polynomial regression.

**The Mouse TNF- $\alpha$  ELISA** was carried out according to the manufacturer's protocol [Invitrogen 2018]. Briefly, anti-mouse TNF- $\alpha$  capture antibody was diluted 1:250 in coating buffer (1X PBS, provided by manufacturer) and 100  $\mu$ L per well was added to a F96 Maxisorp Nunc-Immuno 96-well plate and stored at 4°C overnight. Next day the wells were aspirated and washed three times with 275  $\mu$ L washing buffer (**Appendix I**). The plates were then blocked in ELISA Diluent (1X) and incubated at RT for 1 h. Meanwhile, recombinant mouse TNF- $\alpha$  standards were reconstituted in distilled water to a 1000 pg/mL and left for 10-30 min at RT to dissolve completely. Then a seven-point standard curve was created using 2-fold serial dilutions in 1X assay diluent (15.6 - 1000 pg/mL). Likewise, samples (except basal control) were diluted in assay diluent at 2-fold. Following blocking, the washing step was repeated and 100  $\mu$ L of each known standard, sample or internal control in technical duplicates were added to wells. The plate was sealed and incubated for 2 h at RT. Then, the washing step was repeated for five times before adding 100  $\mu$ L detection antibody (1:250 in ELISA/ Diluent)

and incubated at RT for 1 h. Next, the washing step was repeated and 100  $\mu$ L Streptavidin-HRP (1:100 in ELISA/ Diluent) was added to plate, incubated 30 min at RT. Then the plate was washed seven times and 100  $\mu$ L TMB solution was added to each well and the plate was incubated at RT for 5 min. Finally, 50  $\mu$ L stop solution (Appendix I) was added to each well and the OD was measured and analysed as described above for human TNF- $\alpha$ .

### **2.5.3 IL-6 ELISA**

#### **2.5.3.1 Cell Stimulation and Sample Preparation**

**THP-1** Cell stimulation and sample preparation were as per human TNF- $\alpha$  method, with the following exceptions: cells were stimulated with 1  $\mu$ g/mL LPS for 24 h; 10  $\mu$ M Bay 11-7082 was used as a positive control to reduce IL-6 secretion and only the effect of 20  $\mu$ M FA, FA-Hex-Es and FA-Pro-Es were investigated.

**BV2** cells stimulation for IL-6 and sample preparation were carried out exactly as per BV2 cell stimulation and sample preparation for TNF- $\alpha$  (per description above) with the following exceptions: cells were stimulated with 1  $\mu$ g/mL LPS for 24 h; the treatment with PCA-Hex-E was at 0.1  $\mu$ M and the dose response effect of FA-Hex-Es and IFA-Et-Es were investigated at 0.1, 1, 10  $\mu$ M.

#### **2.5.3.2 IL-6 ELISA Assay Procedure**

**The Mouse IL-6 ELISA** was carried out according to the manufacturer's protocol [R & D Systems 2019]. Briefly, rat anti-mouse IL-6 capture antibody was diluted in PBS without carrier protein (2  $\mu$ g/mL) and 100  $\mu$ L per well was added to a F96 Maxisorp Nunc-Immuno 96-well plate. The coated plate was sealed and incubated overnight at RT to allow the capture antibody to

bind to the coating. Next day the wells were aspirated and washed with 250  $\mu$ L ELISA assay washing buffer (recipe in **Appendix I**) three times and the plate was blocked with 250  $\mu$ L Reagent Diluent (RD) (**Appendix I**), sealed and left for 1 h at RT. For each assay, a seven-point standard curve using 2-fold serial dilutions was prepared from recombinant mouse IL-6 standards (15.6 - 1000 pg/mL) in RD and likewise, samples were prepared by diluting (1:1) in RD (except basal control). After blocking, the washing step was repeated before adding 100  $\mu$ L/well of each known standard or sample. The plate was sealed and incubated at RT for 2 h to allow binding of IL-6 protein to the capture antibodies. Next, the washing step was repeated and 100  $\mu$ L of biotinylated goat anti-mouse IL-6 detection antibody (75 ng/mL) diluted in RD was added to each well. The plate was sealed and incubated for another 2 h at RT. After incubation, the aspiration and washing step was repeated to remove any unbound detection antibody. Then, 100  $\mu$ L of working dilution of streptavidin-HRP (1:40) in RD was added to each well and the plate was covered, incubated for 20 min at RT, avoiding direct light. The aspiration/wash step repeated before adding 100  $\mu$ L Substrate Solution (1:1 A&B) (**Appendix I**) to each well and the plate was covered and incubated for another 20 min at RT, avoiding direct light. Finally, 50  $\mu$ L/well stop solution (**Appendix I**) was added and the optical density of each well was immediately measured at 450 nm and 570 nm by using a POLARstar Optima microplate reader (BMG Labtech, Aylesbury, UK). Absorbance values were corrected by extracting 570 nm values from 450 nm values. The quantification of IL-6 secretion was calculated by extrapolating from the standard curve plotted between 0-1000 pg/mL recombinant IL-6 standard, using a linear regression.

**The Human IL-6 ELISA** was carried out according to the manufacturer's protocol [R & D Systems 2019] and exactly as per the mouse IL-6 method (per description above), with the following exceptions: mouse anti-human IL-6 capture antibody (2  $\mu$ g/mL), biotinylated goat anti-human IL-6 detection antibody (50  $\mu$ g/mL), and recombinant human IL-6 standards (9.4-600 pg/mL) were used.

## **2.5.4 MCP-1 ELISA**

### **2.5.4.1 Cell Stimulation and Sample Preparation**

**HL-60** cells were differentiated into neutrophil like cells (HL60-differentiated neutrophils) with 1.3% DMSO for three days. For differentiation:  $10^5$  cells/mL in 10 mL differentiation media (RPMI complete medium + DMSO), in a T25 flask were incubated at 37°C. As control a flask of 10 mL cells ( $10^5$  cells/mL) in non-differentiation media was incubated alongside. After 3 days, the colour change of the control flask was compared to the differentiated flask, and the morphology of the cells were examined under microscopy. Then, differentiated cells were centrifuged at 1200 rpm for 5 min. The cell pellet was washed with 10 mL warm DPBS followed by resuspending in equal volume of RPMI complete media. 1 mL cells/well were seeded in a 24-well plate and pre-treated for 30 min with 10  $\mu$ M of each flavonoid metabolite or related phenolic acids. On each plate eight wells were with controls: two wells for fMLP treatment, two wells pre-treated with 10  $\mu$ M PD 098059 as positive control to reduce MCP-1 secretion, two wells with 0.1% DMSO as vehicle control (VC), two wells left for fMLP treatment, and two wells for basal (untreated cells). After pre-incubation cells were stimulated with 1  $\mu$ M fMLP and returned to the incubator for another 30 min. Cells were spun at 2000 rpm for 2 min, and supernatant were immediately used for MCP-1 ELISA assay.

### **2.5.4.2 MCP-1 ELISA Assay Procedure**

Human MCP-1 ELISA was carried out as per human TNF- $\alpha$  ELISA assay procedure with the following exceptions: anti-human MCP-1 capture antibody (1:250), biotinylated goat anti-human MCP-1 detection antibody (1:500), streptavidin-horseradish peroxidase conjugate (Sav-HRP) enzyme reagent (1:250), and recombinant human MCP-1 standards (7.8-1000 pg/mL) were used.



## **2.5.5 HO-1 ELISA**

### **2.5.5.1 Cell Stimulation and Sample Preparation**

Two days after passaging, THP-1 cells were seeded in a T25 flask at  $5 \times 10^6$  cells in an approximate 10 mL volume and incubated for 20 h at 37°C, 5% CO<sub>2</sub> under a humidified atmosphere to settle the cells. Next day, 20 µM treatments of ferulic acid and its esters, 20 µM quercetin, 30 µM DMF (positive control) or 0.1% DMSO (vehicle control) were added into the referred flasks. The flasks were returned to the incubator for another 20 h. Following incubation, the cells were harvested by centrifugation at 2000 x g for 5 min and washed twice with 1.5 mL PBS. The pellet was resuspended in 1 mL HO-1 cell lysis buffer (recipe in **Appendix I**) and incubated on ice for 15 min, then transferred into -80 °C and assessed within one week. Before the HO-1 ELISA assay, cell lysates were defrosted and centrifuged at 2000 x g for 5 min and the clear supernatant with protein fraction was transferred into a new clean test tube.

### **2.5.5.2 Protein Quantification**

Total protein concentration and quality in supernatant was measured using the NanoDrop® ND-1000 (Labtech, Uckfield, UK). The quantification is based on the light absorption property of proteins at 280nm. The estimation is based on using the Beer-Lambert Law, whereby:

For proteins: Optical Density at 280 nm = extinction coefficient x concentration x path length

(extinction coefficient of protein = 1 mg/mL; path length = 1 mm)

Furthermore, the quality of total protein in supernatants was assessed based on the ratio between 260/280. Nucleic acids having an absorbance (at 260 nm) close to protein absorbance (280 nm). The ration was taken to assess the presence of co-purified nucleic acids in protein supernatants. A

ratio of ~ 1.8 was considered as pure, and a ratio lower than ~1.5 was handled with caution.

### **2.5.5.3 HO-1 Sandwich ELISA Assay Procedure**

The HO-1 ELISA was carried out according to the manufacturer's instructions [R & D Systems 2015]. Briefly, rat anti-human HO-1 capture antibody (Part 842355) was diluted to 8 µg/mL in PBS and 100 µL per well was added to a F96 Maxisorp Nunc-Immuno 96-well plate. The coated plate was sealed and stored at RT overnight. Next day the wells were aspirated and washed three times with 250 µL washing buffer (**Appendix I**). The plate was then blocked with 250 µL blocking buffer (**Appendix I**) and incubated for 2 h at RT. For each assay, a seven-point standard curve using 2-fold serial dilutions and a high standard of 10ng/mL was created from recombinant human HO-1 (Part 842357) in IC Diluent#4 (**Appendix I**). The blocked plate was washed three times in washing buffer and 100 µL of each known standard, sample ( $\pm$  1-3 mg/mL) or blank were added to the ELISA plate. The plate was sealed and incubated for 2 h at RT. Following this, the unbound proteins were washed three times with washing buffer. Then, 200 ng/mL biotinylated goat anti-human HO-1 detection antibody in a volume of 100 µL IC Diluent#1 (**Appendix I**) was added to each well and the plate was incubated for a further 2 h at RT. After incubation, the plate was aspirated and washed three times with washing buffer, then 1:200 diluted Streptavidin-HRP in 100 µL IC Diluent#4 was added to each well and incubated for 20 min at RT, avoiding placing the plate in direct light. Then, the aspiration/washing step was repeated and 100 µL substrate solution (A:B) (**Appendix I**) was added to each well and incubated for 20 min at RT. Finally, the reaction was stopped by adding 50 µL/well stop solution (**Appendix I**) and the plate was gently tapped to ensure mixing thoroughly. The optical density of each well was determined at 450 nm and 570 nm by a POLARstar Optima microplate reader (BMG Labtech, Aylesbury, UK) and further assessed as described for the TNF- $\alpha$  ELISA. Briefly, the

quantification of HO-1 protein was calculated by extrapolating from the standard curve plotted between 0-10 ng/mL recombinant human HO-1/HMOX1 standard, using a linear regression. The HO-1 protein levels were used to calculate fold change compared to basal control. The data obtained from three independent experiments was analysed as described for TNF- $\alpha$  protein expression.

## **2.6 NQO1 Enzyme Activity Assay**

### **2.6.1 Reagents**

Flavin adenine dinucleotide (FAD) (Cat# F6625), glucose-6-phosphate sodium salt (G-6-P) (Cat# G7879), recombinant glucose-6-phosphate dehydrogenase from *Leuconostoc mesenteroides*, expressed in *E. coli* (G-6-P-DH), in lyophilized form (Cat# G8529),  $\beta$ -nicotinamide adenine dinucleotide phosphate hydrate (NADP<sup>+</sup>) (Cat# N5755), thiazolyl blue tetrazolium bromide (MTT) (Cat# M2128), menadione (Cat# M5625) and recombinant human DT diaphorase (NQO1) (in *E. coli*) (Cat# D1315), digitonin (Cat# D141) and EDTA were obtained from Sigma-Aldrich.

### **2.6.2 Cell Stimulation and Sample Preparation**

Two days after passaging, THP-1 cells were seeded at  $1 \times 10^5$  cells/well in 200  $\mu$ l in a 96-well plate and incubated for 20 h at 37 °C, 5% CO<sub>2</sub> atmosphere to allow the cells to settle. Next day, treatment solutions of 20  $\mu$ M ferulic acid and its esters and quercetin or 30  $\mu$ M DMF (positive control) or 0.1% DMSO (vehicle control) were added into the referred wells and the plate was returned to the incubator for another 20 h of incubation. Following this, treated cells were immediately carried forward for measuring NQO1 enzymatic activity.

### **2.6.3 NQO1 Assay Procedure**

NQO1 enzymatic activity assay was carried out according to Prochaska and Santamaria (1988) <sup>424</sup>. Briefly, at the end of the incubation time point, the cells were collected into a 1.5 mL Eppendorf tube and centrifuged at 2000 x g for 5 min. The media was discarded, and the pellet was resuspended in 50  $\mu$ L cell lysis buffer (recipe in **Appendix I**). To allow cell lysis, the tubes were incubated for 10 min at 37 °C, then agitated on an orbital shaker at

100 rpm for another 10 min at RT. For each assay, a seven-point standard curve using 2-fold serial dilutions and a high standard of 300 mU/mL (60 µg/mL) was created from recombinant NQO1 in cell lysis buffer. 50 µL of samples or standards were added to each referred well. For each assay, two wells were reserved for a blank and a negative control both having 50 µL cell lysis buffer. Then, 200 µL complete reaction buffer (**Appendix I**) was added to all standards, samples, and the blank wells by means of a multichannel pipette. A negative control (200 µL reaction buffer without menadione) was also added. The plate was incubated in the dark for 3-10 min and absorbance was read immediately at 610 nm on a ClarioStar multi-plate reader (BMG Labtech, Aylesbury, UK). The quantification of NQO1 enzymatic activity was calculated by extrapolating from the standard curve plotted between 300-5 mU/mL recombinant human NQO1 standard, using a linear regression. The levels of NQO1 enzymatic activity were used to calculate fold change compared to the vehicle control and the data analysis was performed as described for TNF- $\alpha$  protein expression.

## 2.7 Real Time-QPCR

### 2.7.1 Reagents

TRI Reagent® (Cat#: AM9738) was purchased from Invitrogen (Fisher Scientific). 1-bromo-3-chloro-propane, 2-propanol, ethanol (all Molecular Biology Grade) and SYBR Green Jumpstart Taq Ready Mix for Quantitative PCR were purchased from Sigma-Aldrich. High Capacity cDNA Reverse Transcription kit (Cat#: 4368814) and RNase Inhibitor (Cat#: N8080119) were obtained from Applied Biosystems™ (Thermo Fisher Scientific). Custom primers for all target genes and the housekeeping gene (**Table 2. 2**) were purchased from Life Technologies (Paisley, UK). Sterile filter pipette tips and 0.1 mL and 0.2 mL tubes were from Fisher Scientific.

Table 2. 2 Primer sequences for RT-qPCR.

Gene	Direction	Primer Sequence
hGAPDH	Forward	5'-TCA ACG ACC ACT TTG TCA AGC TCA-3'
	Reverse	5'-GCT GGT GGT CCA GGG GTC TTA CT-3'
hTNF- $\alpha$	Forward	5'-GCC CAG GCA GTC AGA TCA TC-3'
	Reverse	5'-CGG TTC AGC CAC TGG AGC T-3'
hHO-1	Forward	5'-ATG GCC TCC CTG TAC CAC ATC-3'
	Reverse	5'-TGT TGC GCT CAA TCT CCT CCT-3'
hNQO1	Forward	5'-CGC AGA CCT TGT GAT ATT CCA G-3'
	Reverse	5'-CGT TTC TTC CAT CCT TCC AGG-3'
mGAPDH	Forward	5'-AAT GGA TTT GGA CGC ATT GGT-3'
	Reverse	5'-TTT GCA CTG GTA CGT GTT GAT-3'
mIL-6	Forward	5'-GAC AAA GCC AGA GTC CTT CAG AGA G-3'
	Reverse	5'-CTA GGT TTG CCG AGT AGA TCT C -3'

## **2.7.2 Cell stimulation and Sample collection**

### **a) THP-1 cells for TNF- $\alpha$ , HO-1, NQO1**

Two days after splitting, cells were counted and seeded in 24-well plates, at a density of  $1 \times 10^6$  cells/well in a volume of 2 mL ( $5 \times 10^5$  cells/mL) for mRNA expression of TNF- $\alpha$ , NQO1 and HO-1. Plates were incubated overnight at 37°C, 5% (v/v) CO<sub>2</sub> under a humidified atmosphere. Next day, without disturbing the cells, 1 mL of medium was removed from the top of each well and cells were treated with 20  $\mu$ M FA, FA-Pro-Es, FA-Hex-Es (for TNF- $\alpha$ ) or FA-Hex-Es and quercetin (for HO-1 and NQO1). In the case of TNF- $\alpha$ , on every plate, one well was left untreated to provide a basal control; one to provide an LPS control; one with both DMSO (0.1%) and LPS to provide vehicle control (VC) and one well had 20  $\mu$ M Bay 11-7082 (BAY) to provide a positive control for reducing TNF- $\alpha$  mRNA expression. Then the plate was returned to the incubator for 30 min before adding 1 ng/mL LPS for 2 h. In the case of **NQO1** and **HO-1**, on every plate one well was treated with DMSO (0.1%) to provide a basal control and one well had 30  $\mu$ M Dimethyl fumarate (DMF) to provide a positive control for induction of HO-1 and NQO1 mRNA expression. Then the plates were returned to the incubator for 4 h for HO-1 and NQO1 activation. After the stated incubation time, cells were re-suspended by pipetting up and down and transferred to a 1.5 mL Eppendorf tube. The cells were harvested by centrifugation at 5,000 rpm for 5 min. The supernatant was discarded, and the cell pellet was re-suspended in 1 mL TRI Reagent<sup>®</sup> and incubated at RT for 5 min prior to overnight storage at -80 °C.

### **b) BV2 cells for IL-6**

Two days after passaging, BV2 cells were counted and the cell density was adjusted to  $5 \times 10^4$  cells/mL. From this cell suspension,  $1 \times 10^5$  cells/well were seeded in a 6-well plate and incubated overnight at 37°C, 5% CO<sub>2</sub>. Next day, from each well 1 mL media was removed, and cells treated with

10  $\mu\text{M}$  selected phenolic metabolites and their esters with exception of PCA-Hex-E (0.1  $\mu\text{M}$ ). For each experiment, three wells were left untreated: one with only cells to provide basal control; one with DMSO (0.1%) to provide a vehicle control (VC) and one with 0.1  $\mu\text{M}$  BAY 11-7082 (an NF- $\kappa\text{B}$  inhibitor) to provide a positive control for reducing IL-6 production. The treated plates were returned to the incubator for 30 min, prior to stimulation with 10 ng/mL LPS for 4 h. At the end of the incubation period, media was removed and 1 mL TRI Reagent® was added to each well and incubated for 10 min to allow cell lysis. The lysate was then collected into Eppendorfs and stored at  $-80^{\circ}\text{C}$  for overnight incubation or up to one week.

### **2.7.3 RNA Extraction**

Samples were thawed at RT and 100  $\mu\text{L}$  1-bromo-3-chloro- propane was added to each sample. The tubes were shaken by hand, vigorously for 10 sec and left at RT for 10 min prior to centrifugation at 12,000 x g,  $4^{\circ}\text{C}$  for 20 min. Following centrifugation, 400  $\mu\text{L}$  of the top, clear aqueous layer was transferred to a new tube and the remnant was discarded. To each tube, 500  $\mu\text{L}$  2-propanol was added prior to hard vortexing for 10 sec. The tubes were incubated at RT for 10 min, followed by centrifugation for 15 min at 12,000 x g,  $4^{\circ}\text{C}$ . The supernatant was thoroughly removed, and 1 mL 70% ethanol was added to each tube to wash the pellet. The tubes were gently vortexed, using 6 x 1 sec pulses prior to centrifugation at 12,000 x g,  $4^{\circ}\text{C}$  for 10 min. Without disturbing the pellet, the ethanol was carefully removed by pipetting out and the remaining ethanol was left evaporation at RT for a maximum of 30 min. Next, the pellet was re-suspended in 20  $\mu\text{L}$  nuclease-free  $\text{H}_2\text{O}$  by pipetting up and down and gently vortexing. Samples were stored at  $-80$  until further processing.



## 2.7.4 RNA Quantification & Reverse Transcription

The total RNA concentration and quality was measured using the NanoDrop® ND-1000 spectrophotometer (Labtech, Uckfield, UK). The quantification based on light absorption property of nucleic acids at 260nm on the UV spectrum. The estimation is based on using the Beer-Lambert Law, whereby:

Optical Density at 260 nm = extinction coefficient x concentration x path length

(extinction coefficient of RNA = 40 µg/µL; path length = 1 mm)

Whereas, the purity of sample was evaluated by two ratios, A260/280 and A260/230. Lower ratios indicate impurity of nucleic acids (absorbance at 260 nm) with proteins (having an absorbance at 280 nm), and polyphenols (TRIzol traces) (absorbance at 230 nm, and at 270). A value between ~ 1.8 - 2.0 was considered as pure RNA for both ratios. Samples having lower ratio than ~1.5 were handled with caution.

In the case of THP-1, for each sample 240 ng RNA was prepared in 5 µL nuclease free water. For BV2, for each sample 250 ng RNA was prepared in 5 µL water. Samples were mixed with 5 µL Reverse Transcription mastermix (**Appendix I**). Reverse transcription of RNA to cDNA was performed by incubation of the samples at 25°C for 10 min, 37°C for 2 h, 85°C for 5 min and hold on 4°C using a MJ Research PTC-100 Peltier Thermal Cycler (Biorad, Herts, UK). Following transcription, the samples were diluted 1:2 by adding 10 µL nuclease free H<sub>2</sub>O prior to RT-qPCR with exception of samples from BV2 cells, which were used directly without dilution.

### 2.7.5 RT-qPCR Procedure

Real-time quantitative PCR (RT-qPCR) was carried out using 2  $\mu$ L cDNA template with the addition of 18  $\mu$ L RT-qPCR mastermix (**Appendix I**) containing 250 nM forward and 250 nM reverse target gene primers (**Table 2. 2**) to a final reaction volume of 20  $\mu$ L with the exception of BV2 cells. For gene expression in BV2 cells, the same volume of cDNA template and SYBR Green Jumpstart Taq Ready Mix was used. However, the primer concentration was modified to prevent primer dimer formation due to lower gene expression concentrations (primer concentration optimisation can be found in (**Appendix III**)). For this purpose, 0.5  $\mu$ L 10  $\mu$ M mouse GAPDH primers (250 nM) and 0.3  $\mu$ L 10  $\mu$ M mouse IL-6 primers (150 nM) were used and the volume of water adjusted to a final volume of 20  $\mu$ L. For each assay, 2  $\mu$ L nuclease free H<sub>2</sub>O was used to provide a non-template control (NTC) for each gene to confirm no DNA contamination and no primer dimer formation. RT-qPCR was carried out using the rotor-Gene Q real-time PCR cycler (Qiagen, Manchester, UK), wherein the reaction was activated at 95°C for 2 min prior to 40 cycles of denaturation and amplification: 15 sec at 95°C and 40 sec at 60°C per cycle, respectively. A melt analysis was performed by incrementally increasing the temperature from 60°C - 94°C to assess contamination and primer dimer formation. The recorded C<sub>t</sub> values for the target genes TNF- $\alpha$ , HO-1, NQO1, IL-6, and the reference gene GAPDH (housekeeping gene) were used to calculate fold change. The delta C<sub>t</sub> values was calculated using  $2^{-[\text{target}_{C_t} - \text{reference}_{C_t}]}$  determination, which implies the expression level of each gene as fold change relative to GAPDH. In the case of HO-1 and NQO1, the fold change was normalised to basal control. In the case of TNF- $\alpha$  and IL-6 investigation, the fold change was normalised to LPS control and to vehicle control respectively. Differences for all genes were compared to the vehicle control.

## 2.8 Western Blotting

### 2.8.1 Reagents

Western blotting was carried out as previously described in the laboratory [Steel et al. 2012]. p38 MAPK control cell extract (cat#: 9213) and NF-kappa-B control cell extract (cat#: 9243) were from Cell Signaling Technology® (Hitchin, UK). Novex™ Tris-Glycine SDS Sample Buffer (2X) (Cat#: LC2676), NuPAGE® MOPS SDS Running Buffer (20X) (Cat#: NP000), NuPAGE™ 4-12% Bis-Tris protein gels (cat#: NP0322BOX), SeeBlue™ Pre-stained protein standard (cat#: LC5625), NuPAGE™ Sample Reducing Agent (10X) (cat#: NP0004), NuPAGE™ Antioxidant (cat#: NP0005), SimplyBlue™ SafeStain and Novex® ECL HRP Chemiluminescent Substrate Reagent Kit (cat#: WP20005) were obtained from Invitrogen (Fisher Scientific). Immun-Blot® PVDF Membrane was purchased from Bio-Rad (Hemel Hempstead, UK). Marvel Original dried skimmed milk was from Premier International Foods (Lincolnshire, UK). Pierce™ Western Blotting Filter Papers were from Thermo Fischer Scientific. ReBlot Plus Mild Antibody Stripping Solution (10X) (cat#: 2502) was obtained from Millipore (Darmstadt, Germany).

### 2.8.2 Cell Stimulation and Sample Preparation

#### 2.8.2.1 Nrf2 and p38 MAP kinase in THP-1 cells

Two days after splitting,  $1 \times 10^6$  cells/well in a volume of 2 mL were seeded in 24-well plates and incubated overnight at 37°C, 5% CO<sub>2</sub> and under a humidified atmosphere. In the case of **Nrf2**: next day, 20 µM of selected common flavonoid metabolites and their esters or 30 µM DMF (positive control) or 0.1% DMSO (vehicle control) were added into the referred wells and one well left untreated to provide a basal control. The plate was returned to incubator for 3h. In the case of **p38 MAP kinase**: next day, 1 mL medium was removed and 20 µM FA, FA-Hex-Es, FA-Pro-Es, quercetin

or 10  $\mu\text{M}$  SB203580 (positive control) or 0.1%DMSO were added to the referred wells. The plate was returned to the incubator for 30 min prior to stimulation with 1  $\mu\text{g}/\text{mL}$  LPS for 1h.

### **2.8.2.2 NF- $\kappa\text{B}$ , c-Jun/c-Fos and JNK, in BV2 cells**

Two days after passaging, BV2 cells were counted and the cell density was adjusted to  $10^5$  cells/mL. Then  $2 \times 10^5$  cells/well were seeded in a 6-well plate and incubated overnight at  $37^\circ\text{C}$ . Next day, 1 mL media was removed and 20  $\mu\text{M}$  FA, 10  $\mu\text{M}$  F-Hex-Es and 10  $\mu\text{M}$  IFA-Et-Es were added and pre-incubated for 30 minutes at  $37^\circ\text{C}$ . For each experiment three wells were treated as control: one with only cells to provide basal control; one with DMSO (0.1%) to provide a vehicle control and one well with positive control. For those, 10  $\mu\text{M}$  BAY 11-7082 was used to inhibit NF- $\kappa\text{B}$  phosphorylation, 10  $\mu\text{M}$  SP600125 was used for JNK and c-Jun, and 10  $\mu\text{M}$  PD 098059 for c-fos. Following pre-incubation, cells were further treated with LPS and returned to the incubator. For NF- $\kappa\text{B}$  and, c-Jun & c-Fos 1  $\mu\text{g}/\text{mL}$  LPS stimulation for 2 h, and for JNK phosphorylation 10 ng/mL LPS for 30 min at  $37^\circ\text{C}$ .

### **2.8.3 Cell Lysate Preparation**

After the prescribed period of incubation time, for suspension cells (**THP-1**) the cells were homogenized and transferred into 1.5 eppendorf tubes and pelleted by centrifugation at 5000 rpm for 5 min. The supernatant was removed, and the pellet was washed with 1 mL ice-cold PBS by centrifugation at 5000 rpm for 5 min at  $4^\circ\text{C}$ . The PBS was removed, and the cell pellet was resuspended in 100  $\mu\text{L}$  ice-cold cell lysis buffer (recipe in Appendix I). This suspension was then sonicated for 10 pulses and returned to the ice. For adherent cells (**BV2**) the media was removed, and cells were lysed with 200  $\mu\text{L}/\text{well}$  cell lysis buffer on ice, then the lysates were transferred into pre-chilled eppendorf tubes on ice. Finally, cell lysates were boiled for 5 min and stored at  $-80^\circ\text{C}$  for further use. Protein concentrations

of cells lysates were measured using the NanoDrop® ND-1000 (Labtech, Uckfield, UK) as described in Section 2.5.5.2. Based on the total protein concentrations, sample loading volumes were calculated to ensure that each sample had an equal protein loading on electrophoresis gel.

### **2.8.4 Gel Electrophoresis**

In preparation for gel electrophoresis, a pre-cast NuPAGE® Novex 4 - 12% Bis-Tris gel was clamped into the XCell SureLock® Mini-Cell gel rig (Invitrogen) and the central chamber was filled with 1X Running Buffer (**Appendix I**). 500 µL NuPAGE® antioxidant was added to the central chamber and the gel wells were flushed out. The outer chamber was then filled with running buffer up to a level specified by the chamber case. In preparation for loading samples, 20-69 µg total protein lysates were reduced with NuPAGE™ Sample Reducing Agent (1:10) by short vortexing and boiling for 5 min. Then, protein lysates (15 µL for small gel (9-well); 20 µL for big gel (12-well) or 5 µL SeeBlue™ pre-stained protein standard (containing comparative molecular weight markers of 3-198 kDa) were loaded on the gel and run at 150 V until the leading bands had passed through the stacking gel. The voltage was then increased to 200 V and the samples run until the leading bands reached the foot of the gel.

### **2.8.5 Transfer**

Immun-Blot PVDF membrane was activated in methanol for 30 sec prior to equilibration in 1X complete transfer buffer (**Appendix I**) for at least 15 min on a shaker. Six blotting pads were equilibrated, and two filter papers were soaked in transfer buffer. Then the gel was sandwiched with pre-soaked filter paper and further placed between six blotting pads prior to placing in transfer chamber. The XCell II Blotting module was secured in the XCell rig and filled with 1X complete transfer buffer. The outer chamber was filled with 600 mL of deionized water. Finally, the transfer was run at 30 V for 1 h.

### **2.8.6 Immunoblotting**

The membranes were briefly stained with Ponceau S solution (0.1% (w/v) in 5% (v/v) acetic acid) for 3 min to visually assess protein transfer. The membrane was then rinsed off with 1X Tris Buffered Saline with 0.1% Tween-20 (TBS-T) (**Appendix I**). The membrane was blocked with blocking buffer (5% milk in 1X TBS-T) (**Appendix I**) at RT for 1 h on an orbital shaker (MaxQ 2000, Thermo Scientific). Primary antibodies were diluted to the optimised concentration (**Table 2. 3**) in BSA (5% BSA (w/v) in 1X TBS-T) except for Nrf2, which was diluted in blocking buffer. The membranes were incubated at RT on a roller (Bottle/Tube Roller, Thermo Fisher Scientific) at 45 rpm for 2 h at RT. Then the membranes were washed three times in blocking buffer and three times in TBS-T (5 min each). The membrane was then incubated with HRP- conjugated secondary antibody in blocking buffer on a roller at 45 rpm for 1 h at RT. The wash steps were repeated to remove non-bound antibodies from the membrane prior to detection of proteins.

Novex<sup>®</sup> ECL HRP Chemiluminescent Substrate Reagent Kit was removed from 4°C and allowed to reach RT for 30 min prior to imaging. The membrane was placed onto a clear plastic acetate and excess liquid was removed by blotting with filter paper. The Novex<sup>®</sup> ECL solution A and B were mixed at 1:1 ratio and pipetted onto the membrane and left to develop for 60 sec. Then the ECL solution was removed by blotting and the membrane was covered with another piece of clear plastic acetate to prevent drying. The membrane was imaged using an ImageQuant LAS 4000 series (GE Healthcare Life Sciences).

Table 2. 3 Primary and Secondary antibodies used in Western blotting assays.

<b>Target</b>	<b>Host</b>	<b>Suppliers</b>	<b>Product code</b>	<b>Dilution</b>
Nrf2 antibody- CHIP Grade	Rabbit mAb [EP1808Y]	Abcam	ab62352	1:500
P-p38 MAPK (Thr180/Tyr182)	Rabbit mAb (D3F9) XP®	CTS <sup>1</sup>	#4511	1:500
p38 MAPK	Rabbit mAb (D13E1 XP®)	CTS <sup>1</sup>	#8690	1:500
P-SAPK/JNK (Thr183/Tyr185)	Mouse (G9)	CTS <sup>1</sup>	#9255	1:500
SAPK/JNK	Rabbit mAb (56G8)	CTS <sup>1</sup>	#9258	1:500
P-NF-κB p65 (Ser536)	Rabbit mAb (93H1)	CTS <sup>1</sup>	#3033	1:500
NF-κB p65	Rabbit mAb (D14E12) XP®	CTS <sup>1</sup>	#8242	1:500
P-c-Jun (Ser63)	Rabbit mAb (54B3)	CTS <sup>1</sup>	#2361	1:500
c-Jun	Rabbit mAb (60A8)	CTS <sup>1</sup>	#9165	1:500
P-c-Fos (Ser32)	Rabbit mAb (D82C12)	CTS <sup>1</sup>	#5348	1:500
c-Fos	Rabbit mAb (9F6)	CTS <sup>1</sup>	#2250	1:500
β-Tubulin	Rabbit mAb (9F3)	CTS <sup>1</sup>	#2128	1:500
Rabbit IgG, HRP-Linked	Goat	CTS <sup>1</sup>	#7074	1:1000
Mouse IgG <sub>1</sub> , HPR-Linked	Goat	SCB <sup>2</sup>	Sc-2060	1:1000

<sup>1</sup>Cell Signaling Technology® (Hitchin, UK).

<sup>2</sup>Santa Cruz Biotechnology.

### **2.8.7 Re-Probing**

After imaging, the membranes were stripped for a second protein re-probing if needed. Briefly the membrane was stripped with 1X ReBlot Plus Mild Antibody Stripping Solution for 30 min on a shaker at RT, then washed twice for 5 min with TBS-T before probing with another primary antibody as per the afore mentioned immunoblotting procedure.

### **2.8.8 Densitometry**

To assess the changes in protein expression observed by western blot analysis, a semiquantitative method, the densitometry was used quantify the protein band density of each immunoblotting image. For this purpose, the bands on each single gel image were measured using gel analysis software in Fiji is Just Image J (1.52n, Wayne Rasband National Institute of Health, USA). Band density of proteins were normalized to the  $\beta$ -tubulin, then the ratio of phospho/non-phospho protein expressions were calculated using Excel, with the exception of Nrf2. The latter protein expression was relative to  $\beta$ -tubulin.



## 2.9 Transendothelial Migration Assay

### 2.9.1 Reagents

The polycarbonate trans-well inserts (3  $\mu\text{m}$  pore) of a 96-well plate were from Corning. Stock solution aliquots of N-formyl-methionyl-leucyl-phenylalanine (fMLP) (Sigma-Aldrich) provided at 1 mM in absolute ethanol and monocyte chemoattractant protein 1 (MCP-1) (CCL2) and CX3CL1 (fractalkine) were both provided at 100  $\mu\text{g}/\text{mL}$  in sterile water, stored at  $-80^{\circ}\text{C}$ . Gelatine (2% in water) was from Sigma-Aldrich, stored in  $4^{\circ}\text{C}$ . Paraformaldehyde (4% (w/v)) was from Molecular Probes (Life Technology). Antibodies against human leukocytes cell surface markers were from BioLegend and purchased from ITK Diagnostics BV, Uithoorn, Netherlands (detailed in **Table 2. 3**). 96-well round-bottom polystyrene plates were purchased from Fisher Scientific. Whole human blood or buffy coats (ABO/Rh A+/A-/B-) were obtained commercially from Sanquin Blood supply (Rotterdam, Netherlands) in accordance with Dutch regulations and following approval from the Dutch Medical Committee (NVT0034.01).

### 2.9.2 Seeding HMEC-1

To provide a better attachment of HMEC-1 to the trans-well, the inserts (apical compartment) of a 96-well plate were coated with 50  $\mu\text{L}$  0.01% gelatine (**Appendix I**) for 2 h at  $37^{\circ}\text{C}$ , 5%  $\text{CO}_2$ . After incubation, the excess gelatine was discarded, and HMEC-1 were seeded on the inserts at  $25 \times 10^4$  cells/insert (in 75  $\mu\text{L}$  volume) in HMEC-1 medium. The lower compartment (reservoir) of the 96-well plate was filled with 225  $\mu\text{L}$  HMEC-1 medium and the cells were allowed to grow for 48 h at  $37^{\circ}\text{C}$ , 5%  $\text{CO}_2$  atmosphere to form a monolayer on the filter. Twelve hours prior to the assay, the cells were starved by replacing the HMEC-1 medium with serum and antibiotic free DMEM media at both compartments.

### **2.9.3 PBMC Isolation from Whole blood**

Peripheral blood mononuclear cells (PBMCs) were isolated from whole blood by adding an 11x volume of red blood cell (RBC) lysis buffer (**Appendix I**), followed by incubation at RT for approximately 10 min until the solution became clear and dark red. Then the solution was transferred into a 50 ml falcon tube and centrifuged at 300 x g for 3 min to separate the PBMCs from lysed RBC debris. The cell pellet containing PBMC was further resuspended and washed twice with 50 mL DPBS (without Ca<sub>2</sub><sup>+</sup> and Mg<sub>2</sub><sup>+</sup>), containing 1 g/L glucose (to prevent osmotic shock) and remove remaining debris. Then, the isolated PBMCs were resuspended in 10 mL HMEC-1 medium, and the cell concentration was determined with an automated cell counter, the Nexcelom cellometer T4 (Nexcelom Bioscience LLC, Lawrence, MA, USA). Finally, the cell concentration was adjusted to 8 x 10<sup>6</sup> cells/mL in HMEC-1 medium and used immediately for transendothelial migration assay.

### **2.9.4 Seeding PBMCs & Adding Treatment and Fixing Migrated Cells**

After 12 h starvation, the media was removed from the inserts apical compartment and replaced with 6 x 10<sup>5</sup> cells/insert of total PBMCs (in 75 µL volume/insert). Then, the PBMCs were stimulated with 1 µM of each phenolic acid or 0.01% DMSO. The basal compartment of the reservoirs was filled with 215 µL/well of HMEC-1 medium with 10 nM fMLP, freshly prepared in warm HMEC-1 medium as described in **Figure 2. 1**. The transwell plate was then incubated for 3 h at 37 °C, 5% CO<sub>2</sub> atmosphere to allow transmigration of the PBMCs. Two equal volumes of isolated PBMCs were also incubated under the same conditions to provide pre- transendothelial migration controls for further flow cytometry analysis. After the stated incubation time, the migrated cells were then harvested from the basal compartments by re-suspending the cells with a pipette and transferred to

a new (v-shaped) plate followed by centrifugation at 400 g for 3.3 min. The pellet was washed with 230  $\mu\text{L}$  DPBS (washing buffer) and fixed with 50  $\mu\text{L}$  4% para-formaldehyde for 15 min at RT. Fixed cells were washed with 200  $\mu\text{L}$  DPBS to remove remaining formaldehyde. Finally, fixed samples were resuspended in 150  $\mu\text{L}$  DPBS and stored at 4°C for flow cytometry analysis up to one week.

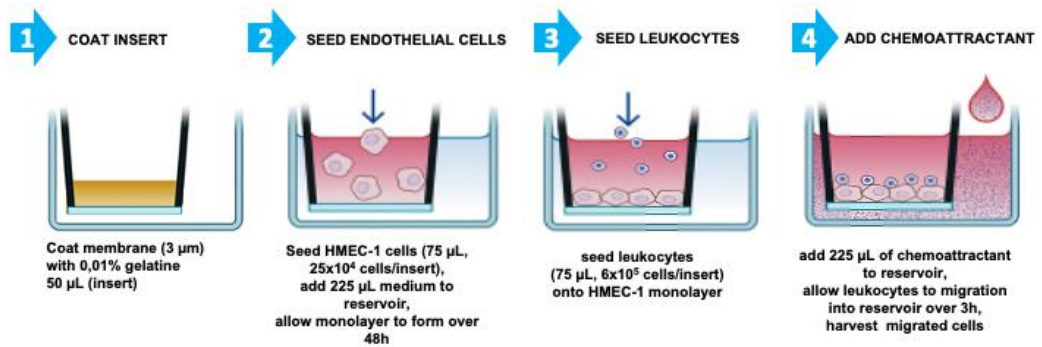


Figure 2. 1 Schematic overview of the transendothelial migration assay.

## 2.9.5 Flow Cytometry

Prior to flow cytometry, the fixed PBMCs from the transendothelial migration assay were removed from the fridge, 50  $\mu\text{L}$  FACS buffer added (**Appendix I**) and centrifuged at 450 x g for 3.3 min. The cell pellet of the pre-transendothelial migration sample (un-stained) was resuspended in 200  $\mu\text{L}$  FACS buffer and analysed to determine the background noise and to adjust threshold (voltage) for forward scatter (FSC), side scatter (SSC) and auto-fluorescence of un-stained cells. To phenotype and quantify transmigrated PBMCs, all samples were labelled with an antibody cocktail containing conjugated-antibodies for the total number of CD14, CD66b and CD45 positive cells, to differentiate between migrated monocytes, neutrophils, and all hematopoietic cells, respectively (**Table 2. 4**). The antibody labelling

was performed by incubating the cell pellet in 25  $\mu$ L Antibody cocktail (**Appendix I**) for 20-30 min in the dark at RT. To remove unbound antibody labels the cell content was washed with 200  $\mu$ L FACS buffer at 450 x g for 3.3 min. The stained cells were then resuspended in 150  $\mu$ L FACS buffer and transferred to a 96-well round-bottom polystyrene plate to analyse with the BD FACSVerser<sup>TM</sup> flow cytometry (BD Bioscience). CD markers were measured with a medium flow rate (60  $\mu$ L/min) and the positive events of each CD marker were gated (the gating strategy can be found in **Appendix III: Method optimisation**) and then counted as the number of transmigrated cells/ $\mu$ L sample by using BD FACSuite (v.1.0.6) software. The technical workflow of flow cytometry is stated in the scheme below (**Figure 2. 2 Schematic Workflow of Flow Cytometr**).

Table 2. 4 Cell surface markers for flow cytometry analysis.

<b>Characteristic(s) being measured</b>	<b>Analyte/ CD marker</b>	<b>Analyte Detector/ Antibody conjugate</b>	<b>Supplier/ Manufacturer</b>	<b>Clone</b>	<b>Cat#</b>	<b>Volume for staining of 10<sup>6</sup> cells</b>
All WBCs	CD45	Brilliant Violet 421™ anti-human CD45		HI30	304032	1.5 µL
Granulocytes, Neutrophils	CD66b	Alexa Fluor® 647 anti-human CD66b	ITK Diagnostics BV	G10F5	305110	1.25 µL
Monocytes	CD14	Alexa Fluor® 488 anti-human CD14		M5E2	301811	1.25 µL

## FACSVerse Experimental / Worklist

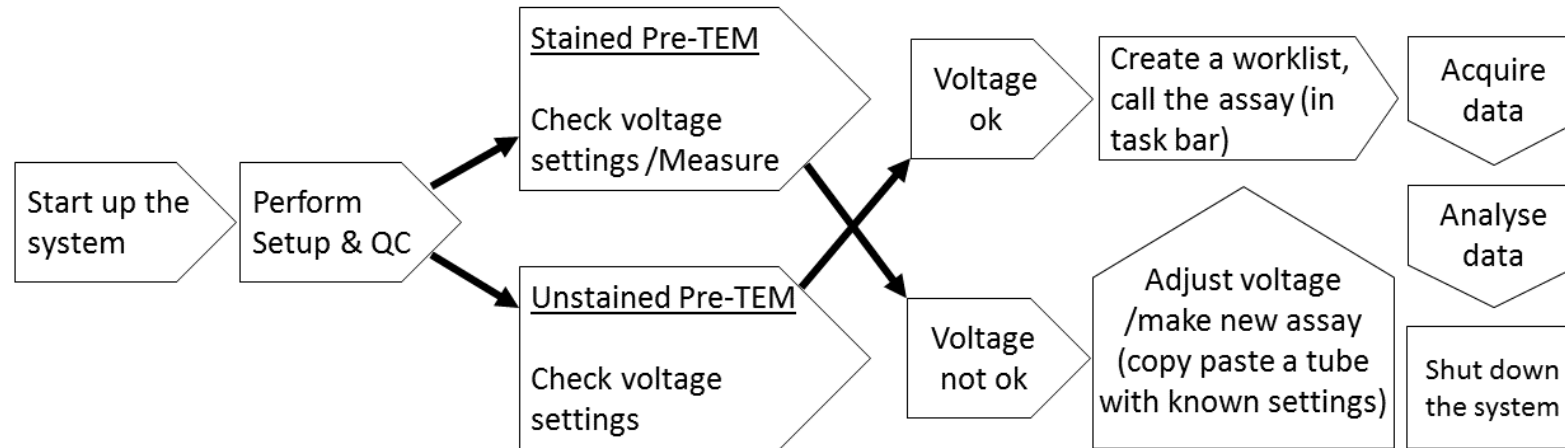


Figure 2. 2 Schematic Workflow of Flow Cytometry.

## 2.10 Chemotaxis and Calcium Flux

### 2.10.1 Reagents

The ChemoTx® Disposable Chemotaxis system (ChemoTx #: 101-5) with 5 µm pore size, a 96-well cell migration system, was purchased from Neuro Probe, Inc (MD 20877 USA). Black, opaque 96-well plates were from Thermo Fisher Scientific. Fura-2 AM calcium indicator was provided from Invitrogen. N-Formyl-Met-Leu-Phe (fMLP) (F3506) was from Sigma-Aldrich. Recombinant human MCP-1 (CCL2) was purchased from PeproTech EC, Ltd (London, UK) and recombinant human CCL3 was generously donated by Dr Lloyd Czaplewski of British Biotech and provided by Dr. Anja Mueller (from School of Pharmacy, University of East Anglia).

### 2.10.2 Chemotaxis Assay

**THP-1:** The chemotaxis assay was carried out using a ChemoTx® 5 µm pore transwell chemotaxis plate as previously described<sup>425</sup>. Briefly the wells to be used of a 96-well cell migration system were blocked with 30 µL blocking buffer (recipe in **Appendix I**) for 30 min at RT. Meanwhile, chemokine working solutions (0.3 nM MCP-1 or 1 nM CCL3) and phenolic acid working solutions (10 µM) were prepared in working buffer (**Appendix I**). THP-1 cells were harvested and spun down at 1200 rpm for 5 min, washed once with working buffer and then re-suspended to give an approximate concentration of  $1.25 \times 10^6$  cells/mL. THP-1 cells were then pre-treated with 1 µM phenolic acid working solutions or vehicle control (0.001% DMSO) or working buffer (basal control) and incubated for 30 min at 37°C with 5% CO<sub>2</sub>. Following blocking, the blocking buffer was removed from each well and replaced with either 31 µL of the relevant chemokine solution or 31 µL working buffer (basal control) with duplicates of each condition being conducted. Then the membrane (a polyvinylpyrrolidone-free polycarbonate filter with 5 µm pores) was carefully secured on the top of the 96-well plate and pre-treated cells in a volume of 20 µL  $125 \times 10^4$  cells/mL

( $25 \times 10^4$  cells/well) were pipetted on the top of the filter. Finally, the plate was covered and placed inside a humidified chamber and left to incubate at 100% humidity for 4 h at 37°C with 5% (v/v) CO<sub>2</sub>. After incubation, the remaining cells on the top of membrane were wiped off and the filter was carefully removed. Then, the content of each well was mixed by a pipette to re-suspend the cells before taking 10 µL for counting the migrated cells into the bottom of the compartment by using a Malassez haemocytometer and light microscopy.

**HL-60:** HL-60 cells were differentiated into neutrophil like cells (HL60-differentiated neutrophils) with 1 µM ATRA or 1.3 % DMSO for 3 days as per description above (in section 8.3.3.3 of **Appendix III**). HL60-differentiated neutrophils and HL-60 cells (non-differentiated control) were centrifuged at 1200 rpm for 5 min and cell pellet was resuspended in working buffer to a cell density of  $2.5 \times 10^5$  cells/mL. From this suspension, 20 µL was used as per description here above for THP-1 chemotaxis with the following exceptions: 10 nM fMLP and 5 nM CXCL12 were used in comparison to working buffer and the cells were allowed to migrate for 3h at 37°C.

### **2.10.3 Calcium Release Assay**

The calcium flux assay was conducted as described previously (Mills et al., 2018). Briefly THP-1 cells were collected and centrifugation at 1200 rpm for 5 min and washed once with 4 mL PBS (see recipe in **Appendix I**). The cell pellet was further washed twice with 1 mL calcium flux (CFX) buffer (**Appendix I**) at 1000 rpm for 11 sec before being re-suspended to give an approximate concentration of  $2 \times 10^6$  cells/mL. Cells were then probed with acetoxymethyl ester form of Fura-2 (Fura-2 AM; 4 µM) in 1 mL CFX buffer and incubated for 30 min at 37°C with 5% CO<sub>2</sub> in the dark to protect the dye from photobleaching. Fura-2 is a UV light-excitable, ratiometric Ca<sup>2+</sup> indicator. And acetoxymethyl ester form of Fura-2 (Fura-2 AM) is a



membrane permeant derivative of Fura-2. When added to cells, Fura-2 AM rapidly penetrated through the membrane to the cytosol where the AM-groups are hydrolysed by cellular esterases, generating Fura-2 which bind to intracellular free  $\text{Ca}^{2+}$  ions. (Oakes et al., 1988). Upon binding to  $\text{Ca}^{2+}$ , Fura-2 exhibits an absorption shift that can be observed by measuring the excitation spectrum between 300 and 400 nm, while monitoring the emission at ~510 nm (Spencer & Johnson, 2010). Following this, the cells were centrifuged at 1200 rpm and washed twice with CFX buffer to remove extra-cellular unbound Fura-2 AM and resuspended in 1 mL CFX buffer. Finally, 100  $\mu\text{L}$  cells were pipetted into a black, opaque 96-well plate and loaded into a BMG LabTech FLUOstar Optima Fluorometer (BMG Labtech, Germany). The Fluorometer microinjector pump was primed and back flushed twice with ice cold  $\text{H}_2\text{O}$  and the Gain set at 30% before running assay. Then, 20  $\mu\text{L}$  1  $\mu\text{M}$  (200  $\mu\text{M}$ ) chemokine was injected after 15 sec of assay running time and then monitored for a further 60 sec. Fura-2 fluorescence was measured at 340nm (bound to  $\text{Ca}^{2+}$ )/ 380nm (unbound to  $\text{Ca}^{2+}$ ) via a ratiometric analysis where a fixed emission frequency was set at 510 nm. The data was recorded and expressed as a change in fluorescence ratio (340nm/380nm) where the basal fluorescence prior to the addition of chemokine (15 sec) is subtracted from peak fluorescence (after 30-40 sec) following addition of chemokine. A ratio  $>0.2$  was considered a good response of receptor activation and vice versa.

## **2.11 Cytospin**

### **2.11.1 Reagents**

Reastain Quick-Diff kit staining solution and Reagena (Cat# 102164) were obtained from Invitech, (Huntingdon, UK). Thermo Scientific™ Polysine adhesion slides (Cat# 10219280) and Thermo Scientific™ Shandon™ TPX Single Sample Chamber, Caps, and Filter Cards (Cat# 11922355), and DPX mounting media were from Fisher Scientific.

### **2.11.2 Cytospinning and staining**

Cells were counted and density was adjusted to  $10^6$  cells/mL in RPMI complete media and 100  $\mu$ L ( $10^5$  cells) was pipetted on a polysine coated slide. Prior to sample pipetting, slides were prepared as followed: each slide was inserted in a cytoclip, then a filter card and a cytofunnel placed on the top of slide. The cytoclip was fastened and placed in a balanced position in cytospin (Thermo Scientific, Cytospin 4). Then, the sample was pipetted by gentle spinning motions into a cytofunnel followed by gently spinning at 450 rpm for 5 min. The slides were checked for even distribution of cells and left to air dry on a wet tissue overnight at RT. Air dried slides were stained with Reastain quick-diff kit staining solution according to the manufacturer's instructions (Reastain quick-diff Instructions for use Ver 2.0 ENG). Briefly, slides were fixed in ice-cold methanol for 5 min, then stained for 2 min in Quick-Diff red solution and 2 min in Quick-Diff blue solution. The excess stain was washed gently under running tap water. The slides were checked under the microscope and air dried overnight at RT. Slides were sealed with a droplet of DPX mounting media and a coverslip glass and left to dry at RT for up to 1 h. Finally, cell morphology was examined and imaged by using the Leica Microsystems CMS GmbH Fluorescence Microscope and Leica Application Suite software (Leica, Mannheim, Germany).

## **2.12 General Flow Cytometry**

### **2.12.1 Reagents**

CD11b mouse anti-human antibody (Clone: ICRF44) was from eBioscience™ and obtained from Fisher Scientific. Alexa Fluor® 488 goat anti-mouse (Cat# A11001) was from Life Technologies™ (Thermo Fisher Scientific) and Human BD Fc Block™ (Cat# 564219) was from BD Biosciences (Oxford, UK). Mouse anti-human TNF- $\alpha$  membrane form FITC-conjugated monoclonal antibody (Clone# 6401, Cat# FAB210F), and FITC-conjugated mouse IgG<sub>1</sub> control (Clone# 11711, Cat# IC002F) were obtained from R & D Systems (Biotechne, Abingdon, UK). DAPI (Cat# D9542) was from Sigma-Aldrich.

### **2.12.2 Differentiated HL-60 Flow Cytometry**

HL-60 were differentiated for 3 days with 1 $\mu$ M ATRA or 1.3% DMSO (section 2.11.2). Then, cell density was determined and 3x 10<sup>6</sup> cells per sample were spun at 300xg for 5 min. The cell pellet was washed with 1.5 mL PBS. Cells were then resuspended in 300  $\mu$ L staining buffer (0.5% BSA in DPBS) with FC blocker (1:200) and divided into three pre-labelled tubes for unstained, isotype (goat anti mouse IgG) and CD11b stained. Tubes were incubated 10 min at RT. Then, the primary antibody CD11 (1:100) was added to the referred tubes and incubated on ice for 30 min. The unstained samples were kept on ice until the last washing step. After incubation, stained samples were washed with 1.5 mL staining buffer and resuspended in 100  $\mu$ L secondary antibody mouse IgG Alexa Fluor® 488 (1:200) (to both isotype and CD11b stained samples) and incubated for 30 min on ice in the dark. Following incubation, all sample were washed with 1.5 mL staining buffer. Finally, the cells were resuspended in 300  $\mu$ L staining buffer and markers were measured by CytoFLEX Flow Cytometry and acquisition and analysis carried out using CytExpert (V2.10) (Beckman Coulter Life Sciences). For each sample, 10,000 events were recorded with a slow flow

rate (10  $\mu\text{L}/\text{min}$ ). Gate (P1 [X-axis, forward scattered area; Y-axis side scattered area]) was drawn around dots representing viable cells to exclude cell debris, doublets, and other particles. Data collected in P1 was then plotted for FITC intensity (x-axis) against cell count (y-axis) to assess the fluorescence intensity of differentiated cells in comparison to non-differentiated cells, and isotype control.

### **2.12.3 mTNF- $\alpha$ Flow Cytometry**

In the case of mTNF- $\alpha$ , THP-1 cells were seeded at a density of  $5 \times 10^5$  cells/mL in 1 mL in 24-well plate and pre-treated for 30 min with SB 203580 (10, 20  $\mu\text{M}$ ) or Celastrol (10  $\mu\text{M}$ ). Pre-treatment was followed by 4 h stimulation with 1  $\mu\text{g}/\text{mL}$  LPS. Afterwards, cells were collected in an eppendorf and spun at 300xg for 5 min, then washed with 1 mL PBS. Cells were then resuspended in 100  $\mu\text{L}$  staining buffer (0.5% BSA in DPBS) with FC blocker (1:200) and divided into three pre-labelled tubes for unstained, isotype, and mTNF- $\alpha$ . Tubes were incubated 10 min at RT. Then, primary antibody mTNF- $\alpha$  (specific to membrane form, FITC-conjugated) (1:15) and isotype (mouse IgG<sub>1</sub> FITC -conjugated) (1:15) was added to the referred tubes and incubated on ice for 30 min in the dark. The unstained samples were kept on ice until last washing step. After incubation, all samples were washed with 1 mL staining buffer and resuspended in 300  $\mu\text{L}$  staining buffer. Markers were measured by CytoFLEX Flow Cytometry and acquisition and analysis were carried out using CytExpert (V2.10) (Beckman Coulter Life Sciences). 10,000 events per sample was recorded with a medium flow rate (30  $\mu\text{L}/\text{min}$ ). Gating strategy was exactly as above for the differentiated HL-60 flow cytometry.

## **2.13 Fluorescent Microscopy**

mTNF- $\alpha$  stained for flow cytometry (previous section) was assessed with fluorescence microscopy to assess antibody binding efficiency to membrane form of TNF- $\alpha$ . For this purpose, following flow cytometry analysis, the samples were kept at 4°C overnight. Next day, cells were spun at 300xg for 5 min and the cell pellet was resuspended in 100  $\mu$ L DAPI stain (1:1000 in PBS) and incubated on ice for 5 min in the dark to allow the nuclear staining. The cells were washed with 1 mL PBS and resuspended in 30  $\mu$ L PBS. 10  $\mu$ L was pipetted on a clean slide and covered with a cover slip. The edges of the cover slip were sealed with nail polish and stored in a cupboard in the dark. Next day, cell images were taken by using the Leica Microsystems CMS GmbH Fluorescence Microscope and Leica Application Suite software (Leica, Mannheim, Germany).

Table 2.5. Antibodies and controls used in General Flow Cytometry & Fluorescent Microscopy.

<b>Target</b>	<b>Host/ clone</b>	<b>Suppliers</b>	<b>Product code</b>	<b>Dilution</b>
Human CD11b	Mouse [ICRF44]	eBioscience™	12-0118-42	1:100
Human BD Fc Blocker	n.a.	BD	564219	1:200
Mouse IgG (Alexa Fluor® 488)	goat	Life Technologies	A11001	1:200
Human TNF- $\alpha$ Membrane Form (FITC)	Mouse [6401]	R & D Systems	FAB210F	1:15
IgG <sub>1</sub> control (FITC)	Mouse [11711]	R & D Systems	IC002F	1:15

## **2.14 Statistical Analysis**

For LPS experiments, the data obtained from each independent experiment was normalized to LPS control unless otherwise stated. Effects of the phenolic acids were assessed compared to 0.1% DMSO (vehicle control (VC)) unless otherwise stated. In the case of more than two comparisons, the treatment effects were established by One-way analysis of variance (ANOVA), Post-Hoc Dunnett's test by using SPSS (v23.0, IBM, New York, USA), unless otherwise stated. In the case of two comparisons (comparing a control to VC), data was assessed by a two-tailed independent sample t-test using Excel (version 2016, (Microsoft Corporation, WA, USA). The statistical significance was set at  $p < 0.05$ . Error bars, where shown, indicates the standard error of means between three biological replicates. \* $p < 0.05$ , \*\* $p < 0.01$ , \*\*\* $p < 0.001$ , \*\*\*\* $p < 0.0001$ . For the transendothelial migration assay, samples were tested for normality with the D'Agostino & Pearson omnibus normality test. Pearson's correlation coefficient was determined with Microsoft Excel and a normal distribution was assumed.

**Chapter 3. Effect of Phenolic  
Metabolites and Their Synthetic  
Conjugates on Inflammatory and  
Oxidative Stress Biomarkers in THP-1  
monocytes**



### 3.1 Introduction

Flavonoid consumption is inversely correlated with a reduced risk of developing CVD <sup>34,48,180,426</sup>. High consumption is associated with an improvement in vascular and endothelial function <sup>427</sup>, lower blood pressure <sup>182,212</sup>, and a reduction in other CVD-associated biomarkers (incl. endothelin-1, pulse wave velocity <sup>211</sup>, LDL, ox-LDL, CRP, TNF- $\alpha$ , IL-6, IL-10, MCP-1, ICAM, VCAM <sup>198,229</sup>, <sup>34,179</sup>). Low grade chronic inflammation and oxidative stress are two key underlying factors in the pathogenesis of CVD and the beneficial health effects of flavonoids has been attributed to their anti-inflammatory and anti-oxidative properties. More recent evidence suggests that their observed health effects are likely to occur through crosstalk between multiple pathways <sup>89</sup> including inhibition of NF- $\kappa$ B and the MAPK pathways as well as through activation of Nrf2.

Until recently, *in vitro* studies predominantly focused on the anti-inflammatory effects of flavonoids in their native form and at supraphysiological concentrations. However, following ingestion, flavonoids are extensively metabolised in the body via bacterial catabolism in the gut or conjugation by phase II drug metabolizing enzymes in the liver and kidney. Physiological concentrations of flavonoid metabolites identified in the serum have been reported to be between 0.1- 40  $\mu$ M <sup>42</sup>. The most common microbial catabolites found in the serum are the benzoic acid derivatives including protocatechuic acid (PCA), vanillic acid (VA) and 4-hydroxy benzoic acid (4HBA), and the cinnamic acid derivatives including caffeic acid (CA) and ferulic acid (FA) <sup>20,89,147</sup>. It is worth mentioning that these phenolic acids are also naturally found in food stuffs and hence bioavailability is possibly even higher <sup>79</sup>. Furthermore, evidence from the literature indicates that in addition to metabolites derived from bacterial catabolism, their conjugation with glucuronide, sulfate, methyl and glycine are possible, resulting from phase II drug metabolizing enzymes <sup>41</sup>. Previous research has focused on the presence and the effect of sulfate and glucuronide conjugates <sup>19,46,47</sup>. However, glycine conjugation has in

general been regarded as a detoxification mechanism of xenobiotics<sup>428,429</sup> and a plausible route for flavonoid metabolism and excretion, the research on the presence and effect glycine conjugated metabolites is lacking.

Flavonoids and their metabolites are diverse, and studies of their structure activity relationships (SAR) are lacking despite the availability of numerous unnatural synthetic analogues and such approaches may reveal the mechanism of the interaction between functional groups and the target molecules. It is promising to study the SAR of common phenolic acids with a low molecular weight, with one benzene ring that bear one or two hydroxyl groups (seen in **Table 3. 1**, e.g. 4HBA, PCA) or one hydroxy and one methoxy group (e.g. VA, FA) to understand which group(s) at which position are important for greater bioactivity by comparing their bioactivity to non-natural simple phenolic acids (hydroxy or methoxy group replaced with a chloro, bromo, amino or nitro group).

Moreover, in addition to sulfates and glucuronides, metabolism of flavonoids with other small chemical group conjugation by phase II enzymes are in theory possible. For instance, glycation of xenobiotics is possible<sup>428–430</sup>. As previously reported by our group and others, flavonoid metabolites as conjugated phenolic acids (e.g. sulfate- and glucuronide conjugates) of PCA, VA, IVA, 4HBA have been synthesised and screened<sup>18,19,46,47,431</sup> for their effects on pro-inflammatory biomarkers (e.g. TNF- $\alpha$ , IL-1 $\beta$ , IL-6 and sVCAM-1) in THP-1 cells and HUVEC<sup>19,46,47</sup>. Furthermore, those studies also investigated the combined effect of flavonoid metabolites on inflammatory biomarkers for their additive or synergistic effects. On the other hand, studies of additive or synergistic effects of flavonoid metabolites with anti-inflammatory food bioactives such as omega-3 fatty acids<sup>432</sup> are lacking despite well documented cardio protective effects of omega-3 fatty acids, *cis*-5,8,11,14,17-eicosapentaenoic acid (EPA) and *cis*-4,7,10,13,16,19-docosahexaenoic acid (DHA)<sup>433–437</sup>.

Furthermore, in *in vivo* and *in vitro* studies, flavonoids and their metabolites display a moderate non-linear U-shaped concentration response curve

<sup>19,426</sup>. Our group have previously found that at physiological concentrations, specific flavonoids and metabolites modestly inhibit secretion of the pro-inflammatory biomarker TNF- $\alpha$  and induce expression of the anti-oxidant biomarker HO-1, a downstream target of Nrf2 in THP-1 monocytes. The observed effects are not dose-dependent, possibly due to colloidal formation in culture <sup>153,438,439</sup>. It is unclear if the effect of flavonoid metabolites at physiological concentrations can be enhanced by altering the structure without changing the functional groups.

## 3.2 Aims and objectives

- Screen and compare 7 naturally occurring phenolic acids with 14 non-natural analogues for their effects on LPS-induced TNF- $\alpha$  secretion in THP-1 cells (**Table 3. 1**) and establish SAR
- Investigate the additive (sum of their separate effect) or synergistic (greater than their sum) effects of naturally occurring phenolic acids with omega-3 fatty acids on LPS-induced TNF- $\alpha$  secretion in THP-1 cells
- Synthesise and screen glycinated forms of these 7 naturally occurring phenolic acids (**Table 3. 1**) for their effects on LPS-induced TNF- $\alpha$  secretion in THP-1 cells
- To understand the absorption and solubility of metabolites in *in vitro* assays, synthesise and screen esterified forms of these 7 phenolic acids (**Table 3. 1**) and establish SAR to study mechanisms of action (MOA)
- Understand the mechanisms of action (MOA) of the most active metabolites on inflammatory and antioxidant pathways

Table 3. 1 List of common parental flavonoid metabolites and analogues used in this study.

No	Metabolites	Acronym
<b>Common parental/ flavonoid metabolites</b>		
1	4-Hydroxybenzoic acid	4HBA
2	3,4-Dihydroxybenzoic acid ( <b>Protocatechuic acid</b> )	PCA
3	3,4-Dihydroxycinnamic acid ( <b>Caffeic acid</b> )	CA
4	3-Hydroxy-4-methoxybenzoic acid ( <b>Isovanillic acid</b> )	IVA
5	4-Hydroxy-3-methoxybenzoic acid ( <b>Vanillic acid</b> )	VA
6	3-Hydroxy-4-methoxycinnamic acid ( <b>Isoferulic acid</b> )	IFA
7	4-Hydroxy-3-methoxycinnamic acid ( <b>Ferulic acid</b> )	FA
<b>Synthetic analogues</b>		
8	Benzoic acid	BA
9	2-Iodobenzoic acid	2IBA
10	3-Iodobenzoic acid	3IBA
11	3-Chlorobenzoic acid	3CBA
12	3-Aminobenzoic acid	3ABA
13	3-Hydroxybenzoic acid	3HBA
14	4-Aminobenzoic acid (para-aminobenzoic acid)	4ABA
15	4-Nitrobenzoic acid	4NBA
16	4-Bromobenzoic acid	4BBA
17	2,4-Dihydroxybenzoic acid	24DHBA
18	2,4-Dimethoxybenzoic acid	24DMBA
19	3,5-Diaminobenzoic acid	35DABA
20	3-Chloro-4-methoxybenzoic acid	3C4MBA
21	5-Chloro-2-methoxybenzoic acid	5C2MBA
<b>Novel synthetic analogues, Glycinated</b>		
22	4HBA-glycine	4HBA-Gly
23	PCA-glycine	PCA-Gly
24	CA-glycine	CA-Gly
25	IVA-glycine	IVA-Gly
26	VA-glycine	VA-Gly
27	IFA-glycine	IFA-Gly
28	FA-glycine	FA-Gly
<b>Novel synthetic analogues, Esters</b>		

29	PCA-methyl ester	PCA-Met-Es
30	PCA-ethyl ester	PCA-Et-Es
31	PCA-isopropyl ester	PCA-Prop-Es
32	PCA-hexyl ester	PCA-Hex-Es
33	VA-hexyl ester	VA-Hex-Es
34	IFA-methyl ester	IFA-Met-Es
35	IFA-ethyl ester	IFA-Et-Es
36	IFA-hexyl ester	IFA-Hex-Es
37	FA-methyl ester	FA-Met-Es
38	FA-ethyl ester	FA-Et-Es
39	FA-propyl ester	FA-Prop-Es
40	FA-hexyl ester	FA-Hex-Es

## **3.3 Results**

### **3.3.1 Effect of flavonoid metabolites, related phenolic acids, and synthetic analogues on LPS-induced TNF- $\alpha$ secretion in THP-1 cells**

#### **3.3.1.1 Optimisation of TNF- $\alpha$ measurement in THP-1 cells**

The assay for measuring LPS-induced TNF- $\alpha$  secretion in THP-1 cells previously established in the laboratory was first further optimised to enable higher throughput screening of selected compounds. The cell seeding density ( $5 \times 10^5$  cells/well) and incubation time point for metabolites (30 min) and LPS (3 h) were previously established and TNF- $\alpha$  secretion measured by ELISA (di Gesso, 2015). Note to mention that, the pre-incubation time point of flavonoids was established by using only PCA. Cells were pre-incubated with 0.1, 1, 10, 100  $\mu$ M PCA prior to stimulation with LPS for 0.5, 4, 18 and 24 h. The TNF- $\alpha$  protein secretion was reduced maximally at 0.5 h for all tested concentrations and therefore chosen as optimal pre-incubation time. The rationale to choose the 30 min pre-incubation time point for all metabolites in the present study was based on the previous work from our lab <sup>19,47</sup>, and the assumption that the tested compound, PCA was a representative compound for all selected metabolites <sup>440</sup>. In the present study, three experiments were conducted to (1) determine optimal LPS concentration (1 ng/mL), (2) provide the assay with a positive control (10  $\mu$ M SB 203580) and (3) use an optimal plate for a high-throughput screening (24-well) as illustrated in **Figure 3. 1 (details in Appendix III)**.

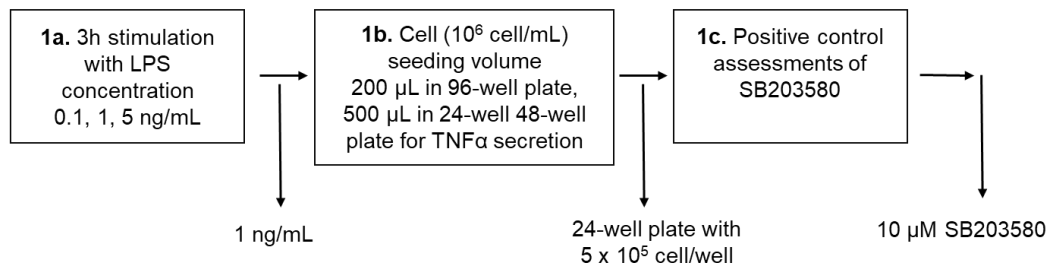


Figure 3. 1 Flow chart of method optimisation for measuring LPS-induced TNF- $\alpha$  secretion in THP-1 cells.

In order to evaluate the optimal concentration of LPS for TNF- $\alpha$  secretion in THP-1 cells, the following concentrations were assessed: 0.1, 1 and 5 ng/mL. **Figure 3. 2 (A)** indicates a concentration-dependent response in THP-1 cells. 1 ng/mL LPS was selected as a suitable concentration for further experiments. Previous studies have used various positive controls for LPS-induced TNF- $\alpha$  secretion in THP-1 cell assays, including bardoxolone, PD 98059 and SB203580. For this study SB203580, a p38 MAPK inhibitor was validated as a positive control for reducing LPS-induced TNF- $\alpha$  secretion. **Figure 3. 2 (B)** demonstrates that 10  $\mu$ M SB203580 significantly decreased LPS-induced TNF- $\alpha$  secretion measured by ELISA. This control was used in all subsequent experiments.



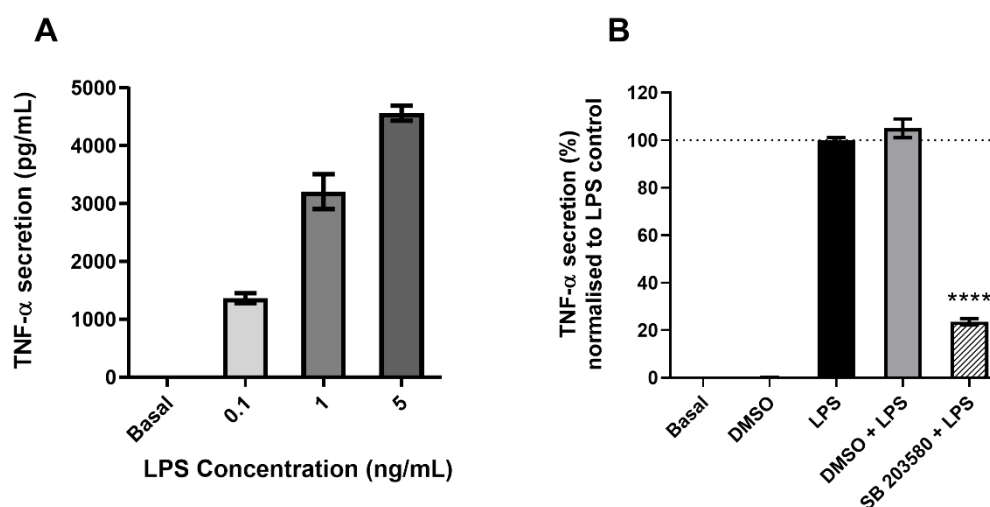


Figure 3. 2 Optimisation of LPS concentration and positive control for TNF- $\alpha$  secretion in THP-1 cells.  $5 \times 10^5$  cells/well were incubated with LPS (0.1, 1 and 5 ng/mL) for 3 h (A) or pre-incubated with 0.1% DMSO (vehicle control) and 10  $\mu$ M SB203580 (positive control) for 30 min, prior to treatment with LPS (1 ng/mL) for 3 h (B). TNF- $\alpha$  secretion was measured by ELISA assay. (A) Mean  $\pm$  SEM,  $n=2$ , expressed as pg/ml secreted TNF- $\alpha$  and (B) protein concentration expressed as percentage of LPS control, mean  $\pm$  SEM,  $n=4$ . Significant reduction by positive control compared to VC analysed by T-test. \*\*\*\* $p \leq 0.0001$ .

### 3.3.1.2 Effects of flavonoid metabolites and related phenolic acid analogues on LPS-induced TNF- $\alpha$ secretion in THP-1 cells

The most common flavonoid metabolites found in serum are the phenolic acids ferulic acid (FA), isoferulic acid (IFA), vanillic acid (VA), isovanillic acid (IVA), caffeic acid (CA), protocatechuic acid (PCA) and 4-hydroxybenzoic acid (4HBA). Prior to screening, the effects of these and related compounds were assessed for their effects on cell viability to ensure any observed effects were not due to cell death or senescence. Compounds of interest were tested at 1  $\mu$ M and 10  $\mu$ M concentrations. THP-1 cells were incubated with each compound for 24 h prior to the addition of MTS assay reagent for 3 h. None of the compounds affected cell viability (in **Appendix II**),

suggesting they could be used in cell assays at these concentrations. The effects of these metabolites on LPS-induced TNF- $\alpha$  secretion were then assessed in THP-1 cells. For this purpose, 1  $\mu$ M and 10  $\mu$ M concentrations were chosen to represent physiologically achievable levels found in the serum <sup>20,42</sup>. In addition to naturally occurring phenolic acid metabolites, phenolic acid analogues with chloro, bromo, amino and nitro-benzoic acid were included to determine any SAR of phenolic acid metabolites. SB203580 was included to ensure the assay was working. **Figure 3. 3** demonstrates that SB consistently reduced TNF- $\alpha$  secretion by approximately 65%. Although the selected phenolic acids slightly reduced LPS-induced TNF- $\alpha$  secretion (14-18% relative to VC), there was no significant reductions at either of the tested concentrations.

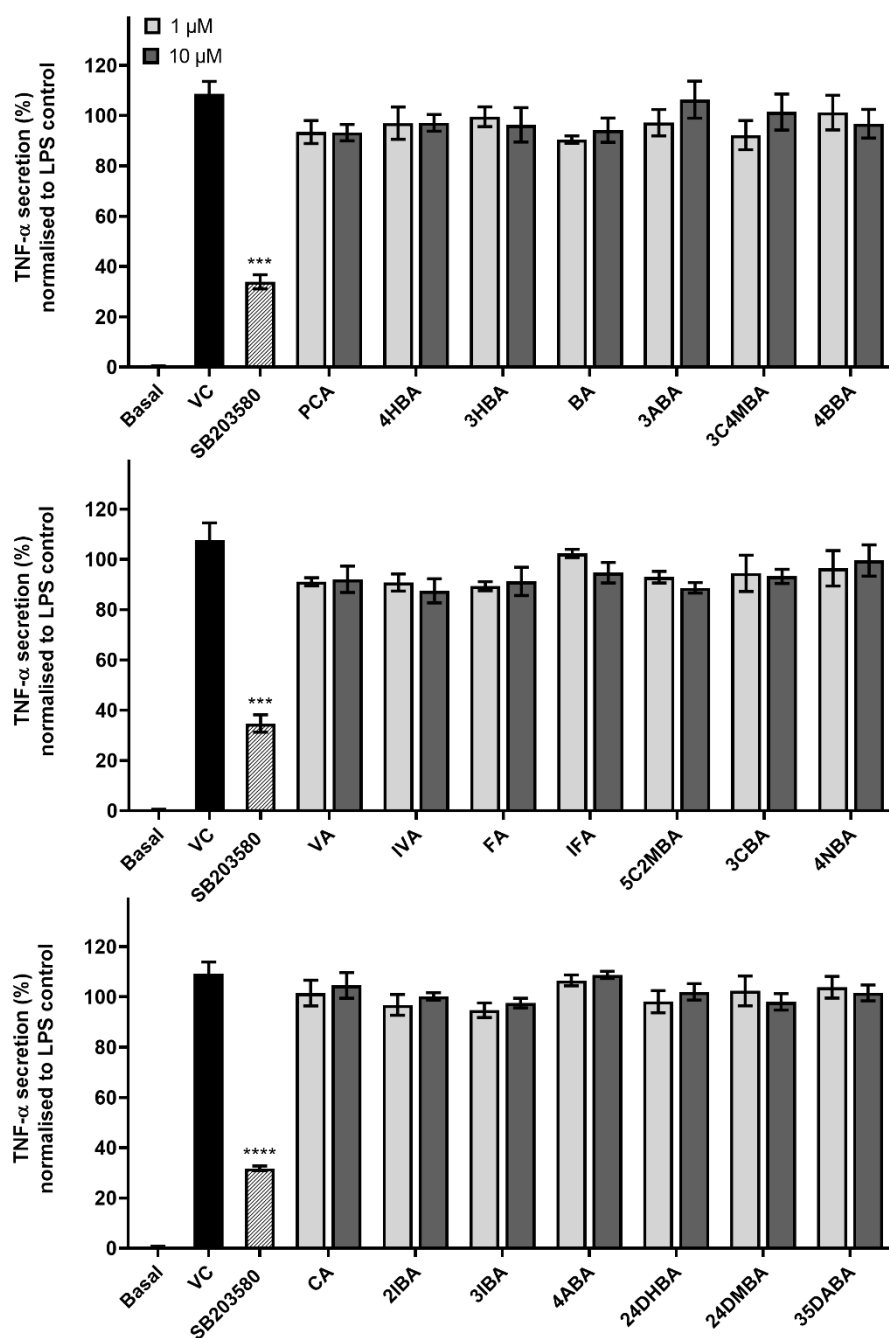


Figure 3. 3 Flavonoid metabolites and related phenolic acids do not reduce LPS-induced TNF- $\alpha$  secretion in THP-1. Cells ( $5 \times 10^5$ ) were treated with 1 and 10  $\mu$ M phenolic acids or 0.1% DMSO (vehicle control, VC) and 10  $\mu$ M SB 203580 (positive control) for 30 min prior to stimulation with LPS (1 ng/ml) for 3 h. TNF- $\alpha$  secretion measured by ELISA and protein concentrations expressed as a percentage of LPS control (not shown). Data mean + SEM,  $n = 3$ . No significant difference between phenolic acids and VC by one-way ANOVA with post hoc Dunnett's test. Significant difference ( $p < 0.05$ ) between SB 203580 and VC by t-test. \*\*\*\* $p \leq 0.0001$ .

### **3.3.2 Combined effect of flavonoid metabolites with $\Omega$ -3 fatty acids on LPS-Induced TNF- $\alpha$ secretion in THP-1 monocytes and macrophages**

Omega-3 polyunsaturated fatty acids (PUFAs) such as EPA and DHA are essential fatty acids with reported benefits in various diseases including mental health <sup>441</sup>, CVD <sup>435,442</sup> and atherosclerosis <sup>436</sup> and they improve endothelial function <sup>443</sup>. Although omega-3 fatty acids effectively incorporate into the cellular membrane of virtually all immune cells, their specific mechanisms of action on immune cell function is cell type specific (e.g. activation, infiltration and migration) <sup>444</sup>. The anti-inflammatory effect of EPA and DHA is partly due to competing with formation of pro-inflammatory prostaglandins <sup>432</sup> but mainly due to their bioactive lipid metabolites such as resolvins D(RvD) and E (RvE) series, maresins (MaR) and protectins (PD), which are collectively termed specialised pro-resolving mediators (SPMs) <sup>432,434</sup>. The SPMs are generated in the body by aspirin and Cox2 enzymatic conversion <sup>432</sup> and involved in resolution of inflammation and tissue homeostasis <sup>445</sup>. The anti-inflammatory effect of EPA and DHA is widely studied in macrophages <sup>444,446</sup> as they are the key player in lipid metabolism and widely used model for fatty acid work <sup>447</sup>. Moreover, in response to omega-3 fatty acids, macrophages are the only immune cell types that polarise towards M2 phenotype (anti-inflammatory type) with reduced pro-inflammatory cytokine production and secretion <sup>444</sup>. Therefore, they are a valid model to study anti-inflammatory effects. Treatment of THP-1-derived, LPS-activated macrophages with EPA and DHA induces changes in gene expression involved in the immune response, cell cycle, apoptosis and oxidative stress <sup>448</sup> and combination treatment of EPA and DHA shows greater inhibitory effect on pro-inflammatory gene expression including MCP-1, IL-6 and TNF- $\alpha$  <sup>449</sup> than either alone.

Previously studies have shown that combination treatment of flavonoid metabolites have an additive effect for preventing expression of VCAM-1 and IL-6 in HUVECs <sup>20</sup> and TNF- $\alpha$  in THP-1 monocytes <sup>19</sup>. Aspirin is the

acetylated form of salicylic acid, which is a common phenolic acid. We hypothesised that structurally related, common simple phenolic acids might have an additive or synergistic effect with EPA or DHA. Therefore, we investigated the combined effects of common phenolic acids with EPA and DHA on TNF- $\alpha$  secretion in THP-1 monocytes and macrophages.

Optimisation of THP-1 differentiated into macrophage and pre-incubation of EPA & DHA treatment

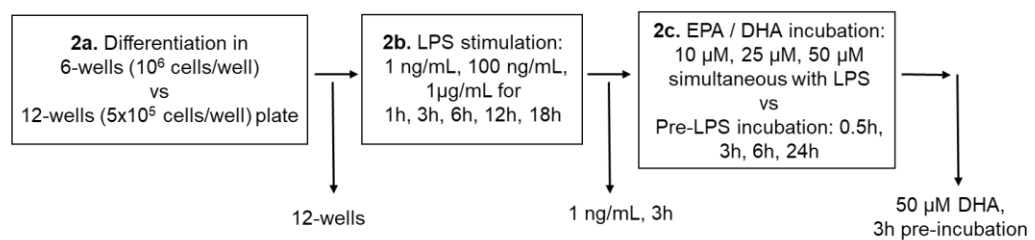


Figure 3. 4 Flow chart of method optimisation for effects of combined omega-3 fatty acids and flavonoid metabolites in THP-1 macrophages.

### 3.3.2.1 THP-1 differentiation into macrophages

THP-1 cells can be differentiated into macrophage-like phenotypes by using phorbol-12-myristate-13-acetate (PMA) or  $1\alpha, 25$ -dihydroxyvitamin D<sub>3</sub> (vD<sub>3</sub>) and macrophage colony-stimulating factor (M-CSF) <sup>450</sup>. PMA-induced THP-1-derived macrophages secrete similar levels of IL-1 $\beta$  and TNF- $\alpha$  to human PBMC monocyte-derived macrophages. THP-1 cells were differentiated with 200 nM PMA for 3 days (**Figure 3. 4**) to investigate the combination effects of flavonoid metabolites with EPA and DHA on LPS-induced TNF- $\alpha$  secretion. Various cell densities for THP-1 differentiation and LPS stimulation for TNF- $\alpha$  secretion have been previously reported <sup>446,448,449,451</sup>. Cell differentiation experiments were optimised using various parameters including optimal size of wells and concentrations and kinetics

of LPS, EPA and DHA used (**Appendix III**). THP-1 monocytes without PMA were also seeded as a control. **Figure 3. 5** shows that PMA-treated cells were attached to the wells and demonstrated elongated or expanding morphologies, indicating that cells were differentiated into macrophage-like cells. No major difference was observed between cells differentiated in 6-well and 12-well plates. In contrast, non-differentiated cells looked crowded in the wells, indicating cell division and growth. Similarly, to previous experiments, LPS (1 ng/mL for 3 h) was suitable for further experiments.

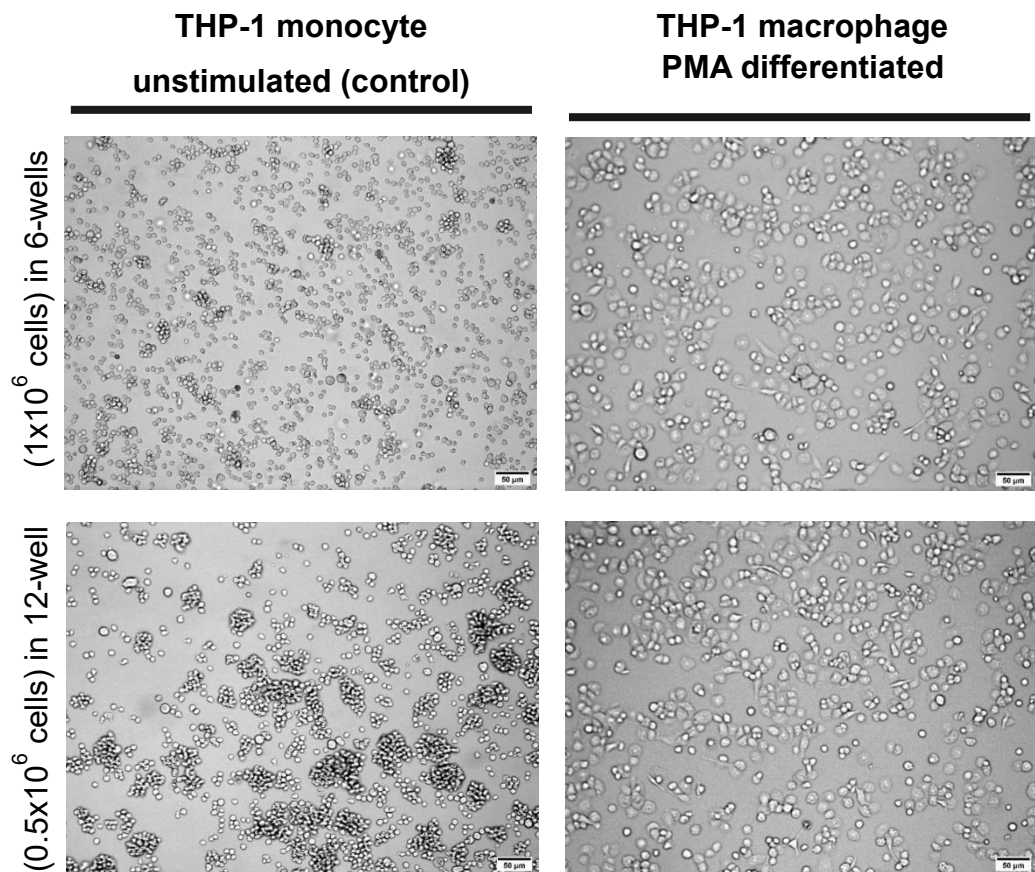


Figure 3. 5 PMA differentiation of THP-1 monocytes. THP-1 cells (1x10<sup>6</sup>/mL) were treated with 200 nM PMA in 6-well-plates and 12-well-plates for 72 h at 37°C. Microscopy images taken with 10X magnification (scale bar=50 µm).

### **3.3.2.2 Optimisation of addition of EPA, DHA or a mixture of both on LPS-induced TNF- $\alpha$ Secretion in THP-1 monocytes and macrophages**

Prior to the screening of combination effects of flavonoid metabolites with  $\omega$ -3 fatty acids, optimisation experiments were conducted to test the pre-incubation effect of fatty acids on LPS-induced TNF- $\alpha$  secretion in THP-1 monocytes and macrophages. THP-1 macrophages were differentiated as described above. Then, treatments of 10  $\mu$ M, 25  $\mu$ M or 50  $\mu$ M EPA, DHA or a mixture of EPA+DHA were co-incubated with 1 ng/mL LPS for 3 h. A vehicle control (VC) (0.1% DMSO) and a positive control, 10  $\mu$ M SB 203580, were also included. None of these showed any significant effect on LPS-induced TNF- $\alpha$  secretion, measured by ELISA (**Appendix III**). Next, undifferentiated, or differentiated THP-1 cells were pre-incubated with 10, 25, 50  $\mu$ M EPA, DHA or EPA+DHA or 0.1% DMSO (VC) for 0.5, 3 or 6 h prior to addition of LPS for 3 h and TNF- $\alpha$  secretion measured by ELISA. **Figure 3. 6 (A,B,C)** indicates that in THP-1 monocytes, pre-treatment up to 6 h with DHA or EPA (50  $\mu$ M) reduced TNF- $\alpha$  secretion with the 3 h pre-treatment demonstrating the most reduction. In THP-1 macrophages (**Figure 3. 6 D, E, F**), 50  $\mu$ M DHA alone inhibited LPS-induced TNF- $\alpha$  secretion with 0.5-6 h pre-treatment and 10  $\mu$ M DHA inhibited with 6 h pre-treatment. 50  $\mu$ M DHA showed the most reduction with 3 h pre-incubation and the combination of EPA+DHA showed similar effects as DHA alone in both monocytes and macrophages. 50  $\mu$ M DHA with 3 h pre-incubation time was therefore used in further experiments in both cell types.

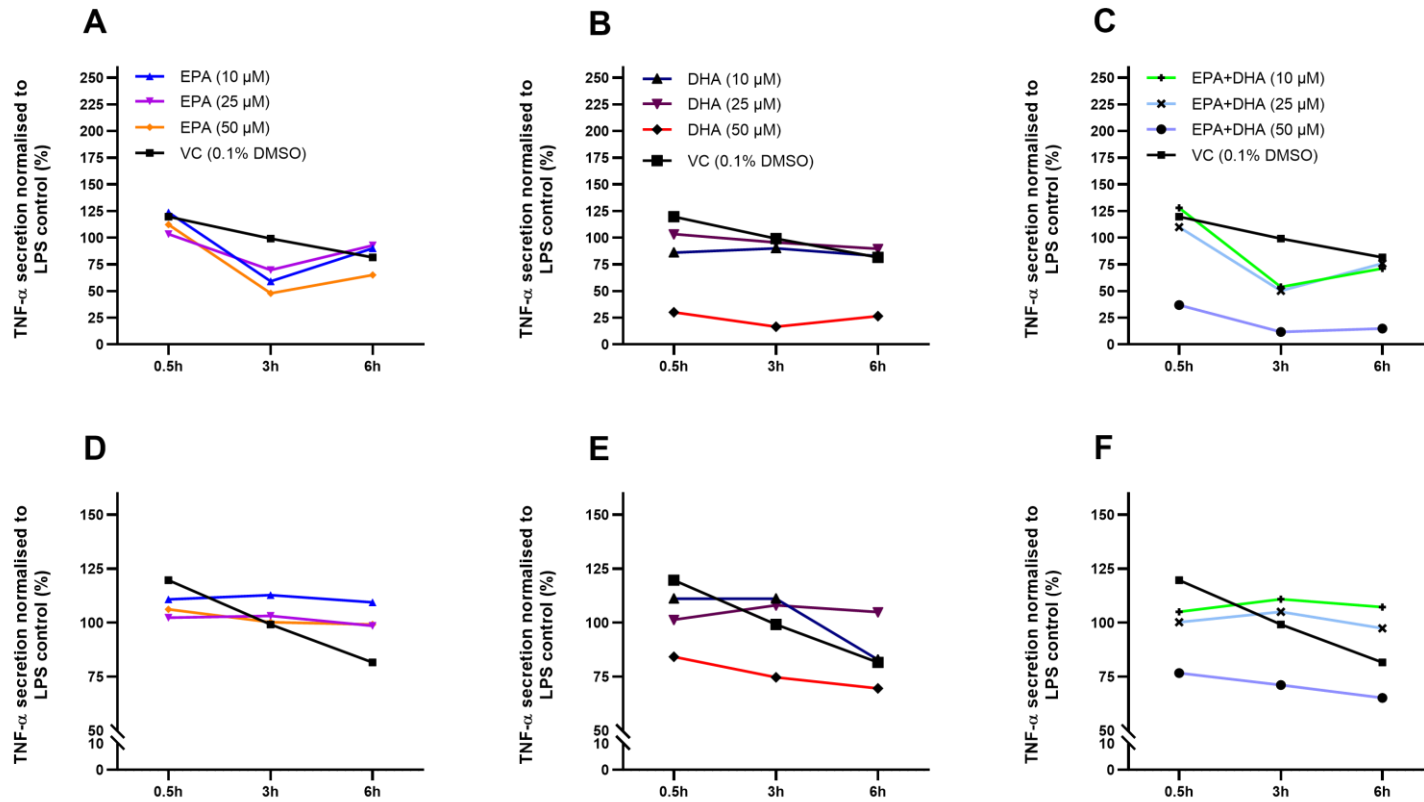


Figure 3.6 Pre-incubation of DHA, EPA and EPA+DHA reduces LPS-stimulated TNF- $\alpha$  secretion in THP-1 monocytes and macrophages. THP-1 monocytes ( $5 \times 10^5$  cells/well) (A, B, C) or differentiated macrophages (D, E, F) were pre-incubated with 10, 25, 50  $\mu$ M EPA, DHA and EPA+DHA or 0.1% DMSO (VC) for 0.5, 3 or 6 h prior to treatment with 1 ng/mL LPS for 3 h. TNF- $\alpha$  secretion was measured by ELISA. Data is from a single biological experiment and expressed as percentage of LPS control (not shown).



### **3.3.2.3 Combined effects of flavonoid metabolites with DHA on LPS-induced TNF- $\alpha$ secretion in THP-1 monocytes and macrophages**

THP-1 monocytes or macrophages were pre-treated with 50  $\mu$ M DHA for 2.5 h before addition of PCA, VA, IVA, CA, FA, or IFA (10  $\mu$ M) for 30 min. Finally, LPS was added for 3 h. As before, none of the tested flavonoid metabolites alone showed any effect on LPS-induced TNF- $\alpha$  secretion in monocytes but 50  $\mu$ M DHA alone significantly reduced it (**Figure 3. 7**). Similar to monocytes, single treatments of tested flavonoid metabolites showed no significant reduction in macrophages (**Figure 3. 8**) but 50  $\mu$ M DHA alone significantly reduced LPS-induced TNF- $\alpha$  secretion. Combination treatments of 50  $\mu$ M DHA with 10  $\mu$ M selected metabolites showed similar significant effects on TNF- $\alpha$  secretion as DHA alone suggesting no additive or synergistic effects of the selected flavonoid metabolites with DHA.

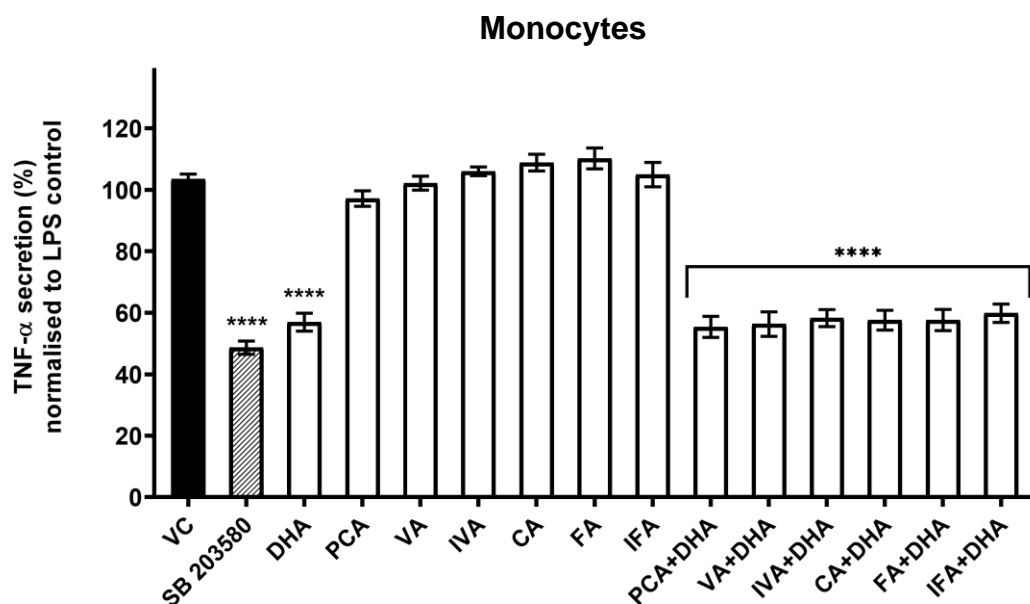


Figure 3. 7 Combined effects of 10  $\mu$ M phenolic acids with 50  $\mu$ M DHA on LPS-induced TNF- $\alpha$  secretion in THP-1 monocytes. Cells ( $5 \times 10^5$ /well) were pre-incubated for 2.5 h with 50  $\mu$ M DHA prior to treatment with 10  $\mu$ M phenolic acids (alone or in combination with DHA) or 0.2% DMSO (vehicle control, VC), and 10  $\mu$ M SB 203580 (positive control) for 30 min. After this, cells were stimulated with LPS (1ng/mL) for 3 h. TNF- $\alpha$  secretion was measured by ELISA. Data is expressed as a percentage of LPS-control. Mean  $\pm$  SEM, n=3. Significant ( $p < 0.05$ ) difference between treatment and VC analysed by one-way ANOVA with post hoc Dunnett's test and between VC and SB203580 by t-test. \*\*\*\*  $p < 0.00001$ .

### Macrophages

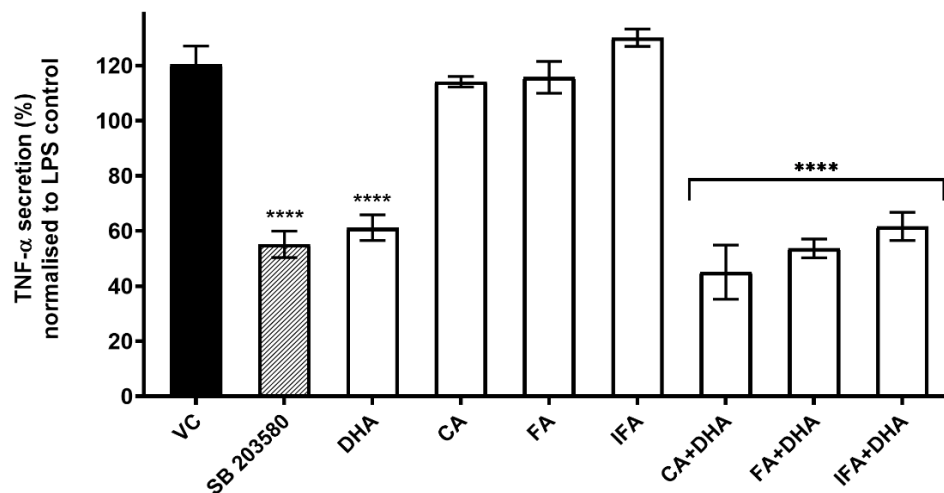
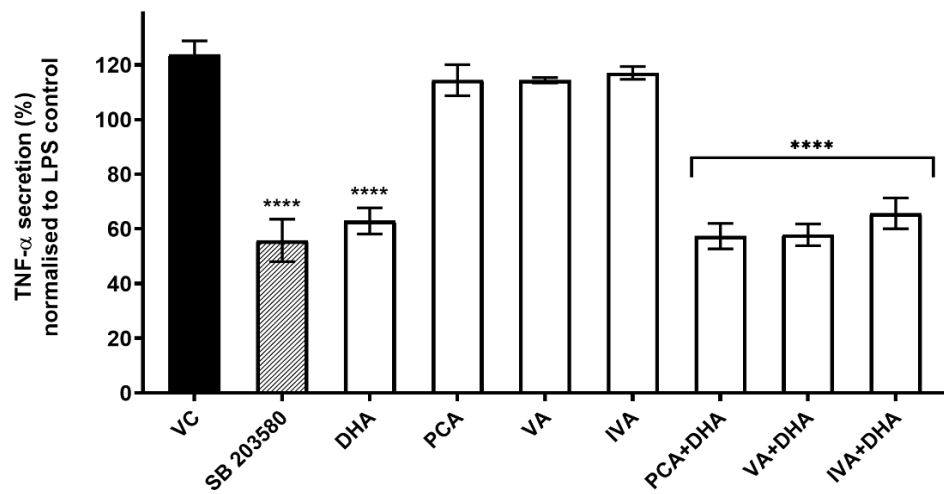


Figure 3.8 Combined effects of 10  $\mu$ M phenolic acids with 50  $\mu$ M DHA on LPS-induced TNF- $\alpha$  secretion in THP-1 macrophages. Cells ( $5 \times 10^5$ /well) were differentiated with PMA (200nM) for 3 days. They were then pre-incubated for 2.5 h with 50  $\mu$ M DHA prior to treatment with 10  $\mu$ M phenolic acids (alone or in combination with DHA) or 0.2% DMSO (vehicle control, VC), and 10  $\mu$ M SB 203580 (positive control) for 30 min. After this, cells were stimulated with LPS (1ng/mL) for 3 h. TNF- $\alpha$  secretion was measured by ELISA. Data is expressed as a percentage of LPS-control. Mean  $\pm$  SEM, n=3. Significant ( $p < 0.05$ ) difference between treatment and VC analysed by one-way ANOVA with post hoc Dunnett's test and between VC and SB203580 by t-test. \*\*\*\*  $p < 0.00001$ .

### **3.3.3 Effects of glycine-conjugated phenolic acids on LPS-induced TNF- $\alpha$ secretion in THP-1 monocytes**

Previous studies by our group and others have concluded that specific flavonoid metabolites are more active than their parent compounds. Our previous studies have focused on sulphate or glucuronide metabolites<sup>18,19,47,431</sup>. Although conjugation of flavonoids with glycine in theory is possible<sup>452</sup>, their presence and extent in the circulation is unclear and to our knowledge, there are no previous studies of their effects on pro-inflammatory biomarkers.

The lack of research on glycine conjugation as flavonoid metabolites is partly due to the lack of reference compounds as analytical standards to investigate their presence and excretion as glycine conjugates, with the exception of hippuric acid<sup>89</sup>. In addition, the fact that glycation is a common deportation system of drugs and other xenobiotic molecules from the body<sup>429,452</sup>, it could be difficult to differentiate whether glycinated metabolites are originating from flavonoids or other dietary precursors. For instance, as a detoxification mechanism, glycine conjugation of aromatic acids, especially benzoates (a commonly used food preservative) have generally been assumed to increase water solubility to facilitate urinary excretion<sup>452</sup>. Consequently, it poses a challenge to differentiate between hippuric acid derived from dietary flavonoid metabolites or from food preservative benzoates.

For this study, we synthesized glycine conjugates to investigate their effect on pro-inflammatory biomarkers as well as to provide reference compounds to be used as analytical standards to enable specific metabolites to be identified in future studies.

The novel glycine conjugates of protocatechuic acid (PCA-Gly), caffeic acid (CA-Gly), ferulic acid (FA-Gly), isoferulic acid (IFA-Gly), vanillic acid (VA-Gly), isovanillic acid (IVA-Gly) and 4-hydroxy benzoic acid (4HBA-Gly) were

studied for their effects on TNF- $\alpha$  secretion in THP-1 cells. Their effects on cell viability at 1  $\mu$ M and 10  $\mu$ M were first examined using the MTS assay. The compounds had no effect on cell viability at the tested concentrations (**Appendix II**). These compounds were then investigated for their effects on LPS-induced TNF- $\alpha$  secretion in THP-1 cells. indicates that there was no significant effect with any metabolite. CA-Gly (10  $\mu$ M) reduced TNF- $\alpha$  secretion by 20%, but this was not statistically significant. However, there were some possible concentration-dependent effects with CA-Gly and FA-Gly, therefore further dose response experiments were carried out.

Table 3. 2 Effects of 1 and 10  $\mu$ M glycine-conjugated phenolic acids on LPS-induced TNF- $\alpha$  secretion in THP-1 cells.

Treatment Effect on TNF- $\alpha$ Level	Average change from VC (% $\pm$ SD)			
	1 $\mu$ M	P value	10 $\mu$ M	P value
Protocatechuic acid glycine ( <b>PCA-Gly</b> )	$\uparrow$ 9.2 $\pm$ 13.2	0.574	$\downarrow$ 4.9 $\pm$ 5.1	0.837
4-hydroxy benzoic acid-glycine ( <b>4HBA-Gly</b> )	$\downarrow$ 4.3 $\pm$ 4.2	0.559	$\downarrow$ 3.41 $\pm$ 3.1	0.682
Vanillic acid-glycine ( <b>VA-Gly</b> )	$\downarrow$ 0.4 $\pm$ 6.0	0.996	$\downarrow$ 4.4 $\pm$ 7.4	0.690
Isovanillic acid-glycine ( <b>IVA-Gly</b> )	$\uparrow$ 1.6 $\pm$ 3.5	0.945	$\downarrow$ 2.0 $\pm$ 8.4	0.912
Ferulic acid-glycine ( <b>FA-Gly</b> )	$\downarrow$ 4.0 $\pm$ 8.5	0.957	$\downarrow$ 8.8 $\pm$ 32.7	0.812
Isoferulic acid-glycine ( <b>IFA-Gly</b> )	$\uparrow$ 6.3 $\pm$ 0.9	0.914	$\downarrow$ 5.2 $\pm$ 37.3	0.939
Caffeic acid-glycine ( <b>CA-Gly</b> )	$\downarrow$ 10.6 $\pm$ 9.9	0.527	$\downarrow$ 20.7 $\pm$ 19.1	0.157

THP-1 ( $5 \times 10^5$  cells/well) were pre-treated with 1 or 10  $\mu$ M of phenolic acid-glycine or 0.1% DMSO (VC) for 30 min prior stimulation with LPS (1 ng/mL) for 3 h. TNF- $\alpha$  secretion was measured by ELISA. Protein concentration was normalised to LPS control (data not shown) and expressed as percentage. Data mean change from VC  $\pm$ SD, n=3. No significant ( $p < 0.05$ ) difference between glycinated metabolites and VC by one-way ANOVA with post hoc Dunnett's test.

Glycinated conjugates were further tested at 0.1, 1, 10 and 20  $\mu\text{M}$  concentrations. However, although CA-Gly and FA-Gly again demonstrated an apparent trend in reducing secretion in a concentration-dependent manner, there was no significant effect on LPS-induced TNF- $\alpha$  secretion at any concentration (**Figure 3. 9**), suggesting these compounds were not anti-inflammatory at these concentrations.

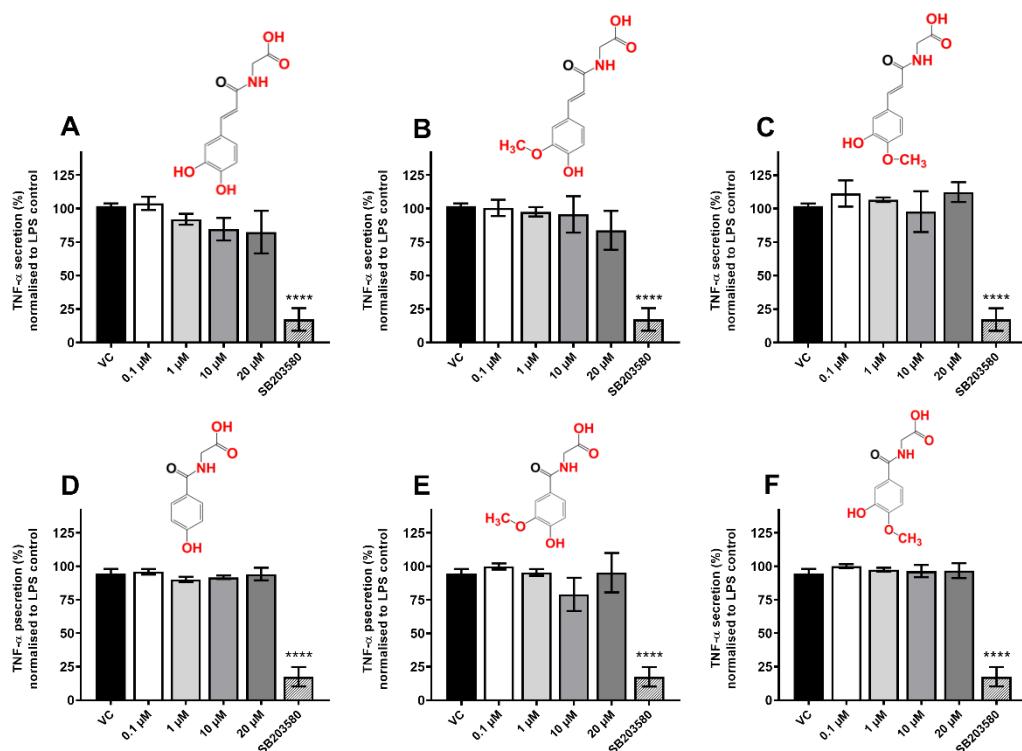


Figure 3. 9 Concentration-dependent effects of glycine-conjugated phenolic acids on LPS-induced TNF- $\alpha$  secretion in THP-1. Cells ( $5 \times 10^5$ /well) were pre-treated with 0.1, 1, 10 or 20  $\mu\text{M}$  CA-Gly (A), FA-Gly (B), IFA-Gly (C), 4HBA-Gly (D), VA-Gly (E), IVA-Gly (F), or 0.1% DMSO (vehicle control, VC) and 10  $\mu\text{M}$  SB203580 (positive control) for 30 min prior to stimulation with LPS (1 ng/mL) for 3 h. TNF- $\alpha$  secretion was measured by ELISA. Data expressed as a percentage of LPS control (not shown). Mean  $\pm$  SEM,  $n=4$ . No significant ( $p < 0.05$ ) difference between treatment and VC by one-way ANOVA with post hoc Dunnett's test. Comparison of SB203580 vs VC done with student's t-test.

### **3.3.4 Effect of esterified phenolic acids on LPS-induced TNF- $\alpha$ secretion in THP-1 cells**

Esterification of natural products, for example ginsenoside <sup>453</sup>, quercetin <sup>454</sup> and rosmarinic acid <sup>455</sup> can enhance their cellular uptake and bioactivity. Novel ester analogues of common dietary flavonoid metabolites were synthesised. They included -methyl, -ethyl, -propyl and -hexyl esters of the benzoic acid derivatives PCA and VA, and the cinnamic acid derivatives FA and IFA.

Following synthesis, twelve synthetic analogues were first tested for their effects on the viability of THP-1 cells. None of the analogues at the concentrations used in any experiments had any significant effect on cell viability (**Appendix II**). Then all twelve analogues were investigated at 1 and 10  $\mu$ M concentrations for their effects on LPS-induced TNF- $\alpha$  secretion in THP-1 cells. **Table 3.3** indicates that 10  $\mu$ M FA-hexyl ester (FA-Hex-Es) and the FA-propyl ester (FA-Pro-Es) significantly reduced TNF- $\alpha$  secretion compared to the VC. In each experiment PCA, VA, IVA, FA, and IFA were included to compare the effect of ester analogues with their parent compound (data not shown). Moreover, a concentration-dependent response was apparent for some analogues. To examine if these compounds at higher concentrations would be more potent, dose response experiments were performed for those compounds with a hexyl ester.

Table 3. 3 Effect of phenolic acid esters on LPS-induced TNF- $\alpha$  secretion.

Treatment Effect on TNF- $\alpha$ Level	Average change from VC (% $\pm$ SD)			
	1 $\mu$ M	P value	10 $\mu$ M	P value
Protocatechuic acid-methyl ester (PCA-Met-Es)	↓ 8.4 $\pm$ 17.5	0.791	↓ 4.9 $\pm$ 17.9	0.936
Protocatechuic acid-ethyl ester (PCA-Et-Es)	↓ 11.1 $\pm$ 8.2	0.619	↓ 7.8 $\pm$ 20.1	0.778
Protocatechuic acid-isopropyl ester (PCA-Pro-Es)	↓ 22.3 $\pm$ 26.3	0.517	↓ 8.3 $\pm$ 33.3	0.898
Protocatechuic acid-hexyl ester (PCA-Hex-Es)	↑ 2.3 $\pm$ 12.2	0.857	↓ 7.7 $\pm$ 5.1	0.420
Vanillic acid hexyl-ester (VA-Hex-Es)	↑ 0.4 $\pm$ 6.8	0.993	↑ 1.5 $\pm$ 4.8	0.905
Ferulic acid methyl-ester (FA-Met-Es)	↓ 14.6 $\pm$ 22.6	0.725	↑ 4 $\pm$ 34.8	0.974
Ferulic acid ethyl-ester (FA-Et-Es)	↑ 3.0 $\pm$ 5.5	0.760	↓ 9.3 $\pm$ 8.2	0.163
Ferulic acid propyl-ester (FA-Pro-Es)	↓ 2.5 $\pm$ 1.0	0.054	↓ <b>6.6 <math>\pm</math> 1.5</b>	<b>0.001</b>
Ferulic acid hexyl-ester (FA-Hex-Es)	↓ 8.7 $\pm$ 8.4	0.371	↓ <b>24.8 <math>\pm</math> 10.6</b>	<b>0.016</b>
Isoferulic acid-methyl ester (IFA-Met-Es)	↑ 3.7 $\pm$ 4.3	0.787	↓ 0.6 $\pm$ 12.7	0.994
Isoferulic acid-ethyl ester (IFA-Et-Es)	↓ 21.2 $\pm$ 10.7	0.086	↓ 13.7 $\pm$ 12.4	0.270
Isoferulic acid-hexyl ester (IFA-Hex-Es)	↑ 1.3 $\pm$ 10.4	0.977	↑ 0.1 $\pm$ 11.4	1.000

THP-1 ( $5 \times 10^5$  cells/well) were pre-treated with phenolic acid esters or 0.1% DMSO (vehicle control, VC) for 30 min prior to incubation with LPS (1 ng/mL) for 3 h. TNF- $\alpha$  secretion was measured by ELISA and data was expressed as mean percentage change from VC  $\pm$  SD, n=3. Significant ( $p < 0.05$ ) difference between treatment and VC by one-way ANOVA with post hoc Dunnett's test.

The parent compounds FA and CA as well as ester analogues with the longest alkyl chains (PCA-Hex-Es, IFA-Hex-Es and FA-Hex-Es) were included to investigate effects at higher concentrations and potential SAR. **Figure 3. 10** demonstrates that FA-Pro-Es (D) and FA-Hex-Es (F) significantly reduced LPS-induced TNF- $\alpha$  secretion in a concentration-dependent manner.



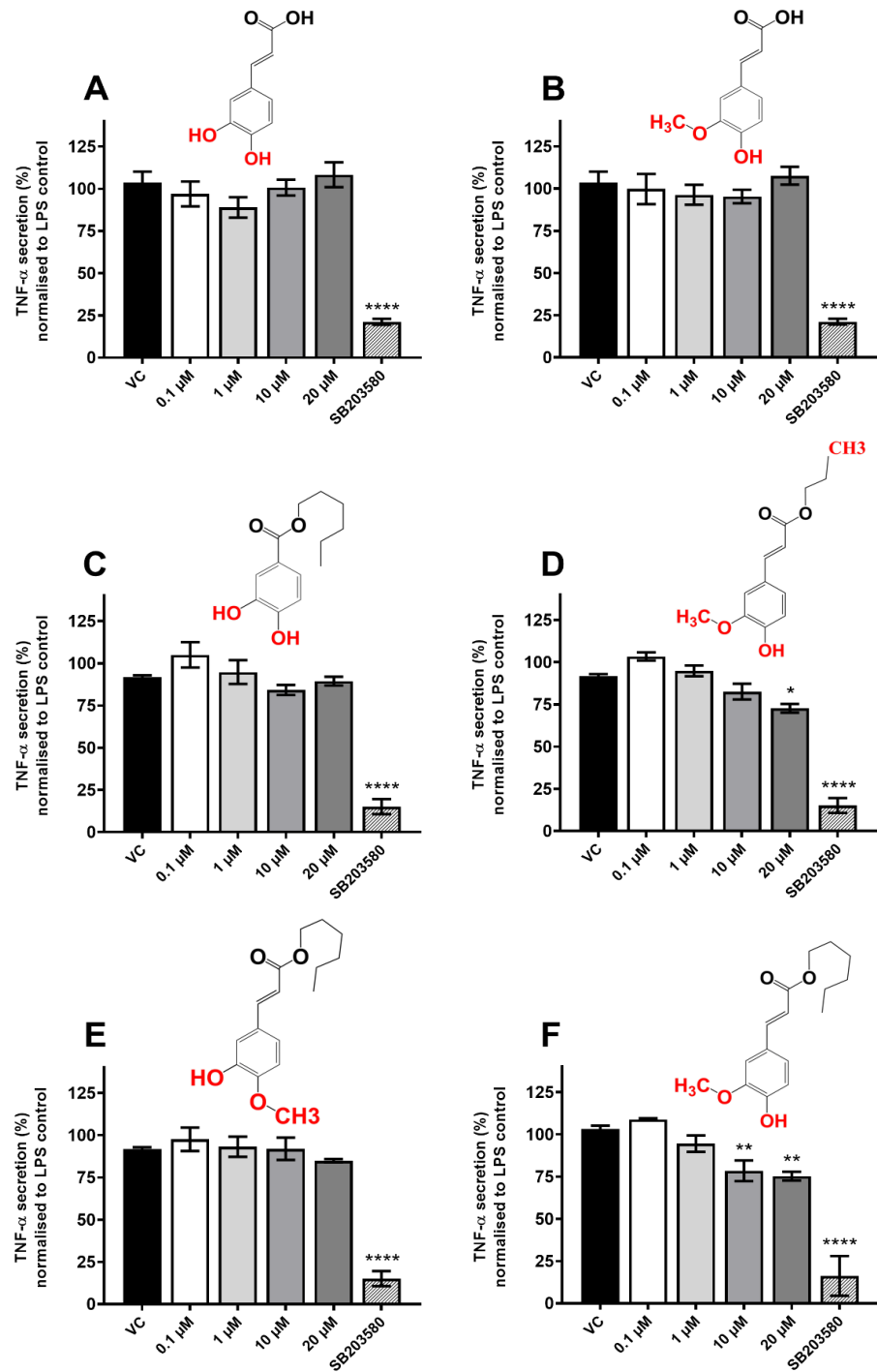


Figure 3. 10 FA-Hex-Es and FA-Pro-Es significantly and dose-dependently reduce LPS-stimulated TNF- $\alpha$  secretion in THP-1. Cells ( $5 \times 10^5$ /well) were pre-treated with 0.1, 1, 10, 20  $\mu$ M of caffeic acid (A), ferulic acid (B), PCA-Hex-Es (C), FA-Pro-Es (D), IFA-Hex-Es (E), FA-Hex-Es (F), or 0.1% DMSO (VC) and 10  $\mu$ M SB 203580 (positive control) for 30 min prior stimulation with LPS (1 ng/mL) for 3 h. TNF- $\alpha$  secretion was measured by ELISA and results normalised to LPS control. Mean  $\pm$  SEM,  $n=3$ . Significant difference ( $p < 0.05$ ) between treatment and VC by one-way ANOVA with post hoc Dunnett's test. Comparison of positive control vs VC done by Student's t-test. \* $p \leq 0.05$ ; \*\*  $p \leq 0.01$ ; \*\*\*\*  $p \leq 0.0001$ .

### **3.3.5 FA-Hex-Es and FA-Pro-Es do not affect LPS-induced TNF- $\alpha$ mRNA expression in THP-1 cells**

Since FA-Hex-Es and FA-Pro-Es at 20  $\mu$ M significantly reduced LPS-induced TNF- $\alpha$  secretion, their intracellular mechanism of action was studied. Firstly, we determined whether the effect was upstream of mRNA translation by examining mRNA expression. THP-1 cells were seeded at  $1 \times 10^6$  cells/well and pre-treated for 30 min with of 20  $\mu$ M FA, FA-Pro-Es, FA-Hex-Es, or 0.1 % DMSO (VC). In addition, 20  $\mu$ M BAY 11-7082 (BAY) was included as a positive control. This inhibits I $\kappa$ B $\alpha$  phosphorylation and has previously been reported to decrease LPS-induced TNF- $\alpha$  mRNA expression<sup>456</sup>. SB203580 was not suitable as it inhibits p38 mediated post-translational repression of TNF- $\alpha$  mRNA<sup>283</sup>. After pre-treatment, cells were stimulated with 1 ng/mL LPS for 2 h as previously described<sup>440</sup>. **Figure 3.11** indicates that treatment with LPS elevated TNF- $\alpha$  mRNA expression compared to basal control. The positive control, BAY, completely suppressed LPS-induced TNF- $\alpha$  mRNA expression. However, neither FA-Hex-Es, FA-Pro-Es nor FA affected TNF- $\alpha$  mRNA expression, suggesting that the mechanism of action is likely through post-transcription or post-translational modification of the TNF- $\alpha$  protein rather than effects on upstream gene expression.

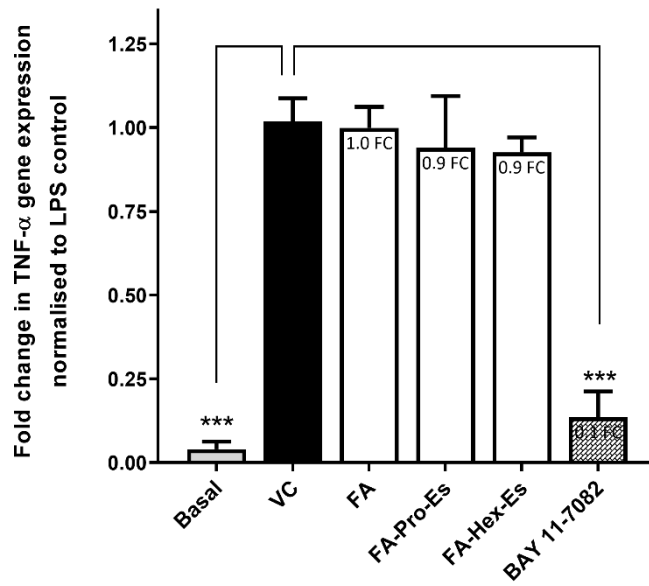


Figure 3. 11 FA, FA-Pro-Es and FA-Hex-Es do not affect LPS-induced TNF- $\alpha$  mRNA expression in THP-1. Cells ( $1 \times 10^6$ /well) were treated with 20  $\mu$ M FA, FA-Pro-Es and FA-Hex-Es, or 0.1 % DMSO (vehicle control, VC) and 20  $\mu$ M BAY 11-7082 (positive control) for 30 min prior to stimulation with LPS (1 ng/mL) for 2 h. Basal is untreated cells. TNF- $\alpha$  mRNA expression was measured by RT-qPCR and normalised to GAPDH levels. Data is expressed as a percentage of LPS control (not shown), mean  $\pm$  SEM, n=3. No significant ( $p \leq 0.05$ ) difference between VC and FA, FA-Pro-Es, FA-Hex-Es by one-way ANOVA with post-hoc Dunnett's test. Comparisons of basal control and BAY with VC were established via student t-test. \*\*\*  $p \leq 0.001$ .

### **3.3.6 Post translational mechanisms of action of FA-Hex-Es and FA-Pro-Es**

TNF- $\alpha$  is a highly potent inflammatory mediator and its expression is tightly controlled by transcription, mRNA turnover and translation. The post-transcriptional regulators include micro RNA and MAPK<sup>283</sup> while post-translation is controlled by TNF- $\alpha$  converting enzyme (TACE)<sup>457</sup>. Thus, MAPK are master regulators controlling protein translation and TACE controlling protein secretion. Moreover, p38 MAP kinase has been reported to upregulate TACE activity<sup>458,459</sup>. Inhibition of p38 by SB 203580 attenuates TNF- $\alpha$  protein secretion and celastrol, a triterpenoid has been reported to block inhibition of TACE enzymatic activity and TNF- $\alpha$  secretion, causing accumulation of membrane-form TNF- $\alpha$  on the cell surface<sup>278</sup>.

#### **3.3.6.1 Optimisation of p38 MAPK phosphorylation in THP-1 cells**

Our group has previously shown that LPS induces p38 MAPK phosphorylation in response to LPS in THP-1 cells<sup>460</sup>. To determine a suitable timepoint to investigate the effects of FA and its esters on p38 MAPK activation, a time course of its phosphorylation in response to LPS was established.  $1 \times 10^6$  cells/mL were treated with 1  $\mu$ g/mL LPS for 10, 20, 30, 45 and 60 min following the literature<sup>461–463</sup>, and p38 phosphorylation examined by western blot analysis. **Figure 3. 12** demonstrates that p38 MAP kinase is phosphorylated within 20 min in response to LPS and continues to increase to 1 h. Since the latter timepoint had the highest phosphorylation levels, this timepoint was chosen for further experiments. The optimal buffer for the primary antibody (5% BSA in TBST) was also determined (**Appendix III**).

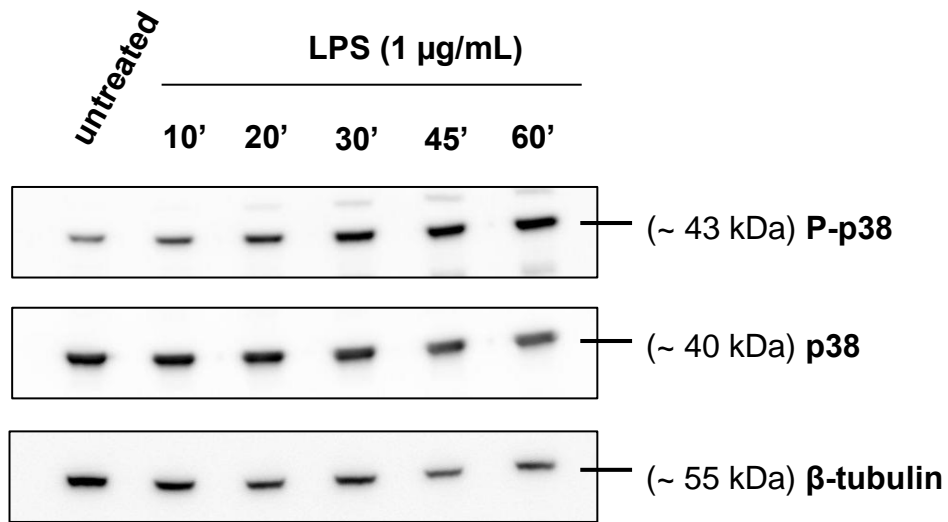


Figure 3. 12 Kinetics of LPS induced p38 phosphorylation in THP-1. Cells ( $1 \times 10^6$  /well) were treated with LPS ( $1 \mu\text{g/mL}$ ) for 10, 20, 30, 45 and 60 min. Total protein was extracted and protein expression analysed by western blot assay,  $n=1$ .

### 3.3.6.2 FA-Hex-Es and FA-Pro-Es do not modulate p38 MAPK phosphorylation in THP-1 cells

Cells were pre-treated with  $20 \mu\text{M}$  FA, FA-Pro-Es, FA-Hex-Es or  $10 \mu\text{M}$  SB203580 (a p38 MAP kinase inhibitor) for 30 min prior to addition of LPS ( $1 \mu\text{g/mL}$ ) for 1 h. Following SDS-PAGE, immunoblotting was carried out for unphosphorylated and phosphorylated p38 MAP kinase expression **Figure 3. 13** demonstrates that LPS-induced p38 phosphorylation expression was reduced by SB203580. However, it was not significantly affected by FA, FA-Pro-Es or FA-Hex-Es.

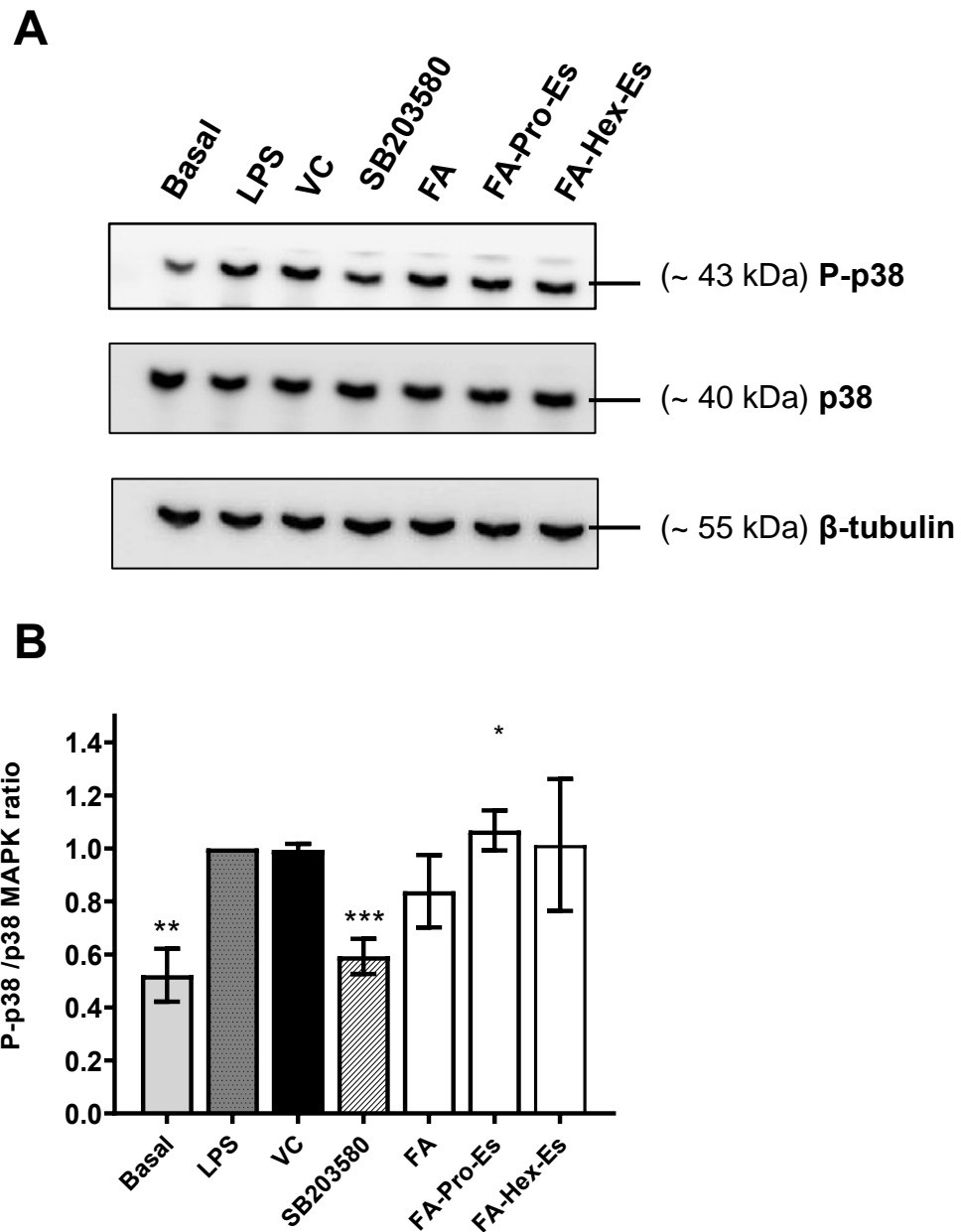


Figure 3. 13 FA and its propyl and hexyl esters do not modulate LPS-induced p38 MAPK phosphorylation in THP-1. Cells ( $1 \times 10^6$ /well) were pre-treated with 20  $\mu$ M FA, FA-Pro-Es, FA-Hex-Es, or with 0.1% DMSO (vehicle control, VC) and 10  $\mu$ M SB 203580 (positive control) for 30 min prior to stimulation with LPS (1  $\mu$ g/mL) for 1 h. Unphosphorylated and phosphorylated p38 MAP kinase expression was measured by western blot assay. Tubulin was used as a loading control. A) Immunoblot representative of 3 independent experiments. B) Densitometry of protein detection levels normalised to tubulin control and relative fold change to LPS control, expressed as phospho-p38/p38 ratio. Mean  $\pm$  SEM,  $n=3$ . Relative change from VC was analysed by One Way Anova with post hoc Dunnett's' test. Non-treated cells (basal) and SB203580 vs VC performed by student t-test. Significant change from VC, \*\*  $p < 0.01$ , \*\*\*  $p < 0.001$ .

### **3.3.6.3 Membrane-bound TNF- $\alpha$ expression in THP-1 cells**

Since p38 MAP kinase was unlikely to be involved in the mechanism of action of FA-Hex-Es, effects on membrane-bound TNF- $\alpha$  were then examined. Cells were incubated with SB203580 or celastrol (10  $\mu$ M) or 0.1% DMSO (VC) for 30 min before stimulation with LPS (1  $\mu$ g/mL) for 4 h as described earlier in the literature<sup>278</sup>. Membrane bound TNF- $\alpha$  expression was examined by immunofluorescence microscopy. **Figure 3. 14** shows that the membrane form of TNF- $\alpha$  was expressed in unstimulated cells but absent in the IgG isotype control. LPS and celastrol slightly increased expression but the staining was weak and results inconclusive.

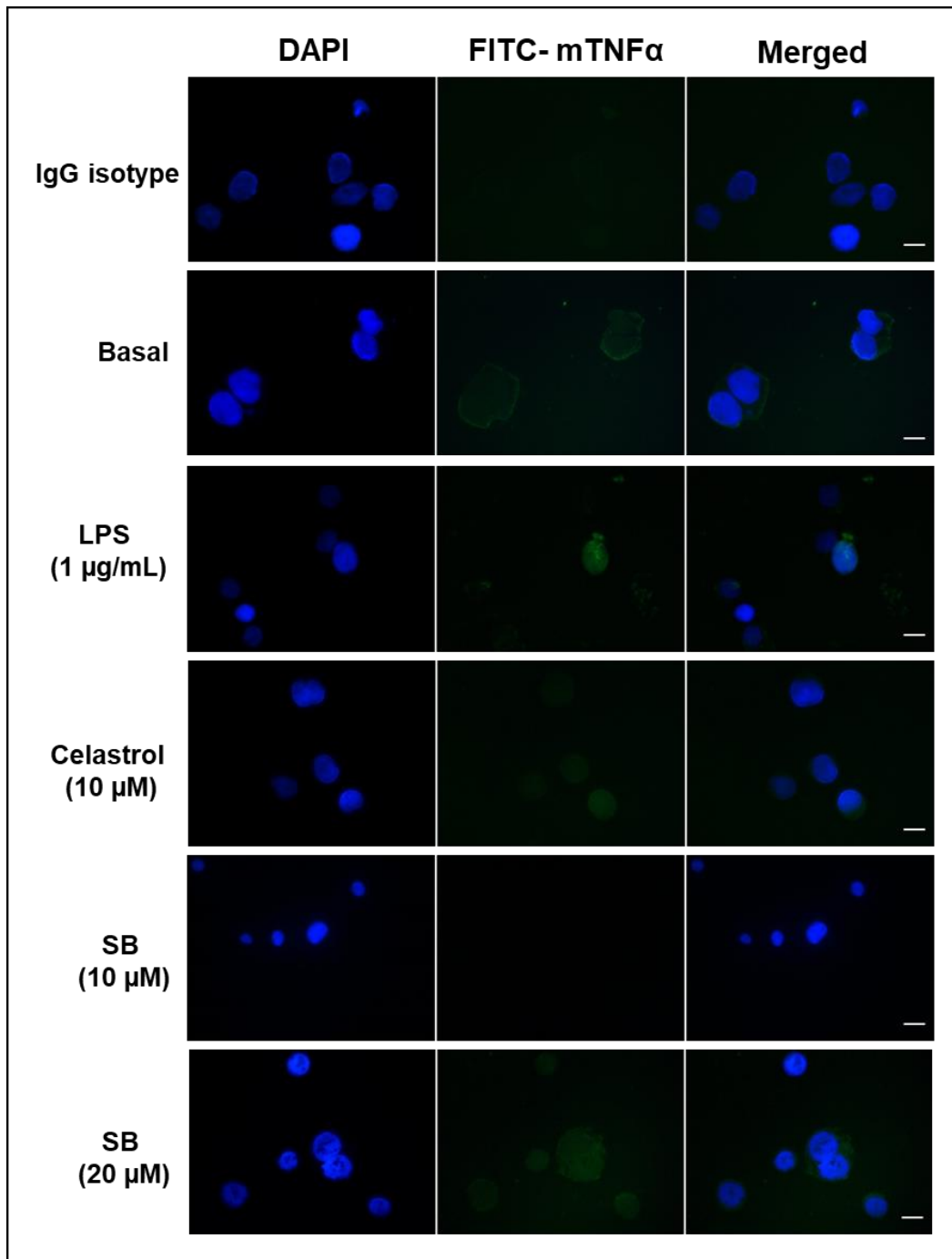


Figure 3. 14 LPS-induced membrane-bound TNF- $\alpha$  expression in THP-1. Cells ( $5 \times 10^5$ /well) were pre-treated with celastrol (10  $\mu$ M) or SB203580 (10, 20  $\mu$ M) for 30 min prior to stimulation with LPS (1  $\mu$ g/mL) for 4 h. Cells were either stained FITC-conjugated anti-human mTNF- $\alpha$  antibody (specific to membrane-bound TNF- $\alpha$ ) or FITC-conjugated mouse IgG isotype control prior staining nucleus with DAPI. Basal is untreated cells. Membrane-bound TNF- $\alpha$  (green), analysed by immunofluorescence microscopy. 63X magnification. n=1. Scale bar = 10  $\mu$ m.



#### **3.3.6.4 Flow Cytometry of Membrane Bound TNF- $\alpha$ expression in LPS-induced THP-1**

Membrane bound TNF- $\alpha$  in LPS-induced THP-1 cells was then assessed by flow cytometry. Cells were incubated for 30 min with FA, FA-Pro-Es, FA-Hex-Es, celastrol (10  $\mu$ M) or 0.1% DMSO (**VC**) prior to stimulation with LPS (1  $\mu$ g/mL) for 4 h. **Figure 3. 15** shows that membrane-bound TNF- $\alpha$  expression in the basal control was slightly increased by DMSO but that there was no change in fluorescence with FA, FA-Pro-Es, FA-Hex-Es or even the positive control, celastrol, possibly suggesting that the antibody was weak and therefore the results were inconclusive.

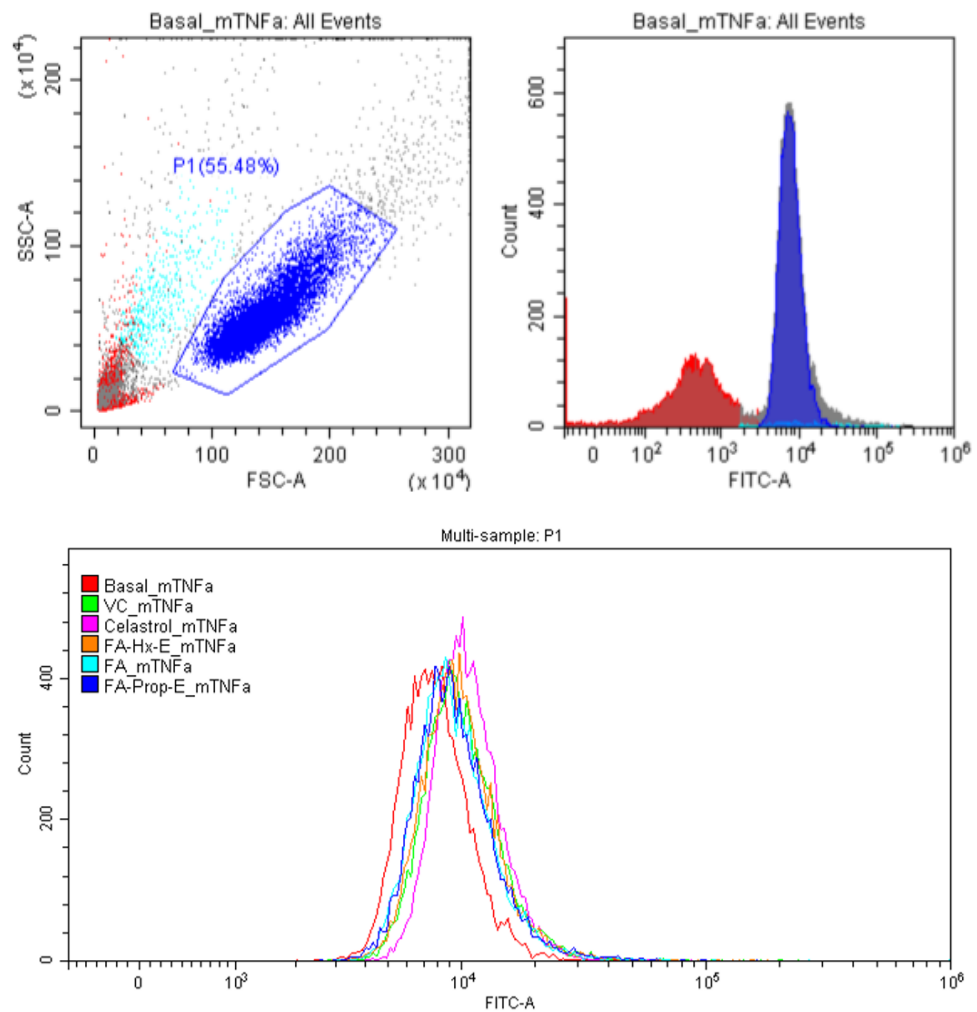


Figure 3. 15 Membrane-bound TNF- $\alpha$  expression in THP-1 cells by flow cytometry. Cells ( $5 \times 10^5$  /well) were incubated with 20  $\mu$ M FA, FA-Pro-Es, FA-Hex-Es or 0.1% DMSO (vehicle control, VC) or 10  $\mu$ M celestrol (positive control) or for 30 min prior to stimulation with LPS (1  $\mu$ g/mL) for 4 h. Basal is untreated cells. Membrane-form TNF- $\alpha$  was stained with FITC-conjugated anti-human mTNF- $\alpha$  antibody or FITC-conjugated mouse IgG isotype control and analysed by flow Cytometry. Graphs are representative of three independent experiments.

### **3.3.7 FA esters activate HO-1 expression and NQO1 activity in THP-1 cells**

The health effects of flavonoid consumption are attributed to both their anti-inflammatory and antioxidant effects. We have previously reported that some flavonoids, including quercetin, activate the Nrf2 pathway and its downstream targets, HO-1 and NQO1<sup>387,394,408,440,464</sup>. Upregulation of Nrf2, HO-1 and NQO1 all lead to anti-inflammatory effects including TNF- $\alpha$  inhibition. FA, FA-Hex-Es and FA-Pro-Es were therefore investigated to determine if this was a potential mechanism of action of these compounds. Following a time course to determine optimal HO-1 expression (data not shown), cells were stimulated with 20  $\mu$ M of FA or its esters for 20 h and their effects on HO-1 protein expression measured by ELISA. Dimethyl fumarate (DMF, 30  $\mu$ M), a previously reported potent activator of Nrf2<sup>465</sup>, was included as a positive control. DMF significantly increased HO-1 protein expression (3.9-fold increase over control) and FA-Hex-Es induced a similar response (3.7-fold increase) (**Figure 3. 16**). FA-Pro-Es also significantly increased HO-1 protein expression to a lesser extent (2.3-fold increase). FA had no significant effect on HO-1 expression. Following this, different concentrations of FA-Hex-Es (1, 10 and 20  $\mu$ M) were used to determine if the observed effects could be reached at lower concentrations. **Figure 3. 17** demonstrates that FA-Hex-Es at both 10  $\mu$ M and 20  $\mu$ M significantly increased HO-1 protein expression to a similar extent and similarly to DMF.

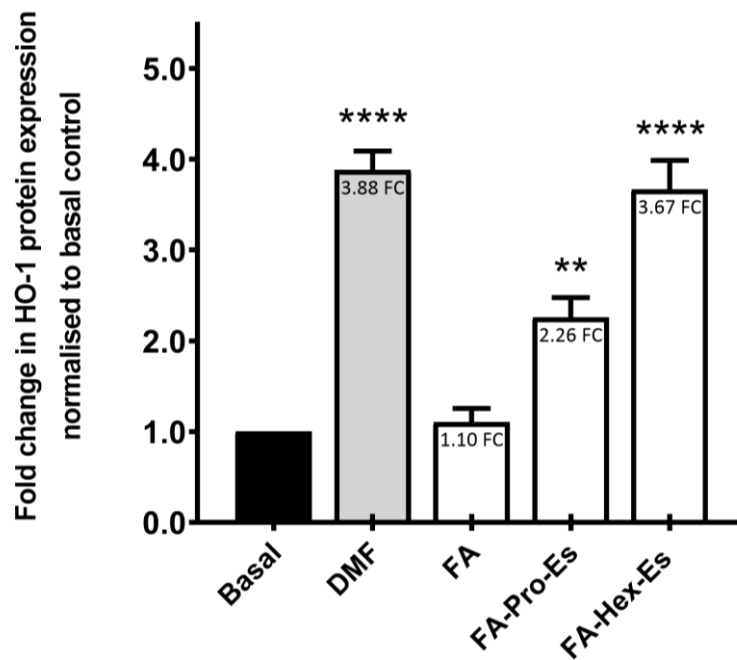


Figure 3. 16 FA-Hex-Es and FA-Pro-Es significantly increase HO-1 protein expression in THP-1. Cells ( $5 \times 10^6$ /T25 flask) were treated with 20  $\mu$ M FA, FA-Pro-E and FA-Hex-Es or 0.1% DMSO (basal control) and 30  $\mu$ M Dimethyl fumarate (DMF, positive control) for 20 h. HO-1 protein expression measured by ELISA assay. Data expressed as fold change relative to basal control. Mean  $\pm$  SEM,  $n=3$  independent biological experiments. Significant ( $*p \leq 0.05$ ) difference between basal and FA, FA-Hex-Es, FA-Pro-Es analysed by one-way ANOVA with post hoc Dunnett's test. Comparisons of DMF relative to basal by Student t-test.  $*p \leq 0.05$ ,  $**p \leq 0.01$ ,  $****p \leq 0.0001$ .

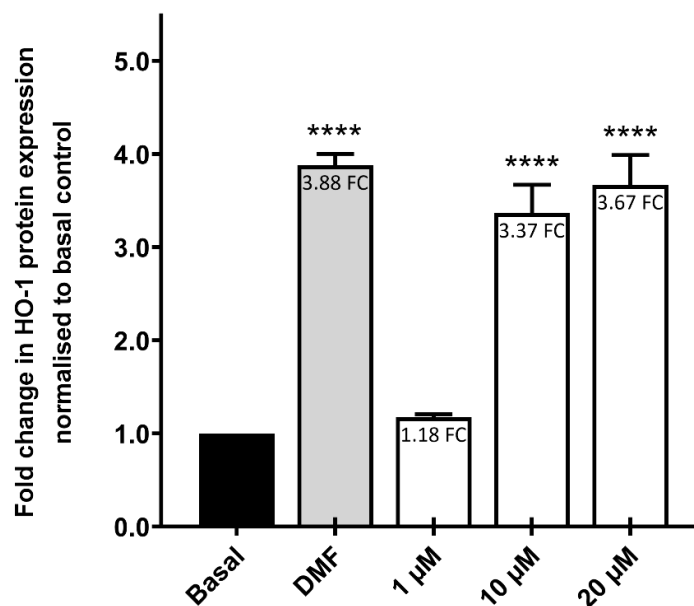


Figure 3. 17 FA-Hex-Es dose-dependently increases HO-1 protein expression in THP-1. Cells ( $5 \times 10^6$ /T25 flask) were treated with 1  $\mu$ M, 10  $\mu$ M or 20  $\mu$ M FA-Hex-Es or 0.1% DMSO (basal) and 30  $\mu$ M Dimethyl fumarate (DMF, positive control) for 20 h. Data is expressed as fold change over basal control (VC). Mean  $\pm$  SEM, n=3. Significant ( $p \leq 0.05$ ) difference between basal and treatment by one-way ANOVA with post hoc Dunnett's test. Comparisons of DMF relative to VC via student t-test. \*\*\*  $p \leq 0.001$ , \*\*\*\*  $p \leq 0.0001$ .

The effects of FA and its esters on NQO1 activity in THP-1 cells were then investigated. NQO1 activity was measured by direct measurement of NQO1 from cells cultured in 96-well plates <sup>424</sup>. Optimisation of the assay is described in **Figure 3. 18** and **Appendix III**. Cells were untreated or treated with FA, FA-Pro-Es, FA-Hex-Es, quercetin (Que) (20  $\mu$ M), DMF (30  $\mu$ M) or 0.1% DMSO (VC) for 20 h. DMF significantly increased NQO1 enzymatic activity (2.2-fold over control) (**Figure 3. 19**). FA-Hex-Es and FA-Pro-Es both showed a mild and comparable significant increase in NQO1 activity similarly to Que.

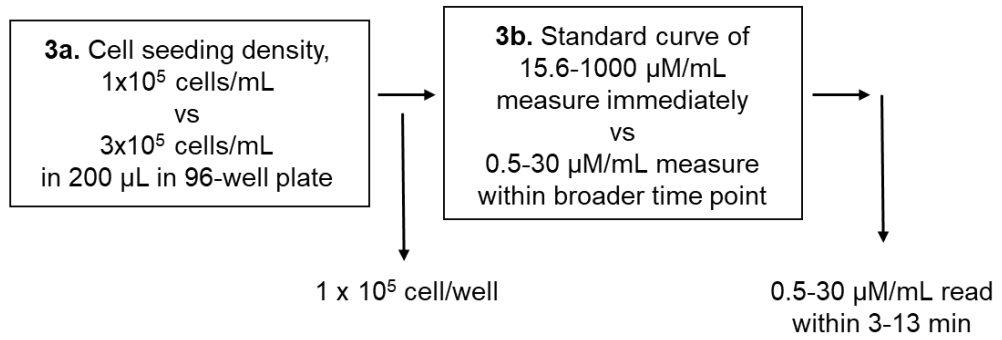


Figure 3. 18 Flow chart of method optimisation for NQO1 enzymatic assay in THP-1 monocytes.

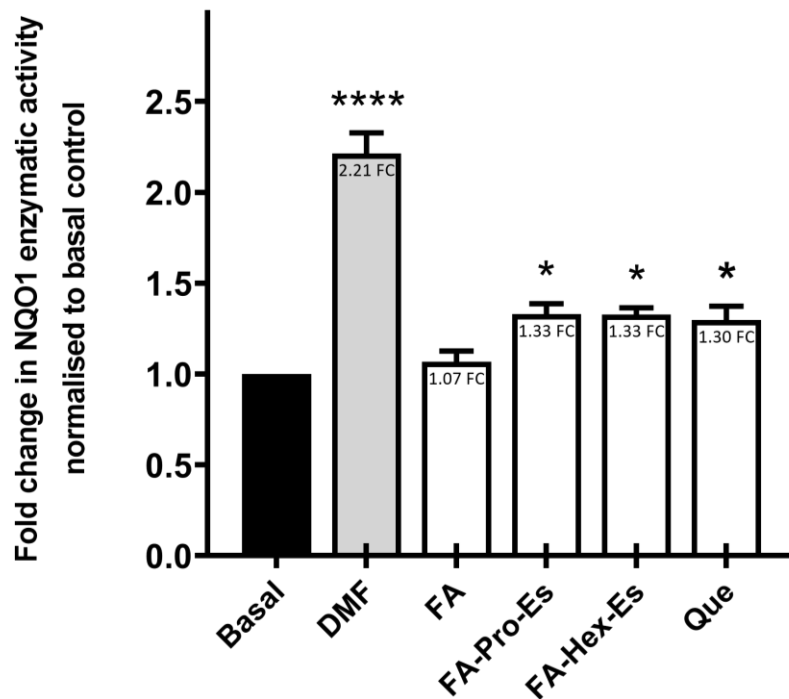


Figure 3. 19 FA-Hex-Es and FA-Pro-Es significantly increase NQO1 enzyme activity in THP-1. Cells ( $1 \times 10^5$ /well) were treated with 20  $\mu$ M FA, FA-Pro-Es, FA-Hex-Es and Quercetin (Que, as positive control) or 0.1% DMSO (basal control) and 30  $\mu$ M Dimethyl fumarate (DMF, positive control). NQO1 protein level measured by direct enzymatic activity from cell culture in a 96-well plate. Data expressed as fold change relative to basal control. Mean  $\pm$  SEM,  $n=3$  independent biological experiments. Significant ( $*p \leq 0.05$ ) difference between basal and FA, FA-Hex-Es, FA-Pro-Es and Que analysed by one-way ANOVA with post hoc Dunnett's test. Comparisons of DMF relative to basal by Student t-test.  $*p \leq 0.05$ ,  $**p \leq 0.01$ ,  $***p \leq 0.0001$ .

### 3.3.8 Effect of FA esters on HO-1 and NQO1 mRNA expression in THP-1 cells

We have previously reported that the flavonoids curcumin and quercetin increase HO-1 mRNA expression<sup>394,440</sup>. The kinetics of HO-1 and NQO1 mRNA induction in response to FA-Hex-Es and DMF were examined at 4 and 8 h (**Appendix III**). Both DMF and FA-Hex-Es increased HO-1 and NQO1 mRNA expression and to a higher extent at 4 h than 8 h and therefore this time-point was used in further experiments. **Figure 3. 20** indicates that DMF significantly increased both HO-1 and NQO1 mRNA expression by 4.5 and 2.7-fold respectively. FA-Hex-Es and Que significantly increased HO-1 mRNA expression by nearly 2-fold. The effect on NQO1 mRNA expression was not significant but a comparable non-significant increase in expression was observed with both FA-Hex-Es and Que.

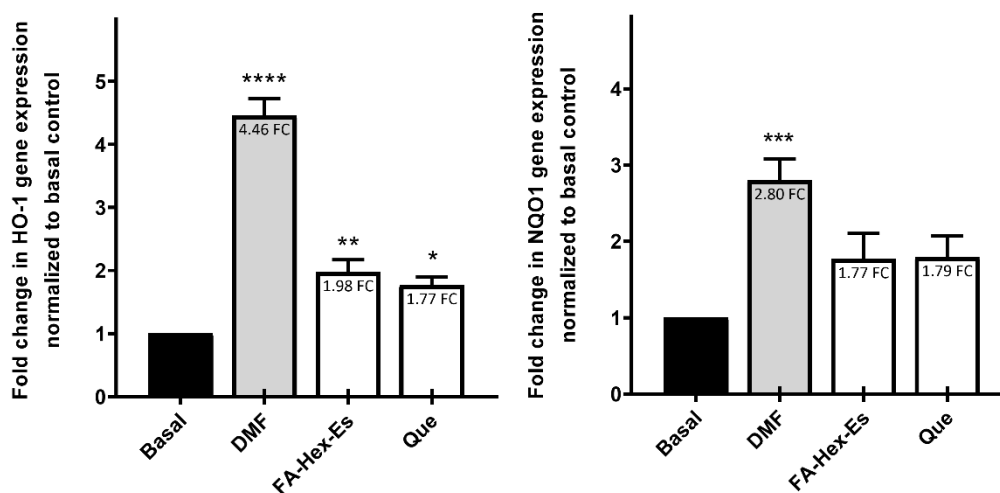


Figure 3. 20 Treatment effect FA-Hex-Es on HO-1 and NQO1 gene expression in THP-1. Cells ( $1 \times 10^6$ /well) were treated with 20  $\mu$ M FA-Hex-Es and Quercetin (Que, as positive control) or 30  $\mu$ M Dimethyl fumarate (DMF, positive control) and with 0.1% DMSO (basal control) for 4h and mRNA expression measured by RT-qPCR. mRNA values were expressed as fold change (relative to GAPDH) normalised to basal control. Mean  $\pm$  SEM, n=4 independent biological experiments. Significant difference between basal and treatment by one-way ANOVA with post hoc Dunnett's test. Comparisons of DMF relative to basal via student t-test. \*  $p \leq 0.05$ , \*\*  $p \leq 0.01$ , \*\*\*  $p \leq 0.001$ , \*\*\*\*  $p \leq 0.0001$ .

### **3.3.9 Effect of FA and FA esters on Nrf2 protein expression in THP-1 cells**

HO-1 and NQO1 are both regulated by Nrf2 and therefore the effects of the esters on Nrf2 protein accumulation in THP-1 cells was examined. Cells were untreated or treated with 20  $\mu$ M FA, FA-Hex-Es, FA-Pro-Es or Que, 30  $\mu$ M DMF or 0.1% DMSO for 3 h and Nrf2 protein expression measured by western blot analysis (**Figure 3.**). DMF and Que significantly increased Nrf2 expression (2.8-fold and 2.1-fold over basal control, respectively). FA did not affect Nrf2 expression and although not significant, both FA-Hex-Es and FA-Pro-Es increased Nrf2 by  $\pm$ 1.5-fold and 1.6-fold respectively. This suggests that FA-Hex-Es and FA-Pro-Es may be partly involved in Nrf2 signalling pathway.



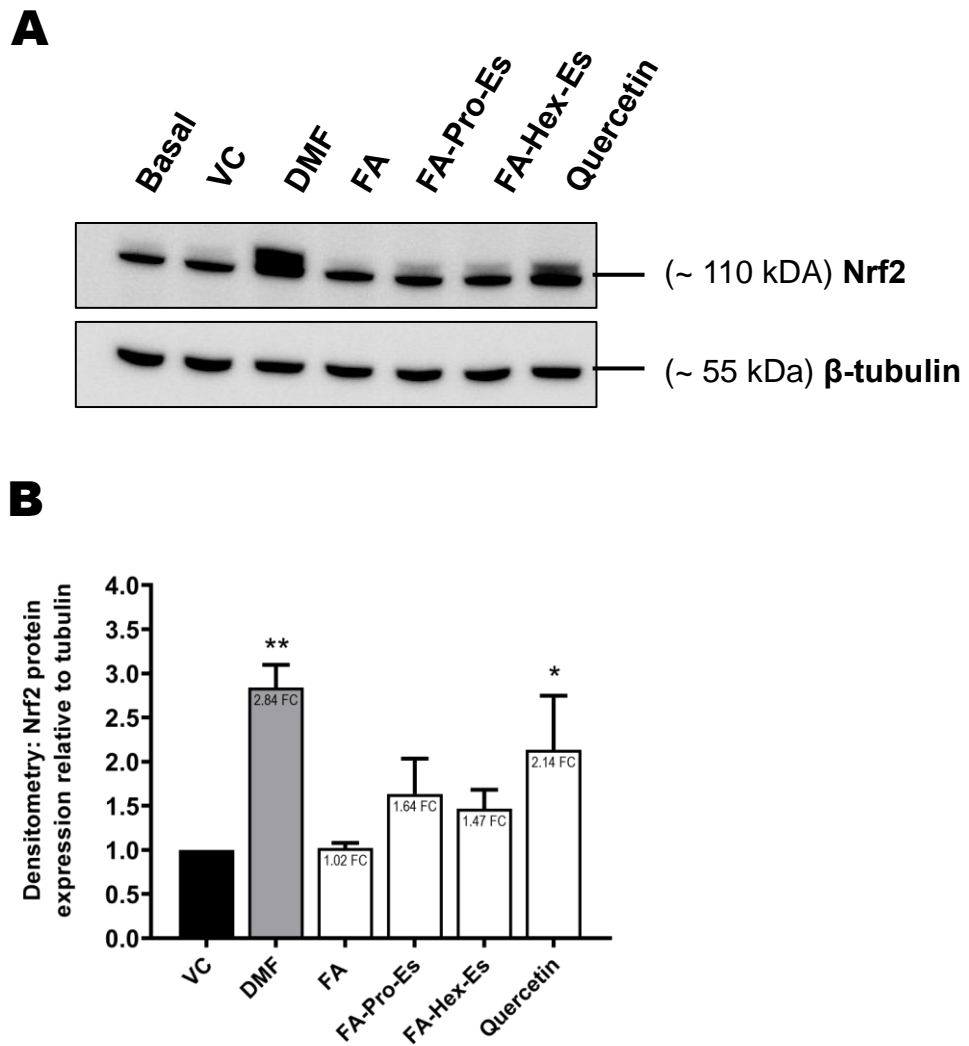


Figure 3. 21 Nrf2 protein expression is not modulated by FA and its esters in THP-1. Cells ( $1 \times 10^6$ /wells) were treated with 20  $\mu$ M FA, FA-Pro-Es, FA-Hex-Es and Quercetin or 0.1% DMSO (vehicle control, VC) and 30  $\mu$ M Dimethyl fumarate (DMF, positive control) for 3 h. Nrf2 protein expression was measured by Western blot assay. Tubulin was used as a loading control. A) Immunoblot representative of 4 independent experiments. B) Densitometry of protein detection levels, Nrf2 normalised tubulin and expressed relative to VC. Mean  $\pm$  SEM,  $n=4$ . No significant change from VC by One Way Anova with post hoc Dunnett's' test. DMF vs VC performed by student t-test. \* $p < 0.05$ , \*\* $p < 0.01$ .

### 3. 4 Discussion

Habitual intake of phenolic compounds is associated with reduced inflammation and prevention of atherosclerosis. Phenolic acids are the second most abundant class of phenolic compounds in the common diet. They are derived from the metabolism of flavonoids and as they are low molecular weight, may be more bioavailable and therefore may be responsible for these beneficial effects. In this study, seven of the most common diet-derived simple phenolic acids together with 14 commercially available, related phenolic acids, 7 related glycinated metabolites and 12 related esterified phenolic acids were investigated for their anti-inflammatory effects in THP-1 monocytes. FA propyl ester and FA hexyl ester were the only phenolic acids that inhibited LPS-induced TNF- $\alpha$  secretion at physiological concentrations. They did not inhibit TNF- $\alpha$  mRNA expression or p38 MAP kinase expression. However, they increased HO-1 and NQO1 expression, whose activation we have previously shown to inhibit LPS-induced TNF- $\alpha$  expression in these cells.

Although not significant, a slight reduction in LPS-induced TNF- $\alpha$  secretion was observed, ranging between 10-18%, but this slight effect was not dose-dependent, suggesting phenolic acids might not be taken up or absorbed by the cell in *in vitro* assays. However, the screening results from this study, in accordance with our previous work <sup>440</sup>, further revealed that at physiological concentrations, flavonoid metabolites show a mild effect and the effect is rather non-dose dependent. This is an important point and might be relevant from a nutritional point of view when considering these compounds are highly bioavailable and very high bioactivity might interfere with the immune response. A limited number of studies have reported the effect of phenolic acids on TNF- $\alpha$  expression in monocytes or macrophages but mainly at supraphysiological concentrations. In LPS-induced THP-1 macrophages, ferulic acid inhibited TNF- $\alpha$  gene expression at 125-500  $\mu$ M <sup>466</sup> while caffeic acid reduced TNF- $\alpha$  secretion at 14-39  $\mu$ M <sup>467</sup>. Vanillic acid also inhibited TNF- $\alpha$  secretion at 10-100  $\mu$ M in LPS-induced mouse

peritoneal macrophages <sup>263</sup>. PCA inhibited TNF- $\alpha$  secretion at 1-5  $\mu$ M in LPS-induced murine RAW macrophages <sup>262</sup>. Studies with relevant concentrations are rare and to our knowledge only di Gesso investigated the anti-inflammatory effect of flavonoid metabolites and phenolic acids in THP-1 monocytes. In this study several metabolites, including phenolic acids PCA, VA, IVA and 4HBA, were tested for their effect on LPS induced TNF- $\alpha$  secretion at 1  $\mu$ M <sup>19</sup>. Except IVA, none of these exerted any significant effect but a mild reduction of 10-24% in TNF- $\alpha$  secretion. The reduction levels are in the same range as the current study and confirmed the mild bioactivity. Moreover, PCA together with 4HBA and PCA with 4HBA and VA (at 1, 10  $\mu$ M) also inhibited TNF- $\alpha$  secretion <sup>19</sup>. Our group also reported bioactivity of a combination of PCA and VA at 10  $\mu$ M in RASMC cells <sup>137</sup>.

We postulated that phenolic acids with mild effects may have additive or synergistic effects with other anti-inflammatory food bioactives from the diet such as peptides <sup>468</sup> or omega-3 fatty acids <sup>444</sup>. For instance, curcumin, a food bioactive that is also metabolised into FA, is poorly bioavailable <sup>469</sup>, but when taken in combination with piperin, a naturally occurring food alkaloid that is bioactive, it increases its absorption and bioavailability <sup>469</sup>. EPA and DHA inhibit LPS-induced TNF- $\alpha$  expression in RAW macrophages <sup>470</sup> and THP-1 macrophages <sup>446,449</sup>. Macrophages are involved in lipid metabolism in atherosclerosis and are the logical cell type to study the anti-inflammatory effects of fatty acids. Anti-inflammatory effects of EPA and DHA have also been reported in other immune cells <sup>444</sup>. In this study, the effects of EPA, DHA or both in combination with diet-derived phenolic acids were investigated in THP-1 monocytes and macrophages. Pre-incubation with EPA inhibited TNF- $\alpha$  in monocytes but not macrophages, while DHA inhibited in both cell types. The effect in monocytes was more rapid, suggesting cellular mechanisms might be different, in line with previous reports that both EPA and DHA have differential effects on gene expression at different concentrations in THP-1 macrophages <sup>448</sup>. Pre-incubation with the mixture of EPA+DHA was effective at all concentrations in monocytes,

while in macrophages only 50  $\mu\text{M}$  was effective. Previous studies have explored the pre-, post- and co-incubation of EPA and DHA with LPS-stimulated monocytes and macrophages <sup>449</sup>. In contrast to other studies, EPA did not affect TNF- $\alpha$  secretion in macrophages in our study, which may have been due to shorter incubation times for both EPA and LPS and previous studies have reported that the anti-inflammatory effect of EPA and DHA is time and dose-dependent <sup>446,449</sup>. Furthermore, the varied effect of EPA and DHA on TNF- $\alpha$  secretion might be due to cellular location of EPA and DHA and the differential molecular mechanisms involved <sup>444</sup>. DHA undergoes rapid conformational changes in the lipid bilayer of membranes where it causes cholesterol enrichment and membrane fluidity while EPA is postulated to intercalate into membrane phospholipid hydrocarbon core regions where it inhibits free radical formation and is involved in antioxidant defence while maintaining a more homogenous cholesterol distribution <sup>435</sup>. Thus, EPA is involved in quenching lipid and membrane associated ROS and suppressing inflammatory signalling. In this study, 50  $\mu\text{M}$  DHA showed the greatest inhibition in both monocytes and macrophages and this treatment was tested for additive/synergistic effects with phenolic acids. DHA alone, as well as in combination with phenolic acids, significantly decreased TNF- $\alpha$  secretion in a similar fashion in both monocytes and macrophages. However, no additive or synergistic effects were observed when selected phenolic acids at physiological concentrations were combined with DHA. Due to time limitation, it was not possible to study the combination effects of phenolic acid with EPA or different concentration ratios and pre-incubation times with both EPA and DHA. Further studies could include a mixture of phenolic acids with relevant concentrations.

We also synthesised novel metabolites of phenolic acids with glycine conjugates as glycine conjugation is widely accepted as the primary mechanism of detoxification of xenobiotic aromatic acids especially polyphenolic compounds from the body by increasing the water solubility of these compounds, facilitating urinary excretion <sup>452</sup>. However, none of the glycine conjugates significantly affected TNF- $\alpha$  secretion in THP-1 cells

suggesting no additive effect of glycation of parental phenolic acids. It is worth mentioning that we observed a wide variation in results which may be the reason for no significant effects.

Studies investigating the cellular uptake and absorption of phenolic acids into immune cells are lacking. Previous studies from our lab have demonstrated a U-shaped (or bell-shaped) curve for inhibition of TNF- $\alpha$  secretion in THP-1 cells, which could be due to colloid formation by those molecules that may result in physical exclusion from the cells at relevant concentrations <sup>438</sup>. Moreover, U-shaped curve responses might indicate more complex biological effects, such as multiple targets or binding sites, as exemplified by phytoestrogens which are aromatase inhibitors at lower concentrations ( $\leq 1 \mu\text{M}$ ) while exhibiting estrogen activity at higher concentrations ( $\geq 1 \mu\text{M}$ ), resulting in a U-shaped dose response <sup>471</sup>. We hypothesised that synthetic analogues with varying lipophilicity might increase uptake of the phenolic acids and help us to understand their mechanisms of action. Esterification is a widely applied chemical modification for drug uptake and absorption and an emerging method to improve uptake and absorption of food bioactives. Esterification of poorly bioavailable EGCs with fatty acids such as DHA, stearic-, lauric-, caprylic- and propionic-acid increased their bioactivity in both hydrophilic and lipophilic media <sup>472</sup>. Moreover, DHA and EPA supplements on the market are also esterified with ethyl or triglyceride to increase their absorption <sup>473</sup>. Hybrids of CA-FA have also shown greater bioactivity compared to CA and FA alone in murine microglial cells <sup>336</sup>, which may be due to higher lipophilicity. We synthesised and tested synthetic ester analogues of phenolic acids with varying chain length corresponding to their increasing lipophilicity. Phenolic acids with shorter ester chains such as methyl- and ethyl esters are in theory possible by phase II conjugation <sup>97,474</sup> but longer ester chains such as propyl- and hexyl-esters are novel and thus non-natural. Alkyl esters of PCA, VA, FA and CA with methyl-, ethyl-, propyl-, butyl- and hexyl- groups were previously synthesised and screened for their anti-bacterial properties <sup>475</sup> but to our knowledge we are the first to

investigate their anti-inflammatory effects in immune cells. Among all phenolic acid analogues that we tested, FA-Hex-Es and FA-Pro-Es were the only compounds to significantly inhibit LPS-induced TNF- $\alpha$  secretion in a concentration-dependent manner. These results suggest that longer alkyl groups of FA combined with propyl- and hexyl-ester enhance the lipophilicity, which may contribute to greater cellular absorption and/or the prevention of colloidal formation.

For future studies it is advisable to further clarify if phenolic acids are transported into immune cells. For instance, a fluorescent probe specific to phenolic acids could be developed and used to detect intra-cellular phenolic acids<sup>476,477</sup>. Alternatively, an analytical approach with a high throughput screening property, such as ultra-high performance liquid chromatography tandem mass spectrometry (UHPLC MS/MS) or RapidFire tandem mass spectrometry (RapidFire MS/MS) could be used to quantify the selected phenolic acid concentrations in immune cells following incubation of cells with test compounds<sup>478</sup>.

To understand the cellular MOA of FA-Pro-Es and FA-Hex-Es on TNF- $\alpha$  secretion, we examined the effects on gene expression. Similar to our previous studies with other flavonoid metabolites at physiological concentrations in THP-1 cells and HUVEC<sup>137,334,440,479</sup>, neither the parent FA, or the ester analogues FA-Pro-Es and FA-Hex-Es affected mRNA expression. LPS-induced TNF- $\alpha$  secretion is regulated post-translationally by p38 MAP kinase<sup>283</sup>. However, none of the three phenolic acids affected LPS-induced p38 MAPK phosphorylation suggesting an alternative mechanism was involved.

TNF- $\alpha$  is expressed on the membrane prior to secretion. The membrane - located enzyme TACE cleaves the ectodomain of membrane-anchored TNF- $\alpha$ , giving rise to its circulating soluble form. TACE is also responsible for releasing soluble VCAM-1 and ICAM-1<sup>480</sup>. Several studies have reported the effect of flavonoids on TACE activity by looking at gene and protein expression<sup>232,291,481,482</sup> as well as by measuring enzymatic activity

by colorimetric assays <sup>232,456,482</sup> or by molecular modelling <sup>483</sup>. However, protein and gene expression might not be directly correlated with enzymatic activity. We used an enzymatic activity assay, the InnoZyme TACE activity kit <sup>291</sup> which measures TACE activity from cell lysates to study the effect of FA, FA-Hex-Es and FA-Pro-Es on TNF- $\alpha$  secretion. However, this assay was problematic and even the controls were not reproducible, and optimisation of this kit did not improve TACE activity from cell lysates (data not shown). As an alternative, we studied the effect of our compounds on retention of membrane-bound TNF- $\alpha$  by flow cytometry as blocking TACE activity should result in membrane retention and accumulation. Celastrol, a wide spectrum anti-inflammatory compound <sup>484</sup>, has been reported to inhibit TACE enzymatic activity and increases membrane-bound TNF- $\alpha$  in LPS-induced THP-1 cells <sup>278</sup>. However, in our hands neither Celastrol or the phenolic acids inhibited LPS-induced membrane bound TNF- $\alpha$ , which could have been due to insufficient antibody binding or weakly expressed mTNF- $\alpha$  combined with the use of a dim fluorochrome FITC <sup>485</sup>. Future studies should include a TACE specific inhibitor such as Ro 32-7315 <sup>278</sup>, instead of any broad spectrum inhibitors such as Celastrol. And for immunofluorescence experiments, perhaps a brighter or an ultrabright fluorochrome such as PE or Brilliant Violet™ could be used. Catalán and co-workers have reported that LPS stimulation alone in THP-1 cells did not affect TACE activity and basal levels of THP-1 might be sufficient for TNF- $\alpha$  secretion. However, they used a fluorimetric assay <sup>456</sup> which could have missed detection of the transient inhibitory activity in cell lysates. Further studies should consider using validated live-cell based assays with FRET-based biosensors where both inducer (LPS) and inhibitors (positive control and compounds of interest) are simultaneously present <sup>458</sup>. Future studies for TACE activity should also consider use of primary cells or cell lines with TACE activity similar to primary cells, rather than THP-1 in which TACE catalytic activity was reported to be different than in primary cells <sup>278</sup>.

We have previously shown that activation of HO-1 or NQO1 can inhibit LPS-induced TNF- $\alpha$  secretion in THP-1 cells and that flavonoids and flavonoid

metabolites can induce their expression <sup>19,47,387</sup>. This may be an alternative cellular mechanism for the esterified ferulic acids. In contrast to FA, both FA-Hex-Es and FA-Pre-Es significantly increased HO-1 protein expression and the magnitude of FA-Hex-Es was similar to the positive control DMF. A moderate but significant effect was also observed with NQO1 enzymatic activity relative to basal control. Further examination showed that FA-Hex-Es increased HO-1 gene expression but did not significantly alter NQO1 gene expression. Finally, we studied the effect of these two compounds together with FA on expression of Nrf2, which regulates these genes. FA-Hex-Es and FA-Pro-Es slightly induced Nrf2 protein expression by 1.5-fold but this was statistically non-significant. Various studies have consistently reported quercetin as a robust Nrf2 activator in different types of cells, including hepatocytes <sup>379,380,486</sup>, endothelial cells <sup>137</sup>, macrophages <sup>416,487,488</sup>, monocytes <sup>440</sup>, and microglia <sup>382</sup>, and so we used thus as a control. Our results are in line with previous studies showing a robust increase in Nrf2 protein expression by quercetin.

Nrf2 has been reported to be upregulated by various parent flavonoids at higher supraphysiological concentrations including: hesperidin (20-80  $\mu$ M) in human hepatic L02 cells <sup>384</sup>, naringenin (20-80  $\mu$ M) in human neuroblast SH-SY5Y cell line <sup>383</sup>, EC (10  $\mu$ M) in HepG2 cells <sup>388</sup>, EGCG (50  $\mu$ M) in bovine aortic endothelial cells (BAECs) <sup>386</sup> and EGC (80-100  $\mu$ M) in THP-1 cells <sup>387</sup>. In a rabbit study, 3 weeks of daily oral administration of C3G and its metabolites FA but not PCA reduced light-exposure induced oxidative stress in the retina via Nrf2 induced HO-1 upregulation <sup>266</sup>. Regarding phenolic acids, in high-glucose induced primary rat hepatocytes and cardiomyocytes, FA increased Nrf2 nuclear accumulation in a dose dependent manner (1-10  $\mu$ g/kg) <sup>264</sup>. Also, IFA induced HO-1 expression via Nrf2 in microglial cells at 100-150  $\mu$ M <sup>489</sup> and CA induced HO-1 and NQO1 expression via Nrf2 in acetaminophen-induced hepatocytes L-02 and HepG2 cells at 50  $\mu$ M <sup>490</sup>. Recent studies from our lab focused on bioactivity at physiological achievable concentrations (1-10  $\mu$ M) and investigated the effect of several parent flavonoids, their sulfate and glucuronide conjugates



as well as benzoic acid derived phenolic acids (PCA, VA, IVA, 4HBA) on HO-1 and Nrf2 expression. In HUVEC, PCA-4-sulfate (PCA4S), 4HBA and quercetin at 1  $\mu$ M upregulated HO-1 expression, but only quercetin and 4HBA upregulated mRNA expression and only quercetin affected Nrf2<sup>137</sup>. In THP-1 cells, quercetin induced Nrf2 and HO-1 expression<sup>440</sup> but similarly to this study, none of the other parents or metabolites had any significant effect on Nrf2 expression, even at 50-100  $\mu$ M. This suggests that alternative mechanisms are responsible, and that benzoic acid derived phenolic acids and metabolites most likely involve different regulatory mechanisms for HO-1 expression that is independent of Nrf2, contrasting with cinnamic acid derivatives (CA, FA, IFA) and parent flavonoids such as quercetin and curcumin, which involves Nrf2 regulation via an upstream signalling pathway<sup>394</sup>. More recently, Croft and co-workers investigated the structural requirements of flavonoids for HO-1 induction in HAECs<sup>491</sup> by comparing ten flavonoids and two caffeic acid-derived synthetic compounds containing either an ortho-dihydroxy or ortho-dioxo group. At 10  $\mu$ M only quercetin, luteolin and 7,8,4'-trihydroxyflavone and the two synthetic compounds induced HO-1 expression. Further comparison of quercetin with these synthetic compounds revealed that the ortho-dioxo compound was the most potent, suggesting a high oxidized state of flavonoids is most likely contributing to HO-1 induction in endothelial cells. This compound induced both HO-1 and NQO1 gene expression, probably via Nrf2 although other mechanisms may also be involved.

Furthermore, we and others have shown the anti-inflammatory effect of both NQO1 and HO-1 might be partly independent of Nrf2 activity. For instance, our lab (Rushworth et al., 2008) showed that overexpression of NQO1 alone as well as in combination with HO-1 can inhibit LPS-induced TNF- $\alpha$  expression in THP-1 cells and this inhibition is NF- $\kappa$ B independent. Further evidence indicates that NQO1 has an RNA-binding property, thus a direct involvement in post-translational modification of proteins<sup>414</sup>. Although in this study we mainly observed a marked effect of FA-Hex-Es and FA-Pro-Es on HO-1 and TNF- $\alpha$  at protein level, no evidence from the current

literature indicates any post-translational involvement of HO-1 or its enzymatic products on TNF- $\alpha$  protein or any other proteins, although it is worth further investigating whether reduced TNF- $\alpha$  protein is linked to HO-1 upregulation at the post-translational level. Further work could include experiments such as silencing RNA (siRNA) to knock down HO-1 and Nrf2 prior to treatment with FA-Hex-Es and FA-Pro-Es and measuring TNF- $\alpha$  secretion. Another experiment could be treating cells with HO-1 and Nrf2 inhibitors alone or in combination with FA-Hex-Es and FA-Pro-Es. In addition to these experiments, more importantly the effect of these two potent compounds on HO-1 and Nrf2 should be tested in the presence of 1 ng/mL LPS, the same condition as the effect on LPS-induced TNF- $\alpha$  secretion, to see if these compounds still upregulates anti-oxidant proteins.

A limitation of this study is that we did not investigate the effect of other phenolic acids and analogues on HO-1 and NQO1 expression. For instance, CA-Gly showed a trend in suppressing TNF- $\alpha$  secretion and caffeic acid derivatives, as in the study of Croft et al., 2017, increased HO-1. Furthermore, although THP-1 are a validated cell line model to study inflammation and oxidative stress and their LPS-induced Nrf2 and pro-inflammatory signalling pathways are similar to primary monocytes, they have some limitations. As a cancer cell line, it may be less responsive to oxidative and other stress. Use of primary monocytes or macrophages could have been more responsive to physiological concentrations of the phenolic acids and future studies should take this into consideration. Another limitation of this study is the use of LPS. Even though LPS is a well established inflammatory model for immune cells, alternative models of inflammation specific to CVD such as oxLDL or CD40L to induce inflammation rather than LPS should be considered in future studies.

In conclusion, most phenolic acids examined did not exert anti-inflammatory effects at physiological concentrations in THP-1 cells. However, esterification of natural phenolic acids enhanced the activity of FA, likely due to increased lipophilicity combined with presence of a longer alkyl chain

of FA itself, together mediating a better cellular uptake or absorption. The mechanism of action of these esterified compounds is post-transcriptional similar to other flavonoid metabolites previously studied in our laboratory. The esters induced HO-1 and NQO1 expression independently of Nrf2 suggesting alternative regulatory mechanisms are involved. These results suggest that synthetic esterified analogues of dietary-derived phenolic acids have anti-inflammatory properties with potential pharmaceutical application as anti-inflammatory drugs.

# **Chapter 4. Anti-Inflammatory Effects of Flavonoid Metabolites and Their Esters in Microglial Cells**

## **Acknowledgements**

Gabriela Burianova performed the MTS assay for the dose response of PCA-Hex-Es and LPS kinetics for IL-6 secretion.

## 4.1 Introduction

Consumption of flavonoid rich foods e.g. berries, tea and chocolate, is associated with a reduced risk of developing various neurological disorders including stroke <sup>492,493</sup> depression <sup>185,186</sup> and neurodegenerative disorders e.g. Parkinson's disease (PD) and Alzheimer's disease (AD) <sup>24,26,190</sup>. Neuroinflammation is a major contributor to the development of these diseases <sup>242,243,246,494,495</sup>. The cause of neuroinflammation in AD and PD is mainly unknown but in stroke and ischemia, the signalling is mediated by several key pro-inflammatory cytokines (TNF- $\alpha$ , IL-1 $\beta$  and IL-6), chemokines (MCP-1, CCL5, CXCL1), reactive oxygen species (ROS) and secondary messengers (prostaglandins and NO) <sup>240</sup>. Accumulating evidence suggests that neuroinflammation is mediated by microglial cells <sup>241,245,250,496</sup>.

Microglial cells are the resident macrophage-like immune cells in the brain, playing a central role in maintaining homeostasis and repairing brain injury <sup>241</sup>. Recent evidence suggests that in diseases such as PD and AD, neuroinflammation can be initiated by chronic microglial activation (classical activation) <sup>243,245</sup>. The activation of microglia is induced by pro-inflammatory stimuli such as LPS, IFN- $\gamma$  or GM-CSF leading to activation of transcription factors such as AP1 and NF- $\kappa$ B, which regulate secretion of pro-inflammatory cytokines (e.g. IL-6 and TNF- $\alpha$ ) <sup>245</sup>. IL-6 plays a critical role in the nervous system. A dramatic increase in IL-6 levels is observed in various neurological disorders including major depressive disorder <sup>497</sup> PD, AD and brain ischemia <sup>318</sup>.

Emerging evidence suggests that flavonoids exert anti-inflammatory effects in microglial cells. Various flavonoids such as hesperetin, isorhamnetin and luteolin inhibit pro-inflammatory cytokines such as TNF- $\alpha$ , IL-1 $\beta$ , and IL-6 in LPS-induced BV2 cells <sup>498-501</sup>. More recent studies have postulated that the anti-inflammatory properties of flavonoids are likely due to their low molecular weight phenolic metabolites (including FA, CA, PCA and VA)

<sup>54,55,184</sup>. Furthermore, a recent study with raspberry extract enriched in ellagitannins, their degradation products, and ellagic acid (1 µg/mL) reduced the pro-inflammatory biomarkers TNF-α, CD40, NO and intracellular superoxide production via NF-κB, NFAT and MAPK pathways in LPS-stimulated N9 murine microglial cells <sup>502</sup>. The blood brain barrier (BBB) is highly selective with limited bioaccessibility and certain low-molecular metabolites (including PCA, VA, CA, FA, IFA) have been shown to pass the BBB in murine brain <sup>503</sup>. PCA administration has been shown to reduce ischemia-induced neuronal cell death by decreasing oxidative stress, microglial activation and disruption of BBB in rats <sup>504,505</sup>. In mice exposed to chronic unpredictable mild stress, FA administration showed an anti-depressant effect, inhibiting microglial activation via reduced pro-inflammatory cytokine expression and NF-κB signalling <sup>265</sup>. IFA has been reported to suppress LPS-induced NF-κB activity via dephosphorylation of PI3K/Akt in BV2 cells <sup>489</sup>. The use of animal studies indicates that bioaccessible phenolic acids PCA, FA and IVA are bioactive in the brain.

Since in the previous chapter synthetic esters were shown to be bioactive, we investigated these esters together with their parent compounds for their anti-inflammatory effects in murine BV2 microglial cells.

## **4.2 Aim**

- To compare three common naturally occurring phenolic acids, FA, IFA and PCA and their synthetic esterified analogues for their effects on TNF- $\alpha$  and IL-6 secretion in BV2 microglial cells and investigate their intracellular mechanisms of action.

## 4.3 Results

### 4.3.1 Effect of phenolic acids and ester analogues on BV2 microglial cell viability

Cytotoxicity of selected compounds on murine BV2 microglial cells was assessed by MTS assay to ensure any subsequent observed effects were not due to cell death. BV2 cells were treated with 10  $\mu\text{M}$  FA, IFA, PCA or their methyl (Met), ethyl (Et), propyl (Pro) or hexyl (Hex) esters (Es) or DMSO (vehicle control, VC) for 24h and cell viability measured by MTS assay. **Figure 4. 1 (A)** indicates that none of the treatments had any significant effect on cell viability with the exception of PCA-Hex-Es. To determine a non-toxic dose for this compound, a further MTS assay was performed with 1  $\mu\text{M}$ , 5  $\mu\text{M}$ , 10  $\mu\text{M}$  and 20  $\mu\text{M}$  (**Figure 4. 1 (B)**). PCA-Hex-Es markedly reduced cell viability at all tested concentrations. Although 1  $\mu\text{M}$  PCA-Hex-Es reduced cell viability by 30%, it was not statistically significant and therefore 10X lower concentration (0.1  $\mu\text{M}$ ) was used in further experiments.



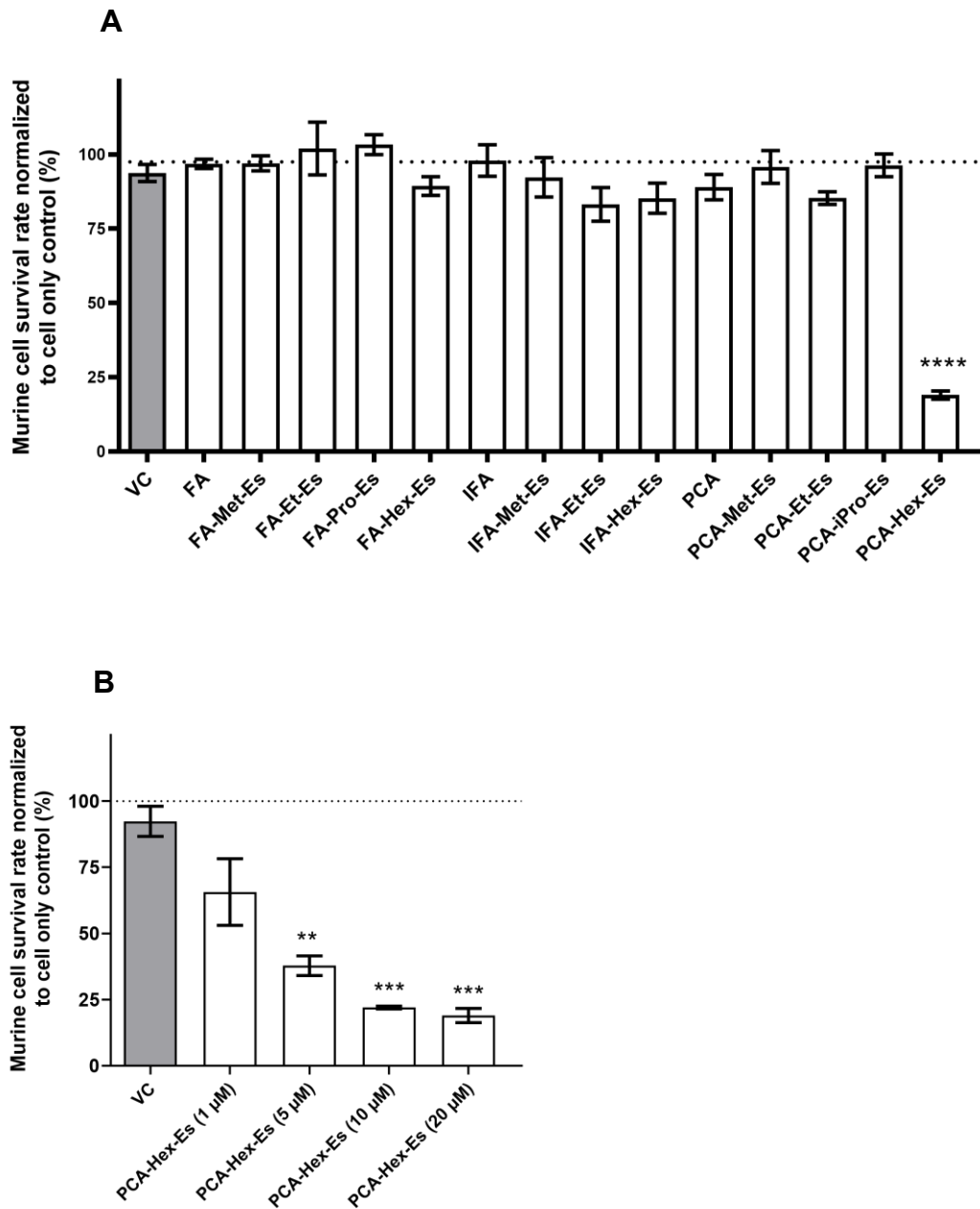


Figure 4. 1 Effect of phenolic acids esters on murine BV2 microglial cell viability measured by MTS assay. Cells ( $3 \times 10^3$ ) were treated with 10  $\mu$ M of each compound (A), or with 1, 5, 10, or 20  $\mu$ M PCA-Hex-Es (B) or 0.1 % DMSO (vehicle control, VC) for 24h and cell viability measured by MTS assay. Cell viability was expressed as percentage of non-treated cells (cell only, not shown) mean  $\pm$  SEM, n=3. Treatment effects compared with VC were determined by one-way ANOVA with post-hoc Dunnett's. \*\* p < 0.01; \*\*\* p < 0.001; \*\*\*\* p < 0.0001.

### 4.3.2 Kinetics of LPS-induced TNF- $\alpha$ secretion in BV2 cells

TNF- $\alpha$  is a key proinflammatory cytokine and elevated TNF- $\alpha$  in the central nervous system is associated with neurodegenerative disease pathology and progression<sup>244</sup>. To assess the optimal concentration and time for LPS-induced TNF- $\alpha$  secretion in the microglial cells, BV2 cells were treated with 1, 10 or 100 ng/mL LPS for 2, 4 or 6 h. TNF- $\alpha$  secretion was measured by ELISA. TNF- $\alpha$  secretion steadily increased with time in response to 10 and 100 ng/ml LPS (**Figure 4. 2**). A dose response was observed at 4 and 6 h. 10 ng/mL LPS for 4 h was chosen for further experiments.

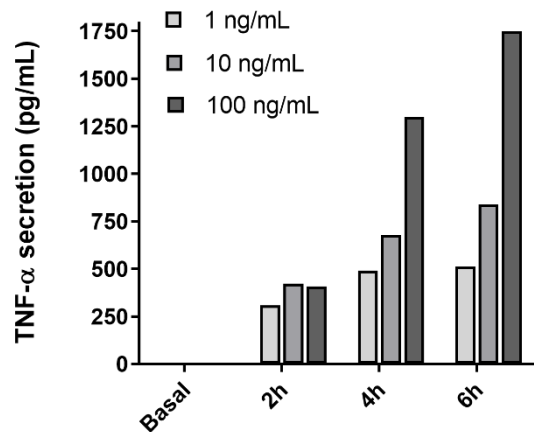


Figure 4. 2 LPS-induced TNF- $\alpha$  secretion in BV2. Cells ( $1 \times 10^5$ /well) were treated with 1, 10, or 100 ng/mL LPS for 2, 4 or 6h or left untreated (Basal). TNF- $\alpha$  secretion was measured by ELISA and expressed as pg/mL, n=1.

### 4.3.3 Phenolic acids and ester analogues do not significantly inhibit TNF- $\alpha$ Secretion in BV2 cells

The common phenolic acids PCA, FA, and IFA and their esters were screened at 10  $\mu$ M (except PCA-Hex-Es, 0.1  $\mu$ M) for their effect on LPS-induced TNF- $\alpha$  secretion in BV2 cells. BAY 11-7082, an NF- $\kappa$ B inhibitor, has previously been reported to reduce LPS-induced TNF- $\alpha$  secretion in BV2 cells<sup>501</sup> was included as a positive control. **Figure 4. 3** shows that BAY 11-7082 (1  $\mu$ M) significantly inhibited LPS-induced TNF- $\alpha$  secretion. Of the phenolic acids and esters, FA-Hex-Es was the most promising, reducing LPS-induced TNF- $\alpha$  secretion by 15% compared with VC but this did not reach statistical significance and none of the other phenolic acids or related esters had any significant effect. A higher concentration of FA-Hex-Es (20  $\mu$ M) was not investigated as it reduced cell viability by ~43% (data not shown).

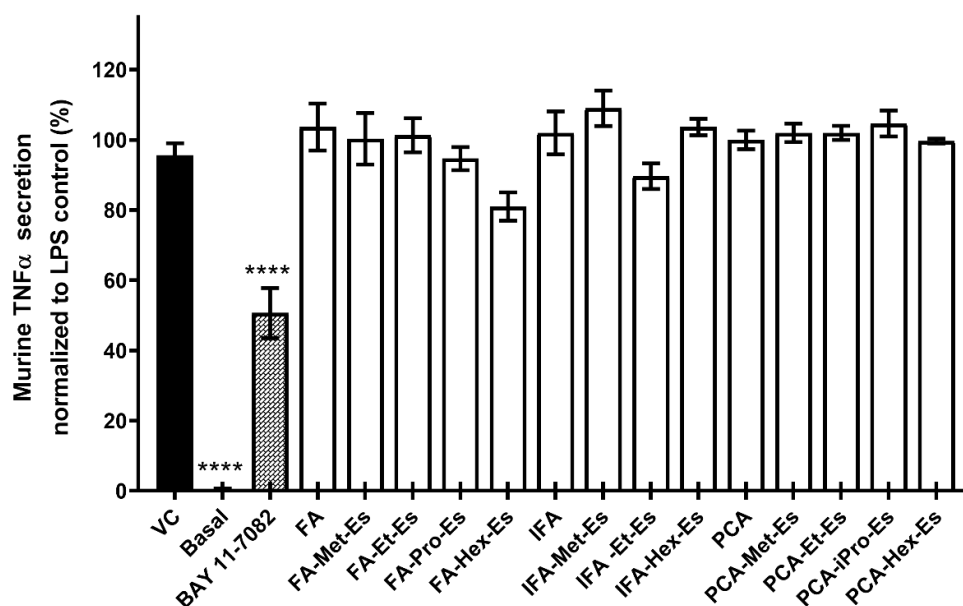


Figure 4. 3 Effect of FA, IFA, PCA and their esters on LPS-induced TNF- $\alpha$  secretion in BV2. Cells ( $1 \times 10^5$ /well) were pre-treated with 10  $\mu$ M of each compound (except PCA-Hex-Es, 0.1  $\mu$ M) or 0.1% DMSO (vehicle, VC) and 1  $\mu$ M BAY 11-7082 (positive control) for 30 min prior to stimulation with LPS (10 ng/mL) for 4h and TNF- $\alpha$  secretion measured by ELISA. Data expressed as percentage LPS control, mean  $\pm$  SEM, n=3. Treatment effects compared with VC were determined by one-way ANOVA with post-hoc Dunnett's test. \*\*\*\* p<0.0001.

#### 4.3.4 LPS-induced IL-6 secretion in BV2 cells

Since IL-6 plays a critical role in neuroinflammation and is secreted by microglial cells<sup>310,318</sup>, the effect of the phenolic acids and their esters on LPS-induced IL-6 secretion was investigated. While LPS induces TNF- $\alpha$  secretion rapidly, IL-6 secretion is delayed and has been reported to be highest after 24 h<sup>317</sup>. Prior to investigating the effects of the phenolic acids, the optimum concentration of LPS required for the ELISA was obtained. BV2 cells were stimulated with 1-1000 ng/ml LPS for 24 h. **Figure 4. 4** indicates that LPS increased IL-6 secretion in a concentration-dependent manner. Since 10 ng/mL LPS induced approximately 500 pg/mL IL-6, this concentration was considered the most suitable concentration within the detection range of the IL-6 ELISA assay standard curve (7.5-1000 pg/mL).

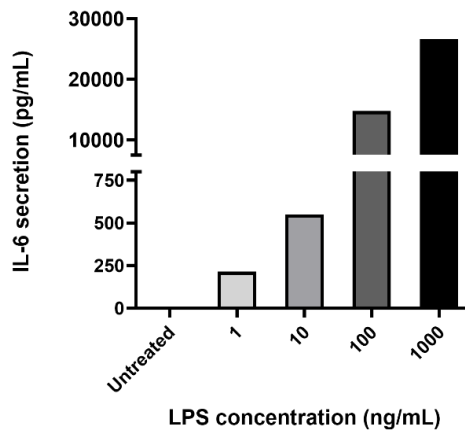


Figure 4. 4 LPS-induced IL-6 secretion in BV2. Cells ( $1 \times 10^5$ /well) were untreated or stimulated with 1, 10, 100 or 1000 ng/mL LPS for 24h. IL-6 secretion was measured by ELISA and expressed as pg/mL,  $n=1$ .

### 4.3.5 FA-Hex-Es suppresses LPS-induced IL-6 secretion in BV2 cells

Prior to LPS stimulation for 24 h, BV2 cells were pre-treated with 0.1% DMSO (VC) or 10  $\mu$ M FA, PCA or IFA or their esters, with the exception of PCA-Hex-Es, which had a concentration of 0.1  $\mu$ M to avoid cytotoxicity. 1  $\mu$ M Bay 117082 was included as a positive control. **Figure 4. 5** shows that 1  $\mu$ M BAY 117082 completely suppressed LPS-induced IL-6 secretion. Among the phenolic acids and esters, FA-Hex-Es significantly inhibited IL-6 secretion. The FA methyl and ethyl esters slightly reduced IL-6 secretion (7 and 12% vs VC) and IFA-Et-Es showed a moderate but non-significant attenuation of IL-6 secretion (16% vs VC). FA, FA-Hex-Es and IFA-Et-Es were further assessed for a possible dose response effect.

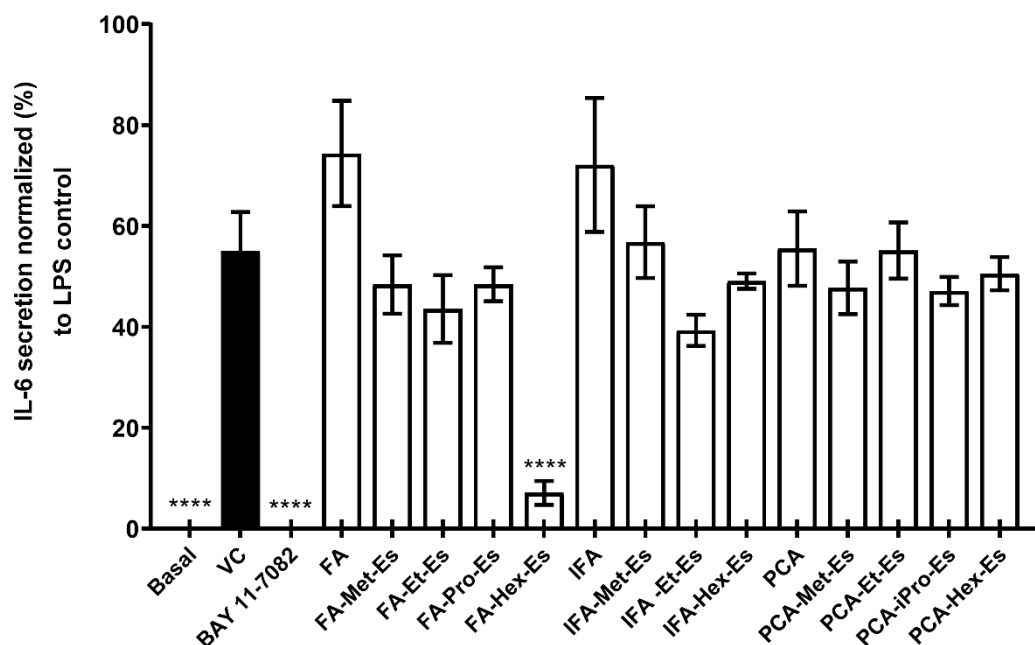


Figure 4. 5 Effect of 10  $\mu$ M flavonoid metabolites and their esters on LPS-induced IL-6 protein secretion in BV2. Cells ( $1 \times 10^5$ /well) were pre-treated with 10  $\mu$ M of each phenolic acid or their esters (except PCA-Hex-Es, 0.1  $\mu$ M), or 0.1% DMSO (vehicle control, VC) or 1  $\mu$ M BAY 11-7082 (positive control) for 30 min prior to treatment with LPS (10 ng/mL) for 24h and IL-6 secretion measured by ELISA. Data is expressed as percentage of LPS control, mean  $\pm$  SEM, n=3. Treatment effects compared to VC were determined by one-way ANOVA with post-hoc Dunnett's test or t test for BAY11-7082 \*\*\*\* p<0.0001.

### 4.3.6 FA-Hex-Es significantly reduces LPS-induced IL-6 secretion in a dose-dependent manner in BV2 cells

The effects of different concentrations (0.1  $\mu$ M, 1  $\mu$ M and 10  $\mu$ M) of FA-Hex-Es and IFA-Et-Es on LPS-induced IL-6 secretion were investigated. FA was included as a control. **Figure 4. 6** indicates that FA-Hex-Es (**4.6 B**) significantly inhibited LPS-stimulated IL-6 secretion and the effect was dose-dependent (16%, 52% and 76% vs VC). In contrast no significant effect was observed with FA alone (**4.6 A**) and a non-significant trend with IFA-Et-Es (**4.6 C**) was observed.

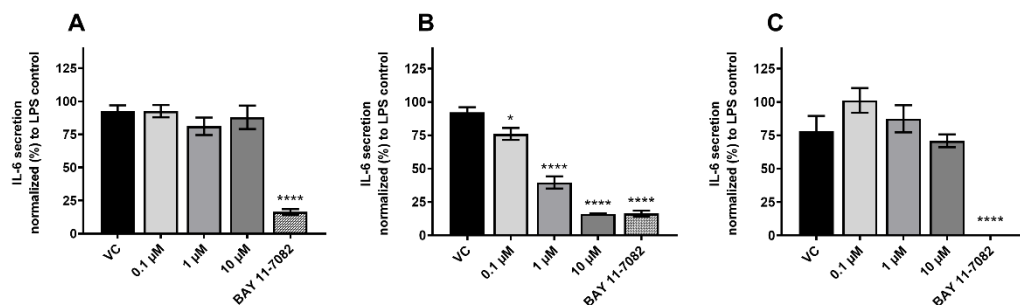


Figure 4. 6 FA-Hex-Es dose dependently inhibits LPS-induced IL-6 secretion in BV2. Cells ( $1 \times 10^5$ /well) were pre-treated with 0.1  $\mu$ M, 1  $\mu$ M or 10  $\mu$ M of FA (A), FA-Hex-Es (B) or IFA-Et-Es (C), 0.1% DMSO (vehicle control, VC) or 1  $\mu$ M BAY 11-7082 (positive control) for 30 min prior to treatment with LPS (10 ng/mL) for 24h and IL-6 secretion measured by ELISA. Data is expressed as percentage of LPS control, mean  $\pm$  SEM, n=3. Treatment effects compared to VC were determined by one-way ANOVA with post-hoc Dunnett's test or t test for BAY11-7082 vs VC \* $p < 0.05$ ; \*\*\*\* $p \leq 0.0001$ .

### 4.3.7 LPS-induced IL-6 mRNA expression in BV2 cells

To understand whether the observed effect on IL-6 secretion in BV2 cells was post-translational as in the case of TNF- $\alpha$ , HO-1 and NQO1 expression in THP-1 cells or affected gene expression, effects on mRNA expression were examined. A time-course of LPS-induced mRNA expression for 2, 4, 6 and 8 h was conducted and analysed by qPCR. **Figure 4. 7** indicates IL-6 mRNA expression in response to LPS was elevated at all time-points, peaking at 4 h and therefore this time point was used in further experiments.

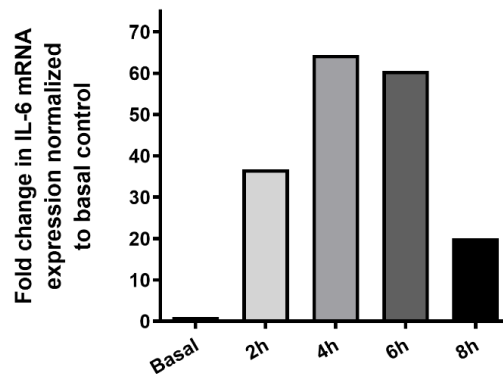


Figure 4. 7 Kinetics of LPS-induced IL-6 mRNA expression in BV2. Cells ( $1 \times 10^5$ /well) were untreated or treated with 10 ng/mL LPS for 2h, 4h, 6h, and 8h and mRNA expression measured by RT-qPCR. IL-6 mRNA expression levels were normalised to GAPDH and expressed as fold change over basal control, n=1.

### 4.3.8 Effect of FA-Hex-Es, FA-Pro-Es and FA on IL-6 mRNA expression in BV2 cells

BV2 cells were pre-treated with FA and esters (10  $\mu$ M) or 0.1% DMSO (VC) prior to stimulation with LPS (10 ng/mL) for 4 h. BAY 11-7082 (1  $\mu$ M) was included as a positive control. **Figure 4. 8** demonstrate that LPS-induced IL-6 mRNA expression was significantly inhibited by FA-Hex-Es (90% inhibition) to a similar level as the positive control (BAY 11-7082). IFA-Et-Es also significantly inhibited LPS-induced IL-6 mRNA expression to a lesser extent. As expected, no significant effect was observed with FA.

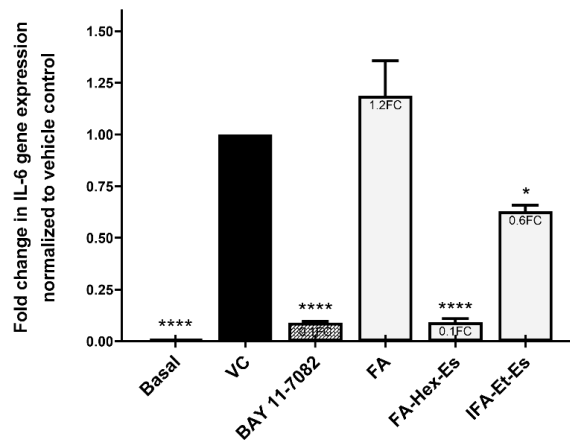


Figure 4. 8 Effects of FA, FA-Hex-Es and IFA-Et-Es on LPS-induced IL-6 mRNA expression in BV2. Cells ( $1 \times 10^5$ /well) were untreated or treated with 10  $\mu$ M of FA, FA-Hex-Es, IFA-Et-Es, 0.1% DMSO (VC) or 1  $\mu$ M BAY 11-7082 (positive control) for 30 min prior to adding LPS (10 ng/mL) for 4 h. IL-6 mRNA expression was measured by RT-qPCR. mRNA values were expressed as fold change (relative to VC) and normalised to GAPDH. Mean  $\pm$  SEM, n=3. Treatment effects with FA, FA-Hex-Es, and IFA-Et-Es compared to VC were determined by one-way ANOVA with post hoc Dunnett's test. Significant difference between BAY 11-7082 and VC and basal versus VC by t-test. \* $p < 0.05$ ; \*\*\*\* $p \leq 0.0001$ .



### **4.3.9 Effect of FA-Hex-Es on upstream regulators of IL-6 gene expression**

IL-6 gene expression is regulated by several transcription factors including NF- $\kappa$ B and AP-1. AP-1, a heterodimer of c-Fos and c-Jun is activated by JNK, which is an essential mediator of the pro-inflammatory response in microglia<sup>506,507</sup>. The flavone luteolin (5-50  $\mu$ M) has been reported to inhibit IL-6 gene expression via JNK and AP-1 activation in LPS-induced BV2 cells<sup>498</sup>, suggesting that this may be a possible mechanism of action also for the phenolic acid esters. To understand how FA-Hex-Es and IFA-Et-Es inhibited IL-6 gene expression, we studied JNK, AP-1 and NF- $\kappa$ B activation in BV2 cells.

### **4.3.10 Optimisation of LPS-induced JNK protein phosphorylation in BV2 Cells**

The kinetics of JNK phosphorylation in response to 10 ng/mL LPS was first investigated. Cells were treated with 10 ng/mL LPS for 0, 5, 15, 30, 45, and 60 min western blot analysis used to measure phosphorylation of JNK. Unphosphorylated JNK and  $\beta$ -tubulin (a housekeeping gene) were included as loading controls. **Figure 4. 9** indicates that LPS stimulated JNK phosphorylation by 15 min, remained high at 30 min and decreased by 45 min. This suggested that 30 min stimulation was suitable for further experiments.

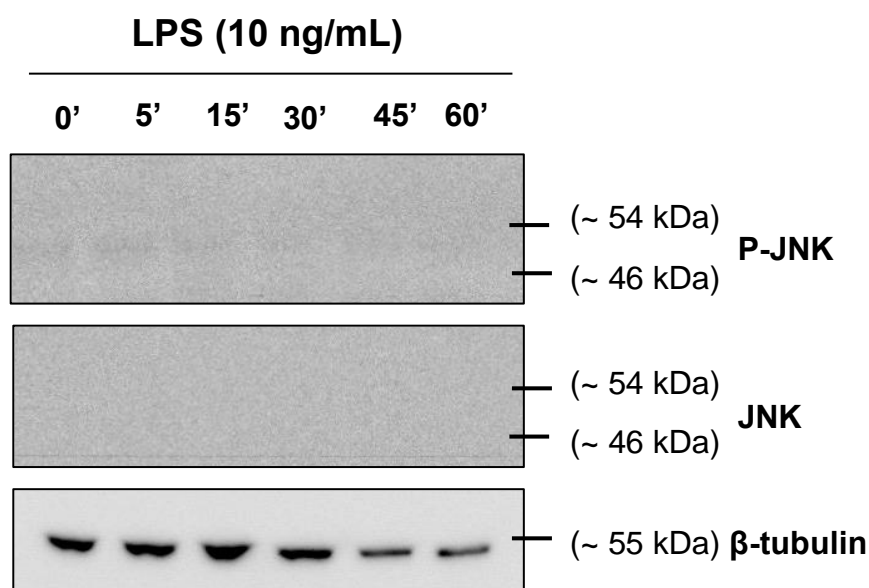


Figure 4. 9 Kinetics of LPS-induced JNK protein phosphorylation in BV2. Cells ( $2 \times 10^5$ /well) were stimulated with 10 ng/mL LPS for 0-60 min. Total protein was extracted and phosphorylated and unphosphorylated JNK protein expression measured by western blot analysis. Beta tubulin was used as a loading control. Representative of three independent experiments.

#### **4.3.11 Effect of FA-Hex-Es, IFA-Et-Es and FA on JNK phosphorylation in BV2 cells**

BV2 cells were pre-treated for 30 min with 20  $\mu$ M FA and 10  $\mu$ M FA-Hex-Es, IFA-Et-Es or SP600125, a JNK inhibitor (positive control) or 0.1% DMSO (VC) prior to treatment with LPS (10 ng/mL) for 30 min. JNK phosphorylation was assessed by western blot analysis. **Figure 4. 10 (A)** shows that although SP600125 inhibited LPS-induced JNK phosphorylation compared to the VC, neither FA nor the two esters had any effect. This was confirmed by densitometric analysis (**Figure 4. 10 (B)**).

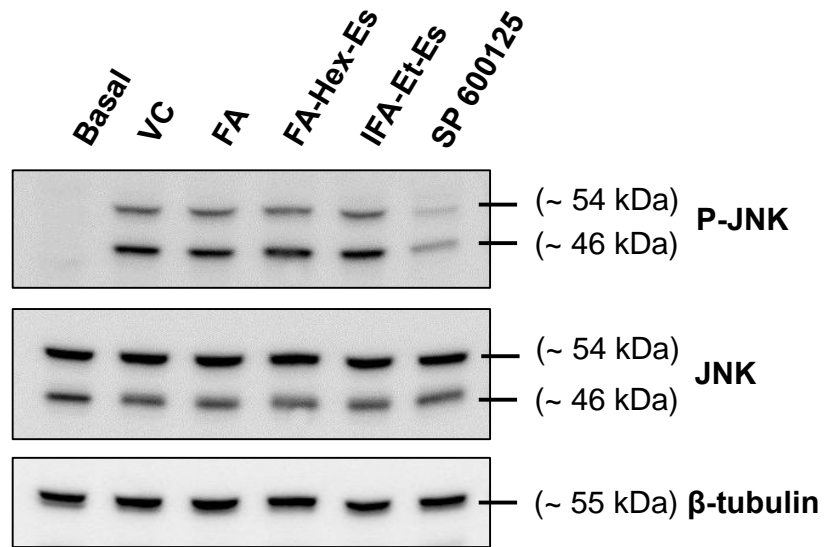
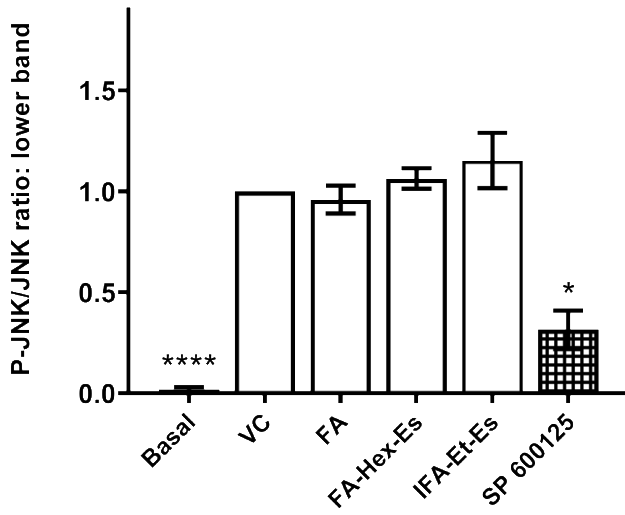
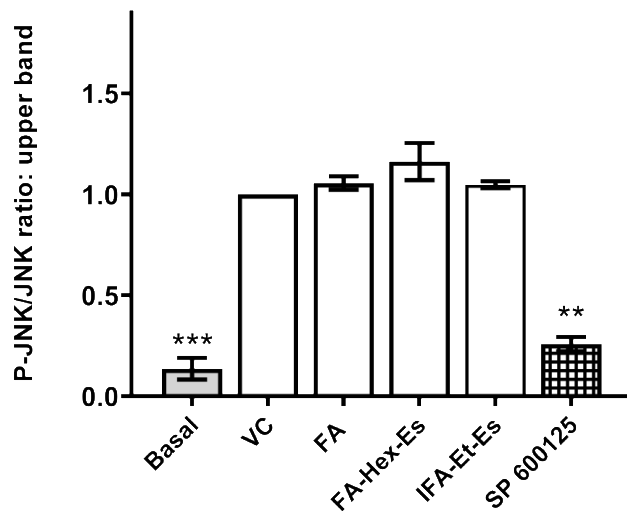
**A**

Figure 4. 10 LPS-stimulated JNK phosphorylation is not affected by treatment with FA, FA-Hex-Es or IFA-Et-Es in BV2. Cells ( $2 \times 10^5$ /well) were treated for 30 min with 20  $\mu$ M FA or 10  $\mu$ M FA-Hex-Es, IFA-Et-Es or SP 600125 (positive control) or 0.1% DMSO (VC) prior to stimulation with LPS (10 ng/mL) for 30 min. A) JNK protein expression and phosphorylation was measured by western blot analysis from whole cell lysates and  $\beta$ -tubulin used as a loading control. Representative of three independent experiments. B) Image J densitometric analysis of unphosphorylated and phosphorylated JNK expression, normalised to  $\beta$ -tubulin and relative to VC control. Ratio of P-JNK/JNK for FA, FA-Hex-Es and IFA-Et-Es was analysed by one-way ANOVA with post hoc Dunnett's test. Significant difference between basal and VC and SP600125 and VC were analysed by Student's t-test. Mean  $\pm$  SEM,  $n=3$ . \* $p \leq 0.05$ , \*\*\*\* $p \leq 0.0001$ .

**B**



#### **4.3.12 Kinetics of LPS-induced c-Jun and c-Fos phosphorylation in BV2 cells**

AP-1 is a heterodimer of c-jun and c-fos<sup>329</sup>. In order to determine an optimal time-point to study the effects of FA and the esters on LPS-induced c-Jun and c-Fos phosphorylation, a time course was performed. Cells were unstimulated or treated with 1 µg/mL LPS for 1, 2, 3, or 4 h phosphorylation measured by western blot analysis. The concentration of LPS used in this assay was based on the assay sensitivity as well as on previous work from our lab and others<sup>460,508,509</sup>. **Figure 4. 11** indicates that compared to basal levels (0 h), c-Jun and c-Fos were phosphorylated following LPS treatment at all timepoints, peaking at 1 h. Furthermore, protein level of c-jun was elevated by LPS treatment at all time points. 1h treatment with LPS also seemed to elevate c-Fos protein level however this may have been due non-specific signal enhancement and low quality of antibody which could be seen from the size of bands. Further studies in serum-free media did not alter the effects of LPS on phosphorylated or non-phosphorylated c-Jun or c-Fos expression (**Figure 8.16, Appendix III**). 1 µg/mL LPS stimulation for 2 h in usual media was therefore utilised in further studies.

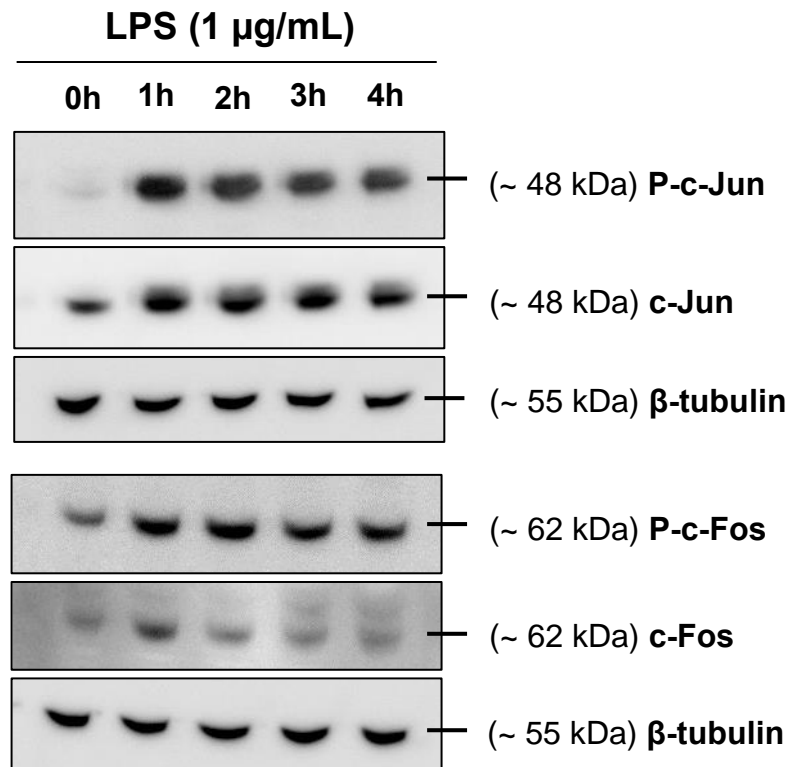


Figure 4. 11 Kinetics of c-Jun and c-Fos protein phosphorylation and expression in response to LPS stimulation in BV2. Cells ( $2 \times 10^5$ /well) were stimulated with 1 µg/mL LPS for 0-4 h and total protein extracted. cells were lysed for protein extract. Per sample 50 µg total protein was used to examine protein expression by western blot assay. And β-Tubulin expression was used to assess equal protein loading for all samples.

#### **4.3.13 Effect of FA-Hex-Es, FA-Pro-Es and FA on c-Jun and c-Fos phosphorylation in BV2 Cells**

FA, FA-Hex-Es and IFA-Et-Es were then tested for their effect on c-Jun and c-Fos. Cells were pre-treated with 20 µM FA or 10 µM FA-Hex-Es, IFA-Et-Es, SP 600125 (which inhibits c-Jun and to some extent c-Fos phosphorylation<sup>510</sup>), PD 98059 (which inhibits c-Fos phosphorylation<sup>511</sup>) or 0.1% DMSO (VC) for 30 min prior to stimulation with LPS (1 µg/mL) for 2 h except control (non-treated cells). Protein expression and phosphorylation levels of c-Jun and c-Fos were assessed by western blot analysis. **Figure**

4.12 shows that LPS increased phosphorylation of c-Jun and c-Fos but these were not affected by treatment with FA, FA-Hex-Es or IFA-Et-Es. In contrast, SP 600125 markedly inhibited both c-Jun and c-Fos phosphorylation, while PD 98059 inhibited c-Fos phosphorylation. These results suggest that FA-Hex-Es and IFA-Et-Es do not act through the AP-1 signalling pathway. Their effects on NF- $\kappa$ B were then investigated.

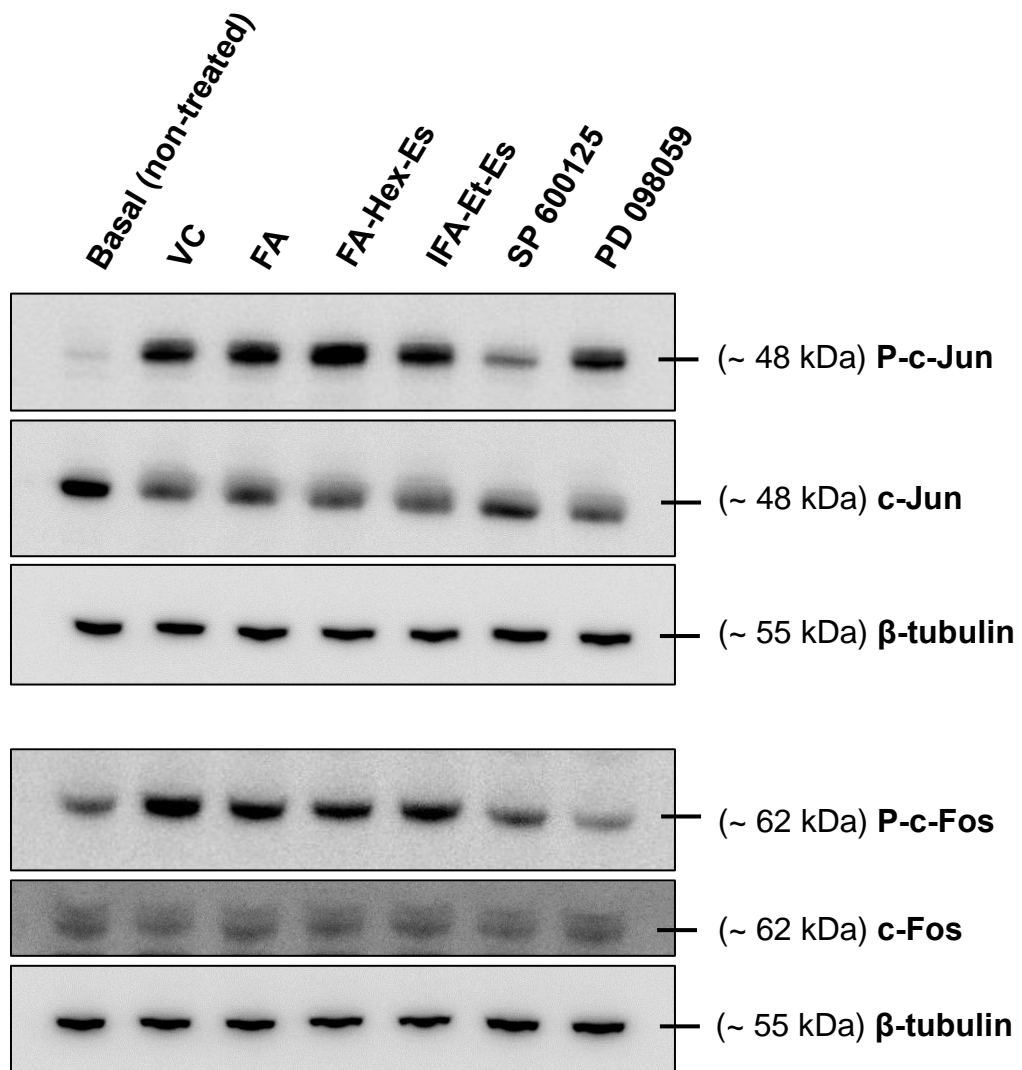


Figure 4. 12 FA, FA-Hex-Es and IFA-Et-Es do not significantly reduce LPS-induced c-Fos/c-Jun phosphorylation in BV2. Cells ( $2 \times 10^5$ /well) were untreated or pre-treated for 30 min with 20  $\mu$ M FA, 10  $\mu$ M FA-Hex-Es, IFA-Et-Es, SP 600126, PD 098059 or 0.1% DMSO (vehicle control, VC) prior to stimulation with 1  $\mu$ g/mL LPS for 2 h. Western blot analysis of c-jun and c-fos using whole cell lysates. was used as a protein loading control. Immunoblot is representative of three independent experiments.

#### **4.3.14 FA-Hex-Es inhibits p65 NF-κB phosphorylation in BV2 cells**

The transcription factor NF-κB is a major regulator of pro-inflammatory cytokines, including IL-6. NF-κB is a family of transcription factors that heterodimerise and IL-6 is regulated by the p50/p65 heterodimer. p65 becomes phosphorylated upon activation and therefore its phosphorylation status is useful to determine if the pathway is activated or inhibited. Previously LPS-induced p65 phosphorylation in BV2 cells has been reported for various-time points (15 min-6 h <sup>232,512,513</sup>) and different concentrations (0.1-1 µg/ml <sup>232,512,514</sup>) have been reported to induce p65 phosphorylation. A preliminary experiment conducted in our lab showed 10 ng/mL LPS for 2 h induces phosphorylation of p65 NF-κB (data not shown). The effects of FA, IFA-Et-Es and FA-Hex-Es on LPS-induced p65 phosphorylation in BV2 cells was then examined at 2 h with 10 ng/mL LPS. **Figure 4. 13 (A)** demonstrates that LPS induces p65 phosphorylation by 2 h and that this is significantly reduced by FA-Hex-Es and BAY 11-7082 (1 µM), an NFκB inhibitor that suppresses IκBα phosphorylation, (**Figure 4. 13 (B)**). FA did not show any observable effect on p65 phosphorylation while IFA-Et-Es did show a non-significant inhibitory trend. FA-Hex-Es showed a marked inhibition by reducing NF-κB phosphorylation by 0.56-fold relative to VC control.



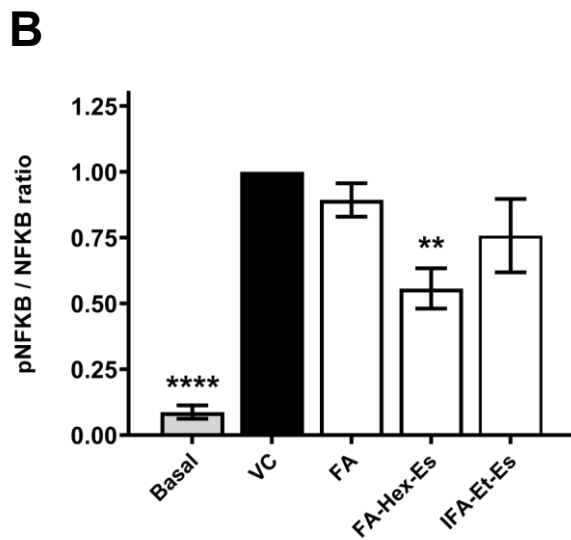
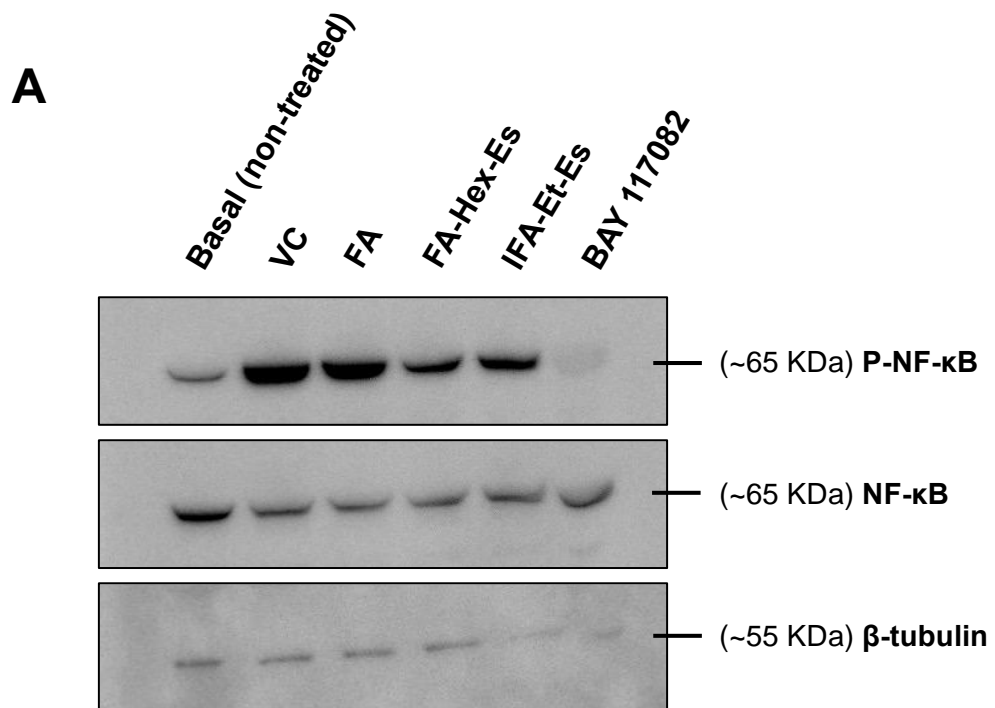


Figure 4. 13 FA-Hex-Es reduces LPS-induced p65 NF-κB phosphorylation in BV2. Cells ( $2 \times 10^5$ /well) were untreated or pre-treated for 30 min with 20  $\mu$ M FA, 10  $\mu$ M FA-Hex-Es or IFA-Et-Es for 30 min prior to stimulation with 10 ng/mL LPS for 2 h. A) p65 protein expression measured by western blot analysis.  $\beta$ -tubulin expression was used as a loading control. Representative of four independent experiments. B) Densitometric analysis of the expression levels of NF-κB and P-NF-κB normalised to  $\beta$ -tubulin and compared with VC. Data is expressed as P-NF-κB/NF-κB ratio. Mean  $\pm$  SEM, n=5. Significant differences between VC and FA, FA-Hex-Es, IFA-Et-Es were assessed by one-way ANOVA with post hoc Dunnett's test and difference between VC and basal, and positive controls by Student's t-test. \*\* $p \leq 0.01$ ; \*\*\*\* $p \leq 0.0001$ .

## 4.4 Discussion

Flavonoid intake is positively associated with a reduced risk of neurological disorders including stroke and age-related neurodegeneration <sup>492,493</sup>. Neuroinflammation is central to the pathogenesis of these diseases and microglial cells play a key role in inflammatory processes in the brain. Parent flavonoids have been extensively studied for their anti-inflammatory effects in microglial cell models and have been shown to inhibit the pro-inflammatory cytokines TNF- $\alpha$  and IL-6 <sup>498,501</sup>. However, these are metabolised before they reach the brain and the concentrations used were supraphysiological. Here, we investigated the effects of three common dietary-derived phenolic acids and their unnatural esters on pro-inflammatory mediators in the BV2 microglial cell line. FA-Hex-Es significantly inhibited LPS-induced IL-6 secretion and mRNA expression and significantly reduced NF- $\kappa$ B expression suggesting that this signalling pathway was the regulatory mechanism responsible for this effect.

Prior to screening, the effect of these compounds on BV2 cell viability was assessed by MTS assay. With the exception of PCA-Hex-Es, none of the tested PA were cytotoxic to BV2 cells at 10  $\mu$ M concentration. Even at 1  $\mu$ M, PCA-Hex-Es reduced cell viability by  $\pm$  35%. PCA-Hex-Es has previously been shown to inhibit tyrosinase <sup>515</sup>, an enzyme regulating melanogenesis in mammals and enzymatic browning in mushrooms, fruits and vegetables. Interestingly, intracellular neuromelanin levels have been proposed to set the threshold for Parkinson's disease initiation <sup>516</sup>, hence further studies are warranted to investigate the effect of PCA-Hex-Es on tyrosinase, perhaps a new target for phenolic metabolites in neuroinflammation.

None of the screened compounds showed any significant effect on LPS-induced TNF- $\alpha$  secretion in BV2 cells. However, FA-hexyl-ester (FA-Hex-Es) and IFA-ethyl-ester (IFA-Et-Es) showed a non-significant inhibitory trend towards attenuation of TNF- $\alpha$  levels. Several flavonoids have

previously been reported to inhibit TNF- $\alpha$  secretion in microglial cells. Isorhamnetin (100-200  $\mu$ M) was shown to suppress TNF- $\alpha$  and IL-1 $\beta$  secretion in LPS-induced BV2 cells via TLR4/NF- $\kappa$ B signalling pathway<sup>500</sup>. This pathway was also reported to be targeted by hesperetin in LPS treated mice and in LPS-activated BV2 and mouse hippocampal (HT-22) cells at 50  $\mu$ M<sup>501</sup>. Sophoraflavanone G, a medicinal plant flavonoid also inhibited LPS-induced TNF- $\alpha$  secretion in a dose-dependent manner between 5-20  $\mu$ M via MAPKs, JAK/STAT and Nrf2/HO-1 signalling pathway<sup>499</sup>. However, the concentrations used are supraphysiological and it is unclear whether parent flavonoids pass the BBB. On the other hand, PA have been reported to pass BBB and recent studies<sup>55,517</sup> have listed various phenolic acids with neuroprotective effects including FA, CA and PCA with an inhibitory effect on TNF- $\alpha$ . Oral administration of CA (30 mg/kg) to mice prior to LPS challenge reduced IL-6 serum levels but had no significant effect on TNF- $\alpha$ , while in brain tissue samples TNF- $\alpha$  level was significantly reduced<sup>518</sup>. Treatment of BV2 with 2.5-22.5  $\mu$ g/mL FA was also shown to reduce TNF- $\alpha$  secretion<sup>519</sup>. Similarly, in another study pre-treatment of BV2 with 5-20  $\mu$ M PCA for 1 h and 24 h stimulation with LPS (0.5  $\mu$ g/mL) dose-dependently inhibited TNF- $\alpha$  as well as IL-1 $\beta$  and IL-6 secretion<sup>520</sup>. The disagreement between these studies and ours may be due to the concentration of PA used, the pre-incubation time and LPS treatment concentration and time-points.

Similarly, to TNF- $\alpha$ , IL-6 is involved in the inflammatory initiation and progression stages of chronic age-related disorders. More importantly, IL-6 is a major cytokine in the central nervous system (CNS)<sup>310</sup> and plays a central role in CNS neuroinflammation<sup>318,495</sup>. In this study, most of the screened PA at 10  $\mu$ M did not affect IL-6 secretion. However, the key finding of this chapter was the effect of FA-Hex-Es and IFA-Et-Es, where both concentration-dependently reduced IL-6 secretion in contrast to the parent FA. More interestingly, IL-6 mRNA expression was suppressed by FA-Hex-Es in a similar fashion as the positive control BAY 11-7082, an NF- $\kappa$ B inhibitor, while IFA-Et-Es showed a modest though significant reduction.

Other studies have reported that FA, CA and PCA inhibit IL-6 secretion. Again, the differences may be due to the concentrations used for CA<sup>518</sup> and FA<sup>519</sup>. While in the case of PCA<sup>520</sup>, even though relevant concentrations (5-20  $\mu$ M) were used, the discrepancy could be due to duration of pre-exposure and higher LPS concentration. However, similarly to this study, FA even at supraphysiological concentration neither affected IL-6 nor TNF- $\alpha$  secretion in a murine MG6 microglial cell line, where FA (10-250  $\mu$ M) co-incubated with LPS (300 ng/mL) for 24 h<sup>521</sup>.

IL-6 gene expression is under the control of several transcription factors including NF- $\kappa$ B and AP-1<sup>522</sup>. JNK, upstream of AP-1, is a potent effector in neuroinflammation and neuronal death<sup>506,523</sup> and a recent study reported that tea polyphenols down-regulated JNK phosphorylation to inhibit neuronal apoptosis in rats with cardiac arrest<sup>524</sup>. Another early study, has shown that expression of inflammatory genes e.g. IL-1 $\beta$ , IL-6 and MCP-1 induced by  $\beta$ -amyloid peptides in human Alzheimer's brain and endothelial cell culture was mediated by the JNK/AP-1 pathway<sup>525</sup>. In this study, neither FA, FA-Hex-Es nor IF-Et-Es showed any effect on JNK, c-JUN or c-FOS phosphorylation levels, suggesting that AP-1 does not regulate the effects of FA-Hex-Es.

Here, LPS induced NF- $\kappa$ B phosphorylation was significantly attenuated by FA-Hex-Es but not IFA-Et-Es or FA, suggesting the effect is MAPK-independent and specific to the NF- $\kappa$ B signalling pathway. Similarly, Wang and co-workers<sup>520</sup> showed that BV2 pre-treatment with 5-20  $\mu$ M PCA for 1h prior stimulation with LPS inhibits pro-inflammatory markers including IL-6 via NF- $\kappa$ B<sup>520</sup>. Recently, 2 h -pre-incubation of FA (10-100  $\mu$ M) prior 24h post-incubation with 1  $\mu$ g/mL LPS was reported to inhibit NF- $\kappa$ B phosphorylation in BV2 cells<sup>526</sup>.

Although FA-Hex-Es is not naturally occurring it has pharmaceutical value, and this could be having therapeutical application for neuroinflammatory disorders. A limitation of this study is that an immortalised murine microglial

cell line was used. BV2 cells were derived from raf/myc-immortalised murine neonatal microglia and are the most frequently used alternative model system for primary microglia research<sup>527</sup>. Further validation of these results in primary human microglial cells is needed in order to claim a beneficial effect of these compounds. Utilisation of primary microglial cell cultures are time-consuming, expensive, and of ethical concern. A few immortalised human microglial cell lines have been established<sup>528–530</sup>, however lack of validation against human primary microglial cells and concern over cross contamination with rat glioma cells (CHME-5)<sup>531</sup> are limiting factors.

An esterification reaction is the most widely used strategy in drug design to enhance the lipophilicity and hence the passive membrane permeability<sup>532</sup>. Accordingly, our results suggest that the observed effect of FA-Hex-Es is likely due to its longer alkyl chain tail, and thus its lipophilicity. In line with our findings, in another recent study by Kwon and co-workers (2019)<sup>336</sup>, they synthesised and evaluated the anti-inflammatory effect of a caffeic-ferulic acid hybrid together with parent FA and CA. The latter two failed to show any effect while the hybrid compound dose-dependently inhibited LPS-induced iNOS and COX-2, IL-1 $\beta$  and IL-6 expression via NF- $\kappa$ B activation in BV2 cells. More interestingly there was no effect on TNF- $\alpha$  expression<sup>336</sup> which is in line with our current finding.

In the context of SAR, the bioactivity of FA-Hex-Es in contrast to VA-Hex-Es suggests the absorption is due to a longer alkyl chain rather than the 4-OH, and 3-Met functional groups. Interestingly, in contrast to FA-Hex-Es, isoferulic acid-hexyl-ester (IFA-Hex-Es) did not show any activity on either TNF- $\alpha$  secretion in both BV2 and THP-1, nor IL-6 secretion in BV2 cells, implying that a methyl group on the third position is more important for the activity rather than a hydroxyl group. Furthermore, the parent phenolic acid, FA, but not IFA has been detected in the brain of rats, injected with a mixture of microbial metabolites of dietary polyphenol at physiological relevant concentrations<sup>503</sup>. Gasperotti and co-workers intravenously administered a

mixture of 23 metabolites (total 2.7  $\mu$ M) (incl. PCA, VA, CA, FA, IFA) into rats (n=4) to mimic a physiological post absorption situation. Tissue, blood, and urinary samples (5 sec-15 min) were taken to analysis by UHPLC-MS/MS. CA, PCA, VA and FA were among 10 metabolites detected in the brain. FA increased rapidly in the brain after 15 sec. In contrast, IFA, was neither detected in the brain of control animals (endogenous metabolite) nor ever appeared in the brain of treated animal despite a low level of plasma elimination rate. Furthermore, PCA and VA were both detected as endogenous metabolites. Indeed VA found in the cerebrospinal fluid (CSF) originates from catecholamine catabolism <sup>533</sup>. Interestingly in traditional Chinese medicine FA is one of the main components found in herbs and spices to treat inflammatory disorders and have been reported to be present in rat brains <sup>503,534,535</sup>. To summarise, FA is likely to be active in the brain and potentially has an effect on the IL-6 signalling pathway. However, its non-dose dependency in cell culture makes it challenging to study its mechanistic effect on inflammation and synthetic ester compound are promising alternative to study the mechanistic effect.

In summary, the chief outcome of this study was the robust effect of FA-Hex-Es on inhibiting LPS-induced IL-6 expression at both protein and mRNA level. We further investigated the mechanism of action of this compound and showed that this effect is potentially via reducing NF- $\kappa$ B activation rather than via JNK/AP-1 axis. Further study would be required to understand the inhibitory effect of FA-Hex-Es in the NF- $\kappa$ B signalling pathway (**Figure 4.4**). Hence, the effect on NF- $\kappa$ B upstream signalling molecules should be investigated. The most logical targets would be I $\kappa$ B and IKK. For instance, western blot analysis could be utilised to study the effect of FA-Hex-Es on phosphorylation state of these targets.

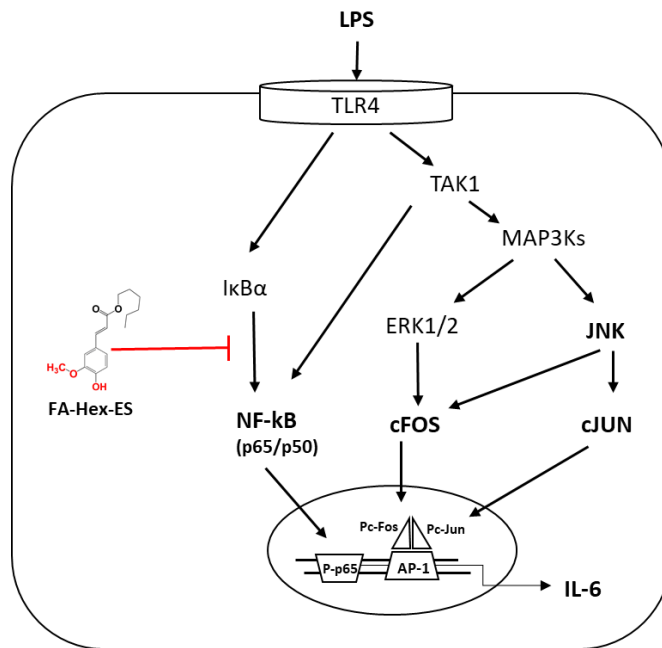


Figure 4. 14 Hypothetical model of the FA-Hex-Es-mediated anti-inflammatory effect via NF-κB pathway inhibition, with subsequent downregulation of IL-6 in BV2 microglial cells.

**Chapter 5. Effect of Phenolic  
Metabolites and Related Phenolic Acids  
on Transendothelial Migration of  
Neutrophils and Monocytes**



## 5.1 Introduction

CVD is the most common cause of death globally, hence bringing a major burden on the health care system, society, and the economy. The single most important contributor to CVD development is atherosclerosis<sup>217</sup>, a progressive inflammatory disease of the arterial wall characterised by the accumulation of lipid-laden lesions and foam cell formation over a long period of time. The first stage of atherosclerosis is initiated by endothelial cell injury and activation in response to multiple stimuli, including hemodynamic forces, hypercholesterolemia, infectious agents, oxidative stress, and circulating pro-inflammatory cytokines<sup>536</sup>. The activated endothelium orchestrates the recruitment of immune cells to the site of injury by inducing various pro-inflammatory mediators, including cell adhesion molecules (VCAM-1, E-selectin), pro-inflammatory cytokines (e.g., IL-1 $\beta$  and IL-6) and chemokines e.g. monocyte chemoattractant protein 1 (MCP-1, CCL2), CCL5<sup>337,537</sup> and CX3CL1 (fractalkine)<sup>538</sup>. In the early stages of atherosclerosis, a typical inflammatory response occurs with recruitment of neutrophils to the site of injury<sup>226,287,539,540</sup>. In response to inflammatory stimuli, neutrophils become activated and externalise a range of pre-made plasma membrane proteins, forming cytonemes (with a range of ready to release signalling proteins), release neutrophil extracellular traps (NETome), secretomes (ROS and lipid mediators), extracellular vesicles as well as pre-formed granular proteins and cytokines<sup>221,541–543</sup>, which are instantly released to instruct the subsequent recruitment and activation of monocytes and macrophages to the site of injury<sup>544,545</sup>.

The consumption of flavonoid-rich foodstuffs is inversely correlated with the risk of cardiovascular disease (CVD)<sup>33,52</sup>. Flavonoids are thought to interfere with the initial stages of atherosclerosis, preventing the development of the disease process through their anti-inflammatory and anti-oxidant properties. For example, the flavonoid fraction of bergamot juice inhibited TNF- $\alpha$ , IL-1 $\beta$  and IL-6 secretion by NF- $\kappa$ B activation in LPS-activated THP-1 monocytes<sup>546</sup>. In addition, cyanidin-3-glucosides

countered the response of TNF- $\alpha$  by inducing HO-1 and NQO1 expression via the Nrf2 pathway in HUVECs <sup>269</sup>. Moreover, FA has been shown to inhibit ICAM-1 and VCAM-1 expression in HUVECs and prevent radiation-induced U937 adhesion to HUVECs <sup>547</sup>. Since flavonoids from the diet are extensively metabolised in the body, our lab has previously focused on these metabolites. We and others have shown that these metabolites significantly reduce TNF- $\alpha$  and IL-1 secretion from monocytes and VCAM, ICAM-1 and IL-6 expression in endothelial cells at physiological concentrations (0.1-10  $\mu$ M) <sup>18,19,45,47,334,548</sup>. Moreover, phenolic metabolites inhibit monocyte adhesion to endothelial cells and transendothelial migration <sup>46,549</sup>.

Recent studies suggest that neutrophils also play an important role in the atherosclerosis process <sup>287,550,551</sup>. However, less is known about the effects of phenolic metabolites on neutrophils, which are also important in the initial inflammatory stages of atherosclerosis. Furthermore, to date, flavonoid studies have focused on single cell models, rather than the more complex multicellular vascular environment.

***Important note:*** *The rationale of this study was to investigate the effect of the most potent phenolic acids and novel synthetic compounds on trans-endothelial migration of primary immune cells using a high-throughput screening method. This study was meant to be performed toward the end of my PhD (2019-2020), as a 3-month placement at Unilever, Rotterdam, The Netherlands. However, due to unforeseen circumstances at the placement (incl. structural changes in the company, re-location of the research team and facilities) an unfavourable and immediate placement (Oct-Dec, 2017) was required rather than waiting for glycine- and ester-conjugates of phenolic acids to be synthesized (early, 2018). Therefore, the most potent compounds were not included in this study, but a selection of most common dietary phenolic acids and structurally related, commercially available non-natural phenolic acids were included.*

## 5.2 Aims

- Investigate the effect and structure-activity relationship of the seven most common diet-derived PA (PCA, FA, IFA, IVA, VA, CA and 4HBA) and fourteen structurally related PA (**Table 5. 1**) at 1  $\mu$ M on primary monocyte and neutrophil transendothelial migration through endothelial cells in a transendothelial migration assay.
- Investigate the effect of potent phenolic acids found in the transendothelial migration assay on MCP-1 secretion from neutrophils.
- Investigate the effect of potent phenolic acids found in the transendothelial migration assay on MCP-1 induced monocyte chemotaxis.

Table 5. 1 List of screened phenolic acids.

No	Metabolites	Acronym
<b>Common phenolic acids/ flavonoid metabolites</b>		
1	4-Hydroxybenzoic acid	4HBA
2	3,4-Dihydroxybenzoic acid ( <b>Protocatechuic acid</b> )	PCA
3	3-Hydroxy-4-methoxybenzoic acid ( <b>Isovanillic acid</b> )	IVA
4	4-Hydroxy-3-methoxybenzoic acid ( <b>Vanillic acid</b> )	VA
5	3,4-Dihydroxycinnamic acid ( <b>Caffeic acid</b> )	CA
6	3-Hydroxy-4-methoxycinnamic acid ( <b>Isoferulic acid</b> )	IFA
7	4-Hydroxy-3-methoxycinnamic acid ( <b>Ferulic acid</b> )	FA
<b>Synthetic analogues</b>		
8	Benzoic acid	BA
9	2-Iodobenzoic acid	2IBA
10	3-Iodobenzoic acid	3IBA
11	3-Chlorobenzoic acid	3CBA
12	3-Aminobenzoic acid	3ABA
13	3-Hydroxybenzoic acid	3HBA
14	4-Aminobenzoic acid (para-aminobenzoic acid)	4ABA
15	4-Nitrobenzoic acid	4NBA
16	4-Bromobenzoic acid	4BBA
17	2,4-Dihydroxybenzoic acid ( $\beta$ -Resorcylic acid)	24DHBA
18	2,4-Dimethoxybenzoic acid	24DMBA
19	3,5-Diaminobenzoic acid	35DABA
20	3-Chloro-4-methoxybenzoic acid	3C4MBA
21	5-Chloro-2-methoxybenzoic acid	5C2MBA

## **5.3 Results**

### **5.3.1 Transendothelial migration assay optimisation**

The transendothelial migration assay was developed to simulate the in vivo initial inflammatory stages of atherosclerosis <sup>552</sup>. The assay was further optimised as a high throughput functional assay for studying the effect of phenolic acids and related compounds on trans-endothelial migration of leukocytes.

#### **5.3.1.1 HMEC-1 validation by the endothelial cell biomarker PECAM-1**

Although human umbilical vein endothelial cells (HUVEC) are often used for the transendothelial migration assay, they have several limitations, including a limited lifespan and demonstrate variability between donors. Alternatively, the human microvascular endothelial cell line (HMEC-1) <sup>421</sup> has been reported to bear many features of primary endothelial cells, including similar expression of their adhesion molecules such as VCAM-1, ICAM-1 and PECAM-1 (CD31) <sup>421,553</sup>. PECAM-1 is required for extravasation of leukocytes from the blood through the endothelial layer and into the intima <sup>554</sup>. Hence, HMEC-1 cells were chosen for this assay. Firstly, HMEC-1 cells were validated by investigating CD31 expression by flow cytometry. **Figure 5. 1** demonstrates that PECAM-1 is expressed on HMEC-1 cells.

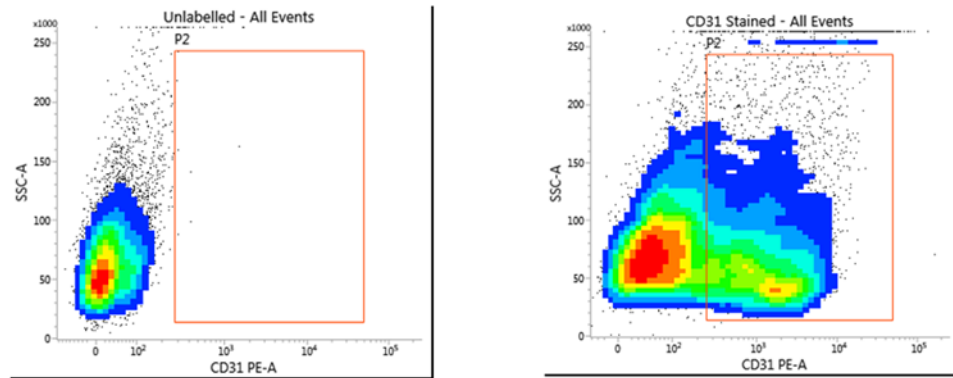


Figure 5. 1 HMEC-1 cells express PECAM-1 (CD31). Cells ( $10^6$ ) unstained (left panel) or stained (right panel) with 5  $\mu$ L PE-labelled CD31 (PE-31) antibody, resuspended in 300  $\mu$ L FACS buffer and run with medium flow rate (60  $\mu$ L/min). Side scatter (SSC) was extrapolated against PE-31 to create a density plot and population gate (P2) was drawn to separate stained cells from auto-fluorescence un-stained cells. Un-stained cells population (left panel) shifts after staining with PE-31 isotope (right panel).

### 5.3.1.2 Effects of the chemoattractants fMLP, MCP-1 and CX3CL1 on neutrophil and monocyte transendothelia migration

Three chemoattractants were compared for their chemotactic effects on both neutrophils and monocytes in the transendothelial migration assay. N-Formyl-Met-Leu-Phe (fMLP) is a well-defined bacterial chemotactic tripeptide for migration of neutrophils<sup>555–558</sup> but also attracts monocytes<sup>342,559–562</sup> to a lesser extent<sup>563</sup>. fMLP attracts both monocytes and neutrophils in a transendothelial migration-model<sup>552</sup>. Monocyte chemoattractant protein-1 (MCP-1/CCL2)<sup>337</sup> and fractalkine (CX3CL1)<sup>564</sup> are pro-inflammatory chemokines, known for their chemotactic activity on various leukocytes<sup>337,564</sup>. While fractalkine is a chemoattractant for monocytes/macrophages, NKs and some T-cells<sup>564</sup>, MCP-1, attracts monocytes, T- and B-cells, NKs, DCs<sup>343</sup>, and neutrophils during chronic inflammation<sup>565</sup>. Both were tested at different concentrations as chemoattractants for both neutrophils and monocytes in comparison to 10

nM fMLP. HMEC-1 cells were grown overnight on the apical compartment of a trans-well to form a monolayer, prior to adding peripheral blood leukocytes (PBL). The lower compartments of the trans-well were filled with media containing aforementioned chemoattractants and cells were allowed to migrate for 4 h. Transmigrated cells were fixed and analysed by flow cytometry as described in Chapter 2.

**Figure 5. 2** indicates that 10 nM fMLP caused approximately a 20-fold increase in neutrophil and 6-fold increase in monocyte migration when compared with unstimulated control cells. As expected, more neutrophils than monocytes migrated alone and in response to fMLP. MCP-1 significantly increased both neutrophil and monocyte migration at the highest tested concentration 1µg/ml, while CX3CL1 only significantly increased monocyte migration at 1-10 ng/mL. When compared to basal controls the significant effect of MCP-1 and CX3CL1 was nearly 2-fold. 10 nM fMLP was utilised in all further experiments.

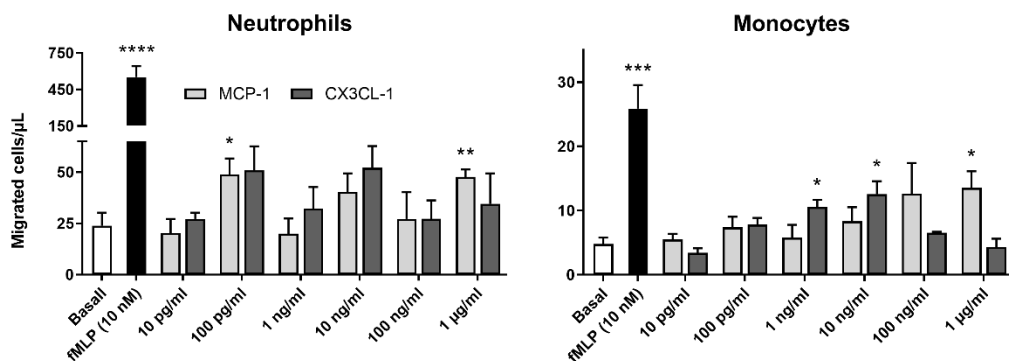


Figure 5. 2 Transendothelial migration of neutrophils and monocytes in response to fMLP, MCP-1 and CX3CL1.  $6 \times 10^5$  leukocytes were added to the HMEC-1 cell monolayer ( $0.25 \times 10^5$  cells/insert) and allowed to migrate for 4 h in response to 10 nM fMLP or 10 pg/mL-1 µg/mL MCP-1 or CX3CL1. Migrated cells were analysed by flow cytometry. Basal, non-treated cells (control). Mean  $\pm$  SEM, n=8 technical replicates. Significant difference between basal control and chemokine treatment by student's t-test. \* P <0.05; \*\* P <0.01; \*\*\* P <0.001; \*\*\*\* P <0.0001.

### 5.3.1.3 Transendothelial migration kinetics of neutrophils and monocytes

A kinetic study was carried out in order to optimise the duration of neutrophil and monocyte transendothelial migration through the HMEC-1 monolayer and analysed by flow cytometry. Briefly, PBL were added to the upper compartment of the trans-wells containing the HMEC-1 monolayer and cells allowed to transmigrate for 2, 3 or 4 h in response to 10 nM fMLP in the lower compartment. **Figure 5. 3** demonstrates that the number of transmigrated cells were highest at 3 h incubation time for all events (total migrated leukocytes) and granulocytes (neutrophils), and 4 h for monocytes. However, there was no major difference between 3 h and 4 h for monocytes. Therefore, the 3 h time point was chosen as the optimal incubation time for further experiments.

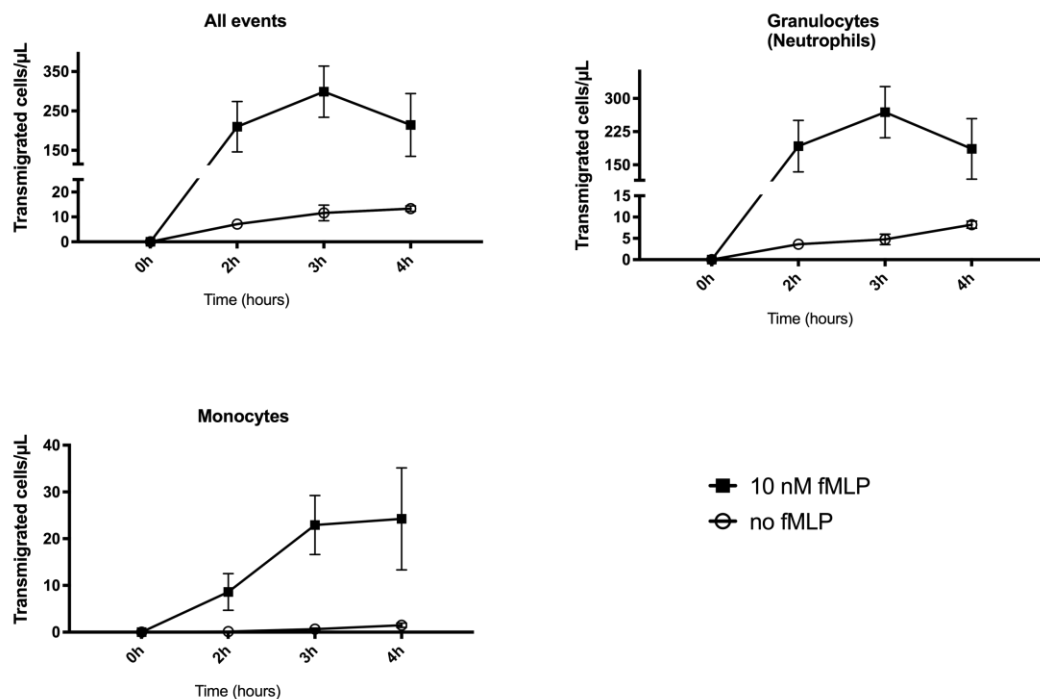


Figure 5. 3 Kinetics of granulocytes (neutrophil) and monocyte migration in response to fMLP in the transendothelial migration model.  $6 \times 10^5$  leukocytes were added to the trans-well with the HMEC-1 monolayer ( $0.25 \times 10^5$  cells) and allowed to migrate in response to 10 nM fMLP for 2-4 h and migrated cells analysed by flow cytometry. Data is expressed as mean number of transmigrated cells/ $\mu$ L  $\pm$  SEM,  $n=8$  technical replicates.



### **5.3.2 Effect of phenolic metabolites of dietary flavonoids and related phenolic acids on neutrophil and monocyte transendothelial migration**

Seven flavonoid metabolites **Figure 5. 5 (A)** of commonly consumed dietary flavonoids were studied for their effects on leukocyte migration in the transendothelial migration assay. Briefly PBL and 1  $\mu\text{M}$  of each PA or 0.01% DMSO were added on top of the HMEC-1 monolayer, in the upper compartment of a 96-trans-well plate and cells were allowed to migrate to the lower compartment for 3 h in the absence or presence of 10 nM fMLP. **Figure 5. 4** indicates that none of the metabolites significantly inhibited neutrophil transendothelial migration when compared with VC. In contrast, PCA significantly inhibited monocyte transendothelial migration and FA and IFA also showed non-significant reductions in monocyte transendothelial migration.

Fourteen non-naturally occurring but structurally similar phenolic acids (**Figure 5. 5 (B)**) were then studied to investigate any potential structure activity relationships of PA on neutrophil and monocyte transendothelial migration. **Figure 5. 6** shows that none of the related analogues had any effect on neutrophil migration, although non-significant reductions were seen with 2IBA, 3IBA, 4NBA, 4ABA and 3ABA. In contrast, 3IBA significantly inhibited monocyte transendothelial migration and non-significant trends were observed with 2IBA, 3CBA, 4BBA, 4ABA and 3ABA. These compounds together with PCA and 3IBA were then investigated for possible mechanisms of action in transendothelial migration.

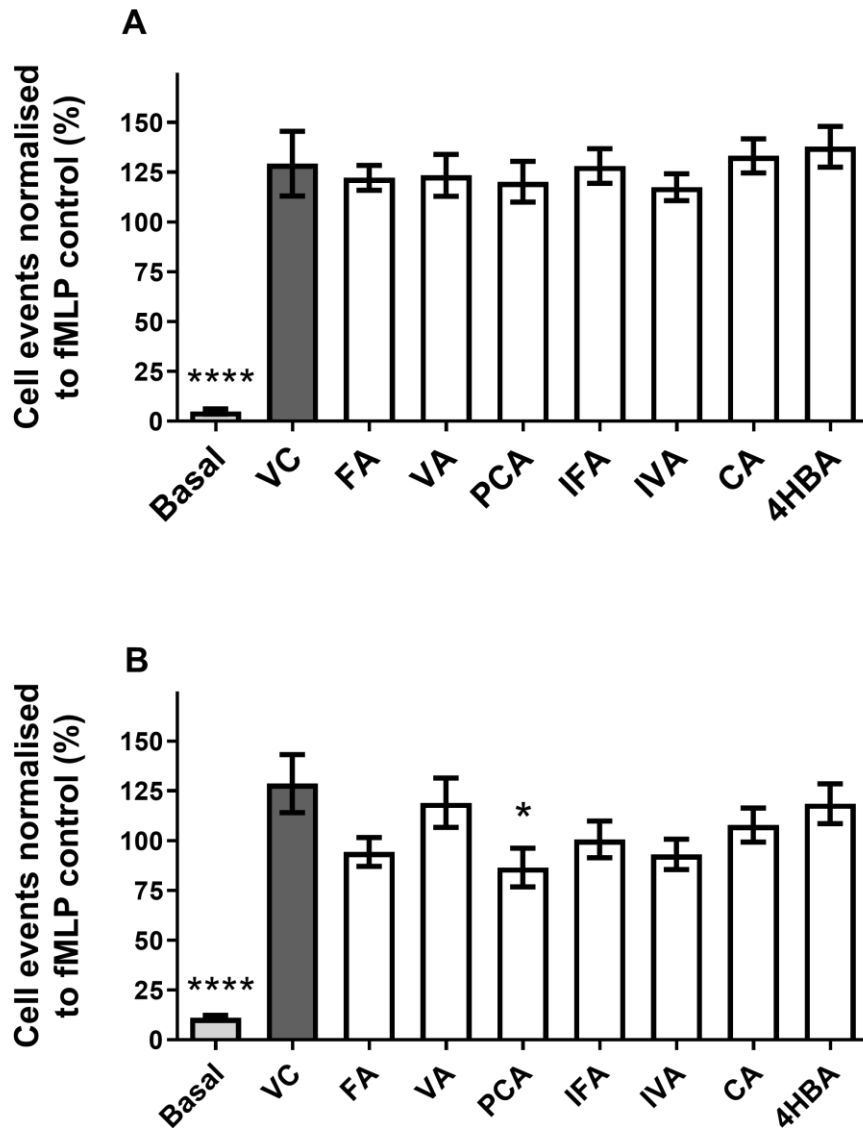


Figure 5. 4 Treatment effect of phenolic acids on neutrophils and monocytes transendothelial migration. HMEC-1 ( $0.25 \times 10^5$  cells/insert) were grown in trans-well (upper compartment) to form a monolayer prior to adding leukocytes ( $6 \times 10^5$  cells/insert) and  $1 \mu\text{M}$  of FA (ferulic acid), VA (vanillic acid), PCA (protocatechuic acid), IFA (isoferulic acid), IVA (isovanillic acid), CA (caffeic acid), 4HBA (4-hydroxybenzoic acid), or 0.001% DMSO (vehicle control, VC) and cells were allowed to migrate for 3 h in response to 10 nM fMLP (in lower compartment). Transmigrated neutrophils (A) and monocytes (B) were quantified by flow cytometry and expressed as a percentage of fMLP control (not shown). Mean  $\pm$  SEM,  $n=3$  independent biological experiments, each in four technical replicates. Inhibition of cell migration is significant ( $p > 0.05$ ) compared to VC analysed by one-way ANOVA with post hoc Dunnett's test. Significant difference between basal control (non-treated cells) and VC by student's t-test. \* $p \leq 0.05$ ; \*\* $p \leq 0.01$ ; \*\*\*\* $p \leq 0.0001$ .

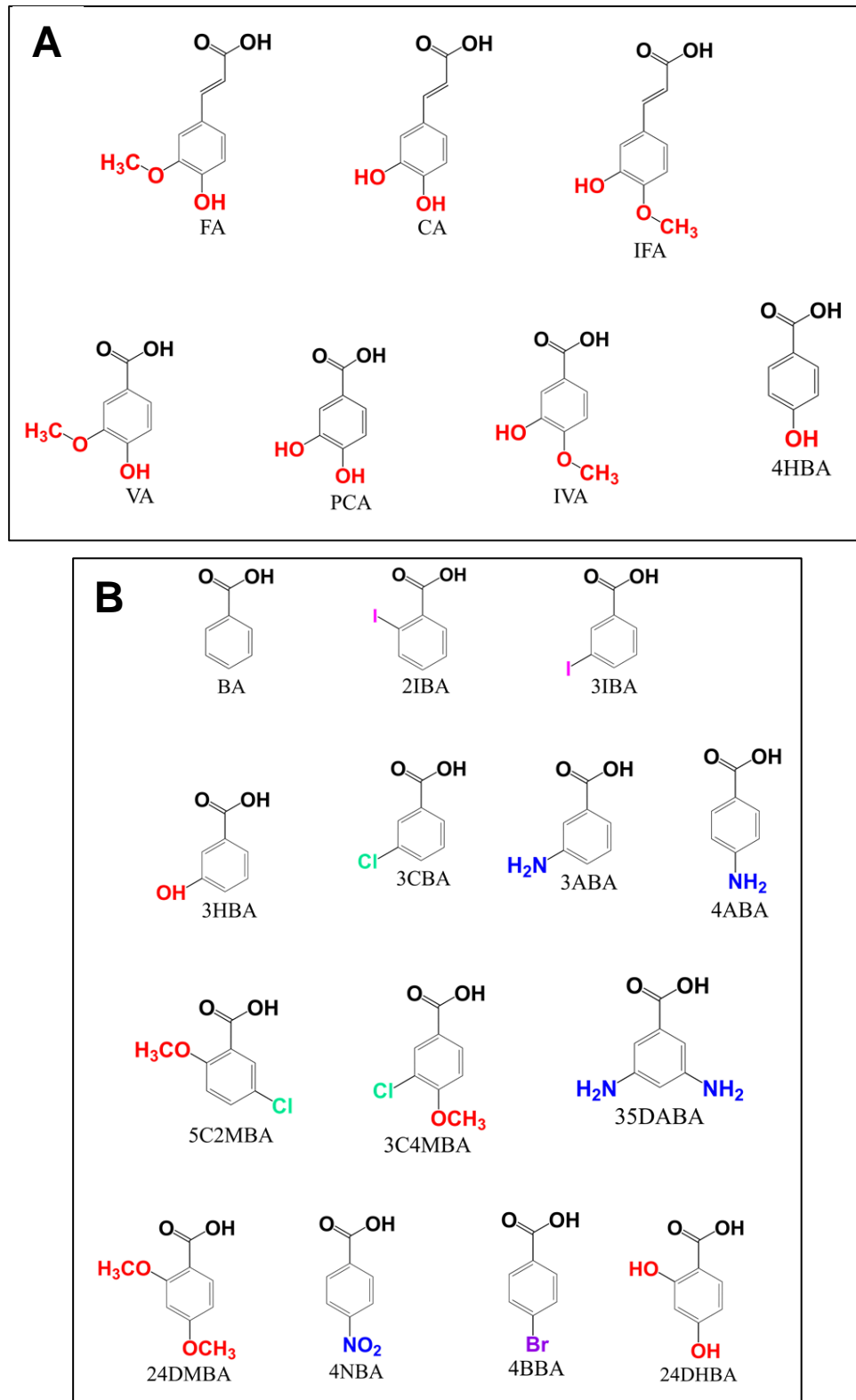


Figure 5. 5 Structures of PAs used in the transendothelial migration assay.

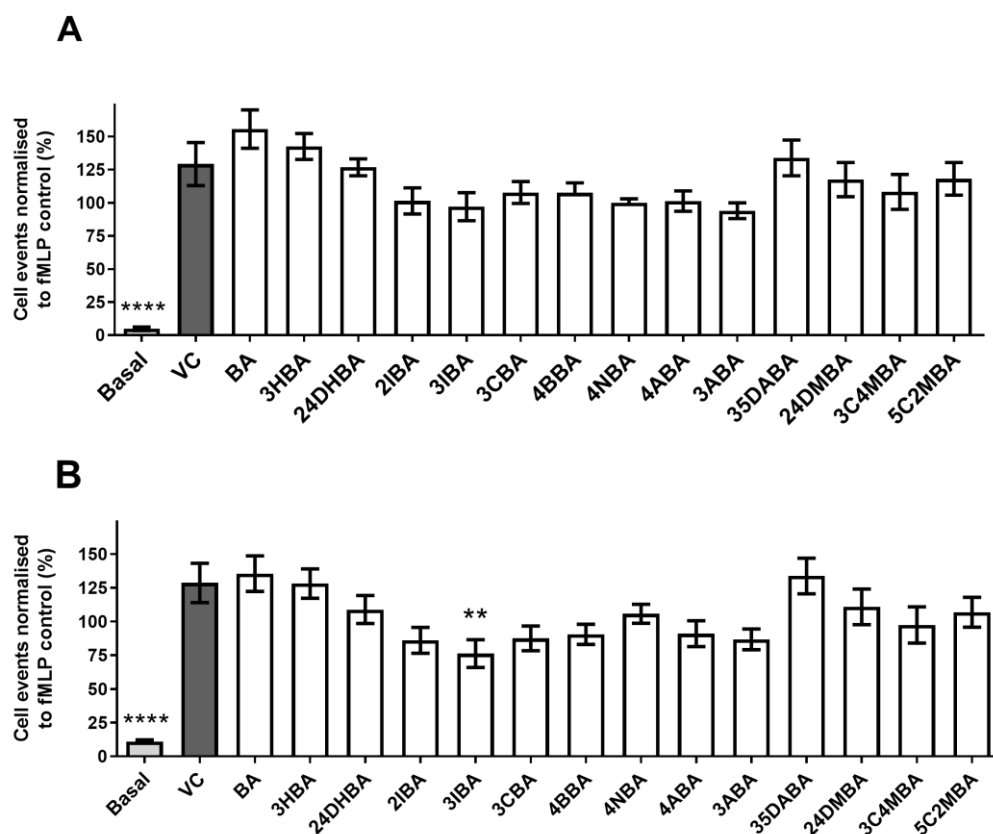


Figure 5.6 Treatment effect of non-natural phenolic acids on neutrophils and monocytes transendothelial migration. HMEC-1 ( $0.25 \times 10^5$  cells/insert) were grown in trans-well (upper compartment) to form a monolayer prior to adding leukocytes ( $6 \times 10^5$  cells/insert) and  $1 \mu\text{M}$  of BA (benzoic acid), 3HBA (3-hydroxybenzoic acid), 24DHBA (2,4-dihydroxybenzoic acid), 2IBA (2-iodobenzoic acid), 3IBA (3-iodobenzoic acid), 3CBA (3-chlorobenzoic acid), 4BBA (4-bromobenzoic acid), 4NBA (4-nitrobenzoic acid), 4ABA (4-aminobenzoic acid), 3ABA (3-aminobenzoic acid), 35DABA (3,5-diaminobenzoic acid), 24DMBA (2,4-dimethoxybenzoic acid), 3C4MBA (3-chloro-4-methoxybenzoic acid), 5C2MBA (5-chloro-2-methoxybenzoic acid), or 0.001% DMSO (vehicle control, VC) and cells were allowed to migrate for 3 h in response to 10 nM fMLP (in lower compartment). Transmigrated neutrophils (A) and, monocytes (B) were quantified by flow cytometry and expressed as a percentage of fMLP control (not shown). Mean  $\pm$  SEM,  $n=3$  independent biological experiments, each in four technical replicates. Inhibition of cell migration is significant ( $p > 0.05$ ) compared to VC analysed by one-way ANOVA with post hoc Dunnett's test. Significant difference between basal control (non-treated cells) and VC by student's t-test. \* $p \leq 0.05$ ; \*\* $p \leq 0.01$ ; \*\*\*\* $p \leq 0.0001$ .

### **5.3.3 Optimisation and validation of differentiated HL-60s as a model for neutrophils**

fMLP induced both neutrophil and monocyte migration in the transendothelial migration assay. However, fMLP is a more classical activator of neutrophils <sup>566,567</sup>, suggesting that the mechanism of action on monocytes might not be a direct action of fMLP signalling. Neutrophils embody the first line of defence in acute inflammation in response to various microbial agents including LPS and fMLP. Recruited to the site of inflammation, neutrophils rapidly release their pre-packed granules containing chemotactic factors and other pro-inflammatory mediators <sup>558</sup>. fMLP synergises with MCP-1 in monocyte chemotaxis <sup>568</sup>. We investigated whether fMLP stimulation of neutrophils might induce MCP-1 secretion from neutrophil granules.

#### **5.3.3.1 Differentiation of HL-60 into neutrophil like cells**

To test our hypothesis, we intended to investigate the effect of phenolic acids on primary neutrophils. However, due to the Covid-19 pandemic the utilisation of primary neutrophils from volunteers was not allowed. Although there are no neutrophil cell lines available, HL-60 cells have been previously reported to be differentiated into neutrophil like cells with 1.3% DMSO or 1  $\mu$ M all-trans retinoic acid (ATRA) <sup>541,569–573</sup>. Differentiated HL60 cells resemble primary neutrophils in function. Differentiation can be confirmed by observing increased nuclear segmentation, a decrease in cell size and proliferation <sup>572</sup> and expression of CD11b which is virtually absent in undifferentiated HL-60 cells <sup>574</sup>.

### 5.3.3.1.1 Kinetics of HL-60 Growth and Differentiation

HL-60 cells ( $1, 2$  or  $5 \times 10^5$  cells/mL) were differentiated with 1.3% DMSO or  $1 \mu\text{M}$  ATRA or undifferentiated (control media) for up to 6 days in T25 flasks. Cell growth was monitored by daily cell count using trypan blue exclusion and media colour change noted (**Figure 8.18, Appendix III**). At  $1 \times 10^5$  cells/mL, cell proliferation was prevented with ATRA and DMSO after 2 days (**Figure 5. 7**). Cell growth in the other two concentrations (data not shown) also slowed down but the lowest concentration showed more consistency and was carried forward.

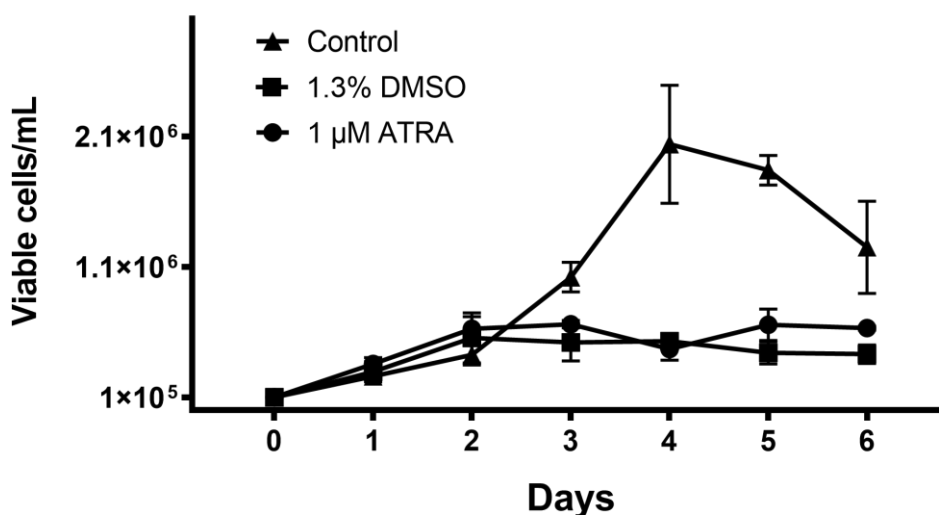


Figure 5. 7 Inhibition of cell HL60 cell growth by DMSO and ATRA. Cells were seeded at  $1 \times 10^5$  cells/mL in 10 mL media alone or with 1.3% DMSO or  $1 \mu\text{M}$  ATRA. Daily cell growth was monitored by trypan blue exclusion for seven consecutive days. Mean  $\pm$  SEM,  $n=2$  of a single biological experiment.

### **5.3.3.1.2 Nuclear morphology of differentiated HL-60 cells**

HL-60 cells are a human myeloid cell line obtained from a patient with acute promyelocytic leukemia and the nuclear morphology of the cells has an ovoid circular shape. Nuclear morphology of neutrophils is distinct from its myeloid progenitor. To check for neutrophil morphology, cells were differentiated for 3 days, cytopun and stained with Reastain quick-diff solution. **Figure 5. 8** shows that non-differentiated HL-60 nuclear morphology is mainly spherical while DMSO and ATRA-treated cells have segmented or invaginated nuclear lobes, resembling nuclear morphology of neutrophils, hence indicating differentiation.

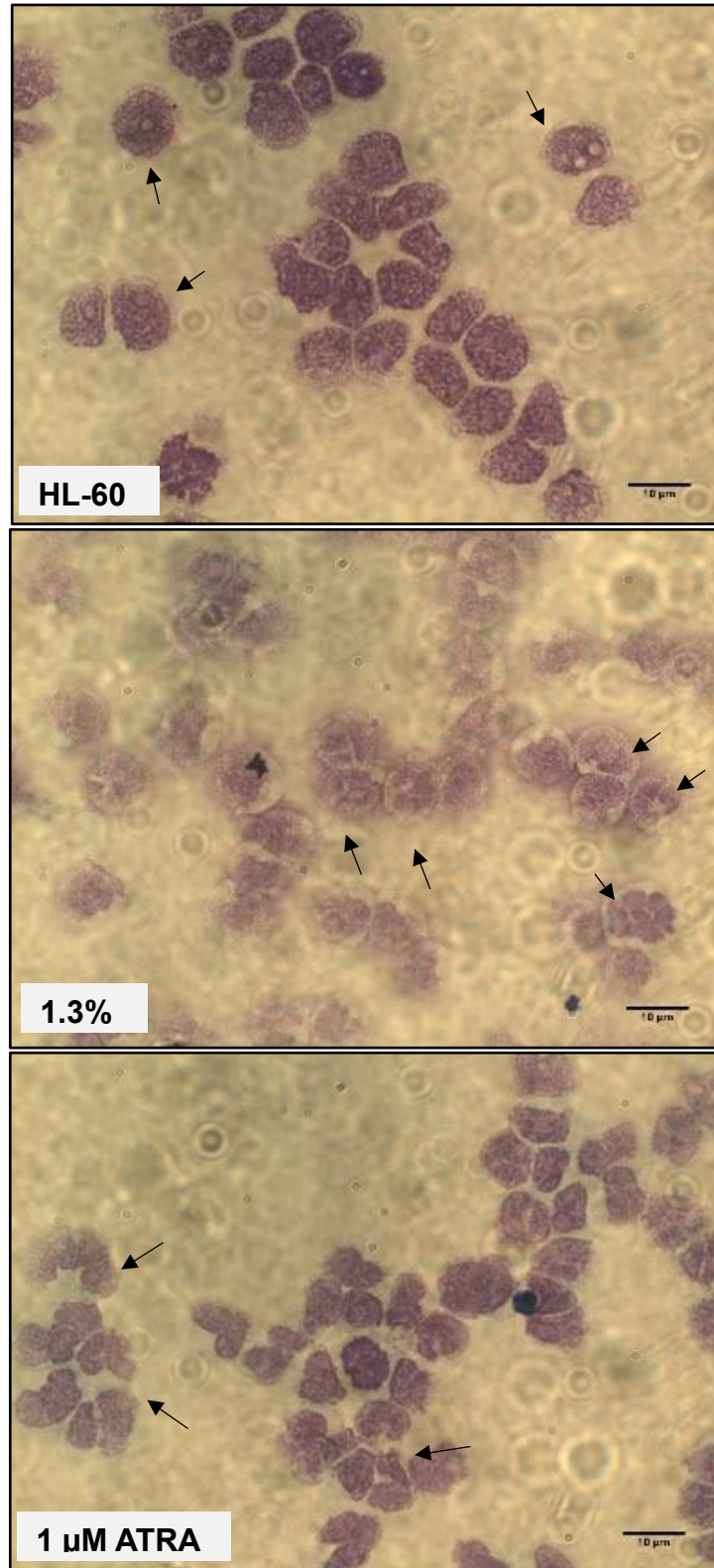


Figure 5. 8 Nuclear morphology of HL60-differentiated cells.  $1 \times 10^5$  cells/mL were differentiated for 3 days with 1.3% DMSO or  $1 \mu\text{M}$  ATRA and  $10^5$  cells were cytopun. Slides with stained with Reastain quick-diff, dried overnight and sealed. Cell morphology was imaged using the Leica Fluorescence Microscope. Arrows indicate nucleus morphological differences. Scale bar,  $10 \mu\text{m}$ .



### 5.3.3.1.3 Differentiated HL60 cells express CD11b

Neutrophils express CD11b, which is virtually absent on non-differentiated HL-60 cells<sup>574</sup>. CD11b membrane expression on non-differentiated and differentiated HL-60 cells was therefore investigated. Cells were differentiated with DMSO and ATRA for 3 days labelled with CD11b antibody conjugated to PE (CD11b-PE) or isotype control (IgG-PE) and analysed by flow cytometry. **Figure 5. 9** demonstrates that both DMSO- and ATRA-treated cells express CD11b compared with isotypic control antibody, indicating differentiation to neutrophil like cells. CD11b expression was higher on DMSO-differentiated cells, while ATRA-differentiated cells had a broad, shorter peak, indicating a more heterogenous cell population with different levels of CD11b expression suggesting that DMSO differentiated cells may be a better model of human neutrophil like cells.

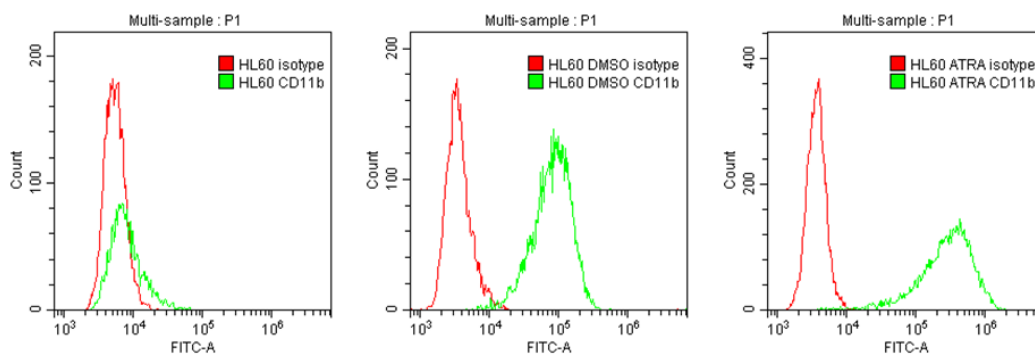


Figure 5. 9 HL-60 cells differentiated with DMSO or ATRA express CD11b. Cells ( $1 \times 10^5$  cells/mL) were differentiated either with 1.3% DMSO or  $1 \mu\text{M}$  ATRA or left unstimulated for 3 days. Cells were blocked with FC blocker (1:200) prior to labelling with CD11b (1:100) or isotype (goat anti-mouse IgG) for 10 min, followed by staining with secondary antibody mouse IgG Alexa Fluor® 488 (1:200) for 30 min and CD11b expression measured by flow cytometry. Data collected in P1 plotted for FITC intensity (x axis) against cell count (y axis) to assess the fluorescence intensity of differentiated cells in comparison to non-differentiated cells and isotype control.

#### **5.3.3.1.4 fMLP and CXCL12-induced chemotaxis of HL60-differentiated neutrophils**

CXCL12 and fMLP induced neutrophil migration <sup>566</sup>. Therefore, HL60-differentiated neutrophils were studied for their ability to migrate towards chemokines. Briefly, 1.3% DMSO- or 1  $\mu$ M ATRA -differentiated (diff) HL-60 or control (non-diff) HL-60 were resuspended in chemotaxis working buffer (0.1% BSA in RPMI) and added to the top of a 96-well ChemoTx filter, secured on the wells with 5 nM CXCL12, 10 nM fMLP or working buffer and the number of cells migrated were counted after 3 h. **Figure 5. 10** shows that undifferentiated HL-60 cells did not migrate in response to both chemokines or working buffer (basal). In contrast, both DMSO and ATRA differentiated HL-60 cells migrated spontaneously as well as in response to chemokines, suggesting neutrophil-like function. fMLP and CXCL12 both significantly induced DMSO-differentiated HL-60 cells compared to basal control. Although ATRA-differentiated cells also migrated in response to these chemoattractants, this did not reach statistical significance, again suggesting that DMSO was a better inducer of neutrophils. DMSO-differentiated HL-60 cells were therefore used in further experiments and henceforth called HL60-differentiated neutrophils.

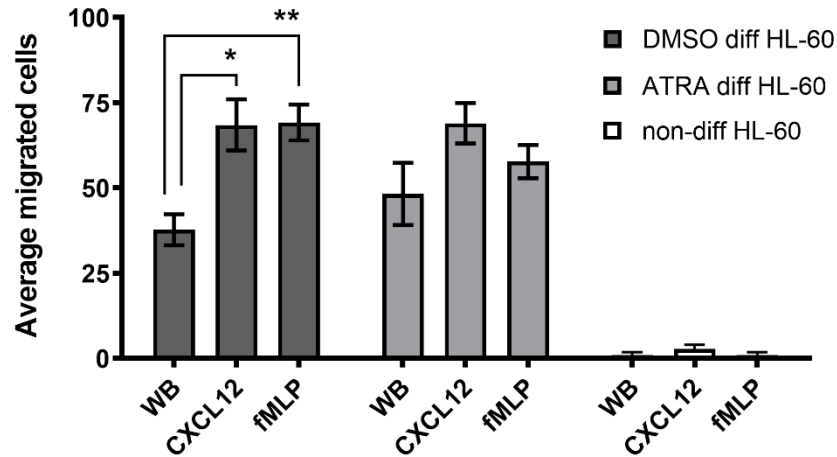


Figure 5. 10 Spontaneous and fMLP and CXCL12-induced chemotaxis of DMSO- and ATRA-differentiated HL-60. Cells ( $1 \times 10^5$  cells/mL) were differentiated with 1.3% DMSO or 1  $\mu$ M ATRA or left untreated for 3 days. Cells resuspended in working buffer (0.1% BSA) added on the top of ChemoTx chemotaxis filter ( $5 \times 10^3$  cells/well), secured on the wells with chemokines CXCL12 (5 nM) and fMLP (10 nM) or working buffer (WB) and incubated for 3 h. The number of cells migrated to the wells were counted. Mean number of migrated cells  $\pm$  SEM, n=2. Significant differences between DMSO- and ATRA-differentiated HL-60 migration with working buffer (WB) and fMLP, and CXCL12 chemokine challenge by student t-test. \* $p < 0.05$ ; \*\* $p < 0.01$ .

### 5.3.4 Effect of Phenolic acids on MCP-1 secretion from HL60-differentiated neutrophils

In the transendothelial migration assays, 3IBA and PCA significantly inhibited monocyte migration and there were non-significant reductions observed also with FA, 2IBA, 3CBA, 3C4MBA, 4BBA, 3ABA and 4ABA.

MCP-1 is the main chemokine responsible for recruiting monocytes<sup>337</sup> and primary monocytes have been shown to migrate towards fMLP<sup>559-561</sup>. fMLP also synergises with MCP-1 in monocyte chemotaxis<sup>568</sup>. We therefore investigated whether fMLP induces MCP-1 secretion from HL60-differentiated neutrophils and if so, whether phenolic acid prevent MCP-1 secretion from HL60-differentiated neutrophils.

### 5.3.4.1 Kinetics of MCP-1 secretion

To determine whether fMLP-induced MCP-1 secretion from HL60-differentiated neutrophils a kinetic study was carried out. Briefly HL60-differentiated neutrophils were treated with 0, 1, 10 and 100 nM fMLP for 15 min, 30 min, 1 h, 2 h and 3 h and MCP-1 secretion was measured by ELISA assay. The cells spontaneously secreted MCP-1 independently of fMLP in the presence of serum (**Figure 5. 11 A**) and fMLP did not induce further secretion. However, in the absence of serum, fMLP induced a concentration-dependent increase in MCP-1 secretion following 30 min stimulation with fMLP (**Figure 5. 11 B**), albeit only a 2.3-fold increase with the highest concentration (1  $\mu$ M) of fMLP. This concentration was therefore used in further experiments.

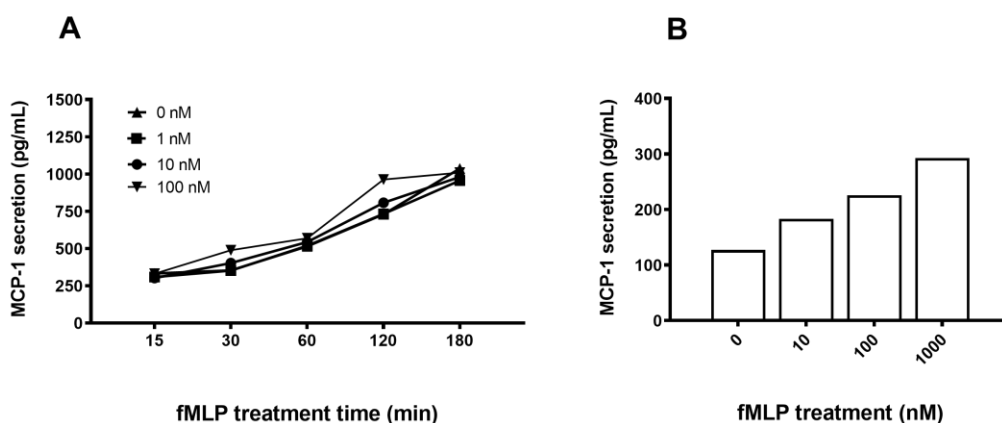


Figure 5. 11 fMLP induced MCP-1 secretion in HL60-differentiated neutrophils. HL-60 ( $10^5$  cells/mL) were differentiated with 1.3% DMSO for 3 days prior to stimulation with fMLP for (A) 15 min-3 h in complete media or (B) 30 min in serum-free media and MCP-1 secretion measured by ELISA. n=1.

### **5.3.5 Phenolic acids do not reduce fMLP-induced MCP-1 secretion in HL60-differentiated neutrophils**

Since the HL60-differentiated neutrophils secreted MCP-1 in response to fMLP, we hypothesised that PA inhibit monocyte migration potentially via interfering with MCP-1 secretion from HL60-differentiated neutrophils. To test our hypothesis, HL60-differentiated neutrophils were treated with 1  $\mu$ M of the above-mentioned PA prior to stimulation with fMLP for 30 min and MCP-1 secretion measured by ELISA. ERK MAP kinase has previously been reported to inhibit fMLP-induced MCP-1 secretion<sup>575,576</sup>, therefore 10  $\mu$ M PD 098059 was included as a positive control. **Figure 5. 12 (A)** demonstrates that fMLP-induced MCP-1 secretion was significantly inhibited by PD 098059. However, none of the PA had any significant effect on MCP-1 secretion (**Figure 5. 12 (B)**), suggesting that the effects of the PA in the transendothelial migration assay are not due to MCP-1 secretion.

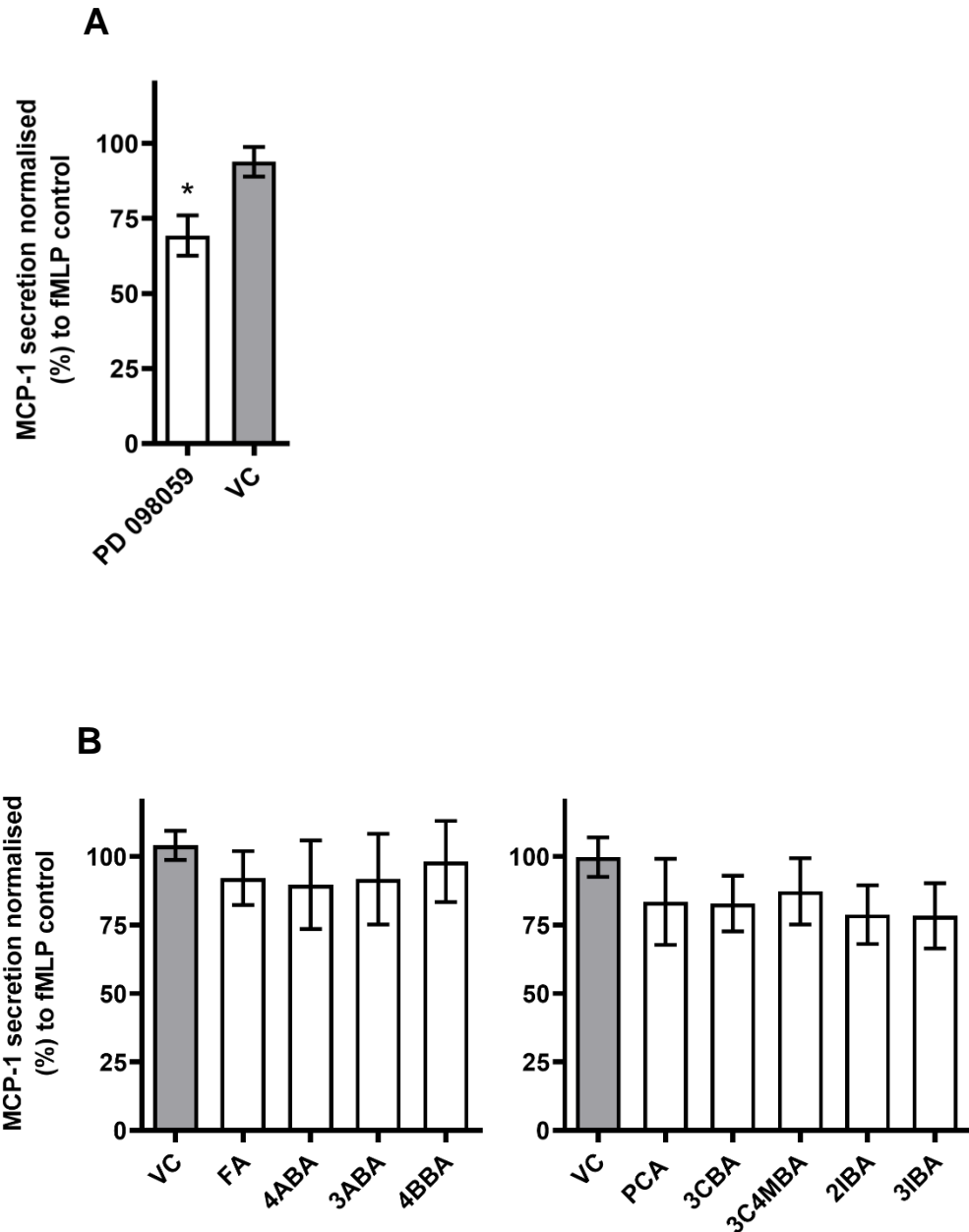


Figure 5. 12 Phenolic acids do not inhibit MCP-1 secretion from HL60-differentiated neutrophils. Cells ( $10^5/\text{mL}$ ) were pre-treated with  $10\ \mu\text{M}$  PD 098059 (positive control) or  $0.01\%$  DMSO (vehicle control, VC) (A) or  $1\ \mu\text{M}$  of each phenolic acid (B) or left untreated for 30 min in serum-free media prior treatment with  $1\ \mu\text{M}$  fMLP for 30 min. MCP-1 secretion was measured by ELISA assay and expressed as percentage of fMLP-treated cells (not shown). Mean  $\pm$  SEM,  $n=3$  biological experiments. Treatment effect of phenolic acids was compared to VC by one-way ANOVA with post-hoc Dunnett's test. Significant difference between PD 098059 vs vehicle control by Student's t-test. \*  $p<0.05$ .

### **5.3.6 Effect of Phenolic acids on Monocyte Migration**

In the transendothelial migration assay, PCA and 2IBA significantly inhibited monocyte migration. Since they did not inhibit neutrophil migration or MCP-1 secretion from HL60-differentiated neutrophils, their direct effects on monocyte migration was measured by a chemotaxis assay utilising THP-1 monocytes.

#### **5.3.6.1 Optimisation of monocyte migration assay**

Prior to testing the effect of the phenolic acids on monocyte migration, the chemotaxis assay was optimised. Four different concentrations of fMLP (1 nM, 10 nM, 100 nM and 1  $\mu$ M) and four of MCP-1 (0.01 nM, 0.1 nM, 0.5 nM, and 1 nM) were tested. CCL3 (aka MIP-1 $\alpha$ , Macrophage Inflammatory Protein 1-alpha) (1 nM) has previously been shown to induce THP-1 chemotaxis by 4 h<sup>425</sup> and was included as a positive control. fMLP had no effect on THP-1 migration compared with basal control (**Figure 5. 13**). CCL3 significantly induced THP-1 monocyte migration and MCP-1 also increased it in a dose dependant manner between 0.1nM- 1nM. 0.3 nM MCP-1 was chosen as a midrange concentration for further experiments.

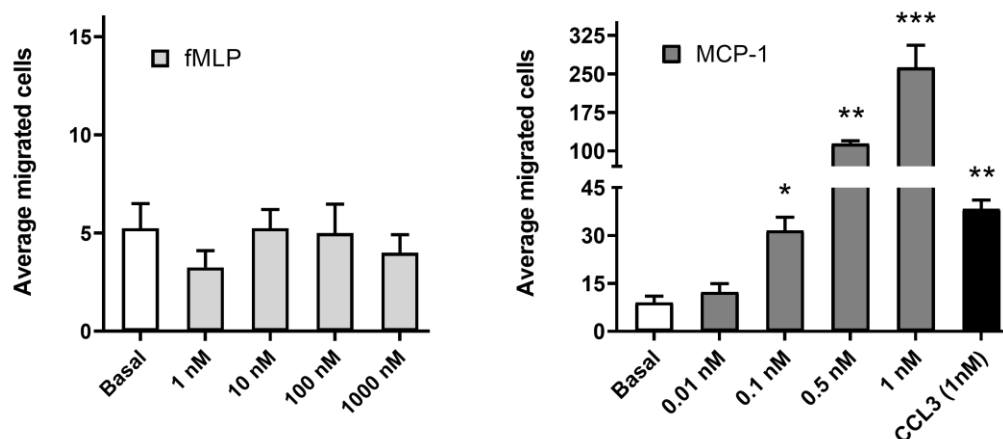


Figure 5. 13 Effects of fMLP and MCP-1 on THP-1 chemotaxis.  $2.5 \times 10^5$  cells were added on the top of ChemoTx chemotaxis filter, secured on wells with different concentrations of fMLP or MCP-1 or 1 nM CCL3 and incubated for 4 h. The number of cells migrated to the wells were counted. Mean number of migrated cells  $\pm$  SEM, n=2. Significant difference between basal control (no chemokine) and CCL3 or MCP-1-challenged cells by t-test. \*  $p < 0.05$ ; \*\*  $p < 0.01$ ; \*\*\*  $p < 0.001$ .

### 5.3.7 Phenolic acids at 1 $\mu$ M do not significantly reduce MCP-1 induced monocyte chemotaxis

Since PCA and 3IBA significantly attenuated the transendothelial migration of monocytes in the transendothelial migration assay and FA, 2IBA, 3CBA, 3ABA, 4ABA, 4BBA and 3C4MBA also non-significantly reduced transendothelial migration by  $> 15\%$ , these were investigated for their effects on monocyte chemotaxis in response to 0.3 nM MCP-1. **Figure 5. 14** shows that there was no significant reduction of any of the tested PA on THP-1 migration by One-way ANOVA. However, a non-significant reduction was observed with the halogenated PA 2IBA, 3IBA, 3C4MBA, 4BBA (30%, 23%, 24%, 23% vs VC). Analysis by student t-test demonstrated a significant inhibition of MCP-1 induced chemotaxis by 2IBA ( $p=0.0239$ ), 4BBA (0.0575) and 3C4MBA (0.0901). Additional halogenated PA were also tested to determine if there were any structure activity



relationships but none of the tested compounds demonstrated any significant reduction on THP-1 chemotaxis (Table 8.1, Appendix III).

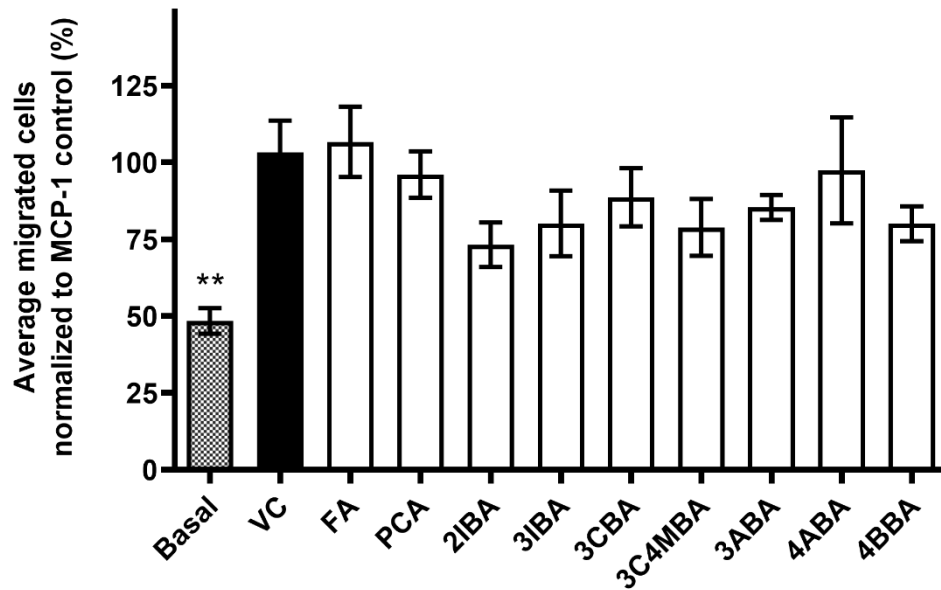


Figure 5. 14 Effects of 1  $\mu$ M PCA, FA or related phenolic acids on MCP-1 induced THP-1 chemotaxis.  $2.5 \times 10^5$  cells/well were seeded in X plates and left untreated or pre-treated with 1  $\mu$ M of phenolic acid or 0.001% DMSO (VC) for 30 min prior to stimulation with 0.3 nM MCP-1 for 4 h. Migrated cells were counted and normalised to MCP-1 control. Mean  $\pm$  SEM, n=4 independent biological experiments, each in two technical replicates, counted twice. Treatment effect of phenolic acids was compared to VC by one-way ANOVA with post-hoc Dunnett's test. Significant difference between basal control and VC by Student's t-test. \*\* p<0.01.

## 5.4 Discussion

Consumption of specific flavonoids and subclasses are beneficial for vascular health. Their protective effects might be due to their structural properties<sup>426,427,577-579</sup> and to their more bioavailable metabolites, which have been shown to mitigate pro-inflammatory cytokines (TNF- $\alpha$ , IL-6) in monocytes and adhesion molecules (VCAM-1 and ICAM-1) in endothelial cells at physiological concentrations (0.1-10  $\mu$ M)<sup>18,19,47,334,548</sup>. Endothelial activation is an important event in the initiation of atherosclerosis in response to various stimuli including oxidative stress and circulating pro-inflammatory cytokines<sup>536</sup>. Upon activation, neutrophils and monocytes are recruited to the site of endothelial injury by multiple cytokines, chemokines, and adhesion molecules, mediating transendothelial migration. Although the effect of flavonoids and their metabolites on cytokine expression from monocytes and adhesion molecules in endothelial cells have been extensively studied in inflammatory models, their effect on neutrophils and chemokines remained to be elucidated. Here, the effects of 7 common flavonoid metabolites and 14 related PA on transendothelial migration were investigated. PCA and 2IBA significantly inhibited monocyte transendothelial migration by 42% and 52% respectively. No structural activity relationships were observed. The mechanisms of action were investigated and from neutrophil and monocyte cell line models, it does not appear that these either directly inhibit monocyte migration or MCP-1 secretion from HL60-differentiated neutrophils. However, there are limitations to this study, which will be discussed below.

No studies to date, to our knowledge, have investigated PA metabolites in a leukocyte transendothelial migration model. In the present study, PCA significantly attenuated monocyte but not neutrophil migration in a transendothelial migration assay. Similarly, PCA significantly reduced THP-1 monocyte adhesion to HUVECs by 47% at physiological concentrations (2  $\mu$ M)<sup>46</sup>. 20-40  $\mu$ M PCA also inhibited HL-60 cells binding to mouse aortic

endothelial cells (MAECs), which was associated with a reduction in ICAM-1 and VCAM-1 expression<sup>233</sup>.

In the present study, VA, FA, and the other common dietary metabolites did not significantly reduce transendothelial migration. FA, however, did reduce monocyte migration by 35% relative to VC. In another study, FA at higher concentrations (10-20  $\mu$ M) attenuated adhesion of U937 monocytic cells to HUVECs and reduced VCAM-1, ICAM-1 secretion<sup>547</sup>. More recently, 2  $\mu$ M VA and FA reduced THP-1 monocyte adhesion to HUVECs<sup>46</sup>. THP-1 adhesion was reduced maximally by 31% with FA and 26% by VA. The differences between our results and these other studies may be due to the concentrations of the PA used and higher concentrations in our study may have led to more significant results.

Structurally related analogues of the PA metabolites were also screened to investigate possible structure activity relationships as these simple PA with one or two different groups could be helpful to understand which positions are important for bioactivity. 3IBA alone significantly reduced monocyte transendothelial migration, which could have been due to its high lipophilicity (LogP 2.9) (**Table 8.2, Appendix III**) However, other structurally-related compounds showed non-significant reductions. For example, 2IBA, 2CBA, 4BBA, 4ABA and 3ABA did reduce monocyte migration by 43, 42, 38, 38 and 42% respectively. Again, higher concentrations could have resulted in significant results. However, due to work done in Unilever under time constraint, it was not possible to examine any further concentrations. Further studies are warranted to test the effect of those compounds at higher physiological concentration (10-20  $\mu$ M) on transendothelial migration of primary leukocytes.

The transendothelial migration model is a high throughput method that allows simultaneous testing of multiple variations and components within the same assay. In fact, it is an invaluable functional assay in terms of capability to study early steps of inflammation in atherosclerosis at the complex molecular, cellular, and whole tissue level. In comparison to simple

assays, it is a more predictive model regarding translation to the *in vivo* situation since it is able to measure the net effect on a functional outcome of all the molecular events that happens upon treatment of the cell or whole tissue (endothelia cells). However, the transendothelial migration assay bears its own limitations as it measures only the behaviour of the cells in a setting mimicking an organ and does not directly give indications of the mechanism of action behind the observed net effect of these cell behaviours. Furthermore, in this assay instead of cell lines we used fresh blood obtained from different donors which results in variation between experiments, which may be due to natural genetic diversity and/or the donors health condition <sup>580</sup>. Moreover, depending on the donors health state, their PBL composition may vary with normal values accounting for 2-8% monocytes; 20-40% lymphocytes and the remaining are granulocytes with neutrophils being 40-60%. Therefore, for mechanistic studies further classical assays are required.

The mechanisms by which PCA and 3IBA inhibited monocyte transendothelial migration were then studied in a classical assay. Transendothelial migration of leukocytes is a complex process, involving multiple signalling and surface molecules <sup>581,582</sup> and is not limited to the action of adhesion molecules. In general adhesion of leukocytes to the endothelial cells is followed by crawling, scanning and protrusion, then transmigration. Since all of these steps aid both monocyte and neutrophil migration, we hypothesised that there may be a different mechanism that specifically aids monocyte migration whilst not affecting neutrophils, and that signal might originate from neutrophils or may result from differences in receptor expression between the two cell types or another specific effect on monocytes. Gonzalez and co-workers (2011) reported a direct effect of flavonoids on neutrophils including quercetin, myricetin, kaempferol and baicalin <sup>583</sup>. Among those, quercetin was reported to cause neutrophil degranulation without effecting cell viability or phagocytosis and its activity was attributed to its lipophilicity. To investigate potential mechanisms of action of the phenolic acids, cell models of neutrophils and monocytes had

to be developed or used as due to COVID-19, no further studies could be carried out with primary cells.

Neutrophils secrete cytokines and chemokines rapidly from pre-packed granules as well as synthesise them *de novo* in response to inflammatory cues<sup>221,541–543</sup>. Naegelen and co-workers<sup>541</sup> reported that LPS-stimulated primary neutrophils and DMSO-differentiated HL-60 cells similarly secreted various chemokines including MCP-1. Neutrophil-derived MCP-1 is released in a circadian manner and involved in monocyte adhesion to arteries<sup>221</sup>. We therefore investigated whether fMLP could induce MCP-1 secretion from neutrophils and whether the phenolic acids could inhibit this. Cells differentiated with either ATRA or DMSO are a validated model of human neutrophils with similar characteristics to primary neutrophils<sup>572</sup>. We compared undifferentiated, ATRA and DMSO-differentiated cells for neutrophil characteristics (CD11b presence, polymorphonuclear staining and CXCL12-induced chemotaxis) and determined that although both were neutrophil-like, DMSO performed better in response to CXCL12 and had higher expression of CD11b. Results were similar to other studies<sup>569,573,584</sup>. These were then used as neutrophils in further studies.

The effects of PA on fMLP-induced MCP-1 secretion in HL60-differentiated neutrophils was then investigated. Although PD 98059 inhibited MCP-1 secretion, no significant effect was observed with the PA. However, a slight inhibitory trend was seen with the PA. Previous *in vitro* and *in vivo* studies have shown inhibitory effects of flavonoids and their metabolites on MCP-1 secretion in human cell lines and rodents. To our knowledge, there are no previous *in vitro* studies with the PA used in this study. Chang and co-workers reported MCP-1 down-regulation in high-fat diet (HFD)-fed rats after 4-week treatment with VA (30 mg/kg body weight)<sup>585</sup>. Zhang and co-workers reported that EGCG (25-100  $\mu$ M) significantly inhibited LPS-induced MCP-1 secretion in human retinal microvascular endothelial cells<sup>290</sup>. High glucose-induced MCP-1 secretion was also suppressed by cyanidin 3-glucoside chloride (C3G) and cyanidin chloride (50  $\mu$ M) in human

kidney (HK-2) cells <sup>367</sup>. These differences could be due to the higher concentrations of phenolic acids used in these studies, the differences in cell types or due to differences in regulation of the signalling pathways activated by the different stimuli activating MCP-1.

In the present study, the effect of PA on MCP-1 induced monocyte migration was then investigated. THP-1 cells are a well characterised model of primary monocytes and migrate similarly to these cells in response to chemokines <sup>450</sup>. However, THP-1 cells did not migrate in response to fMLP in chemotaxis assays in contrast to the response to fMLP in the transendothelial migration assay, suggesting a different mechanism is involved in primary monocytes and THP-1 cells. Another study has reported the lack of fMLP receptor on their THP-1 cells <sup>568</sup>. However, THP-1 cells did migrate in response to MCP-1, similarly to other studies with THP-1 cells and primary monocytes <sup>342</sup>. None of the PA had any effect. In another study, a mixture of three epicatechin metabolites with sulfate and glucuronide (each at 1  $\mu$ M) were shown to inhibit THP-1 chemotaxis towards HUVECs in response to MCP-1 by 27% <sup>586</sup>. Primary cell responses to chemokines have been reported to be better than the leukemic cell lines <sup>562</sup>. Future studies need to consider the effect of PA on primary neutrophils and monocytes to have a better picture of chemokine secretion and chemotaxis in response to PA treatments. In addition to that, further studies could also test the effect of those compounds at higher physiological concentration (10-20  $\mu$ M) on chemotaxis of primary monocyte and neutrophils.

We also included a broad range of halogenated and non-halogenated PA to see if any SAR based on their lipophilicity could be observed, thus with higher and lower logP values (>2 more lipophilic, list in **Appendix III**). In general halogens are widely used in medicinal chemistry for their lipophilicity, electronegativity, and molecule stabilising properties. Cl is mostly used to tune lipophilicity and potency of molecules, while F is most commonly used to prevent oxidation by phase I metabolism. Although none of these phenolic acids at 1  $\mu$ M significantly inhibited THP-1 chemotaxis,

several reduced chemotaxis, for example 2IBA and 3IBA reduced cell migration by 30% and 23% respectively. These results warrant further investigation using higher concentrations of PA as cell lines may be more resistant to small molecules such as PA than primary cells and it is possible that if primary monocytes were utilised the results would have been significant. Future studies should investigate the effect of PA and flavonoid metabolites on primary monocyte chemotaxis by MCP-1.

In conclusion, our findings imply that PA may inhibit chemotaxis and transendothelial migration. A wider range of concentrations should be studied in future as transendothelial migration is a key event in the early stage of atherosclerosis.

## Chapter 6. General Discussion & Future Perspectives

Flavonoids and phenolic acids, the two largest classes of (poly)phenolic compounds found in high quantities in fruits and vegetables, have an extraordinary diversity<sup>64,69,114</sup>. Their protective effects against CVD and neurological disorders have been observed in numerous epidemiological studies, RCTs and meta-analysis studies<sup>6–8,14,26,32–35,169,190,195,202,204,235–237</sup>. The underlying central mechanism of CVD and neurological disorders is postulated to be chronic inflammation<sup>216,217,243,244,250</sup>, characterised by endothelial activation and presence or activity of monocytes and macrophages at the site of arterial injury, and activation of microglial cells in the central nervous system, where a state of imbalance occurs between pro-inflammatory (such as sVCAM, sICAM, MCP-1, TNF- $\alpha$  and IL-6) and anti-inflammatory (IL-12, HO-1 and NQO1) molecules mediated by NF- $\kappa$ B and Nrf2 signalling pathways<sup>216,253,255,372</sup>. To elucidate the bioactivity and the cellular effects of those compounds, numerous *in vitro* studies have been conducted. However, these studies predominantly investigated the effects of parental flavonoids at pharmacological concentrations, overlooking the poor bioavailability of these compounds and their extensive metabolism by gut microbiota.

Evidence from bioavailability studies suggests that the observed health effects of high flavonoid intake are more likely the result of their metabolites that are profoundly found in the circulation rather than their parental flavonoids, which are poorly found in the circulation<sup>41,92,146</sup>, suggesting that the previously observed *in vitro* anti-inflammatory effects on inflammation biomarkers warrant further study.

A large proportion of flavonoid metabolites found in circulation originate from B-ring fission as phenolic metabolites<sup>143</sup>, hence the higher bioavailability of phenolic acids from both colonic metabolism of flavonoids

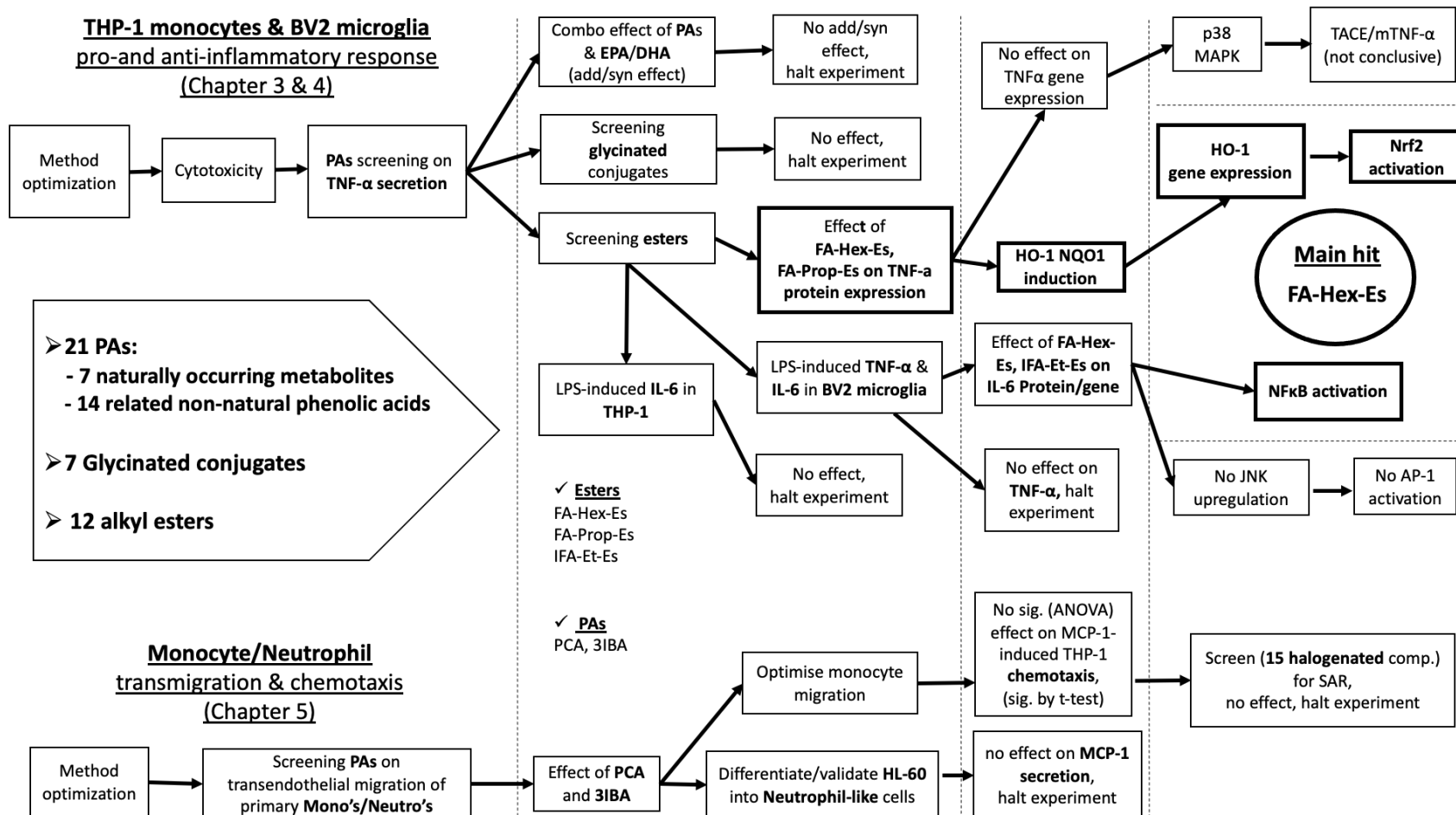


as well as the free form from the common diet and colonic catabolism of their bound forms. These colonic metabolites are not limited to but commonly include PCA, VA, CA and FA <sup>22,60–62</sup>. Furthermore, other major flavonoid metabolites found in the circulation and urine are the methylated, sulphated, glucuronidated and glycosylated conjugates of both flavonoids and phenolic acids <sup>19,24,27,61</sup>.

More recent *in vitro* studies have focused on the bioactivity of flavonoid metabolites at physiological concentrations <sup>18,19,44,46,47,51,168,549,587</sup>. However, the observed effects are rather mild and not dose-dependent, hence the cellular mechanism of action of non-dose dependent compounds in *in vitro* studies has proven to be difficult. It is fundamental to show the effect of any given compound in isolation in order to claim any benefits or make any assumption with certainty for dietary guidelines. However, the non-dose-dependent response could be due to absorption and uptake issues by the immune cells in *in vitro* assays.

The current study sought to address these challenges by screening 40 compounds, including 7 naturally occurring PAs, 4 related non-natural PAs, 7 glycosylated conjugates and 12 alkyl esters, to investigate (primarily) the bioactivity and structure activity relationships (SAR) of the most commonly found PAs and their structurally related non-natural or synthetic analogues, their mechanisms of action and uptake in immune cell types (**Figure 6. 1**).

Figure 6. 1 Schematic overview of overall experiments conducted in chapters 3, 4 and 5.



An initial screening of 7 of the most common PAs and 14 related non-natural PAs was conducted to investigate the effects of the most common PAs on TNF- $\alpha$  secretion in THP-1 cells and to reveal any potential SARs. The initial screening was primarily aimed to reveal SARs, as there is a wide variety of structures from flavonoid metabolism and a SAR could aid future studies to focus on the effect of specific structures rather than screening numerous compounds, which could be rather laborious and time consuming. In this preliminary screening, our results showed that there was no significant effect of any selected PAs on TNF- $\alpha$  secretion in THP-1 cells. However, even though not significant, overall all compounds showed a similar, very mild effect and no dose response, indicating no SAR and confirming previous studies by us and others <sup>18,19,46,47</sup>.

As discussed in Chapter 3, this observation of a mild and non-dose dependent response is likely due to their nature as being food bioactives rather than nutraceuticals. However, from a nutritional perspective, a lower bioactivity is more logical as high intake could result in a compromised immune reaction or toxic reaction. Moreover, considerable evidence shows that flavonoids have a pleiotropic activity <sup>153,588,589</sup>. Potentially, the combined bioactivity on different cell signalling pathways could explain the outcome of cohort or feeding studies.

Furthermore, this set of compounds were also screened for their effect and SAR on transendothelial migration of primary monocytes and neutrophils. In this study a significant effect was observed with 1  $\mu$ M PCA (42%) and 3IBA (52%) on monocyte migration in response to fMLP. However, no SAR was observed and further investigation of the MOA in monocyte and neutrophil cell models indicated neither PCA nor 3IBA directly inhibit monocyte migration or MCP-1 secretion from HL-60 differentiated neutrophils. However, as discussed in Chapter 5, the response of primary cells and cell lines could have been different. Future studies should use primary cells and higher physiological concentrations of PA to reveal their MOA.

This study investigated the effect of novel synthesised PA glycine conjugates which are in theory possible to be present in the circulation. None of these compounds showed any significant effect on LPS-induced TNF- $\alpha$  secretion in THP-1 cells. One of the possibilities is that glycation could have negatively affected the absorption, by making these compounds more water soluble as glycation is one of the primary mechanisms of excreting compounds from the body via urinary excretion <sup>429,451</sup>.

This study also aimed to understand the cellular uptake and absorption, hence synthetic phenolic acid alkyl esters were synthesised, as esterification is a widely used modification for drug uptake and absorption. Screening of 17 alkyl esters and their parental PAs on LPS-induced TNF- $\alpha$  and IL-6 secretion in THP-1 monocytes and BV2 microglial cells revealed a greater effect with only ferulic acids and isoferulic acid with the longest alkyl esters. FA-Hex-Es and FA-Pro-Es showed a marked effect on TNF- $\alpha$  secretion in THP-1 cells and FA-Hex-Es and IFA-Et-Es on IL-6 secretion in BV2 cells, in contrast to their parental PAs, suggesting that cellular uptake might have been increased due to higher lipophilicity. Future studies are warranted to further investigate the mechanism of absorption and/or uptake of natural PAs in immune cells by investigating the potential transporter expression in commonly used cell lines, especially cancer cell lines such as THP-1 cells.

To understand the mechanistic effect of FA-Hex-Es and FA-Pro-Es on LPS-induced TNF- $\alpha$  secretion in THP-1 cells, further experiments were conducted to understand whether the effect is upstream or downstream of gene expression. No effect on gene expression was observed suggesting a post-translational mechanism, in line with our previous studies <sup>137,456</sup>. Further experiments revealed no effect on p38 MAPK, a potential post-translational regulator of TNF- $\alpha$  as suggested by others <sup>283</sup>. The effects on membrane bound TNF- $\alpha$  and TACE enzymatic activity were not conclusive due to assay limitation and non-optimal experimental settings.

The effect of FA-Hex-Es and FA-Pro-Es on HO-1 and NQO1 expression in THP-1 cells were also investigated. A profound effect on HO-1 protein and

gene expression by FA-Hex-Es was observed and further experiments revealed that the effect is likely via Nrf2 pathway activation. This effect warrants further study *in vivo*.

The anti-inflammatory effects of alkyl esters together with their parental compounds were further investigated in BV2 microglial cells, the major source of inflammatory mediators in the brain. Again, FA-Hex-Es as well as IFA-Et-Es showed remarkable effects on IL-6 secretion and gene expression, likely via NF- $\kappa$ B. Future studies should investigate the potential effect of FA-Hex-Es *in vivo* as discussed here below.

In summary, the current study has shown anti-inflammatory effects of FA-Hex-Es in both human monocytic THP-1 cells and murine BV2 microglial cells. The observed effect of this compound is robust compared to FA-Pro-Es and IFA-Et-Es. Although this compound is not a natural PA, its significant effect on pro-inflammatory cytokines as well as its effect on anti-inflammatory signalling proteins in different cells suggest that this compound has potential as a therapeutic for inflammatory disorders and warrants further preclinical study to test its bioactivity in animal models of inflammatory disorders.

Numerous animal models are in use to study chronic inflammatory diseases<sup>590–594</sup>. Among those, two simple disease models with immune cells involvement could be used to test the effect of FA-Hex-Es on inflammation: (1) the murine model of dextran sulfate sodium (DSS)-induced colitis for inflammatory bowel disease (IBD) and (2) a murine model with experimental autoimmune encephalomyelitis (EAE) as a model of multiple sclerosis (MS).

IBD is a collective term used to describe Ulcerative Colitis (UC) and Crohn's Disease (CD), characterised by functional impairment of the gut wall causing both acute and chronic inflammation of the intestine with unknown multifactorial aetiology. Inflammation associated with IBD is thought to be due to the inappropriate activation of the mucosal immune system in response to antigens<sup>595</sup>. Moreover, several pro-inflammatory mediators

play an important role in IBD pathogenesis including TNF- $\alpha$ , IL-6, IL-1 $\beta$ , IFN $\gamma$  as well as the key role of macrophages and neutrophils in this process<sup>593,596</sup>. As we have shown a direct and robust effect of FA-Hex-Es on TNF- $\alpha$  secretion and HO-1 expression, perhaps this animal model would be relevant for a pre-clinical study.

### **Testing the effect of FA-Hex-Es in a murine model of DSS-induced colitis for IBD**

Numerous murine models of intestinal inflammation have been developed to study IBD<sup>590,593</sup> and among those, DSS-induced colitis is a widely used model for its simplicity, rapidity, reproducibility, controllability, and high resemblance with human UC<sup>595</sup>. In this model, the colitogenic chemical DSS, which is a water-soluble and negatively charged polysaccharide, is thought to damage the epithelial monolayer lining the large intestine and altering mucosal barrier alteration throughout the colonic epithelium, causing dissemination of pro-inflammatory intestinal agents into the underlying tissue and infiltration of immune cells. Thus, administration of DSS to mice in their drinking water for a short period of time results in induction of a very reproducible inflammatory response<sup>593</sup>. In this model, the outcome or effect of treatment can be easily monitored and quantified (body weight, stool, intestinal morphology, and expression level of cytokines (IL-6, TNF- $\alpha$ , IL-1 $\beta$ , IL-17 etc.)<sup>591,597</sup>. For instance, a study could be conducted to test the effect of FA-Hex-Es on DSS-induced colitis in murine model animals as described by Algieri et al., 2014. In this study two animal groups could be randomly assigned to a non-colitic (control group) or a DSS colitic group. The colitis could be induced by adding DSS (5-40 kDa) in the drinking water at a concentration of 1-5% for a period of 1 week, after which the DSS would be removed. Then, the colitic mouse could be further divided into two groups: one receiving FA-Hex-Es and the other (colitic control mice) receiving vehicle control (200  $\mu$ L of carboxymethylcellulose (CMC)) for another week, while non-colitic mice would receive tap water during the whole experiment. Before and during the experiment, animal body weight, food, and water intake as well as stool would be daily evaluated. Once the

animal is sacrificed, the colonic tissue could be removed and further examined for histological studies as well as for biochemical determinations or for RNA isolation.

FA-Hex-Es showed a remarkable effect on IL-6 protein and gene expression via the NF- $\kappa$ B pathway in BV2 murine microglial cells. Microglial cells play a central role in neuroinflammation, the underlying mechanism of numerous neurological disorders. The neuroprotective effect of FA-Hex-Es could be further investigated in animal models, such as EAE, resembling MS, involving immune cell infiltration and microglial activation <sup>598</sup>.

### **Testing the effect of FA-Hex-Es in a murine model with EAE, resembling MS**

MS, a chronic inflammatory autoimmune disease of the CNS with unknown etiology and pathogenesis, involves a complex interaction between the immune system and neuronal cells. MS is characterised by demyelination, neuroinflammation, axonal damage or loss, and gliosis. The neuroinflammation is thought to be the main trigger of the events leading to CNS tissue damage. EAE is widely used for preclinical testing of a wide range of potential therapeutic intervention <sup>599</sup>.

In the EAE murine model autoimmunity is induced in susceptible mice through immunisation with self-CNS derived antigens such as myelin basic protein (MBP), myelin oligodendrocyte glycoprotein (MOG), or proteolipid protein (PLP). Usually, these proteins are emulsified in Complete Freund's Adjuvant (CFA) and supplemented with inactivated *Mycobacterium tuberculosis* (MT). Upon immunisation, the pertussis toxin (PT) is administered to potentiate the humoral immune response and to induce oscillatory symptoms typical of the relapsing-remitting MS (RRMS) or chronic EAE <sup>600</sup>.

To test the effect of FA-Hex-Es on microglial activation and inflammatory response in the EAE model, an experiment could be designed where a susceptible mice strain such as C57BL/6 could be used. In this setting, mice

could be randomly assigned to four different groups: (1) non-EAE mice (non-immunised control group), (2) EAE mice, (3) EAE mice treated with FA-Hex-Es and a positive treatment group where (4) EAE mice is treated with DMF or fingolimod, common oral drugs used to treat MS symptoms<sup>465,601,602</sup>. In this experiment, the first group would be administered normal saline (NS) alone, while EAE mice would be immunised by subcutaneous injection of MOG<sub>35-55</sub> peptide in CFA with MT in NS. Following immunisation, mice would be administered PT on day 2 to induce chronic EAE. Following treatment daily, the clinical signs of EAE would be assessed by the five-point scoring system, the neurological function scores of the EAE mice as described by others<sup>602</sup>.

After a period of 12 days, to evaluate the treatment effect, the EAE mice would be then further chronically treated with FA-Hex-Es and DMF or fingolimod (0.3 mg/kg) solution in drinking water for a further 10-20 days, while the non-immunised mice would be given water alone as described by others<sup>602,603</sup>. The treatment effect on EAE mice would be further assessed post-mortem for neurodegeneration and neuroinflammation. For instance, the neurodegenerative process of the EAE vs control mice could be examined by histological assessment. Such assays could involve staining the CNS tissue with Luxol Fast Blue for myelin evaluation and cresyl violet or haematoxylin/eosin for routine histological analysis. Furthermore, the neuroinflammation in the CNS tissues of EAE mice could be assessed by immunofluorescent labelling of leucocytes with CD45 and activated microglial cells with Iba1/TMEM119 to examining the presence and extend of infiltrated immune cells and activated microglial cells in CNS<sup>602,604</sup> and the plasma and CNS expression level of pro-inflammatory cytokines could be assessed by RT-qPCR.

In conclusion we have screened various natural and non-natural phenolic acids, including synthetic analogues, for their anti-inflammatory and antioxidant effects on human and murine immune cells. We have shown that the synthetic analogues of ferulic acid, ferulic acid hexyl ester (FA-Hex-



Es), has a robust effect on both anti-inflammatory and antioxidant proteins in cell culture. This compound has potential therapeutic properties. Further *in vivo* preclinical studies are required to validate the therapeutic properties of FA-Hex-Es in order to confirm that this compound is a valid candidate for future clinical studies.

## Chapter 7 References

1. Middleton, E. Biological properties of plant flavonoids: An overview. *Pharmaceutical Biology* vol. 34 344–348 (1996).
2. Cook, N. C. & Samman, S. Flavonoids—Chemistry, metabolism, cardioprotective effects, and dietary sources. *J. Nutr. Biochem.* **7**, 66–76 (1996).
3. Ono, E. *et al.* Yellow flowers generated by expression of the aurone biosynthetic pathway. *Proc. Natl. Acad. Sci. U. S. A.* **103**, 11075–11080 (2006).
4. Wang, Q., Liu, J. & Zhu, H. Genetic and molecular mechanisms underlying symbiotic specificity in legume-rhizobium interactions. *Front. Plant Sci.* **9**, 313 (2018).
5. Okazaki, S., Kaneko, T., Sato, S. & Saeki, K. Hijacking of leguminous nodulation signaling by the rhizobial type III secretion system. *Proc. Natl. Acad. Sci.* **110**, 17131–17136 (2013).
6. Agati, G., Azzarello, E., Pollastri, S. & Tattini, M. Flavonoids as antioxidants in plants: Location and functional significance. *Plant Sci.* **196**, 67–76 (2012).
7. Mierziak, J., Kostyn, K. & Kulma, A. Flavonoids as important molecules of plant interactions with the environment. *Molecules* **19**, 16240–16265 (2014).
8. Crozier, A., Jaganath, I. B. & Clifford, M. N. Dietary phenolics: chemistry, bioavailability and effects on health. *Nat. Prod. Rep.* **26**, 1001 (2009).
9. Pérez-Jiménez, J., Neveu, V., Vos, F. & Scalbert, A. Identification of the 100 richest dietary sources of polyphenols: An application of the Phenol-Explorer database. *Eur. J. Clin. Nutr.* **64**, S112–S120 (2010).
10. van der Watt, E. & Pretorius, J. C. Purification and identification of active antibacterial components in *Carpobrotus edulis* L. *J. Ethnopharmacol.* **76**, 87–91 (2001).
11. Duda-Chodak, A., Tarko, T., Satora, P. & Sroka, P. Interaction of dietary compounds, especially polyphenols, with the intestinal microbiota: a review. *Eur. J. Nutr.* **54**, 325–341 (2015).
12. Selma, M. V., Espin, J. C. & Tomas-Barberan, F. A. Interaction between Phenolics and Gut Microbiota: Role in Human Health. *J. Agric. Food Chem* **57**, 6485–6501 (2009).
13. Kuster, R. M., Arnold, N. & Wessjohann, L. Anti-fungal flavonoids from *Tibouchina grandifolia*. *Biochem. Syst. Ecol.* **37**, 63–65 (2009).
14. Lopes, N. P., Kato, M. J. & Yoshida, M. Antifungal constituents from roots of *Virolasurinamensis*. *Phytochemistry* **51**, 29–33 (1999).
15. Lalani, S. & Poh, C. L. Flavonoids as antiviral agents for enterovirus A71 (EV-A71). *Viruses* **12**, 184 (2020).
16. Mohammadi Pour, P., Fakhri, S., Asgary, S., Farzaei, M. H. & Echeverría, J. The

signaling pathways, and therapeutic targets of antiviral agents: Focusing on the antiviral approaches and clinical perspectives of anthocyanins in the management of viral diseases. *Front. Pharmacol.* **10**, 1–23 (2019).

17. Dai, W. *et al.* Antiviral efficacy of flavonoids against enterovirus 71 infection in vitro and in newborn mice. *Viruses* **11**, 625 (2019).
18. Amin, H. P. *et al.* Anthocyanins and their physiologically relevant metabolites alter the expression of IL-6 and VCAM-1 in CD40L and oxidized LDL challenged vascular endothelial cells. *Mol. Nutr. Food Res.* **59**, 1095–1106 (2015).
19. di Gesso, J. L. *et al.* Flavonoid metabolites reduce tumor necrosis factor- $\alpha$  secretion to a greater extent than their precursor compounds in human THP-1 monocytes. *Mol. Nutr. Food Res.* **59**, 1143–1154 (2015).
20. Warner, E. F. *et al.* Signatures of anthocyanin metabolites identified in humans inhibit biomarkers of vascular inflammation in human endothelial cells. *Mol. Nutr. Food Res.* **61**, (2017).
21. Bondonno, N. P. *et al.* Association of flavonoids and flavonoid-rich foods with all-cause mortality: The Blue Mountains Eye Study. *Clin. Nutr.* **39**, 141–150 (2020).
22. Ma, L. *et al.* Isoflavone intake and the risk of coronary heart disease in US men and women: Results from 3 prospective cohort studies. *Circulation* **141**, 1127–1137 (2020).
23. Bondonno, N. P. *et al.* Flavonoid intake is associated with lower mortality in the Danish Diet Cancer and Health Cohort. *Nat. Commun.* **10**, 3651 (2019).
24. Shishtar, E., Rogers, G. T., Blumberg, J. B., Au, R. & Jacques, P. F. Long-term dietary flavonoid intake and change in cognitive function in the Framingham Offspring cohort. *Public Health Nutr.* **23**, 1576–1588 (2020).
25. Cassidy, A. *et al.* Habitual intake of anthocyanins and flavanones and risk of cardiovascular disease in men. *Am. J. Clin. Nutr.* **104**, 587–594 (2016).
26. Dodd, G. F., Williams, C. M., Butler, L. T. & Spencer, J. P. E. Acute effects of flavonoid-rich blueberry on cognitive and vascular function in healthy older adults. *Nutr. Heal. Aging* **5**, 119–132 (2019).
27. WHO. Cardiovascular diseases. *Health Topics from WHO Web Page* [http://www.who.int/cardiovascular\\_diseases/en/](http://www.who.int/cardiovascular_diseases/en/) (2016).
28. World Health Organization. Mental health: neurological disorders. *Mental health: neurological disorders* <https://www.who.int/news-room/q-a-detail/mental-health-neurological-disorders> (2021).
29. Public Health England. Health matters: preventing cardiovascular disease - GOV.UK. *Published 14 February 2019* <https://www.gov.uk/government/publications/health-matters-preventing-cardiovascular-disease/health-matters-preventing-cardiovascular-disease> (2019).
30. NHS England. Neurological conditions. *NHS England 1*

<https://www.england.nhs.uk/ourwork/clinical-policy/ltc/our-work-on-long-term-conditions/neurological/> (2021).

31. Knekt, P. *et al.* Flavonoid intake and risk of chronic diseases. *Am. J. Clin. Nutr.* **76**, 560–8 (2002).
32. Curtis, P. J. *et al.* Blueberries improve biomarkers of cardiometabolic function in participants with metabolic syndrome—results from a 6-month, double-blind, randomized controlled trial. *Am. J. Clin. Nutr.* **109**, 1535–1545 (2019).
33. Sansone, R. *et al.* Cocoa flavanol intake improves endothelial function and Framingham Risk Score in healthy men and women: A randomised, controlled, double-masked trial: the Flaviola Health Study. *Br. J. Nutr.* **114**, 1246–1255 (2015).
34. Noad, R. L. *et al.* Beneficial effect of a polyphenol-rich diet on cardiovascular risk: A randomised control trial. *Heart* **102**, 1371–1379 (2016).
35. Feliciano, R. P., Pritzel, S., Heiss, C. & Rodriguez-Mateos, A. Flavonoid intake and cardiovascular disease risk. *Curr. Opin. Food Sci.* **2**, 92–99 (2015).
36. Wardyn, J. D., Ponsford, A. H. & Sanderson, C. M. Dissecting molecular cross-talk between Nrf2 and NF- $\kappa$ B response pathways. *Biochem. Soc. Trans.* **43**, 621–626 (2015).
37. Vernocchi, P., Del Chierico, F. & Putignani, L. Gut microbiota profiling: Metabolomics based approach to unravel compounds affecting human health. *Front. Microbiol.* **7**, 1144 (2016).
38. Kawabata, K., Yoshioka, Y. & Terao, J. Role of intestinal microbiota in the bioavailability and physiological functions of dietary polyphenols. *Molecules* **24**, (2019).
39. Bohn, T. Dietary factors affecting polyphenol bioavailability. *Nutr. Rev.* **72**, 429–452 (2014).
40. Cassidy, A. & Minihane, A. M. The role of metabolism (and the microbiome) in defining the clinical efficacy of dietary flavonoids. *Am. J. Clin. Nutr.* **105**, 10–22 (2017).
41. Kay, C. D., Pereira-Caro, G., Ludwig, I. A., Clifford, M. N. & Crozier, A. Anthocyanins and Flavanones Are More Bioavailable than Previously Perceived: A Review of Recent Evidence. *Annu. Rev. Food Sci. Technol.* **8**, 155–180 (2017).
42. Czank, C. *et al.* Human metabolism and elimination of the anthocyanin, cyanidin-3-glucoside: A13C-tracer study. *Am. J. Clin. Nutr.* **97**, 995–1003 (2013).
43. de Ferrars, R. M., Cassidy, A., Curtis, P. & Kay, C. D. Phenolic metabolites of anthocyanins following a dietary intervention study in post-menopausal women. *Mol. Nutr. Food Res.* **58**, 490–502 (2014).
44. Edwards, M., Czank, C., Woodward, G. M., Cassidy, A. & Kay, C. D. Phenolic Metabolites of Anthocyanins Modulate Mechanisms of Endothelial Function. *J.*

- Agric. Food Chem.* **63**, 2423–2431 (2015).
45. Krga, I. *et al.* Anthocyanins and their gut metabolites attenuate monocyte adhesion and transendothelial migration through nutrigenomic mechanisms regulating endothelial cell permeability. *Free Radic. Biol. Med.* **124**, 364–379 (2018).
  46. Krga, I. *et al.* Anthocyanins and their gut metabolites reduce the adhesion of monocyte to TNF $\alpha$ -activated endothelial cells at physiologically relevant concentrations. *Arch. Biochem. Biophys.* **599**, 51–59 (2016).
  47. Warner, E. F. *et al.* Common Phenolic Metabolites of Flavonoids, but Not Their Unmetabolized Precursors, Reduce the Secretion of Vascular Cellular Adhesion Molecules by Human Endothelial Cells. *J. Nutr.* **146**, 465–73 (2016).
  48. Rodriguez-Mateos, A. *et al.* Cranberry (poly)phenol metabolites correlate with improvements in vascular function: A double-blind, randomized, controlled, dose-response, crossover study. *Mol. Nutr. Food Res.* **60**, 2130–2140 (2016).
  49. Baeza, G. *et al.* The colonic metabolites dihydrocaffeic acid and dihydroferulic acid are more effective inhibitors of in vitro platelet activation than their phenolic precursors. *Food Funct.* **8**, 1333–1342 (2017).
  50. Feliciano, R. P., Istas, G., Heiss, C. & Rodriguez-Mateos, A. Plasma and urinary phenolic profiles after acute and repetitive intake of wild blueberry. *Molecules* **21**, (2016).
  51. Claude, S. *et al.* Flavanol metabolites reduce monocyte adhesion to endothelial cells through modulation of expression of genes via p38-MAPK and p65-Nf-kB pathways. *Mol. Nutr. Food Res.* **58**, 1016–1027 (2014).
  52. Rodriguez-Mateos, A. *et al.* Circulating Anthocyanin Metabolites Mediate Vascular Benefits of Blueberries: Insights from Randomized Controlled Trials, Metabolomics, and Nutrigenomics. *Journals Gerontol. - Ser. A Biol. Sci. Med. Sci.* **74**, 967–976 (2019).
  53. Feliciano, R. P., Mills, C. E., Istas, G., Heiss, C. & Rodriguez-Mateos, A. Absorption, metabolism and excretion of cranberry (poly)phenols in humans: A dose response study and assessment of inter-individual variability. *Nutrients* **9**, 268 (2017).
  54. Figueira, I. *et al.* Polyphenols journey through blood-brain barrier towards neuronal protection. *Sci. Rep.* **7**, (2017).
  55. Carregosa, D., Carecho, R., Figueira, I. & Santos, C. N. Low-Molecular Weight Metabolites from Polyphenols as Effectors for Attenuating Neuroinflammation. *J. Agric. Food Chem.* (2019) doi:10.1021/acs.jafc.9b02155.
  56. Williams, C. A. & Grayer, R. J. Anthocyanins and other flavonoids. *Nat. Prod. Rep.* **21**, 539–573 (2004).
  57. Wang, Y., Chen, S. & Yu, O. Metabolic engineering of flavonoids in plants and

- microorganisms. *Appl. Microbiol. Biotechnol.* **91**, 949–956 (2011).
58. Barros, L., Dueñas, M., Ferreira, I. C. F. R., Baptista, P. & Santos-Buelga, C. Phenolic acids determination by HPLC-DAD-ESI/MS in sixteen different Portuguese wild mushrooms species. *Food Chem. Toxicol.* **47**, 1076–1079 (2009).
59. Martín, J., Navas, M. J., Jiménez-Moreno, A. M. & Asuero, A. G. Anthocyanin Pigments: Importance, Sample Preparation and Extraction. *Phenolic Compd. - Nat. Sources, Importance Appl. Intech*, 117–152 (2017).
60. Phenol-Explorer. Polyphenol Classes. *Phenol-Explorer, version 3.6* <http://phenol-explorer.eu/compounds/classification> (2015).
61. Neveu, V. *et al.* Phenol-Explorer: an online comprehensive database on polyphenol contents in foods. *Database (Oxford)*. **2010**, bap024–bap024 (2010).
62. Tsao, R. Chemistry and biochemistry of dietary polyphenols. *Nutrients* **2**, 1231–1246 (2010).
63. Frank, J. *et al.* Terms and nomenclature used for plant-derived components in nutrition and related research: Efforts toward harmonization. *Nutr. Rev.* **78**, 451–458 (2020).
64. Xiao, J. Dietary Flavonoid Aglycones and Their Glycosides: Which Show Better Biological Significance? *Crit. Rev. Food Sci. Nutr.* **57**, 00–00 (2015).
65. Rothwell, J. A. *et al.* Systematic analysis of the polyphenol metabolome using the Phenol-Explorer database. *Mol. Nutr. Food Res.* **60**, 203–211 (2016).
66. Phenol-Explorer. Food Compositions-Polyphenols. *Phenol-Explorer, version 3.6* <http://phenol-explorer.eu/compounds> (2015).
67. Gates, P. & Lopes, N. Characterisation of flavonoid aglycones by negative ion chip-based nanospray tandem mass spectrometry. *Int. J. Anal. Chem.* **2012**, 1–7 (2012).
68. Kumar, S. & Pandey, A. K. Chemistry and biological activities of flavonoids: An overview. *Sci. World J.* **2013**, 162750 (2013).
69. Manach, C., Scalbert, A., Morand, C., Rémésy, C. & Jiménez, L. Polyphenols: food sources and bioavailability. *Am. J. Clin. Nutr.* **79**, 727–47 (2004).
70. Corcoran, M. P., McKay, D. L. & Blumberg, J. B. Flavonoid Basics: Chemistry, Sources, Mechanisms of Action, and Safety. *J. Nutr. Gerontol. Geriatr.* **31**, 176–189 (2012).
71. Sisa, M., Bonnet, S. L., Ferreira, D. & Van Der Westhuizen, J. H. Photochemistry of flavonoids. *Molecules* vol. 15 5196–5245 (2010).
72. Panche, A. N., Diwan, A. D. & Chandra, S. R. Flavonoids: An overview. *J. Nutr. Sci.* **5**, (2016).
73. Wan, J. *et al.* UV-B radiation induces root bending through the flavonoid-mediated auxin pathway in Arabidopsis. *Front. Plant Sci.* **9**, 1–15 (2018).

74. Keilig, K. & Ludwig-Müller, J. Effect of flavonoids on heavy metal tolerance in *Arabidopsis thaliana* seedlings. *Bot. Stud.* **50**, 311–318 (2009).
75. Ahatović, A. *et al.* Plantago lanceolata L. from Serpentine Soils in Central Bosnia Tolerates High Levels of Heavy Metals in Soil. *Water, Air, Soil Pollut* **231**, 169 (2020).
76. Coberly, L. C. & Rausher, M. D. Analysis of a chalcone synthase mutant in *Ipomoea purpurea* reveals a novel function for flavonoids: Amelioration of heat stress. *Mol. Ecol.* **12**, 1113–1124 (2003).
77. Sivankalyani, V., Feygenberg, O., Diskin, S., Wright, B. & Alkan, N. Increased anthocyanin and flavonoids in mango fruit peel are associated with cold and pathogen resistance. *Postharvest Biol. Technol.* **111**, 132–139 (2016).
78. Sosa, T. *et al.* Inhibition of mouth skeletal muscle relaxation by flavonoids of *Cistus ladanifer* L.: A plant defense mechanism against herbivores. *J. Chem. Ecol.* **30**, 1087–1101 (2004).
79. Goya, L. *et al.* Effect of cocoa and its flavonoids on biomarkers of inflammation: Studies of cell culture, animals and humans. *Nutrients* **8**, 212 (2016).
80. Korkina, L. G. & Afanas'Ev, I. B. Antioxidant and Chelating Properties of Flavonoids. *Adv. Pharmacol.* **38**, 151–163 (1996).
81. Hanasaki, Y., Ogawa, S. & Fukui, S. The correlation between active oxygens scavenging and antioxidative effects of flavonoids. *Free Radic. Biol. Med.* **16**, 845–850 (1994).
82. Kerry, N. L. & Abbey, M. Red wine and fractionated phenolic compounds prepared from red wine inhibit low density lipoprotein oxidation in vitro. *Atherosclerosis* **135**, 93–102 (1997).
83. Sanhueza, J., Valdes, J., Campos, R., Garrido, A. & Valenzuela, A. Changes in the xanthine dehydrogenase/xanthine oxidase ratio in the rat kidney subjected to ischemia-reperfusion stress: Preventive effect of some flavonoids. *Res. Commun. Chem. Pathol. Pharmacol.* **78**, 211–218 (1992).
84. Pietta, P.-G. Flavonoids as Antioxidants. *J. Nat. Prod.* **63**, 1035–1042 (2000).
85. Sies, H. Total antioxidant capacity: appraisal of a concept. *J. Nutr.* **137**, 1493–5 (2007).
86. Brunetti, C., Di Ferdinando, M., Fini, A., Pollastri, S. & Tattini, M. Flavonoids as antioxidants and developmental regulators: Relative significance in plants and humans. *International Journal of Molecular Sciences* vol. 14 3540–3555 (2013).
87. Halliwell, B., Rafter, J. & Jenner, A. Health promotion by flavonoids, tocopherols, tocotrienols, and other phenols: direct or indirect effects? Antioxidant or not? *Am. J. Clin. Nutr.* **81**, 268S-276S (2005).
88. Hollman, P. C. H. *et al.* The Biological Relevance of Direct Antioxidant Effects of Polyphenols for Cardiovascular Health in Humans Is Not Established. *J. Nutr.*

- 141**, 989S-1009S (2011).
89. Williamson, G., Kay, C. D. & Crozier, A. The Bioavailability, Transport, and Bioactivity of Dietary Flavonoids: A Review from a Historical Perspective. *Compr. Rev. Food Sci. Food Saf.* **0**, 1–59 (2018).
  90. Tena, N., Martín, J. & Asuero, A. G. State of the art of anthocyanins: Antioxidant activity, sources, bioavailability, and therapeutic effect in human health. *Antioxidants* **9**, 451 (2020).
  91. Kalt, W. Anthocyanins and their C6-C3-C6 metabolites in humans and animals. *Molecules* **24**, 4024 (2019).
  92. Lila, M. A., Burton-Freeman, B., Grace, M. & Kalt, W. Unraveling Anthocyanin Bioavailability for Human Health. *Annu. Rev. Food Sci. Technol.* **7**, annurev-food-041715-033346 (2016).
  93. Croft, K. D. Dietary polyphenols: Antioxidants or not? *Arch. Biochem. Biophys.* **595**, 120–124 (2016).
  94. Kay, C. D. Rethinking paradigms for studying mechanisms of action of plant bioactives. *Nutr. Bull.* **40**, 335–339 (2015).
  95. Kay, C. D. The future of flavonoid research. *Br. J. Nutr.* **104**, S91–S95 (2010).
  96. Croft, K. D. The chemistry and biological effects of flavonoids and phenolic acids. *Ann. N. Y. Acad. Sci.* **854**, 435–442 (1998).
  97. Kumar, N. & Goel, N. Phenolic acids: Natural versatile molecules with promising therapeutic applications. *Biotechnol. Reports* **24**, e00370 (2019).
  98. Rashmi, H. B. & Negi, P. S. Phenolic acids from vegetables: A review on processing stability and health benefits. *Food Res. Int.* **136**, 109298 (2020).
  99. Kim, K. H., Tsao, R., Yang, R. & Cui, S. W. Phenolic acid profiles and antioxidant activities of wheat bran extracts and the effect of hydrolysis conditions. *Food Chem.* **95**, 466–473 (2006).
  100. Bento-Silva, A. *et al.* Factors affecting intake, metabolism and health benefits of phenolic acids: do we understand individual variability? *Eur. J. Nutr.* **59**, 1275–1293 (2020).
  101. Călinoiu, L. F. & Vodnar, D. C. Whole grains and phenolic acids: A review on bioactivity, functionality, health benefits and bioavailability. *Nutrients* **10**, (2018).
  102. Laddomada, B., Caretto, S. & Mita, G. Wheat bran phenolic acids: Bioavailability and stability in whole wheat-based foods. *Molecules* **20**, 15666–15685 (2015).
  103. Kumar, N. & Pruthi, V. Potential applications of ferulic acid from natural sources. *Biotechnology Reports* vol. 4 86–93 (2014).
  104. McKay, D. L., Chen, C. Y. O., Zampariello, C. A. & Blumberg, J. B. Flavonoids and phenolic acids from cranberry juice are bioavailable and bioactive in healthy older adults. *Food Chem.* **168**, 233–240 (2015).
  105. Frolinger, T. *et al.* The gut microbiota composition affects dietary polyphenols-



mediated cognitive resilience in mice by modulating the bioavailability of phenolic acids. *Sci. Rep.* **9**, 1–10 (2019).

106. Czank, C. *et al.* Human metabolism and elimination of the anthocyanin, cyanidin-3-glucoside: a <sup>13</sup>C-tracer study. *Am. J. Clin. Nutr.* **97**, 995–1003 (2013).
107. Eker, M. E. *et al.* A review of factors affecting anthocyanin bioavailability: Possible implications for the inter-individual variability. *Foods* **9**, 2 (2020).
108. Zhang, Y. & Li, X. Salicylic acid: biosynthesis, perception, and contributions to plant immunity. *Curr. Opin. Plant Biol.* **50**, 29–36 (2019).
109. Wei, H. *et al.* Utilization of straw-based phenolic acids as a biofungicide for a green agricultural production. *J. Biosci. Bioeng.* **131**, 53–60 (2021).
110. Stuper-Szablewska, K., Kurasiak-Popowska, D., Nawracała, J. & Perkowski, J. Quantitative profile of phenolic acids and antioxidant activity of wheat grain exposed to stress. *Eur. Food Res. Technol.* **245**, 1595–1603 (2019).
111. Hsueh, M.-T., Fan, C. & Chang, W.-L. Allelopathic Effects of *Bidens pilosa* L. var. *radiata* Sch. Bip. on the Tuber Sprouting and Seedling Growth of *Cyperus rotundus* L. *Plants* **9**, 742 (2020).
112. Cheng, F. & Cheng, Z. Research progress on the use of plant allelopathy in agriculture and the physiological and ecological mechanisms of allelopathy. *Frontiers in Plant Science* vol. 6 1020 (2015).
113. Rothwell, J. A. *et al.* Phenol-Explorer 3.0: A major update of the Phenol-Explorer database to incorporate data on the effects of food processing on polyphenol content. *Database* **2013**, 7010–1093 (2013).
114. Phenol-Explorer. Food Classes. *Phenol-Explorer, version 3.6* <http://phenol-explorer.eu/foods/classification> (2015).
115. Phenol-Explorer. Food Composition-Polyphenols. *Phenol -Explorer, version 3.6* <http://phenol-explorer.eu/compounds> (2015).
116. Zamora-Ros, R. *et al.* Dietary polyphenol intake in europe: The european prospective investigation into cancer and nutrition (EPIC) study. *Eur. J. Nutr.* **55**, 1359–1375 (2016).
117. Wisnuwardani, R. W. *et al.* Estimated dietary intake of polyphenols in European adolescents: the HELENA study. *Eur. J. Nutr.* **58**, 2345–2363 (2019).
118. Vogiatzoglou, A. *et al.* Flavonoid intake in European adults (18 to 64 Years). *PLoS One* **10**, e0128132 (2015).
119. Khokhar, S. & Magnúsdóttir, S. G. M. Total phenol, catechin, and caffeine contents of teas commonly consumed in the United Kingdom. *J. Agric. Food Chem.* **50**, 565–570 (2002).
120. Nardini, M., Cirillo, E., Natella, F. & Scaccini, C. Absorption of phenolic acids in humans after coffee consumption. *J. Agric. Food Chem.* **50**, 5735–5741 (2002).
121. Clifford, M. N. Chlorogenic acids and other cinnamates - nature, occurrence,

- dietary burden, absorption and metabolism. *J. Sci. Food Agric.* **80**, 1033–1043 (2000).
122. Rein, M. J. *et al.* Bioavailability of bioactive food compounds: A challenging journey to bioefficacy. *Br. J. Clin. Pharmacol.* **75**, 588–602 (2013).
  123. Miranda, A. M., Steluti, J., Fisberg, R. M. & Marchioni, D. M. Dietary intake and food contributors of polyphenols in adults and elderly adults of Sao Paulo: A population-based study. *Br. J. Nutr.* **115**, 1061–1070 (2016).
  124. Hollman, P. C. H. & Katan, M. B. Absorption, metabolism and health effects of dietary flavonoids in man. *Biomed. Pharmacother.* **51**, 305–310 (1997).
  125. Spencer, J. P. E. Proceedings of the Third International Scientific Symposium on Tea and Human Health: Role of Flavonoids in the Diet Metabolism of Tea Flavonoids in the Gastrointestinal Tract 1,2. *J. Nutr.* **133**, 3255S-3261S (2003).
  126. Keppler, K. & Humpf, H. U. Metabolism of anthocyanins and their phenolic degradation products by the intestinal microflora. *Bioorganic Med. Chem.* **13**, 5195–5205 (2005).
  127. Kay, C. D. Aspects of anthocyanin absorption, metabolism and pharmacokinetics in humans. *Nutr. Res. Rev.* **19**, 137–146 (2006).
  128. Serra, A. *et al.* Metabolic pathways of the colonic metabolism of flavonoids (flavonols, flavones and flavanones) and phenolic acids. *Food Chem.* **130**, 383–393 (2012).
  129. Del Rio, D. *et al.* Dietary (Poly)phenolics in Human Health: Structures, Bioavailability, and Evidence of Protective Effects Against Chronic Diseases. *Antioxid. Redox Signal.* **18**, 1818–1892 (2013).
  130. Hollman, P. C. & Katan, M. B. Bioavailability and health effects of dietary flavonols in man. *Arch. Toxicol. Suppl.* **20**, 237–248 (1998).
  131. Aura, A. M. *et al.* In vitro metabolism of anthocyanins by human gut microflora. *Eur. J. Nutr.* **44**, 133–142 (2005).
  132. Scalbert, A. & Williamson, G. Dietary intake and bioavailability of polyphenols. *J. Nutr.* **130**, 2073S–85S (2000).
  133. Day, A. J., Gee, J. M., DuPont, M. S., Johnson, I. T. & Williamson, G. Absorption of quercetin-3-glucoside and quercetin-4'-glucoside in the rat small intestine: The role of lactase phlorizin hydrolase and the sodium-dependent glucose transporter. *Biochem. Pharmacol.* **65**, 1199–1206 (2003).
  134. Walgren, R. A., Lin, J.-T., Kinne, R. K.-H. & Walle, T. Cellular Uptake of Dietary Flavonoid Quercetin 4'- $\beta$ -Glucoside by Sodium-Dependent Glucose Transporter SGLT1. *J. Pharmacol. Exp. Ther.* **294**, 837–843 (2000).
  135. Gopalan, V., Pastuszyn, A., Galey, W. R. & Glew, R. H. Exolytic hydrolysis of toxic plant glucosides by guinea pig liver cytosolic beta-glucosidase. *J. Biol. Chem.* **267**, 14027–32 (1992).

136. Walle, T. Absorption and metabolism of flavonoids. *Free Radical Biology and Medicine* vol. 36 829–837 (2004).
137. Warner, E. F. Investigating the Impact of Flavonoid Metabolites on Endothelial Function and Vascular Inflammation. *Thesis* (University of East Anglia, 2016).
138. Correa-Betanzo, J. *et al.* Stability and biological activity of wild blueberry (*Vaccinium angustifolium*) polyphenols during simulated in vitro gastrointestinal digestion. *Food Chem.* **165**, 522–531 (2014).
139. Chiou, Y. S. *et al.* Metabolic and colonic microbiota transformation may enhance the bioactivities of dietary polyphenols. *J. Funct. Foods* **7**, 3–25 (2014).
140. Griffiths, L. A. & Barrow, A. Metabolism of flavonoid compounds in germ-free rats. *Biochem. J.* **130**, 1161–1162 (1972).
141. Bowey, E., Adlercreutz, H. & Rowland, I. Metabolism of isoflavones and lignans by the gut microflora: A study in germ-free and human flora associated rats. *Food Chem. Toxicol.* **41**, 631–636 (2003).
142. Das, N. P. & Griffiths, L. A. Studies on flavonoid metabolism. Metabolism of (+)-[14C]catechin in the rat and guinea pig. *Biochem. J.* **115**, 813–836 (1969).
143. Pimpão, R. C., Ventura, M. R., Ferreira, R. B., Williamson, G. & Santos, C. N. Phenolic sulfates as new and highly abundant metabolites in human plasma after ingestion of a mixed berry fruit puré e. *Br. J. Nutr.* **113**, 454–463 (2015).
144. Clarke, K. A. *et al.* High performance liquid chromatography tandem mass spectrometry dual extraction method for identification of green tea catechin metabolites excreted in human urine. *J. Chromatogr. B Anal. Technol. Biomed. Life Sci.* **972**, 29–37 (2014).
145. de Ferrars, R. M. *et al.* The pharmacokinetics of anthocyanins and their metabolites in humans. *Br. J. Pharmacol.* **171**, 3268–3282 (2014).
146. Kay, C. D., Kroon, P. A. & Cassidy, A. The bioactivity of dietary anthocyanins is likely to be mediated by their degradation products. *Mol. Nutr. Food Res.* **53**, S92–S101 (2009).
147. Heleno, S. A. *et al.* Bioactivity of phenolic acids: Metabolites versus parent compounds: A review. *Food Chem.* **173**, 501–513 (2015).
148. Currie, G. M. Pharmacology, part 2: Introduction to pharmacokinetics. *J. Nucl. Med. Technol.* **46**, 221–230 (2018).
149. Melse-Boonstra, A. Bioavailability of Micronutrients From Nutrient-Dense Whole Foods: Zooming in on Dairy, Vegetables, and Fruits. *Front. Nutr.* **7**, 101 (2020).
150. Scalbert, A., Manach, C., Morand, C., Rémésy, C. & Jiménez, L. Dietary Polyphenols and the Prevention of Diseases. *Food Sci. Nutr.* **45**, 287–306 (2005).
151. Heaney, R. P. Factors Influencing the Measurement of Bioavailability, Taking Calcium as a Model. *J. Nutr.* **131**, 1376–1382 (2001).
152. Chow, S. C. Bioavailability and bioequivalence in drug development. *Wiley*

*Interdiscip. Rev. Comput. Stat.* **6**, 304–312 (2014).

153. Russo, G. *et al.* Quercetin: a pleiotropic kinase inhibitor against cancer. in *In Advances in nutrition and cancer* 185–205 (Springer Berlin Heidelberg, 2014).
154. Ottaviani, J. I. *et al.* The metabolome of [2-14C](-)-epicatechin in humans: Implications for the assessment of efficacy, safety, and mechanisms of action of polyphenolic bioactives. *Sci. Rep.* **6**, 1–10 (2016).
155. Borges, G., Ottaviani, J. I., van der Hooft, J. J. J., Schroeter, H. & Crozier, A. Absorption, metabolism, distribution and excretion of (-)-epicatechin: A review of recent findings. *Mol. Aspects Med.* **61**, 18–30 (2018).
156. Cortés-Martín, A. *et al.* The gut microbiota urolithin metabolites revisited: the human metabolism of ellagic acid is mainly determined by aging. *Food Funct.* **9**, 4100–4106 (2018).
157. Espín, J. C., González-Sarrías, A. & Tomás-Barberán, F. A. The gut microbiota: A key factor in the therapeutic effects of (poly) phenols. *Biochem. Pharmacol.* **139**, 82–93 (2017).
158. Tzounis, X. *et al.* Prebiotic evaluation of cocoa-derived flavanols in healthy humans by using a randomized, controlled, double-blind, crossover intervention study. *Am. J. Clin. Nutr.* **93**, 62–72 (2011).
159. Pérez-Cano, F., Massot-Cladera, M., Rodríguez-Lagunas, M. & Castell, M. Flavonoids Affect Host-Microbiota Crosstalk through TLR Modulation. *Antioxidants* **3**, 649–670 (2014).
160. Gil-Cardoso, K. *et al.* Effects of flavonoids on intestinal inflammation, barrier integrity and changes in gut microbiota during diet-induced obesity. *Nutrition Research Reviews* vol. 29 234–248 (2016).
161. Green, R. J., Murphy, A. S., Schulz, B., Watkins, B. A. & Ferruzzi, M. G. Common tea formulations modulate in vitro digestive recovery of green tea catechins. *Mol. Nutr. Food Res.* **51**, 1152–1162 (2007).
162. Clarke, K. A. *et al.* Green tea catechins and their metabolites in human skin before and after exposure to ultraviolet radiation. *J. Nutr. Biochem.* **27**, 203–210 (2015).
163. Legeay, S., Rodier, M., Fillon, L., Faure, S. & Clere, N. Epigallocatechin gallate: A review of its beneficial properties to prevent metabolic syndrome. *Nutrients* **7**, 5443–5468 (2015).
164. Medina, S. *et al.* Physical activity increases the bioavailability of flavanones after dietary aronia-citrus juice intake in triathletes. *Food Chem.* **135**, 2133–2137 (2012).
165. Rodríguez-Mateos, A. *et al.* Bioavailability, bioactivity and impact on health of dietary flavonoids and related compounds: an update. *Arch. Toxicol.* **88**, 1803–1853 (2014).

166. Erlund, I., Freese, R., Marniemi, J., Hakala, P. & Alfthan, G. Bioavailability of quercetin from berries and the diet. in *Nutrition and Cancer* vol. 54 13–17 (2006).
167. Clifford, M. N., Van Der Hooft, J. J. J. & Crozier, A. Human studies on the absorption, distribution, metabolism, and excretion of tea polyphenols1-3. *Am. J. Clin. Nutr.* **98**, (2013).
168. González-Sarrías, A., Núñez-Sánchez, M. Á., Tomás-Barberán, F. A. & Espín, J. C. Neuroprotective effects of bioavailable polyphenol-derived metabolites against oxidative stress-induced cytotoxicity in human neuroblastoma SH-SY5Y cells. *J. Agric. Food Chem.* **65**, 752–758 (2017).
169. Grosso, G. *et al.* Dietary Flavonoid and Lignan Intake and Mortality in Prospective Cohort Studies: Systematic Review and Dose-Response Meta-Analysis. *Am. J. Epidemiol.* **185**, 1304–1316 (2017).
170. Kalt, W. *et al.* Recent Research on the Health Benefits of Blueberries and Their Anthocyanins. *Advances in Nutrition* vol. 11 224–236 (2020).
171. Knekt, P. *et al.* Dietary Flavonoids and the Risk of Lung Cancer and Other Malignant Neoplasms. *Am. J. Epidemiol.* **146**, 223–230 (1997).
172. Yang, Y. K., Kim, J. Y. & Kwon, O. Development of flavonoid database for commonly consumed foods by Koreans. *Korean J. Nutr.* **45**, 283 (2012).
173. Theodoratou, E. *et al.* Dietary Flavonoids and the Risk of Colorectal Cancer. *Cancer Epidemiol. Biomarkers Prev.* **16**, 684–93 (2007).
174. Izzo, S., Naponelli, V. & Bettuzzi, S. Flavonoids as epigenetic modulators for prostate cancer prevention. *Nutrients* vol. 12 1010 (2020).
175. Selvakumar, P. *et al.* Flavonoids and other polyphenols act as epigenetic modifiers in breast cancer. *Nutrients* **12**, 1–18 (2020).
176. Huxley, R. *et al.* Coffee, Decaffeinated Coffee, and Tea Consumption in Relation to Incident Type 2 Diabetes Mellitus. *Arch. Intern. Med.* **169**, 2053 (2009).
177. McCullough, M. L. *et al.* Flavonoid intake and cardiovascular disease mortality in a prospective cohort of US adults. *Am. J. Clin. Nutr.* **95**, 454–464 (2012).
178. Kimble, R., Keane, K. M., Lodge, J. K. & Howatson, G. Dietary intake of anthocyanins and risk of cardiovascular disease: A systematic review and meta-analysis of prospective cohort studies. *Critical Reviews in Food Science and Nutrition* vol. 59 3032–3043 (2019).
179. Daneshzad, E., Shab-Bidar, S., Mohammadpour, Z. & Djafarian, K. Effect of anthocyanin supplementation on cardio-metabolic biomarkers: A systematic review and meta-analysis of randomized controlled trials. *Clin. Nutr.* **38**, 1153–1165 (2019).
180. Cassidy, A. Berry anthocyanin intake and cardiovascular health. *Mol. Aspects Med.* **61**, 76–82 (2018).
181. Woodward, K. A., Draijer, R., Thijssen, D. H. J. & Low, D. A. Polyphenols and

- Microvascular Function in Humans: A Systematic Review. *Curr. Pharm. Des.* **24**, 203–226 (2018).
182. Xu, R., Yang, K., Ding, J. & Chen, G. Effect of green tea supplementation on blood pressure: A systematic review and meta-analysis of randomized controlled trials. *Med. (United States)* **99**, (2020).
  183. Spencer, J. P. E. The impact of fruit flavonoids on memory and cognition. *Br. J. Nutr.* **104**, S40–S47 (2010).
  184. Carregosa, D., Carecho, R., Figueira, I. & dos Santos, C. N. Low molecular weight gut polyphenols metabolites and its nutritional relevance as effectors for attenuating neuroinflammation. *Proc. Nutr. Soc.* **79**, (2020).
  185. Chang, S. C. *et al.* Dietary flavonoid intake and risk of incident depression in midlife and older women. *Am. J. Clin. Nutr.* **104**, 704–714 (2016).
  186. Khalid, S. *et al.* Effects of acute blueberry flavonoids on mood in children and young adults. *Nutrients* **9**, (2017).
  187. Godos, J. *et al.* Diet and mental health: Review of the recent updates on molecular mechanisms. *Antioxidants* **9**, 1–13 (2020).
  188. Flanagan, E., Müller, M., Hornberger, M. & Vauzour, D. Impact of Flavonoids on Cellular and Molecular Mechanisms Underlying Age-Related Cognitive Decline and Neurodegeneration. *Curr. Nutr. Rep.* **7**, 49–57 (2018).
  189. Lampion, D. J. *et al.* Concord grape juice, cognitive function, and driving performance: A 12-wk, placebo-controlled, randomized crossover trial in mothers of preteen children. *Am. J. Clin. Nutr.* **103**, 775–783 (2016).
  190. Nilsson, A., Salo, I., Plaza, M. & Björck, I. Effects of a mixed berry beverage on cognitive functions and cardiometabolic risk markers; A randomized cross-over study in healthy older adults. *PLoS One* **12**, (2017).
  191. NHS. Cardiovascular Disease. *NHS*  
<https://www.nhs.uk/conditions/cardiovascular-disease/> (2018).
  192. Einarson, T. R., Acs, A., Ludwig, C. & Panton, U. H. Economic Burden of Cardiovascular Disease in Type 2 Diabetes: A Systematic Review. *Value in Health* vol. 21 881–890 (2018).
  193. Timmis, A. *et al.* European society of cardiology: Cardiovascular disease statistics 2019. *Eur. Heart J.* **41**, 12–85 (2020).
  194. Barbaresko, J., Rienks, J. & Nöthlings, U. Lifestyle Indices and Cardiovascular Disease Risk: A Meta-analysis. *Am. J. Prev. Med.* **55**, 555–564 (2018).
  195. Woo, H. D. & Kim, J. Dietary Flavonoid Intake and Smoking-Related Cancer Risk: A Meta-Analysis. *PLoS One* **8**, 1–13 (2013).
  196. Mink, P. J. *et al.* Flavonoid intake and cardiovascular disease mortality: a prospective study in postmenopausal women. *Am. J. Clin. Nutr.* **85**, 895–909 (2007).

197. Cassidy, A. *et al.* Habitual intake of flavonoid subclasses and incident hypertension in adults. *Am. J. Clin. Nutr.* **93**, 338–347 (2011).
198. Cassidy, A. *et al.* Higher dietary anthocyanin and flavonol intakes are associated with anti-inflammatory effects in a population of US adults. *Am. J. Clin. Nutr.* **102**, 172–181 (2015).
199. Ellinger, S., Reusch, A., Stehle, P. & Helfrich, H. P. Epicatechin ingested via cocoa products reduces blood pressure in humans: A nonlinear regression model with a Bayesian approach. *Am. J. Clin. Nutr.* **95**, 1365–1377 (2012).
200. Arts, I. C., Hollman, P. C., Feskens, E. J., Bueno de Mesquita, H. B. & Kromhout, D. Catechin intake might explain the inverse relation between tea consumption and ischemic heart disease: the Zutphen Elderly Study. *Am J Clin Nutr* **74**, 227–32 (2001).
201. Geleijnse, J. M., Launer, L. J., Kuip, D. A. van der, Hofman, A. & Witteman, J. C. Inverse association of tea and flavonoid intakes with incident myocardial infarction: the Rotterdam Study. *Am. J. Clin. Nutr.* **75**, 880–886 (2002).
202. Huxley, R. R. & Neil, H. A. W. W. The relation between dietary flavonol intake and coronary heart disease mortality: A meta-analysis of prospective cohort studies. *Eur. J. Clin. Nutr.* **57**, 904–908 (2003).
203. Sesso, H. D., Gaziano, J. M., Liu, S. & Buring, J. E. Flavonoid intake and the risk of cardiovascular disease in women. *Am. J. Clin. Nutr.* **77**, 1400–8 (2003).
204. Morze, J. *et al.* Chocolate and risk of chronic disease: a systematic review and dose-response meta-analysis. *Eur. J. Nutr.* **59**, 389–397 (2020).
205. Wang, Z. M. *et al.* Flavonols intake and the risk of coronary heart disease: A meta-analysis of cohort studies. *Atherosclerosis* **222**, 270–273 (2012).
206. Vogiatzoglou, A. *et al.* Associations between flavan-3-ol intake and CVD risk in the Norfolk cohort of the European Prospective Investigation into Cancer (EPIC-Norfolk). *Free Radic. Biol. Med.* **84**, 1–10 (2015).
207. Geleijnse, J. M. & Hollman, P. C. Flavonoids and cardiovascular health: Which compounds, what mechanisms? *Am. J. Clin. Nutr.* **88**, 12–13 (2008).
208. Spencer, J. P. E. *et al.* Biomarkers of the intake of dietary polyphenols: strengths, limitations and application in nutrition research. *Br. J. Nutr.* **99**, 12–22 (2008).
209. Morand, C. & Tomás-Barberán, F. A. Contribution of plant food bioactives in promoting health effects of plant foods: why look at interindividual variability? *Eur. J. Nutr.* **58**, 13–19 (2019).
210. Gibney, E. R. *et al.* Factors influencing the cardiometabolic response to (poly)phenols and phytosterols: a review of the COST Action POSITIVE activities. *Eur. J. Nutr.* **58**, (2019).
211. Grassi, D. *et al.* Cocoa consumption dose - dependently improves flow - mediated dilation and arterial stiffness decreasing blood pressure in healthy individuals. *J.*

- Hypertens.* **33**, 294–303 (2015).
212. Hodgson, J. M. *et al.* Effects of black tea on blood pressure: A randomized controlled trial. *Arch. Intern. Med.* **172**, 186–188 (2012).
213. Dower, J. I. *et al.* Effects of the pure flavonoids epicatechin and quercetin on vascular function and cardiometabolic health: A randomized, double-blind, placebo-controlled, crossover trial. *Am. J. Clin. Nutr.* **101**, 914–921 (2015).
214. Cifuentes-Gomez, T., Rodriguez-Mateos, A., Gonzalez-Salvador, I., Alañon, M. E. & Spencer, J. P. E. Factors Affecting the Absorption, Metabolism, and Excretion of Cocoa Flavanols in Humans. *J. Agric. Food Chem.* **63**, 7615–7623 (2015).
215. Martini, D. *et al.* Impact of foods and dietary supplements containing hydroxycinnamic acids on cardiometabolic biomarkers: A systematic review to explore inter-individual variability. *Nutrients* **11**, (2019).
216. Libby, P. Inflammation in atherosclerosis. *Nature* **420**, 868–874 (2002).
217. Libby, P. Inflammation and Atherosclerosis. *Nature* **420**, 868–874 (2002).
218. McLeod, O. *et al.* Plasma autoantibodies against apolipoprotein B-100 peptide 210 in subclinical atherosclerosis. *Atherosclerosis* **232**, 242–248 (2014).
219. McLaren, J. E., Michael, D. R., Ashlin, T. G. & Ramji, D. P. Cytokines, macrophage lipid metabolism and foam cells: Implications for cardiovascular disease therapy. *Prog. Lipid Res.* **50**, 331–347 (2011).
220. Steyers, C. & Miller, F. Endothelial Dysfunction in Chronic Inflammatory Diseases. *Int. J. Mol. Sci.* **15**, 11324–11349 (2014).
221. Winter, C. *et al.* Chrono-pharmacological Targeting of the CCL2-CCR2 Axis Ameliorates Atherosclerosis. *Cell Metab.* **28**, 175-182.e5 (2018).
222. Ramji, D. P. & Davies, T. S. Cytokines in atherosclerosis: Key players in all stages of disease and promising therapeutic targets. *Cytokine Growth Factor Rev.* **26**, 673–685 (2015).
223. Hartman, J. & Frishman, W. H. Inflammation and atherosclerosis: A review of the role of interleukin-6 in the development of atherosclerosis and the potential for targeted drug therapy. *Cardiology in Review* vol. 22 147–151 (2014).
224. Blankenberg, S., Barbaux, S. & Tiret, L. Adhesion molecules and atherosclerosis. *Atherosclerosis* vol. 170 191–203 (2003).
225. Lusis, A. Atherosclerosis. *Nature* **407**, 233–241 (2000).
226. Döring, Y., Drechsler, M., Soehnlein, O. & Weber, C. Neutrophils in atherosclerosis: From mice to man. *Arterioscler. Thromb. Vasc. Biol.* **35**, 288–295 (2015).
227. Bourdillon, M. C. *et al.* ICAM-1 deficiency reduces atherosclerotic lesions in double-knockout mice (ApoE(-/-)/ICAM-1(-/-)) fed a fat or a chow diet. *Arterioscler. Thromb. Vasc. Biol.* **20**, 2630–5 (2000).
228. Richard, S. *et al.* E-selectin and vascular cell adhesion molecule-1 as biomarkers



- of 3-month outcome in cerebrovascular diseases. *J. Inflamm.* **12**, 61 (2015).
229. Vasani, R. S. Biomarkers of Cardiovascular Disease. *Circulation* **113**, 2335 LP – 2362 (2006).
230. Kim, H. J., Lee, W. & Yun, J. M. Luteolin Inhibits hyperglycemia-induced proinflammatory cytokine production and its epigenetic mechanism in human monocytes. *Phyther. Res.* **28**, 1383–1391 (2014).
231. Zhang, X., Wang, G., Gurley, E. C. E. C. & Zhou, H. Flavonoid Apigenin Inhibits Lipopolysaccharide-Induced Inflammatory Response through Multiple Mechanisms in Macrophages. *PLoS One* **9**, e107072 (2014).
232. Lee, W., Ku, S. K. & Bae, J. S. Vascular barrier protective effects of orientin and isoorientin in LPS-induced inflammation in vitro and in vivo. *Vascul. Pharmacol.* **62**, 3–14 (2014).
233. Wang, D., Wei, X., Yan, X., Jin, T. & Ling, W. Protocatechuic acid, a metabolite of anthocyanins, inhibits monocyte adhesion and reduces atherosclerosis in apolipoprotein E-deficient mice. *J. Agric. Food Chem.* **58**, 12722–12728 (2010).
234. Lee, K. S. *et al.* Matrix metalloproteinase inhibitor regulates inflammatory cell migration by reducing ICAM-1 and VCAM-1 expression in a murine model of toluene diisocyanate-induced asthma. *J ALLERGY CLIN IMMUNOL* **11**, 1278–1284 (2003).
235. Larsson, S. C., Virtamo, J. & Wolk, A. Chocolate consumption and risk of stroke a prospective cohort of men and meta-analysis. *Neurology* **79**, 1223–1229 (2012).
236. Dong, J. Y., Iso, H., Yamagishi, K., Sawada, N. & Tsugane, S. Chocolate consumption and risk of stroke among men and women: A large population-based, prospective cohort study. *Atherosclerosis* **260**, 8–12 (2017).
237. Gao, X., Cassidy, A., Schwarzschild, M. A., Rimm, E. B. & Ascherio, A. Habitual intake of dietary flavonoids and risk of Parkinson disease. *Neurology* **78**, 1138–1145 (2012).
238. Bowtell, J. L., Aboo-Bakkar, Z., Conway, M. E., Adlam, A. L. R. & Fulford, J. Enhanced task-related brain activation and resting perfusion in healthy older adults after chronic blueberry supplementation. *Appl. Physiol. Nutr. Metab.* **42**, 773–779 (2017).
239. Makkar, R. *et al.* Nutraceuticals in neurological disorders. *Int. J. Mol. Sci.* **21**, 1–19 (2020).
240. DiSabato, D. J., Quan, N. & Godbout, J. P. Neuroinflammation: the devil is in the details. *J. Neurochem.* **139**, 136–153 (2016).
241. Deczkowska, A., Amit, I. & Schwartz, M. Microglial immune checkpoint mechanisms. *Nat. Neurosci.* **21**, 779–786 (2018).
242. Hirsch, E. C., Vyas, S. & Hunot, S. Neuroinflammation in Parkinson's disease. *Park. Relat. Disord.* **18**, (2012).

243. Leng, F. & Edison, P. Neuroinflammation and microglial activation in Alzheimer disease: where do we go from here? *Nat. Rev. Neurol.* (2020)  
doi:10.1038/s41582-020-00435-y.
244. Jung, Y. J., Tweedie, D., Scerba, M. T. & Greig, N. H. Neuroinflammation as a Factor of Neurodegenerative Disease: Thalidomide Analogs as Treatments. *Front. Cell Dev. Biol.* **7**, 313 (2019).
245. Subramaniam, S. R. & Federoff, H. J. Targeting Microglial Activation States as a Therapeutic Avenue in Parkinson's Disease. *Front. Aging Neurosci.* **9**, 176 (2017).
246. Jayaraj, R. L., Azimullah, S., Beiram, R., Jalal, F. Y. & Rosenberg, G. A. Neuroinflammation: Friend and foe for ischemic stroke. *Journal of Neuroinflammation* vol. 16 (2019).
247. Schulz, C. *et al.* A lineage of myeloid cells independent of myb and hematopoietic stem cells. *Science* (80-. ). **335**, 86–90 (2012).
248. Alliot, F., Godin, I. & Pessac, B. Microglia derive from progenitors, originating from the yolk sac, and which proliferate in the brain. *Dev. Brain Res.* **117**, 145–152 (1999).
249. Huang, Y. *et al.* Repopulated microglia are solely derived from the proliferation of residual microglia after acute depletion. *Nat. Neurosci.* **21**, 530–540 (2018).
250. Heneka, M. T. Microglia take centre stage in neurodegenerative disease. *Nat. Rev. Immunol.* **19**, 79–80 (2019).
251. Blaser, H., Dostert, C., Mak, T. W. & Brenner, D. TNF and ROS Crosstalk in Inflammation. *Trends in Cell Biology* vol. 26 249–261 (2016).
252. Pereira, S. G. & Oakley, F. Nuclear factor- $\kappa$ B1: Regulation and function. *Int. J. Biochem. Cell Biol.* **40**, 1425–1430 (2008).
253. Moelants, E. A., Mortier, A., Van Damme, J. & Proost, P. Regulation of TNF- $\alpha$  with a focus on rheumatoid arthritis. *Immunol. Cell Biol.* **91**, 393–401 (2013).
254. Baumgart, D. C. & Carding, S. R. Inflammatory bowel disease: cause and immunobiology. *Lancet* **369**, 1627–1640 (2007).
255. Scicchitano, P. *et al.* The role of endothelial dysfunction and oxidative stress in cerebrovascular diseases. *Free Radic. Res.* **53**, 579–595 (2019).
256. Lawrence, T. The nuclear factor NF- $\kappa$ B pathway in inflammation. *Cold Spring Harb. Perspect. Biol.* **1**, (2009).
257. Jost, P. J. & Ruland, J. Aberrant NF- $\kappa$ B signaling in lymphoma: mechanisms, consequences, and therapeutic implications. *Blood* **109**, 2700–2707 (2007).
258. Hayden, M. S. A less-canonical, canonical NF- $\kappa$ B pathway in DCs. *Nat. Immunol.* **13**, 1139 (2012).
259. Dong, Y., Dekens, D., De Deyn, P., Naudé, P. & Eisel, U. Targeting of Tumor Necrosis Factor Alpha Receptors as a Therapeutic Strategy for Neurodegenerative Disorders. *Antibodies* **4**, 369–408 (2015).

260. Wu, C.-H., Wu, C.-F., Huang, H.-W., Jao, Y.-C. & Yen, G.-C. Naturally occurring flavonoids attenuate high glucose-induced expression of proinflammatory cytokines in human monocytic THP-1 cells. *Mol. Nutr. Food Res.* **53**, 984–995 (2009).
261. Chang, Y.-C., Tsai, M.-H., Sheu, W. H.-H., Hsieh, S.-C. & Chiang, A.-N. The Therapeutic Potential and Mechanisms of Action of Quercetin in Relation to Lipopolysaccharide-Induced Sepsis In Vitro and In Vivo. *PLoS One* **8**, e80744 (2013).
262. Min, S.-W., Ryu, S.-N. & Kim, D.-H. Anti-inflammatory effects of black rice, cyanidin-3-O- $\beta$ -D-glycoside, and its metabolites, cyanidin and protocatechuic acid  
Keyword: Black rice Cyanidin-3-O- $\beta$ -D-glycoside Cyanidin Protocatechuic acid  
Anti-inflammation Metabolism. *Int. Immunopharmacol.* **10**, 959–966 (2010).
263. Kim, M.-C. *et al.* Vanillic acid inhibits inflammatory mediators by suppressing NF- $\kappa$ B in lipopolysaccharide-stimulated mouse peritoneal macrophages. *Immunopharmacol. Immunotoxicol.* **33**, 525–532 (2011).
264. Song, Y. *et al.* Ferulic Acid against Cyclophosphamide-Induced Heart Toxicity in Mice by Inhibiting NF- $\kappa$ B Pathway. *Evidence-Based Complement. Altern. Med.* **2016**, 1–8 (2016).
265. Liu, Y.-M. *et al.* Ferulic acid inhibits neuro-inflammation in mice exposed to chronic unpredictable mild stress. *Int. Immunopharmacol.* **45**, 128–134 (2017).
266. Wang, Y. *et al.* Cyanidin-3-glucoside and its phenolic acid metabolites attenuate visible light-induced retinal degeneration in vivo via activation of Nrf2/HO-1 pathway and NF- $\kappa$ B suppression. *Mol. Nutr. Food Res.* **60**, 1564–1577 (2016).
267. Zhao, J. *et al.* Ferulic acid enhances nitric oxide production through up-regulation of argininosuccinate synthase in inflammatory human endothelial cells. *Life Sci.* **145**, 224–232 (2016).
268. Shin, H. S., Satsu, H., Bae, M.-J., Totsuka, M. & Shimizu, M. Catechol Groups Enable Reactive Oxygen Species Scavenging-Mediated Suppression of PKD-NF $\kappa$ B-IL-8 Signaling Pathway by Chlorogenic and Caffeic Acids in Human Intestinal Cells. *Nutrients* **9**, 165 (2017).
269. Speciale, A. *et al.* Cyanidin-3-O-glucoside counters the response to TNF- $\alpha$  of endothelial cells by activating Nrf2 pathway. *Mol. Nutr. Food Res* **00**, 1–9 (2013).
270. Popa, C., Netea, M. G., van Riel, P. L. C. M., van der Meer, J. W. M. & Stalenhoef, A. F. H. The role of TNF- $\alpha$  in chronic inflammatory conditions, intermediary metabolism, and cardiovascular risk. *J. Lipid Res.* **48**, 751–762 (2007).
271. Bradley, J. R. TNF-mediated inflammatory disease. *J. Pathol.* **214**, 149–160 (2008).
272. Katharina Urschel, I. C. TNF- $\alpha$  in the cardiovascular system: from physiology to

- therapy. *Intern. J Interf. Cytokine Med Res* **Volume 7**, 9–25 (2015).
273. Steeland, S., Libert, C. & Vandembroucke, R. E. A new venue of TNF targeting. *Int. J. Mol. Sci.* **19**, 1442 (2018).
  274. Vulliamoz, M. *et al.* TNF-Alpha Blockers in Inflammatory Bowel Diseases: Practical Recommendations and a User's Guide: An Update. *Digestion* **101**, 16–26 (2020).
  275. Chen, C. & Khismatullin, D. B. Oxidized Low-Density Lipoprotein Contributes to Atherogenesis via Co-activation of Macrophages and Mast Cells. (2015) doi:10.1371/journal.pone.0123088.
  276. Croft, M., Benedict, C. A. & Ware, C. F. Clinical targeting of the TNF and TNFR superfamilies. *Nat. Rev. Drug Discov.* **12**, 147–168 (2013).
  277. Abel, A. M., Yang, C., Thakar, M. S. & Malarkannan, S. Natural killer cells: Development, maturation, and clinical utilization. *Front. Immunol.* **9**, 1 (2018).
  278. Moreira-Tabaka, H. *et al.* Unlike for human monocytes after lps activation, release of TNF- $\alpha$  by THP-1 cells is produced by a TACE catalytically different from constitutive TACE. *PLoS One* **7**, e34184 (2012).
  279. Aslam, N. & Zaheer, I. The biosynthesis characteristics of TTP and TNF can be regulated through a posttranscriptional molecular loop. *J. Biol. Chem.* **286**, 3767–3776 (2011).
  280. Daniel, C., Gerlach, K., V  th, M., Neurath, M. F. & Weigmann, B. Nuclear factor of activated T cells-A transcription factor family as critical regulator in lung and colon cancer. *Int. J. Cancer* **134**, 1767–1775 (2014).
  281. Fan, J., Heller, N. M., Gorospe, M., Atasoy, U. & Stellato, C. The role of post-transcriptional regulation in chemokine gene expression in inflammation and allergy. *Eur. Respir. J.* **26**, 933–947 (2005).
  282. Anderson, P. Post-transcriptional control of cytokine production. *Nature Immunology* vol. 9 353–359 (2008).
  283. Giambelluca, M., Rollet-Labelle, E., Bertheau-Mailhot, G., Laflamme, C. & Pouliot, M. Post-transcriptional regulation of tumour necrosis factor alpha biosynthesis: Relevance to the pathophysiology of rheumatoid arthritis. *OA Inflamm.* **1**, (2013).
  284. Carpenter, S., Ricci, E. P., Mercier, B. C., Moore, M. J. & Fitzgerald, K. A. Post-transcriptional regulation of gene expression in innate immunity. *Nat. Rev. Immunol.* **14**, 361–376 (2014).
  285. Kontoyiannis, D., Pasparakis, M., Pizarro, T. T., Cominelli, F. & Kollias, G. Impaired On/Off Regulation of TNF Biosynthesis in Mice Lacking TNF AU-Rich Elements. *Immunity* **10**, 387–398 (1999).
  286. Tili, E. *et al.* Modulation of miR-155 and miR-125b Levels following Lipopolysaccharide/TNF- $\alpha$  Stimulation and Their Possible Roles in Regulating the Response to Endotoxin Shock. *J. Immunol.* **179**, 5082–5089 (2007).

287. Gomez, I. *et al.* Neutrophil microvesicles drive atherosclerosis by delivering miR-155 to atheroprone endothelium. *Nat. Commun.* **11**, 214 (2020).
288. Palau, V., Pascual, J., Soler, M. J. & Riera, M. Role of ADAM17 in kidney disease. *Am. J. Physiol. - Ren. Physiol.* **317**, F333–F342 (2019).
289. Xu, J. *et al.* A disintegrin and metalloprotease 17 in the cardiovascular and central nervous systems. *Frontiers in Physiology* vol. 7 469 (2016).
290. Zhang, H. Y., Wang, J. Y. & Yao, H. P. Epigallocatechin-3-gallate attenuates lipopolysaccharide- induced inflammation in human retinal endothelial cells. *Int. J. Ophthalmol.* **7**, 408 (2014).
291. Ku, S. K., Lee, I. C., Han, M. S. & Bae, J. S. Inhibitory Effects of Rutin on the Endothelial Protein C Receptor Shedding In Vitro and In Vivo. *Inflammation* **37**, 1424–1431 (2014).
292. Hehlgans, T. & Pfeffer, K. The intriguing biology of the tumour necrosis factor/tumour necrosis factor receptor superfamily: Players, rules and the games. *Immunology* **115**, 1–20 (2005).
293. Naudé, P. J. W., den Boer, J. A., Luiten, P. G. M. & Eisel, U. L. M. Tumor necrosis factor receptor cross-talk. *FEBS J.* **278**, 888–898 (2011).
294. Cabal-Hierro, L. & Lazo, P. S. Signal transduction by tumor necrosis factor receptors. *Cellular Signalling* vol. 24 1297–1305 (2012).
295. Borghi, A., Verstrepen, L. & Beyaert, R. TRAF2 multitasking in TNF receptor-induced signaling to NF- $\kappa$ B, MAP kinases and cell death. *Biochem. Pharmacol.* **116**, 1–10 (2016).
296. Dempsey, P. W., Doyle, S. E., He, J. Q. & Cheng, G. The signaling adaptors and pathways activated by TNF superfamily. *Cytokine Growth Factor Rev.* **14**, 193–209 (2003).
297. Dinarello, C. A. Immunological and Inflammatory Functions of the Interleukin-1 Family. *Annu. Rev. Immunol.* **27**, 519–550 (2009).
298. Razaghi, A., Owens, L. & Heimann, K. Review of the recombinant human interferon gamma as an immunotherapeutic: Impacts of production platforms and glycosylation. *Journal of Biotechnology* vol. 240 48–60 (2016).
299. Kunes, P., Mandak, J., Holubcova, Z., Kolackova, M. & Krejsek, J. Actual position of interleukin(IL)-33 in atherosclerosis and heart failure: Great Expectations or En attendant Godot? *Perfusion* **30**, 356–374 (2015).
300. Miossec, P. & Kolls, J. K. Targeting IL-17 and TH17 cells in chronic inflammation. *Nat. Rev. Drug Discov.* **11**, 763–776 (2012).
301. Akira, S., Uematsu, S. & Takeuchi, O. Pathogen recognition and innate immunity. *Cell* vol. 124 783–801 (2006).
302. Mortellaro, A., Diamond, C., Khameneh, H. J. & Brough, D. Novel perspectives on non-canonical inflammasome activation. *ImmunoTargets Ther.* **4**, 131 (2015).

303. Schumann, R. *et al.* Structure and function of lipopolysaccharide binding protein. *Science (80-. )*. **249**, 1429–1432 (1990).
304. Wan, Y. *et al.* Role of lipopolysaccharide (LPS), interleukin-1, interleukin-6, tumor necrosis factor, and dexamethasone in regulation of LPS-binding protein expression in normal hepatocytes and hepatocytes from LPS-treated rats. *Infect. Immun.* **63**, 2435–42 (1995).
305. O'Neill, L. A. J., Bryant, C. E. & Doyle, S. L. Therapeutic Targeting of Toll-Like Receptors for Infectious and Inflammatory Diseases and Cancer. *Pharmacol. Rev.* **61**, 177–197 (2009).
306. Peri, F., Piazza, M., Calabrese, V., Damore, G. & Cighetti, R. Exploring the LPS/TLR4 signal pathway with small molecules. *Biochemical Society Transactions* vol. 38 1390–1395 (2010).
307. Matsunaga, N., Tsuchimori, N., Matsumoto, T. & Ii, M. TAK-242 (resatorvid), a small-molecule inhibitor of Toll-like receptor (TLR) 4 signaling, binds selectively to TLR4 and interferes with interactions between TLR4 and its adaptor molecules. *Mol. Pharmacol.* **79**, 34–41 (2010).
308. Liu, C. *et al.* The flavonoid cyanidin blocks binding of the cytokine interleukin-17A to the IL-17RA subunit to alleviate inflammation in vivo. *Sci. Signal.* **10**, (2017).
309. Kamimura, D., Ishihara, K. & Hirano, T. IL-6 signal transduction and its physiological roles: the signal orchestration model. *Reviews of physiology, biochemistry and pharmacology* vol. 149 1–38 (2003).
310. Erta, M., Quintana, A. & Hidalgo, J. Interleukin-6, a Major Cytokine in the Central Nervous System. *Int. J. Biol. Sci* **8**, 1254–1266 (2012).
311. Reiss, A. B., Siegart, N. M. & De Leon, J. Interleukin-6 in atherosclerosis: atherogenic or atheroprotective? *Clin. Lipidol.* **12**, 14–23 (2017).
312. McGregor, N. E. *et al.* IL-6 exhibits both cis- And trans-signaling in osteocytes and osteoblasts, but only trans-signaling promotes bone formation and osteoclastogenesis. *J. Biol. Chem.* **294**, 7850–7863 (2019).
313. Waldner, M. J. & Neurath, M. F. Master regulator of intestinal disease: IL-6 in chronic inflammation and cancer development. *Seminars in Immunology* vol. 26 75–79 (2014).
314. Kishimoto, T. Interleukin-6: From basic science to medicine - 40 Years in immunology. *Annual Review of Immunology* vol. 23 1–21 (2005).
315. Su, H., Lei, C.-T. T. & Zhang, C. Interleukin-6 signaling pathway and its role in kidney disease: An update. *Front. Immunol.* **8**, 1–10 (2017).
316. Sikorski, K., Czerwoniec, A., Bujnicki, J. M., Wesoly, J. & Bluysen, H. A. R. STAT1 as a novel therapeutic target in pro-atherogenic signal integration of IFN $\gamma$ , TLR4 and IL-6 in vascular disease. *Cytokine Growth Factor Rev.* **22**, 211–219 (2011).

317. Minogue, A. M., Barrett, J. P. & Lynch, M. A. LPS-induced release of IL-6 from glia modulates production of IL-1 $\beta$  in a JAK2-dependent manner. *J. Neuroinflammation* **9**, 629 (2012).
318. Rothaug, M., Becker-Pauly, C. & Rose-John, S. The role of interleukin-6 signaling in nervous tissue. *Biochim. Biophys. Acta - Mol. Cell Res.* **1863**, 1218–1227 (2016).
319. Hirano, T. *et al.* Purification to homogeneity and characterization of human B-cell differentiation factor (BCDF or BSFp-2) (Ig production). *Immunology* vol. 82 (1985).
320. Snick, J. Van. INTERLEUKIN-6: AN OVERVIEW. *Annu. Rev. Immunol* **8**, 253–78 (1990).
321. Rego, D. *et al.* IL-6 Production Is Positively Regulated by Two Distinct Src Homology Domain 2-Containing Tyrosine Phosphatase-1 (SHP-1)–Dependent CCAAT/Enhancer-Binding Protein  $\beta$  and NF- $\kappa$ B Pathways and an SHP-1–Independent NF- $\kappa$ B Pathway in Lipopolysaccharide-Stimulated . *J. Immunol.* **186**, 5443–5456 (2011).
322. Schmidt-Arras, D. & Rose-John, S. IL-6 pathway in the liver: From physiopathology to therapy. *J. Hepatol.* **64**, 1403–1415 (2016).
323. Hsu, M.-P., Frausto, R., Rose-John, S. & Campbell, I. L. Analysis of IL-6/gp130 family receptor expression reveals that in contrast to astroglia, microglia lack the oncostatin M receptor and functional responses to oncostatin M. *Glia* **63**, 132–141 (2015).
324. Sawada, M., Itoh, Y., Suzumura, A. & Marunouchi, T. Expression of cytokine receptors in cultured neuronal and glial cells. *Neurosci. Lett.* **160**, 131–134 (1993).
325. Kang, S. *et al.* IL-6 trans-signaling induces plasminogen activator inhibitor-1 from vascular endothelial cells in cytokine release syndrome. *Proc. Natl. Acad. Sci. U. S. A.* **117**, 22351–22356 (2020).
326. Horiuchi, S. *et al.* Soluble interleukin-6 receptors released from T cell or granulocyte/macrophage cell lines and human peripheral blood mononuclear cells are generated through an alternative splicing mechanism. *Eur. J. Immunol.* **24**, 1945–1948 (1994).
327. Schaper, F. & Rose-John, S. Interleukin-6: Biology, signaling and strategies of blockade. *Cytokine Growth Factor Rev.* **26**, 475–487 (2015).
328. Chalaris, A., Garbers, C., Rabe, B., Rose-John, S. & Scheller, J. The soluble Interleukin 6 receptor: Generation and role in inflammation and cancer. *Eur. J. Cell Biol.* **90**, 484–494 (2011).
329. Luo, Y. & Zheng, S. G. Hall of fame among pro-inflammatory cytokines: Interleukin-6 gene and its transcriptional regulation mechanisms. *Frontiers in Immunology* vol. 7 604 (2016).

330. Van Dam, H. & Castellazzi, M. Distinct roles of Jun:Fos and Jun:ATF dimers in oncogenesis. *Oncogene* vol. 20 2453–2464 (2001).
331. Akira, S. *et al.* A nuclear factor for IL-6 expression (NF-IL6) is a member of a C/EBP family. *EMBO J.* **9**, 1897–1906 (1990).
332. Yi, L. *et al.* Structural requirements of anthocyanins in relation to inhibition of endothelial injury induced by oxidized low-density lipoprotein and correlation with radical scavenging activity. *FEBS Lett.* **584**, 583–590 (2010).
333. Xia, M. *et al.* Anthocyanin prevents CD40-activated proinflammatory signaling in endothelial cells by regulating cholesterol distribution. *Arterioscler. Thromb. Vasc. Biol.* **27**, 519–524 (2007).
334. Ferrars, R. M. de. The Metabolic Fate and Bioactivity of Anthocyanins in Humans. *Thesis* (University of East Anglia, 2014).
335. Wang, Y., Zhou, J., Fu, S., Wang, C. & Zhou, B. Preventive Effects of Protocatechuic Acid on LPS-Induced Inflammatory Response in Human Gingival Fibroblasts via Activating PPAR- $\alpha$ . *Inflammation* **38**, 1080–1084 (2015).
336. Kwon, M. Y. *et al.* A caffeic acid-ferulic acid hybrid compound attenuates lipopolysaccharide-mediated inflammation in BV2 and RAW264.7 cells. *Biochem. Biophys. Res. Commun.* **515**, 565–571 (2019).
337. Deshmane, S. L., Kremlev, S., Amini, S. & Sawaya, B. E. Monocyte chemoattractant protein-1 (MCP-1): An overview. *J. Interf. Cytokine Res.* **29**, 313–326 (2009).
338. Gerszten, R. E. *et al.* MCP-1 and IL-8 trigger firm adhesion of monocytes to vascular endothelium under flow conditions. *Nature* **398**, 718–725 (1999).
339. Neiken, N. A., Coughlin, S. R., Gordon, D. & Wilcox, J. N. Monocyte chemoattractant protein-1 in human atheromatous plaques. *J. Clin. Invest.* **88**, 1121–1127 (1991).
340. Schechter, A. D. *et al.* MCP-1-dependent signaling in CCR2 $^{-/-}$  aortic smooth muscle cells. *J. Leukoc. Biol.* **75**, 1079–1085 (2004).
341. Boring, L., Gosling, J., Cleary, M. & Charo, I. F. Decreased lesion formation in CCR2 $^{-/-}$  mice reveals a role for chemokines in the initiation of atherosclerosis. *Nature* **394**, 894–897 (1998).
342. Yoshimura, T. The chemokine MCP-1 (CCL2) in the host interaction with cancer: A foe or ally? *Cell. Mol. Immunol.* **15**, 335–345 (2018).
343. Gschwandtner, M., Derler, R. & Midwood, K. S. More Than Just Attractive: How CCL2 Influences Myeloid Cell Behavior Beyond Chemotaxis. *Frontiers in Immunology* vol. 10 2759 (2019).
344. Osaka, M. *et al.* Critical role of the C5a-activated neutrophils in high-fat diet-induced vascular inflammation. *Sci. Rep.* **6**, 21391 (2016).
345. Chen, I.-Y. *et al.* Upregulation of the Chemokine (C-C Motif) Ligand 2 via a



Severe Acute Respiratory Syndrome Coronavirus Spike-ACE2 Signaling Pathway. *J. Virol.* **84**, 7703–7712 (2010).

346. Tang, Y. *et al.* Enhancement of lens extraction-induced MCP-1 upregulation and microglia response in long-term diabetes via c-jun, stat1 and ERK. *Life Sci.* **261**, 118360 (2020).
347. WERLE, M., SCHMAL, U., HANNA, K. & KREUZER, J. MCP-1 induces activation of MAP-kinases ERK, JNK and p38 MAPK in human endothelial cells. *Cardiovasc. Res.* **56**, 284–292 (2002).
348. Ueda, A. *et al.* NF-kappa B and Sp1 regulate transcription of the human monocyte chemoattractant protein-1 gene. *Am. J. Immunol.* **153**, 2052–63 (1994).
349. Ueda, A., Ishigatsubo, Y., Okubo, T. & Yoshimura, T. Transcriptional Regulation of The Human Monocyte Chemoattractant Protein-1 Gene. *J. Biol. Chem.* **272**, 31092–31099 (1997).
350. Ping, D., Jones, P. L. & Boss, J. M. TNF regulates the in vivo occupancy of both distal and proximal regulatory regions of the MCP-1/JE gene. *Immunity* **4**, (1996).
351. Zhang, L. *et al.* Chemokine signaling pathway involved in CCL2 expression in patients with rheumatoid arthritis. *Yonsei Med. J.* **56**, 1134–1142 (2015).
352. Bennett, B. L. c-Jun N-terminal kinase-dependent mechanisms in respiratory disease. *Eur. Respir. J.* **28**, 651–661 (2006).
353. Burysek, L., Syrovets, T. & Simmet, T. The serine protease plasmin triggers expression of MCP-1 and CD40 in human primary monocytes via activation of p38 MAPK and Janus kinase (JAK)/STAT signaling pathways. *J. Biol. Chem.* **277**, 33509–33517 (2002).
354. Maghazachi, A. A., al-Aoukaty, A. & Schall, T. J. C-C chemokines induce the chemotaxis of NK and IL-2-activated NK cells. Role for G proteins. *J. Immunol.* **153**, (1994).
355. Carr, M. W., Roth, S. J., Luther, E., Rose, S. S. & Springer, T. A. Monocyte chemoattractant protein 1 acts as a T-lymphocyte chemoattractant. *Proc. Natl. Acad. Sci. U. S. A.* **91**, 3652–3656 (1994).
356. Janjanam, J., Kumar Chandaka, G., Kotla, S. & Rao, G. N. PLC $\beta$ 3 mediates cortactin interaction with WAVE2 in MCP1-induced actin polymerization and cell migration. *Mol. Biol. Cell* **26**, 4589–4606 (2015).
357. Sozzani, S. *et al.* Receptor-activated calcium influx in human monocytes exposed to monocyte chemotactic protein-1 and related cytokines. *J. Immunol.* **150**, 1544–15453 (1993).
358. Myers, S. J., Lu Min Wong & Charo, I. F. Signal transduction and ligand specificity of the human monocyte chemoattractant protein-1 receptor in transfected embryonic kidney cells. *J. Biol. Chem.* **270**, 5786–5792 (1995).
359. Kuang, Y., Wu, Y., Jiang, H. & Wu, D. Selective G protein coupling by C-C

- chemokine receptors. *J. Biol. Chem.* **271**, 3975–3978 (1996).
360. Dubois, P. M., Palmer, D., Webb, M. L., Ledbetter, J. A. & Shapiro, R. A. Early signal transduction by the receptor to the chemokine monocyte chemoattractant protein-1 in a murine T cell hybrid. *J. Immunol.* **156**, (1996).
361. Cambien, B., Pomeranz, M., Millet, M. A., Rossi, B. & Schmid-Alliana, A. Signal transduction involved in MCP-1-mediated monocytic transendothelial migration. *Blood* **97**, 359–366 (2001).
362. Turner, S. J., Domin, J., Waterfield, M. D., Ward, S. G. & Westwick, J. The CC chemokine monocyte chemoattractant peptide-1 activates both the class I p85/p110 phosphatidylinositol 3-kinase and the class II PI3K-C2 $\alpha$ . *J. Biol. Chem.* **273**, 25987–25995 (1998).
363. Mellado, M. *et al.* The chemokine monocyte chemoattractant protein 1 triggers Janus kinase 2 activation and tyrosine phosphorylation of the CCR2B receptor. *J. Immunol.* **161**, (1998).
364. Mukai, Y., Iwaya, K., Ogawa, H. & Mukai, K. Involvement of Arp2/3 complex in MCP-1-induced chemotaxis. *Biochem. Biophys. Res. Commun.* **334**, 395–402 (2005).
365. Mishra, R. S., Carnevale, K. A. & Cathcart, M. K. iPLA2 $\beta$ : Front and center in human monocyte chemotaxis to MCP-1. *J. Exp. Med.* **205**, 347–359 (2008).
366. Ahn, H. Y., Xu, Y. & Davidge, S. T. Epigallocatechin-3-O-gallate inhibits TNF $\alpha$ -induced monocyte chemoattractant protein-1 production from vascular endothelial cells. *Life Sci.* **82**, 964–968 (2008).
367. Duan, H. *et al.* Anthocyanins inhibit high-glucose-induced cholesterol accumulation and inflammation by activating LXRA pathway in HK-2 cells. *Drug Des. Devel. Ther.* **9**, 5099–5113 (2015).
368. Kowalski, J., Samojedny, A., Paul, M. & Pietsz, G. Apigenin inhibit release and gene expression of monocyte chemoattractant protein 1 (MCP-1) in J774.2 macrophages. *Wiad. Lek.* **59**, (2006).
369. Winterbone, M. S., Tribolo, S., Needs, P. W., Kroon, P. A. & Hughes, D. A. Physiologically relevant metabolites of quercetin have no effect on adhesion molecule or chemokine expression in human vascular smooth muscle cells. *Atherosclerosis* **202**, 431–438 (2009).
370. Sies, H. Oxidative stress: A concept in redox biology and medicine. *Redox Biol.* **4**, 180–183 (2015).
371. Gorrini, C., Harris, I. S. & Mak, T. W. Modulation of oxidative stress as an anticancer strategy. *Nature Reviews Drug Discovery* vol. 12 931–947 (2013).
372. Sporn, M. B. & Liby, K. T. NRF2 and cancer: The Good, the bad and the importance of context. *Nature Reviews Cancer* vol. 12 (2012).
373. Taguchi, K., Motohashi, H. & Yamamoto, M. Molecular mechanisms of the Keap1-

- Nrf2 pathway in stress response and cancer evolution. *Genes to Cells* vol. 16 123–140 (2011).
374. Tonelli, C., Chio, I. I. C. & Tuveson, D. A. Transcriptional Regulation by Nrf2. *Antioxidants Redox Signal.* **29**, 1727–1745 (2018).
375. Kimura, A. *et al.* NQO1 inhibits the TLR-dependent production of selective cytokines by promoting I $\kappa$ B- $\zeta$  degradation. *J. Exp. Med.* **215**, 2197–2209 (2018).
376. Araujo, J. A., Zhang, M., Yin, F. & Maines, M. D. Heme oxygenase-1, oxidation, inflammation, and atherosclerosis. *Front. Pharmacol.* **3 JUL**, 1–17 (2012).
377. Kasai, S., Shimizu, S., Tatara, Y., Mimura, J. & Itoh, K. Regulation of Nrf2 by mitochondrial reactive oxygen species in physiology and pathology. *Biomolecules* **10**, (2020).
378. Zucker, S. N. *et al.* Nrf2 amplifies oxidative stress via induction of Klf9. *Mol. Cell* **53**, 916–928 (2014).
379. Liu, S. *et al.* Heme oxygenase-1 mediates the protective role of quercetin against ethanol-induced rat hepatocytes oxidative damage Heme oxygenase-1 Quercetin Ethanol Oxidative damage Nuclear factor erythroid 2 related factor 2 Extracellular signal-regulated kinase. *Toxicol. Vitro.* **26**, 74–80 (2012).
380. Granado-Serrano, A. B., Martin, M. A., Bravo, L., Goya, L. & Ramos, S. Quercetin modulates Nrf2 and glutathione-related defenses in HepG2 cells: Involvement of p38. *Chem. Biol. Interact.* **195**, 154–164 (2012).
381. Li, C., Zhang, W.-J. & Frei, B. Quercetin inhibits LPS-induced adhesion molecule expression and oxidant production in human aortic endothelial cells by p38-mediated Nrf2 activation and antioxidant enzyme induction. *Redox Biol.* **9**, 104–113 (2016).
382. Sun, G. S. *et al.* Quercetin Attenuates Inflammatory Responses in BV-2 Microglial Cells: Role of MAPKs on the Nrf2 Pathway and Induction of Heme Oxygenase-1. *PLoS One* **10**, 272–279 (2015).
383. Lou, H. *et al.* Naringenin protects against 6-OHDA-induced neurotoxicity via activation of the Nrf2/ARE signaling pathway. *Neuropharmacology* **79**, 380–388 (2014).
384. Chen, M. *et al.* Protective effects of hesperidin against oxidative stress of tert-butyl hydroperoxide in human hepatocytes. *Food Chem. Toxicol.* **48**, 2980–2987 (2010).
385. Xin, X., Li, Y. & Liu, H. Hesperidin ameliorates hypobaric hypoxia-induced retinal impairment through activation of Nrf2/HO-1 pathway and inhibition of apoptosis. *Sci. Rep.* **10**, (2020).
386. Wu, C. *et al.* Upregulation of heme oxygenase-1 by Epigallocatechin-3-gallate via the phosphatidylinositol 3-kinase/Akt and ERK pathways. *Life Sci.* **78**, 2889–2897 (2006).

387. Ogborne, R. M., Rushworth, S. A. & O'Connell, M. A. *Epigallocatechin activates haem oxygenase-1 expression via protein kinase C $\delta$  and Nrf2*. *Biochemical and Biophysical Research Communications* vol. 373  
<http://www.sciencedirect.com/science/article/pii/S0006291X08012448> (2008).
388. Granado-Serrano, A. *et al.* Epicatechin induces NF- $\kappa$ B, activator protein-1 (AP-1) and nuclear transcription factor erythroid 2p45-related factor-2 (Nrf2) via phosphatidylinositol-3-kinase/protein kinase B (PI3K/AKT) and extracellular regulated kinase (ERK) signalling in HepG2 cells. *Br. J. Nutr.* **103**, 168–179 (2010).
389. Vari, R. *et al.* Protocatechuic acid induces antioxidant/detoxifying enzyme expression through JNK-mediated Nrf2 activation in murine macrophages. *J. Nutr. Biochem.* **22**, 409–417 (2011).
390. Vari, R. *et al.* Protocatechuic Acid Prevents oxLDL-Induced Apoptosis by Activating JNK/Nrf2 Survival Signals in Macrophages. *Oxid. Med. Cell. Longev.* **2015**, 351827 (2015).
391. Krajka-Kuźniak, V., Paluszczak, J. J., Szaefer, H. & Baer-Dubowska, W. The activation of the Nrf2/ARE pathway in HepG2 hepatoma cells by phytochemicals and subsequent modulation of phase II and antioxidant enzyme expression. *J. Physiol. Biochem.* **71**, 227–238 (2015).
392. Zakkar, M. *et al.* Activation of Nrf2 in endothelial cells protects arteries from exhibiting a proinflammatory state. *Arterioscler. Thromb. Vasc. Biol.* **29**, 1851–1857 (2009).
393. Dai, Y., Zhang, H., Zhang, J. & Yan, M. Isoquercetin attenuates oxidative stress and neuronal apoptosis after ischemia/reperfusion injury via Nrf2-mediated inhibition of the NOX4/ROS/NF- $\kappa$ B pathway. *Chem. Biol. Interact.* **284**, 32–40 (2018).
394. Rushworth, S. A., Ogborne, R. M., Charalambos, C. A. & O'Connell, M. A. Role of protein kinase C  $\delta$  in curcumin-induced antioxidant response element-mediated gene expression in human monocytes. *Biochem. Biophys. Res. Commun.* **341**, 1007–1016 (2006).
395. Mccoubrey, W. K., Huang, T. J. & Maines, M. D. Isolation and characterization of a cDNA from the rat brain that encodes hemoprotein heme oxygenase-3. *Eur. J. Biochem.* **247**, 725–732 (1997).
396. Ozen, M., Zhao, H., Lewis, D. B., Wong, R. J. & Stevenson, D. K. Heme oxygenase and the immune system in normal and pathological pregnancies. *Front. Pharmacol.* **6**, 84 (2015).
397. Choi, A. M. K. & Alam, J. Heme Oxygenase-1: Function, Regulation, and Implication of a Novel Stress-inducible Protein in Oxidant-induced Lung Injury. *American Journal of Respiratory Cell and Molecular Biology* vol. 15 9–19 (1996).

398. Ponka, P. Cell biology of heme. in *American Journal of the Medical Sciences* vol. 318 241–256 (Lippincott Williams and Wilkins, 1999).
399. Kumar, S. & Bandyopadhyay, U. Free heme toxicity and its detoxification systems in human. *Toxicology Letters* vol. 157 175–188 (2005).
400. Ahmed, S. M. U., Luo, L., Namani, A., Wang, X. J. & Tang, X. Nrf2 signaling pathway: Pivotal roles in inflammation. *Biochimica et Biophysica Acta - Molecular Basis of Disease* vol. 1863 585–597 (2017).
401. Weaver, L., Hamoud, A. R., Stec, D. E. & Hinds, T. D. Biliverdin reductase and bilirubin in hepatic disease. *Am. J. Physiol. - Gastrointest. Liver Physiol.* **314**, G668–G676 (2018).
402. Kang, S. J. *et al.* Elevated serum bilirubin levels are inversely associated with coronary artery atherosclerosis. *Atherosclerosis* **230**, 242–248 (2013).
403. Karadag, F. *et al.* Relationship between serum bilirubin levels and metabolic syndrome in patients with schizophrenia spectrum disorders. *Clin. Psychopharmacol. Neurosci.* **15**, (2017).
404. Wegiel, B. & Otterbein, L. E. Go green: The anti-inflammatory effects of biliverdin reductase. *Front. Pharmacol.* **3 MAR**, (2012).
405. Shen, Y. *et al.* Dietary quercetin attenuates oxidant-induced endothelial dysfunction and atherosclerosis in apolipoprotein e knockout mice fed a high-fat diet: A critical role for heme oxygenase-1. *Free Radic. Biol. Med.* **65**, 908–915 (2013).
406. Scapagnini, G. *et al.* Modulation of Nrf2/ARE pathway by food polyphenols: A nutritional neuroprotective strategy for cognitive and neurodegenerative disorders. *Mol. Neurobiol.* **44**, 192–201 (2011).
407. Tian, R., Yang, Z., Lu, N. & Peng, Y. Y. Quercetin, but not rutin, attenuated hydrogen peroxide-induced cell damage via heme oxygenase-1 induction in endothelial cells. *Arch. Biochem. Biophys.* **676**, (2019).
408. Rushworth, S. A., MacEwan, D. J. & O'Connell, M. A. Lipopolysaccharide-Induced Expression of NAD(P)H:Quinone Oxidoreductase 1 and Heme Oxygenase-1 Protects against Excessive Inflammatory Responses in Human Monocytes. *J. Immunol.* **181**, 6730–6737 (2008).
409. Ross, D. & Siegel, D. Functions of NQO1 in cellular protection and CoQ10 metabolism and its potential role as a redox sensitive molecular switch. *Front. Physiol.* **8**, 595 (2017).
410. Chen, X. L. *et al.* Laminar flow induction of antioxidant response element-mediated genes in endothelial cells: A novel anti-inflammatory mechanism. *J. Biol. Chem.* **278**, 703–711 (2003).
411. Dinkova-Kostova, A. T. & Talalay, P. Persuasive evidence that quinone reductase type 1 (DT diaphorase) protects cells against the toxicity of electrophiles and

- reactive forms of oxygen. *Free Radic. Biol. Med.* **29**, 231–240 (2000).
412. Dinkova-Kostova, A. T. & Talalay, P. NAD(P)H:quinone acceptor oxidoreductase 1 (NQO1), a multifunctional antioxidant enzyme and exceptionally versatile cytoprotector. *Archives of Biochemistry and Biophysics* vol. 501 116–123 (2010).
413. Castello, A. *et al.* Insights into RNA Biology from an Atlas of Mammalian mRNA-Binding Proteins. *Cell* **149**, 1393–1406 (2012).
414. Di Francesco, A. *et al.* Novel RNA-binding activity of NQO1 promotes SERPINA1 mRNA translation. *Free Radic. Biol. Med.* **99**, 225–233 (2016).
415. Kim, J., Cha, Y. N. & Surh, Y. J. A protective role of nuclear factor-erythroid 2-related factor-2 (Nrf2) in inflammatory disorders. *Mutation Research - Fundamental and Molecular Mechanisms of Mutagenesis* vol. 690 12–23 (2010).
416. Vrba, J. Í. *et al.* A Novel Semisynthetic Flavonoid 7-O-Galloyltaxifolin Upregulates Heme Oxygenase-1 in RAW264.7 Cells via MAPK/Nrf2 Pathway. *J. Med. Chem.* **56**, 856–866 (2013).
417. Zhang, Q. *et al.* Flavonoid metabolism: The synthesis of phenolic glucuronides and sulfates as candidate metabolites for bioactivity studies of dietary flavonoids. *Tetrahedron* **68**, 4194–4201 (2012).
418. Tsuchiya, S. *et al.* Establishment and characterization of a human acute monocytic leukemia cell line (THP-1). *Int. J. cancer* **26**, 171–6 (1980).
419. Gallagher, R. *et al.* Characterization of the continuous, differentiating myeloid cell line (HL-60) from a patient with acute promyelocytic leukemia. *Blood* **54**, 713–733 (1979).
420. Blasi, E., Barluzzi, R., Bocchini, V., Mazzolla, R. & Bistoni, F. Immortalization of murine microglial cells by a v-raf / v-myc carrying retrovirus. *J. Neuroimmunol.* **27**, 229–237 (1990).
421. Ades, E. W. *et al.* HMEC-1: Establishment of an immortalized human microvascular endothelial cell line. *J. Invest. Dermatol.* **99**, 683–690 (1992).
422. Promega Corporation. CellTiter 96 Aqueous Non-Radioactive Cell Proliferation Assay. *Technical info MTS-assay* 1–13 <https://www.promega.co.uk/-/media/files/resources/protocols/technical-bulletins/0/celltiter-96-aqueous-non-radioactive-cell-proliferation-systems-protocol.pdf?la=en> (2012).
423. BD-Biosciences. BD OptEIA™ Human TNF ELISA Set. *Technical info ELISA assay* <http://www.bdbiosciences.com/ds/pm/tds/555212.pdf> (2007).
424. Prochaska, H. J. & Santamaria, A. B. Direct measurement of NAD(P)H:quinone reductase from cells cultured in microtiter wells: A screening assay for anticarcinogenic enzyme inducers. *Anal. Biochem.* **169**, 328–336 (1988).
425. Moyano Cardaba, C. *et al.* CCL3 induced migration occurs independently of intracellular calcium release. *Biochem. Biophys. Res. Commun.* **418**, 17–21 (2012).

426. Hooper, L. *et al.* Effects of chocolate, cocoa, and flavan-3-ols on cardiovascular health: a systematic review and meta-analysis of randomized trials. *Am. J. Clin. Nutr.* **95**, 740–51 (2012).
427. Rodriguez-Mateos, A. *et al.* Intake and time dependence of blueberry flavonoid-induced improvements in vascular function: A randomized, controlled, double-blind, crossover intervention study with mechanistic insights into biological activity. *Am. J. Clin. Nutr.* **98**, 1179–1191 (2013).
428. Badenhorst, C. P. S., Van Der Sluis, R., Erasmus, E. & Van Dijk, A. A. Glycine conjugation: Importance in metabolism, the role of glycine N-acyltransferase, and factors that influence interindividual variation. *Expert Opinion on Drug Metabolism and Toxicology* vol. 9 (2013).
429. Beyoğlu, D. & Idle, J. R. The glycine deportation system and its pharmacological consequences. *Pharmacology and Therapeutics* vol. 135 151–167 (2012).
430. Lu, H., Meng, X. & Yang, C. S. Enzymology of methylation of tea catechins and inhibition of catechol-O-methyltransferase by (-)-epigallocatechin gallate. in *Drug Metabolism and Disposition* vol. 31 572–579 (2003).
431. Cowan, J. Targeting Nrf2 in Inflammation and Cancer. (2014).
432. Serhan, C. N. *et al.* Resolvins: A family of bioactive products of omega-3 fatty acid transformation circuits initiated by aspirin treatment that counter proinflammation signals. *J. Exp. Med.* **196**, 1025–1037 (2002).
433. Nelson, J. R., Wani, O., May, H. T. & Budoff, M. Potential benefits of eicosapentaenoic acid on atherosclerotic plaques. *Vascular Pharmacology* vol. 91 1–9 (2017).
434. Serhan, C. N. & Levy, B. D. Resolvins in inflammation: emergence of the pro-resolving superfamily of mediators. *J Clin Invest* **128**, 2657–2669 (2018).
435. Preston Mason, R. New Insights into Mechanisms of Action for Omega-3 Fatty Acids in Atherothrombotic Cardiovascular Disease. *Current Atherosclerosis Reports* vol. 21 2 (2019).
436. Carracedo, M., Artiach, G., Arnardottir, H. & Bäck, M. The resolution of inflammation through omega-3 fatty acids in atherosclerosis, intimal hyperplasia, and vascular calcification. *Semin. Immunopathol.* **41**, 757–766 (2019).
437. Artiach, G., Sarajlic, P. & Bäck, M. Inflammation and its resolution in coronary artery disease: A tightrope walk between omega-6 and omega-3 polyunsaturated fatty acids. *Kardiol. Pol.* **78**, 93–95 (2020).
438. Owen, S. C. *et al.* Colloidal drug formulations can explain 'bell-shaped' concentration-response curves. *ACS Chem. Biol.* **9**, 777–784 (2014).
439. Wong, E. *et al.* Harnessing the natural inhibitory domain to control TNF $\alpha$  Converting Enzyme (TACE) activity in vivo. *Sci. Rep.* **6**, 35598 (2016).
440. di Gesso, Lisa, J. Investigating the Effects of Dietary Flavonoids and their

Metabolites on Biomarkers of Inflammation and Antioxidant Defence. *Thesis* (University of East Anglia in, 2015).

441. Giacobbe, J., Benoiton, B., Zunszain, P., Pariante, C. M. & Borsini, A. The Anti-Inflammatory Role of Omega-3 Polyunsaturated Fatty Acids Metabolites in Pre-Clinical Models of Psychiatric, Neurodegenerative, and Neurological Disorders. *Front. Psychiatry* **11**, (2020).
442. Hu, Y., Hu, F. B. & Manson, J. A. E. Marine Omega-3 Supplementation and Cardiovascular Disease: An Updated Meta-Analysis of 13 Randomized Controlled Trials Involving 127 477 Participants. *J. Am. Heart Assoc.* **8**, (2019).
443. Felau, S. M. *et al.* Omega-3 Fatty acid Supplementation improves Endothelial Function in Primary antiphospholipid Syndrome: a Small-Scale randomized Double- Blind Placebo-Controlled Trial Sheylla. *Front. Immunol.* **9**, 336 (2018).
444. Gutiérrez, S., Svahn, S. L. & Johansson, M. E. Effects of Omega-3 Fatty Acids on Immune Cells. *Int. J. Mol. Sci.* **20**, (2019).
445. Ishihara, T., Yoshida, M. & Arita, M. Omega-3 fatty acid-derived mediators that control inflammation and tissue homeostasis. *Int. Immunol.* **31**, 559–567 (2019).
446. Mullen, A., Loscher, C. E. & Roche, H. M. Anti-inflammatory effects of EPA and DHA are dependent upon time and dose-response elements associated with LPS stimulation in THP-1-derived macrophages. *J. Nutr. Biochem.* **21**, 444–450 (2010).
447. Remmerie, A. & Scott, C. L. Macrophages and lipid metabolism. *Cell. Immunol.* **330**, 27–42 (2018).
448. Allam-Ndoul, B., Guénard, F., Barbier, O. & Vohl, M.-C. C. A study of the differential effects of eicosapentaenoic acid (EPA) and docosahexaenoic acid (DHA) on gene expression profiles of stimulated thp-1 macrophages. *Nutrients* **9**, 7–10 (2017).
449. Allam-Ndoul, B., Guénard, F., Barbier, O. & Vohl, M.-C. Effect of different concentrations of omega-3 fatty acids on stimulated THP-1 macrophages. *Genes Nutr.* **12**, 7 (2017).
450. Chanput, W., Mes, J. J. & Wichers, H. J. THP-1 cell line: An in vitro cell model for immune modulation approach. *Int. Immunopharmacol.* **23**, 37–45 (2014).
451. Williams-Bey, Y. *et al.* Omega-3 free fatty acids suppress macrophage inflammasome activation by inhibiting NF-κB activation and enhancing autophagy. *PLoS One* **9**, e97957 (2014).
452. Badenhorst, C. P. S., Erasmus, E., Van Der Sluis, R., Nortje, C. & Van Dijk, A. A. A new perspective on the importance of glycine conjugation in the metabolism of aromatic acids. *Drug Metabolism Reviews* vol. 46 343–361 (2014).
453. Chen, F. *et al.* Esterification of Ginsenoside Rh2 Enhanced Its Cellular Uptake and Antitumor Activity in Human HepG2 Cells. *J. Agric. Food Chem.* **64**, 253–261



(2016).

454. Hu, J., Zou, X., He, Y., Chen, F. & Deng, Z. Esterification of Quercetin Increases Its Transport Across Human Caco-2 Cells. *J. Food Sci.* **81**, H1825–H1832 (2016).
455. Blažević, T. *et al.* Short Chain ( $\leq$ C4) Esterification Increases Bioavailability of Rosmarinic Acid and Its Potency to Inhibit Vascular Smooth Muscle Cell Proliferation. *Front. Pharmacol.* **11**, 2355 (2021).
456. Catalán, Ú. *et al.* Inhibition of the transcription factor c-Jun by the MAPK family, and not the NF- $\kappa$ B pathway, suggests that peanut extract has anti-inflammatory properties. *Mol. Immunol.* **52**, 125–132 (2012).
457. Black, R. A. *et al.* A metalloproteinase disintegrin that releases tumour-necrosis factor- $\phi$  from cells. *Nature* **385**, 729–733 (1997).
458. Chapnick, D. A., Bunker, E. & Liu, X. A biosensor for the activity of the ‘shedase’ TACE (ADAM17) reveals novel and cell type-specific mechanisms of TACE activation. *Sci. Signal.* **8**, rs1 (2015).
459. Slomiany, B. L. & Slomiany, A. Porphyromonas gingivalis-Stimulated TACE Activation for TGF- $\alpha$  Ectodomain Shedding and EGFR Transactivation in Salivary Gland Cells Requires Rac1-Dependent p38 MAPK Membrane Localization. *J. Biosci. Med.* **03**, 42–53 (2015).
460. Guha, M. *et al.* Lipopolysaccharide activation of the MEK-ERK1/2 pathway in human monocytic cells mediates tissue factor and tumor necrosis factor  $\alpha$  expression by inducing Elk-1 phosphorylation and Egr-1 expression. *Blood* **98**, 1429–1439 (2001).
461. Ma, P. *et al.* Nitric oxide post-transcriptionally up-regulates LPS-induced IL-8 expression through p38 MAPK activation. *J. Leukoc. Biol.* **76**, 278–287 (2004).
462. Dhande, I., Ma, W. & Hussain, T. Angiotensin AT2 receptor stimulation is anti-inflammatory in lipopolysaccharide-activated THP-1 macrophages via increased interleukin-10 production. *Hypertens. Res.* **38**, 21–29 (2015).
463. Smith, S. J. *et al.* Inhibitory effect of p38 mitogen-activated protein kinase inhibitors on cytokine release from human macrophages. *Br. J. Pharmacol.* **149**, 393–404 (2006).
464. Warner, E. F., Rodriguez-Ramiro, I., O’Connell, M. A. & Kay, C. D. Cardiovascular mechanisms of action of anthocyanins may be associated with the impact of microbial metabolites on heme oxygenase-1 in vascular smooth muscle cells. *Molecules* **23**, 898 (2018).
465. Carlström, K. E. *et al.* Therapeutic efficacy of dimethyl fumarate in relapsing-remitting multiple sclerosis associates with ROS pathway in monocytes. *Nat. Commun.* **10**, 1–13 (2019).
466. Navarrete, S., Alarcón, M. & Palomo, I. Aqueous extract of tomato (*Solanum lycopersicum* L.) and ferulic acid reduce the expression of TNF- $\alpha$  and IL-1 $\beta$  in

- LPS-activated macrophages. *Molecules* **20**, 15319–15329 (2015).
467. Weber, L., Mahdi, D. H., Jankuhn, S., Lipowicz, B. & Vissiennon, C. Bioactive plant compounds in coffee charcoal (*Coffeae carbo*) extract inhibit cytokine release from activated human THP-1 Macrophages. *Molecules* **24**, (2019).
468. La Manna, S., Di Natale, C., Florio, D. & Marasco, D. Peptides as therapeutic agents for inflammatory-related diseases. *Int. J. Mol. Sci.* **19**, (2018).
469. Prasad, S., Tyagi, A. K. & Aggarwal, B. B. Recent developments in delivery, bioavailability, absorption and metabolism of curcumin: The golden pigment from golden spice. *Cancer Research and Treatment* vol. 46 2–18 (2014).
470. Honda, K. L., Lamon-Fava, S., Matthan, N. R., Wu, D. & Lichtenstein, A. H. EPA and DHA exposure alters the inflammatory response but not the surface expression of toll-like receptor 4 in macrophages. *Lipids* **50**, 121–129 (2015).
471. Almstrup, K. *et al.* *Dual Effects of Phytoestrogens Result in U-Shaped Dose-Response Curves. Environmental Health Perspectives • VOLUME* vol. 110 <http://ehpnet1.niehs.nih.gov/docs/2002/110p743-748almstrup/abstract.html> (2002).
472. Ambigaipalan, P., Oh, W. Y. & Shahidi, F. Epigallocatechin (EGC) esters as potential sources of antioxidants. *Food Chem.* **309**, 125609 (2020).
473. Chevalier, L. & Plourde, M. Comparison of pharmacokinetics of omega-3 fatty acid supplements in monoacylglycerol or ethyl ester in humans: a randomized controlled trial. *Eur. J. Clin. Nutr.* 1–9 (2020) doi:10.1038/s41430-020-00767-4.
474. Baba, S., Osakabe, N., Natsume, M. & Terao, J. Orally administered rosmarinic acid is present as the conjugated and/or methylated forms in plasma, and is degraded and metabolized to conjugated forms of caffeic acid, ferulic acid and m-coumaric acid. *Life Sci.* **75**, (2004).
475. Merkl, R., Hrádková, I., Filip, V. & Šmidrkal, J. Antimicrobial and antioxidant properties of phenolic acids alkyl esters. *Czech J. Food Sci.* **28**, 275–279 (2010).
476. Collot, M. Recent advances in dioxaborine-based fluorescent materials for bioimaging applications. *Materials Horizons* vol. 8 501–514 (2021).
477. Jun, J. V., Chenoweth, D. M. & Petersson, E. J. Rational design of small molecule fluorescent probes for biological applications. *Organic and Biomolecular Chemistry* vol. 18 5747–5763 (2020).
478. Gordon, L. J. *et al.* Direct Measurement of Intracellular Compound Concentration by RapidFire Mass Spectrometry Offers Insights into Cell Permeability. *J. Biomol. Screen.* **21**, 156–164 (2016).
479. Amin, H. P. The vascular and anti-inflammatory activity of cyanidin-3-glucoside and its metabolites in human vascular endothelial cells. *Thesis* (University of East Anglia, 2014).
480. Proestling, K. *et al.* Enhanced expression of TACE contributes to elevated levels

- of sVCAM-1 in endometriosis. *Mol. Hum. Reprod.* **25**, 76–87 (2018).
481. Liu, S. *et al.* Total flavones of *Abelmoschus manihot* improve diabetic nephropathy by inhibiting the iRhom2/TACE signalling pathway activity in rats. *Pharm. Biol.* **56**, 1–11 (2018).
482. Ku, S. K., Yang, E. J., Song, K. S. & Bae, J. S. Rosmarinic acid down-regulates endothelial protein C receptor shedding in vitro and in vivo. *Food Chem. Toxicol.* **59**, 311–315 (2013).
483. Hermenean, A. *et al.* Hepatoprotective activity of chrysin is mediated through TNF- $\alpha$  in chemically-induced acute liver damage: An in vivo study and molecular modeling. *Exp. Ther. Med.* **13**, 1671–1680 (2017).
484. Cascão, R., Fonseca, J. E. & Moita, L. F. Celastrol: A spectrum of treatment opportunities in chronic diseases. *Frontiers in Medicine* vol. 4 (2017).
485. Cell Signaling Technology. Flow Cytometry Troubleshooting Guide. vol. 2019 <https://www.cellsignal.co.uk/learn-and-support/troubleshooting/flow-cytometry-troubleshooting-guide> (2019).
486. Yao, P. *et al.* Quercetin protects human hepatocytes from ethanol-derived oxidative stress by inducing heme oxygenase-1 via the MAPK/Nrf2 pathways. *J. Hepatol.* **47**, 253–261 (2007).
487. Chow, J. M., Shen, S. C., Huan, S. K., Lin, H. Y. & Chen, Y. C. Quercetin, but not rutin and quercitrin, prevention of H<sub>2</sub>O<sub>2</sub>-induced apoptosis via anti-oxidant activity and heme oxygenase 1 gene expression in macrophages. *Biochem. Pharmacol.* **69**, 1839–1851 (2005).
488. Roubalová, L. *et al.* Semisynthetic flavonoid 7-O-galloylquercetin activates Nrf2 and induces Nrf2-dependent gene expression in RAW264.7 and Hepa1c1c7 cells. *Chem. Biol. Interact.* **260**, 58–66 (2016).
489. Dilshara, M. G. *et al.* Downregulation of NO and PGE<sub>2</sub> in LPS-stimulated BV2 microglial cells by trans-isoferulic acid via suppression of PI3K/Akt-dependent NF- $\kappa$ B and activation of Nrf2-mediated HO-1. *Int. Immunopharmacol.* **18**, 203–211 (2014).
490. Pang, C. *et al.* Caffeic acid prevents acetaminophen-induced liver injury by activating the Keap1-Nrf2 antioxidative defense system. *Free Radic. Biol. Med.* **91**, 236–246 (2015).
491. Croft, K. D. *et al.* Structural requirements of flavonoids to induce heme oxygenase-1 expression. *Free Radic. Biol. Med.* **113**, 165–175 (2017).
492. Mursu, J. *et al.* Flavonoid intake and the risk of ischaemic stroke and CVD mortality in middle-aged Finnish men: The Kuopio Ischaemic Heart Disease Risk Factor Study. *Br. J. Nutr.* **100**, 890–895 (2008).
493. Tang, Z., Li, M., Zhang, X. & Hou, W. Dietary flavonoid intake and the risk of stroke: A dose-response meta-analysis of prospective cohort studies. *BMJ Open*

- 6, (2016).
494. Troubat, R. *et al.* Neuroinflammation and depression: A review. *Eur. J. Neurosci.* **53**, 151–171 (2021).
495. Wang, W. Y., Tan, M. S., Yu, J. T. & Tan, L. Role of pro-inflammatory cytokines released from microglia in Alzheimer's disease. *Annals of Translational Medicine* vol. 3 (2015).
496. ElAli, A. & Rivest, S. Microglia ontology and signaling. *Front. Cell Dev. Biol.* **4**, (2016).
497. Kakeda, S. *et al.* Relationship between interleukin (IL)-6 and brain morphology in drug-naïve, first-episode major depressive disorder using surface-based morphometry. *Sci. Rep.* **8**, 1–9 (2018).
498. Jang, S., Kelley, K. W. & Johnson, R. W. Luteolin reduces IL-6 production in microglia by inhibiting JNK phosphorylation and activation of AP-1. *Proc. Natl. Acad. Sci. U. S. A.* **105**, 7534–7539 (2008).
499. Guo, C. *et al.* Anti-neuroinflammatory effect of Sophoraflavanone G from *Sophora alopecuroides* in LPS-activated BV2 microglia by MAPK, JAK/STAT and Nrf2/HO-1 signaling pathways. *Phytomedicine* **23**, 1629–1637 (2016).
500. Kim, S. Y. *et al.* Isorhamnetin alleviates lipopolysaccharide-induced inflammatory responses in BV2 microglia by inactivating NF- $\kappa$ B, blocking the TLR4 pathway and reducing ROS generation. *Int. J. Mol. Med.* **43**, 682–692 (2019).
501. Muhammad, T., Ikram, M., Ullah, R., Rehman, S. U. & Kim, M. O. Hesperetin, a citrus flavonoid, attenuates LPS-induced neuroinflammation, apoptosis and memory impairments by modulating TLR4/NF- $\kappa$ B signaling. *Nutrients* **11**, (2019).
502. Garcia, G. *et al.* Bioaccessible raspberry extracts enriched in ellagitannins and ellagic acid derivatives have anti-neuroinflammatory properties. *Antioxidants* **9**, 1–20 (2020).
503. Gasperotti, M. *et al.* Fate of Microbial Metabolites of Dietary Polyphenols in Rats: Is the Brain Their Target Destination? *ACS Chem. Neurosci.* **6**, 1341–1352 (2015).
504. Kho, A. R. *et al.* Effects of protocatechuic acid (PCA) on global cerebral ischemia-induced hippocampal neuronal death. *Int. J. Mol. Sci.* **19**, (2018).
505. Hwon Lee, S. *et al.* Administration of Protocatechuic Acid Reduces Traumatic Brain Injury-Induced Neuronal Death. *Int. J. Mol. Sci. Artic.* doi:10.3390/ijms18122510.
506. Waetzig, V. *et al.* c-Jun N-terminal kinases (JNKs) mediate pro-inflammatory actions of microglia. *Glia* **50**, 235–246 (2005).
507. Subedi, L., Lee, J., Yumnam, S., Ji, E. & Kim, S. Anti-Inflammatory Effect of Sulforaphane on LPS-Activated Microglia Potentially through JNK/AP-1/NF- $\kappa$ B Inhibition and Nrf2/HO-1 Activation. *Cells* **8**, 194 (2019).

508. Jeong, D. *et al.* P38/AP-1 pathway in lipopolysaccharide-induced inflammatory responses is negatively modulated by electrical stimulation. *Mediators Inflamm.* **2013**, (2013).
509. Kim, Y. H. *et al.* Regulation of c-fos gene expression by lipopolysaccharide and cycloheximide in C6 rat glioma cells. *Brain Res.* **872**, (2000).
510. Bennett, B. L. *et al.* SP600125, an anthrapyrazolone inhibitor of Jun N-terminal kinase. *Proc. Natl. Acad. Sci. U. S. A.* **98**, 13681–13686 (2001).
511. Alessi, D. R., Cuenda, A., Cohen, P., Dudley, D. T. & Saltiel, A. R. PD 098059 is a specific inhibitor of the activation of mitogen-activated protein kinase kinase in vitro and in vivo. *J. Biol. Chem.* **270**, 27489–27494 (1995).
512. Chen, G. *et al.* Peiminine protects dopaminergic neurons from inflammation-induced cell death by inhibiting the ERK1/2 and NF- $\kappa$ B signalling pathways. *Int. J. Mol. Sci.* **19**, (2018).
513. Park, B. K. *et al.* Antineuroinflammatory and Neuroprotective Effects of Gyejibokryeong-Hwan in Lipopolysaccharide-Stimulated BV2 Microglia. *Evidence-based Complement. Altern. Med.* **2019**, 7585896 (2019).
514. Kim, B. W. *et al.* A novel synthetic compound MCAP suppresses LPS-induced murine microglial activation in vitro via inhibiting NF- $\kappa$ B and p38 MAPK pathways. *Acta Pharmacol. Sin.* **37**, 334–343 (2016).
515. EMBL-EBI. IntEnz - EC 1.14.18.1.  
<https://www.ebi.ac.uk/intenz/query?cmd=SearchID&id=19166&view=INTENZ>.
516. Carballo-Carbajal, I. *et al.* Brain tyrosinase overexpression implicates age-dependent neuromelanin production in Parkinson's disease pathogenesis. *Nat. Commun.* **10**, (2019).
517. Szwajgier, D., Borowiec, K. & Pustelniak, K. The neuroprotective effects of phenolic acids: Molecular mechanism of action. *Nutrients* **9**, 1–21 (2017).
518. Basu Mallik, S. *et al.* Caffeic acid attenuates lipopolysaccharide-induced sickness behaviour and neuroinflammation in mice. *Neurosci. Lett.* **632**, 218–223 (2016).
519. Wu, J. L., Shen, M. M., Yang, S. X., Wang, X. & Ma, Z. C. Inhibitory effect of ferulic acid on neuroinflammation in LPS-activated microglia. *Chinese Pharmacol. Bull.* **31**, (2015).
520. Wang, H. yu *et al.* Protocatechuic Acid Inhibits Inflammatory Responses in LPS-Stimulated BV2 Microglia via NF- $\kappa$ B and MAPKs Signaling Pathways. *Neurochem. Res.* **40**, 1655–1660 (2015).
521. Koshiguchi, M., Komazaki, H., Hirai, S. & Egashira, Y. Ferulic acid suppresses expression of tryptophan metabolic key enzyme indoleamine 2, 3-dioxygenase via NF $\kappa$ B and p38 MAPK in lipopolysaccharidestimulated microglial cells. *Biosci. Biotechnol. Biochem.* **81**, 966–971 (2017).
522. Kaminska, B., Mota, M. & Pizzi, M. Signal transduction and epigenetic

- mechanisms in the control of microglia activation during neuroinflammation. *Biochim. Biophys. Acta - Mol. Basis Dis.* **1862**, 339–351 (2016).
523. Hidding, U. *et al.* The c-Jun N-terminal kinases in cerebral microglia: Immunological functions in the brain. *Biochem. Pharmacol.* **64**, 781–788 (2002).
524. Liu, Y., Nguyen Thi, P. A., Chen, M. & Xie, L. Tea polyphenols down-regulate JNK phosphorylation to inhibit neuron apoptosis in rats with cardiac arrest. *Zhonghua Wei Zhong Bing Ji Jiu Yi Xue* **29**, 1122–1126 (2017).
525. Vukic, V. *et al.* Expression of inflammatory genes induced by beta-amyloid peptides in human brain endothelial cells and in Alzheimer's brain is mediated by the JNK-AP1 signaling pathway. *Neurobiol. Dis.* **34**, 95–106 (2009).
526. Rehman, S. U. *et al.* Ferulic Acid Rescues LPS-Induced Neurotoxicity via Modulation of the TLR4 Receptor in the Mouse Hippocampus. *Mol. Neurobiol.* **56**, 2774–2790 (2019).
527. Henn, A. *et al.* The Suitability of BV2 Cells as Alternative Model System for Primary Microglia Cultures or for Animal Experiments Examining Brain Inflammation Doerenkamp-Zbinden Chair for alternative in vitro methods to replace animal experiments. *ALTEX* **26**, 83–94 (2009).
528. Timmerman, R., Burm, S. M. & Bajramovic, J. J. An overview of in vitro methods to study microglia. *Frontiers in Cellular Neuroscience* vol. 12 (2018).
529. Dello Russo, C. *et al.* The human microglial HMC3 cell line: Where do we stand? A systematic literature review. *J. Neuroinflammation* **15**, 259 (2018).
530. Chiavari, M., Ciotti, G. M. P., Navarra, P. & Lisi, L. Pro-inflammatory activation of a new immortalized human microglia cell line. *Brain Sci.* **9**, 111 (2019).
531. Garcia-Mesa, Y. *et al.* Immortalization of primary microglia: a new platform to study HIV regulation in the central nervous system. *J. Neurovirol.* **23**, 47–66 (2017).
532. Zhang, R., Qin, X., Kong, F., Chen, P. & Pan, G. Improving cellular uptake of therapeutic entities through interaction with components of cell membrane. *Drug Deliv.* **26**, 328–342 (2019).
533. Ebinger, G. & Verheyden, R. On the occurrence of vanillic acid in human brain and cerebrospinal fluid. *J. Neurol.* **212**, 133–138 (1976).
534. Zafra-Gómez, A., Luzón-Toro, B., Jiménez-Díaz, I., Ballesteros, O. & Navalón, A. Quantification of phenolic antioxidants in rat cerebrospinal fluid by GC-MS after oral administration of compounds. *J. Pharm. Biomed. Anal.* **53**, 103–108 (2010).
535. Lü, K., Ding, M. Y., Li, H. X. & Liu, D. L. Determination of ferulic acid in chuanxiong and in animal serum and cerebrospinal fluid by reversed-phase high performance liquid chromatography. *Se Pu* **18**, 518–520 (2000).
536. Gimbrone, M. A. & García-Cardena, G. Endothelial Cell Dysfunction and the Pathobiology of Atherosclerosis. *Circ. Res.* **118**, 620–636 (2016).

537. Hopkins, P. N. MOLECULAR BIOLOGY OF ATHEROSCLEROSIS. *Physiol. Rev.* **93**, 1317–1542 (2013).
538. Mestas, J. & Ley, K. Monocyte-endothelial cell interactions in the development of atherosclerosis. *Trends Cardiovasc. Med.* **18**, 228–32 (2008).
539. Papayannopoulos, V. Neutrophils Stepping Through (to the Other Side). *Immunity* vol. 49 992–994 (2018).
540. Joseph, J. P. *et al.* CXCR2 Inhibition – a novel approach to treating CoronAry heart DiseAse (CICADA): study protocol for a randomised controlled trial. *Trials* **18**, 473 (2017).
541. Naegelen, I. *et al.* An essential role of syntaxin 3 protein for granule exocytosis and secretion of IL-1  $\alpha$  , IL-1  $\beta$  , IL-12b, and CCL4 from differentiated HL-60 cells. *J. Leukoc. Biol.* **97**, 557–571 (2015).
542. Tamassia, N. *et al.* Cytokine production by human neutrophils: Revisiting the “dark side of the moon”. *Eur. J. Clin. Invest.* **48**, e12952 (2018).
543. Cassatella, M. A., Östberg, N. K., Tamassia, N. & Soehnlein, O. Biological Roles of Neutrophil-Derived Granule Proteins and Cytokines. *Trends Immunol.* **40**, 648–664 (2019).
544. Soehnlein, O. Multiple roles for neutrophils in atherosclerosis. *Circulation Research* vol. 110 875–888 (2012).
545. Soehnlein, O., Lindbom, L. & Weber, C. Mechanisms underlying neutrophil-mediated monocyte recruitment. *Blood* vol. 114 4613–4623 (2009).
546. Risitano, R. *et al.* Flavonoid fraction of bergamot juice reduces LPS-induced inflammatory response through SIRT1-mediated NF- $\kappa$ B inhibition in THP-1 monocytes. *PLoS One* **9**, (2014).
547. Ma, Z. C. *et al.* Ferulic acid attenuates adhesion molecule expression in gamma-radiated human umbilical vascular endothelial cells. *Biol. Pharm. Bull.* **33**, 752–758 (2010).
548. Smith, M. J. Implications of Anthocyanin Instability and Metabolism : Impact on Discovery of Intake Biomarkers and In Vitro Mechanisms of Action. *Thesis* (University of East Anglia, 2016).
549. Chanet, A. *et al.* Flavanone metabolites decrease monocyte adhesion to TNF- $\alpha$ -activated endothelial cells by modulating expression of atherosclerosis-related genes. *Br. J. Nutr.* **110**, 587–598 (2013).
550. Qi, H., Yang, S. & Zhang, L. Neutrophil Extracellular Traps and Endothelial Dysfunction in Atherosclerosis and Thrombosis. *Front. Immunol.* **8**, 928 (2017).
551. Moschonas, I. C. & Tselepis, A. D. The pathway of neutrophil extracellular traps towards atherosclerosis and thrombosis. *Atherosclerosis* vol. 288 9–16 (2019).
552. Motta, A. C., Oranje, R. P. A. & Kartawidjajaputra, F. *Development of a high throughput functional assay to study inflammation in vitro.* (2012).

553. Willam, C., Schindler, R., Frei, U. & Eckardt, K.-U. Increases in oxygen tension stimulate expression of ICAM-1 and VCAM-1 on human endothelial cells. *Am. J. Physiol. Circ. Physiol.* **276**, H2044–H2052 (1999).
554. Muller, W. A., Weigl, S. A., Deng, X. & Phillips, D. M. PECAM-1 is required for transendothelial migration of leukocytes. *J. Exp. Med.* **178**, 449–460 (1993).
555. Krump, E., Sanghera, J. S., Pelech, S. L., Furuya, W. & Grinstein, S. Chemotactic peptide N-formyl-Met-Leu-Phe activation of p38 mitogen- activated protein kinase (MAPK) and MAPK-activated protein kinase-2 in human neutrophils. *J. Biol. Chem.* **272**, 937–944 (1997).
556. Schiffmann, E., Corcoran, B. A. & Wahl, S. M. N formylmethionyl peptides as chemoattractants for leucocytes. *Proc. Natl. Acad. Sci. U. S. A.* **72**, 1059–1062 (1975).
557. Haldar, S. *et al.* Dose-dependent increase in unconjugated cinnamic acid concentration in plasma following acute consumption of polyphenol rich curry in the polyspice study. *Nutrients* **10**, 1–14 (2018).
558. Spisani, S. & Selvatici, R. FMLP-OME ANALOGUES TRIGGER SPECIFIC SIGNALLING PATHWAYS IN THE PHYSIOLOGICAL FUNCTIONS OF HUMAN NEUTROPHILS. in *Trends in cellular Signaling* (ed. Caplin, D. E.) 1–40 (Nova Science Publishers, Inc., 2006).
559. Legdeur, M. C. J. C. *et al.* A functional study on the migration of human monocytes to human leukemic cell lines and the role of monocyte chemoattractant protein-1. *Leukemia* **11**, 1904–1908 (1997).
560. Riboldi, E. *et al.* Benzylamine inhibits monocyte migration and MAPK activation induced by chemotactic agonists. *Br. J. Pharmacol.* **140**, 377–383 (2003).
561. Fine, J. S., Byrnes, H. D., Zavodny, P. J. & Hipkin, R. W. Evaluation of signal transduction pathways in chemoattractant-induced human monocyte chemotaxis. *Inflammation* **25**, 61–67 (2001).
562. Yoshimura, T. & Leonard, E. J. Identification of high affinity receptors for human monocyte chemoattractant protein-1 on human monocytes. *J. Immunol.* **145**, (1990).
563. Chen, L.-Y. *et al.* Synergistic Induction of Inflammation by Bacterial Products Lipopolysaccharide and fMLP: An Important Microbial Pathogenic Mechanism. *J. Immunol.* **182**, 2518–2524 (2009).
564. Kukhtina, N. B. *et al.* Peptide fragments of the fractalkine chemokine domain: Influence on migration of human monocytes. *Russ. J. Bioorganic Chem.* **38**, 584–589 (2012).
565. Johnston, B. *et al.* Chronic inflammation upregulates chemokine receptors and induces neutrophil migration to monocyte chemoattractant protein-1. *J. Clin. Invest.* **103**, 1269–1276 (1999).



566. Phillipson, M. & Kubes, P. The neutrophil in vascular inflammation. *Nat. Med.* **2011 1711** **17**, 1381 (2011).
567. Panaro, M. A. & Mitolo, V. Immunopharmacology and Immunotoxicology Cellular Responses to Fmlp Challenging: A Mini-Review. (2008)  
doi:10.3109/08923979909007117.
568. Gouwy, M. *et al.* CC chemokine ligand-2 synergizes with the nonchemokine G protein-coupled receptor ligand fMLP in monocyte chemotaxis, and it cooperates with the TLR ligand LPS via induction of CXCL8. *J. Leukoc. Biol.* **86**, 671–680 (2009).
569. MARTIN, S. J., BRADLEY, J. G. & COTTER, T. G. HL-60 cells induced to differentiate towards neutrophils subsequently die via apoptosis. *Clin. Exp. Immunol.* **79**, 448–453 (1990).
570. Klein, M. B., Hayes, S. F. & Goodman, J. L. Monocytic differentiation inhibits infection and granulocytic differentiation potentiates infection by the agent of human granulocytic ehrlichiosis. *Infect. Immun.* **66**, 3410–3415 (1998).
571. Millius, A. & Weiner, O. D. Manipulation of neutrophil-like HL-60 cells for the study of directed cell migration. *Methods Mol. Biol.* **591**, 147–158 (2010).
572. Rincón, E., Rocha-Gregg, B. L. & Collins, S. R. A map of gene expression in neutrophil-like cell lines. *BMC Genomics* **19**, 573 (2018).
573. Koga, T., Morotomi-Yano, K., Sakugawa, T., Saitoh, H. & Yano, K. ichi. Nanosecond pulsed electric fields induce extracellular release of chromosomal DNA and histone citrullination in neutrophil-differentiated HL-60 cells. *Sci. Rep.* **9**, 8451 (2019).
574. Rosmarin, A. *et al.* Differential expression of CD11b/CD18 (Mo1) and myeloperoxidase genes during myeloid differentiation. *Blood* **73**, 131–136 (1989).
575. Ali, H. *et al.* Chemokine Production by G Protein-Coupled Receptor Activation in a Human Mast Cell Line: Roles of Extracellular Signal-Regulated Kinase and NFAT. *J. Immunol.* **165**, 7215–7223 (2000).
576. Zhang, E. R., Liu, S., Wu, L. F., Altschuler, S. J. & Cobb, M. H. Chemoattractant concentration-dependent tuning of ERK signaling dynamics in migrating neutrophils. *Sci. Signal.* **9**, (2016).
577. Hooper, L. *et al.* Flavonoids, flavonoid-rich foods, and cardiovascular risk: A meta-analysis of randomized controlled trials. *Am. J. Clin. Nutr.* **88**, 38–50 (2008).
578. Taubert, D., Roesen, R. & Schömig, E. Effect of cocoa and tea intake on blood pressure: A meta-analysis. *Arch. Intern. Med.* **167**, 626–634 (2007).
579. Kay, C. D., Hooper, L., Kroon, P. A., Rimm, E. B. & Cassidy, A. Relative impact of flavonoid composition, dose and structure on vascular function: A systematic review of randomised controlled trials of flavonoid-rich food products. *Mol. Nutr. Food Res.* **56**, 1605–1616 (2012).

580. Silvestre-Roig, C., Fridlender, Z. G., Glogauer, M. & Scapini, P. Neutrophil Diversity in Health and Disease. *Trends Immunol.* **40**, 565–583 (2019).
581. Muller, W. A. How endothelial cells regulate transmigration of leukocytes in the inflammatory response. *Am. J. Pathol.* **184**, 886–896 (2014).
582. Nourshargh, S. & Alon, R. Leukocyte Migration into Inflamed Tissues. *Immunity* **41**, 694–707 (2014).
583. González, R. *et al.* Effects of Flavonoids and other Polyphenols on Inflammation. *Crit. Rev. Food Sci. Nutr.* **51**, 331–362 (2011).
584. Schwager, J., Bompard, A., Weber, P. & Raederstorff, D. Ascorbic acid modulates cell migration in differentiated HL-60 cells and peripheral blood leukocytes. *Mol. Nutr. Food Res.* **59**, 1513–1523 (2015).
585. Chang, W.-C. *et al.* Protective Effect of Vanillic Acid against Hyperinsulinemia, Hyperglycemia and Hyperlipidemia via Alleviating Hepatic Insulin Resistance and Inflammation in High-Fat Diet (HFD)-Fed Rats. *Nutrients* **7**, 9946–9959 (2015).
586. Milenkovic, D. *et al.* A systems biology network analysis of nutri(epi)genomic changes in endothelial cells exposed to epicatechin metabolites. *Sci. Rep.* **8**, 15487 (2018).
587. Carregosa, D. *et al.* Polyphenol metabolites and new molecules for attenuation of neuroinflammation. *Free Radic. Biol. Med.* **120**, S161 (2018).
588. Weseler, A. R. & Bast, A. Pleiotropic-acting nutrients require integrative investigational approaches: The example of flavonoids. *J. Agric. Food Chem.* **60**, 8941–8946 (2012).
589. Boesten, D. M. P. H. J., Von Ungern-Sternberg, S. N. I., Den Hartog, G. J. M. & Bast, A. Protective pleiotropic effect of flavonoids on NAD<sup>+</sup> levels in endothelial cells exposed to high glucose. *Oxid. Med. Cell. Longev.* **2015**, (2015).
590. Jurjus, A. R., Khoury, N. N. & Reimund, J. M. Animal models of inflammatory bowel disease. *J. Pharmacol. Toxicol. Methods* **50**, 81–92 (2004).
591. Goyal, N., Rana, A., Ahlawat, A., Bijjem, K. R. V. & Kumar, P. Animal models of inflammatory bowel disease: A review. *Inflammopharmacology* **22**, 219–233 (2014).
592. Jiminez, J. A., Uwiera, T. C., Inglis, G. D. & Uwiera, R. R. E. Animal models to study acute and chronic intestinal inflammation in mammals. *Gut Pathog.* **7**, 1–31 (2015).
593. Kiesler, P., Fuss, I. J. & Strober, W. Experimental Models of Inflammatory Bowel Diseases. *Cell. Mol. Gastroenterol. Hepatol.* **1**, 154–170 (2015).
594. Emini Veseli, B. *et al.* Animal models of atherosclerosis. *Eur. J. Pharmacol.* **816**, 3–13 (2017).
595. Chassaing, B., Aitken, J. D., Malleshappa, M. & Vijay-Kumar, M. Dextran sulfate sodium (DSS)-induced colitis in mice. *Curr. Protoc. Immunol.* **104**, 15–25 (2014).

596. Balbas-Martinez, V. *et al.* A systems pharmacology model for inflammatory bowel disease. *PLoS One* **13**, e0192949 (2018).
597. Algieri, F. *et al.* Intestinal anti-inflammatory activity of the Serpylli herba extract in experimental models of rodent colitis. *J. Crohn's Colitis* **8**, 775–788 (2014).
598. Geladaris, A., Häusler, D. & Weber, M. S. Microglia: The missing link to decipher and therapeutically control MS progression? *Int. J. Mol. Sci.* **22**, 3461 (2021).
599. Constantinescu, C. S., Farooqi, N., O'Brien, K. & Gran, B. Experimental autoimmune encephalomyelitis (EAE) as a model for multiple sclerosis (MS). *Br. J. Pharmacol.* **164**, 1079–1106 (2011).
600. Procaccini, C., De Rosa, V., Pucino, V., Formisano, L. & Matarese, G. Animal models of Multiple Sclerosis. *Eur. J. Pharmacol.* **759**, 182–191 (2015).
601. Derfuss, T. *et al.* Advances in oral immunomodulating therapies in relapsing multiple sclerosis. *Lancet Neurol.* **19**, 336–347 (2020).
602. Yang, T. *et al.* Neuroprotective Effects of Fingolimod Supplement on the Retina and Optic Nerve in the Mouse Model of Experimental Autoimmune Encephalomyelitis. *Front. Neurosci.* **15**, 491 (2021).
603. Bonfiglio, T. *et al.* Prophylactic versus therapeutic fingolimod: Restoration of presynaptic defects in mice suffering from experimental autoimmune encephalomyelitis. *PLoS One* **12**, e0170825 (2017).
604. Giralt, M. *et al.* Induction of atypical EAE mediated by transgenic production of IL-6 in astrocytes in the absence of systemic IL-6. *Glia* **61**, 587–600 (2013).

## **Chapter 8. Appendices**

## **Appendix I: Buffers & Reagent Recipes**

### **10X Phosphate-Buffered Saline (PBS) (1L)**

80.1 g	NaCl
11.6 g	Na <sub>2</sub> HPO <sub>4</sub>
2 g	KH <sub>2</sub> PO <sub>4</sub>
2 g	KCl

Top up to 1 L with deionised H<sub>2</sub>O.

pH to 7.0 - 7.2

For sterile purposes aliquot and autoclave.

For experiments, use 1X e.g., dilute 1:10 with deionised H<sub>2</sub>O (100 mL 10X PBS into 900 mL deionised H<sub>2</sub>O).

### **ELISA Assays Buffers**

#### **PBS-Tween General ELISA Assay Washing Buffer (1L)**

(0.05% Tween-20 in PBS)

1 L PBS buffer

500 µL TWEEN® 20

#### **General ELISA Assay Substrate Solution (10 mL)**

1:1 mixture of reagent A & B

5 mL Colour reagent A (H<sub>2</sub>O<sub>2</sub>)

5 mL Colour reagent B (Tetramethylbenzidine)

## **General ELISA Assay Stop Solution (100 mL)**

1 M sulphuric acid (H<sub>2</sub>SO<sub>4</sub>):

5.439 mL 98% w/w H<sub>2</sub>SO<sub>4</sub> (18.385 M)\*

25 mL deionised H<sub>2</sub>O

Adjust volume up to 100 mL with deionised H<sub>2</sub>O.

*\* Be cautious! Concentrated H<sub>2</sub>SO<sub>4</sub> is extremely corrosive and becoming very hot when mixed with water. Therefore, add the acid slowly to water in a fume cupboard and wear appropriate protection material.*

## **TNF-α ELISA Buffers**

### **TNF-α ELISA Coating Buffer (100 mL)**

713 mg      NaHCO<sub>3</sub>

159 mg      Na<sub>2</sub>CO<sub>3</sub>

Dissolve in ± 80 mL deionised H<sub>2</sub>O, adjust pH to 9.5, top up to 100 mL with water

Store at 2-8°C and used within 7 days of preparation.

### **TNF-α ELISA Assay Diluent (100 mL)**

10% FBS in PBS:

10 mL      Fetal Bovine Serum

90 mL      PBS

## **IL-6 ELISA Buffers**

### **IL-6 ELISA Reagent Diluent (10 mL)**

1% BSA in PBS:

0.1 g          BSA

10 mL        PBS

Filter (0.45 µm) sterilise.

Store at 4 °C and use within one week of preparation.

## **HO-1 ELISA Buffers**

### **HO-1 Assay Cell Lysis Buffer (1 mL)**

<b>Volume reagent / reaction</b>	<b>final concentration</b>
500 µL PBS	
500 µL 2 mM EDTA	1mM
5 µL Triton X-100	0.5%
10 µL 10 mM PMSF	100 µM
20 µL 0.5 mg/mL Leupeptin	10 µg/mL
2 µL 5 mg/mL Pepstatin	10 µg/mL
2.143 µL 1.5 mg/mL Aprotinin	3 µg/mL

Filter sterilise with 0.45 µm filter.

### **HO-1 Assay Blocking Buffer (50 mL)**

1% BSA and 0.05% NaN<sub>3</sub> in PBS:

0.5 g BSA

0.025 g NaN<sub>3</sub>

Top up to 50 mL with PBS

Store at 2-8 °C and use within one week of preparation.

### **IC Diluent #1 (5 mL)**

1% BSA in PBS:

0.05 g BSA

5 mL PBS

Filter sterilise with 0.45 µm filter.

Store at 2-8 °C and use within one week of preparation.

### **IC Diluent #4 (10 mL)**

1 mM EDTA and 0.5% Triton X-100 in PBS:

5 mL 2 mM EDTA

50 µL Triton-X-100

5 mL PBS

Store at 2-8 °C and use within one week of preparation.



## **NQO1 Enzymatic Activity Assay Buffers**

### **NQO1 Cell Lysis Buffer (10 mL)**

0.8% digitonin in 2 mM EDTA:

80 mg digitonin

10 mL 2 mM EDTA

pH to 7.8

Store at 4°C\*.

\* Prior to cell lysis procedure, warm up at 95 °C, until it become clear to dissolve digitonin, then leave it at the RT to cool down before use.

### **NQO1 Assay Reaction Buffer**

For each 24 wells prepare 5 mL:

<b>Volume reagent / reaction</b>	<b>final concentration</b>
4.5 mL Millipore H <sub>2</sub> O	
125 µL 1 M Tris-HCl, pH 7.4	25 mM
33.3 µL 100 mg/mL BSA	0.667 mg/mL
33.3 µL Tween-20	0.7%
33.3 µL 150 mM glucose-6-phosphate (G-6-P)	1 mM
3.3 µL 7.5 mM FAD	5 µM
3 µL 50 mM NADP+	30 µM
5 µL 2 kU/mL Yeast G-6-P dehydrogenase	0.002 kU/mL
250 µL 6 mg/mL (MTT)#	0.3 mg/mL
5 µL 50 mM menadione*	50 µM

\* Adding menadione will start the reaction. So, take out 200 µL reaction buffer for double blank (-M), then add menadione just before the assay.

# Thiazolyl Blue Tetrazolium Bromide

## Real Time-QPCR

### Reverse Transcription (RT) Mastermix (5 $\mu$ L/reaction)

Reagents	1x reaction Volume ( $\mu$ L)
H <sup>2</sup> O (nuclease free)	1.6
10xRT Buffer	1.0
10X Random Hexamers (primers)	1.0
RNase Inhibitor (20 U/ $\mu$ L)	0.5
dNTP's (100 nM)	0.4
MultiScribe™ Reverse Transcriptase (50 U/ $\mu$ L)	0.5
<b>Total volume</b>	<b>5.0</b>

### RT- qPCR Mastermix (18 $\mu$ L/reaction)

Reagents	1x reaction Volume ( $\mu$ L)
H <sup>2</sup> O (nuclease free)	7.0
SYBR Green Jumpstart Taq Ready Mix	10
Forward & Reverse primers (10 $\mu$ M)	1.0
<b>Total volume</b>	<b>18.0</b>

## **Western Blotting**

### **Cell lysis buffer (100 µL/reaction)**

1X Tris-Glycine SDS in PBS (100 µL/reaction)

50 µL Novex™ Tris-Glycine SDS Sample Buffer (2X)\*, at 2-8°C

50 µL PBS

Store on ice.

*\* warm up at RT to dissolve SDS.*

### **1X Running Buffer (800 mL)**

40 mL NuPAGE® 20X MOPS SDS Running Buffer

7600 mL deionised H<sub>2</sub>O.

### **10 X Transfer Buffer (1 L)**

10X Transfer buffer was prepared in the laboratory according to the following recipe:

24.26 g Tris Base

112.6 g Glycine

1 g SDS

Make up to 1 L with deionised H<sub>2</sub>O.

### **1X Complete Transfer Buffer (1 L)**

700 mL	deionised H <sub>2</sub> O
100 mL	10X transfer buffer
200 mL	methanol

### **Immunoblotting**

#### **20X TBS-T Buffer (1 L)**

48.4 g	Tris Base
160 g	NaCl
62 mL	5M HCl
20 mL	TWEEN® 20

Make up to 1 L with deionised H<sub>2</sub>O

pH to 7.6

#### **1X TBS-T Buffer (1 L)**

50 mL 20X TBST

950 mL deionised H<sub>2</sub>O

#### **Membrane Blocking Buffer (400 mL)**

5% milk in TBST:

20 g Marvel Original Dried Skimmed Milk Powder

Topped up to 400 mL 1X TBS-T

Dissolve for at least 20 min on slow stirring magnet stirrer to remove all clumps.

## **Transendothelial Migration Assay Buffers and Solutions**

### **Coating solution for 96-well inserts (20 mL)**

1 mL 2% gelatine

19 mL sterile water

### **Red Blood Cell (RBC) Lysis Buffer (1 L)**

8.26 g  $\text{NH}_4\text{Cl}$

0.84 g  $\text{NaHCO}_3$

0.037 g EDTA

Top up to 1 L with deionised  $\text{H}_2\text{O}$

pH to 7.3.

### **FACS Buffer (500 mL)**

0.1% BSA in DPBS:

0.5 g BSA

Top up to 500 mL with Dulbecco's PBS (without  $\text{Ca}^{2+}$  and  $\text{Mg}^{2+}$ )

Store at 2-8 °C

## **FACS Flow Cytometry Antibody Cocktail**

<b>Antibody</b>	<b>Recommended volume/well</b>	<b>Volume used</b>	<b>Mastermix (104 wells)</b>
Brilliant Violet 412 TM	5 $\mu$ L/ $10^6$ cells	1.5 $\mu$ L	156 $\mu$ L
Alexa Fluor 488	5 $\mu$ L/ $10^6$ cells	1.25 $\mu$ L	130 $\mu$ L
Alexa Fluor® 647	5 $\mu$ L/ $10^6$ cells	1.25 $\mu$ L	130 $\mu$ L
FACS-buffer		21 $\mu$ L	2.184 mL

## **Chemotaxis and Calcium Flux Assay Buffers**

### **Chemotaxis Blocking Buffer (CB buffer) (5 mL)**

1% BSA in cell growth medium\*:

0.05 g BSA

5 mL serum-free RPMI 1640

\* Prior to each assay prepare freshly and sterile.

### **Chemotaxis Working Buffer (10 mL)**

0.1% BSA in cell growth medium

1 mL Chemotaxis Blocking Buffer (1% BSA in cell medium)

9 mL serum-free RPMI 1640.

### **Calcium Flux (CFX) Buffer (500 mL)**

<b>Weight compound</b>	<b>final conc.</b>
4.0031 g NaCl	137 mM
0.1864 g KCl	5 mM
0.1066 g MgCl <sub>2</sub>	1 mM
0.1103 g CaCl <sub>2</sub>	1.5 mM
1.1915 g Hepes	10 mM
2.2520 g D-glucose	25 mM

pH to 7.4.

Store at 4°C.

### **General Flow Cytometry Buffers**

#### **Staining buffer (50 mL)**

0.5% BSA in DPBS

Prepare 5% BSA in DPBS (0.5 g BSA into 10 mL) > filter sterilise, then dilute 10X (5 mL into 45 mL DPBS).

## **Appendix II: Cell Viability Assay**

### **THP-1 cell viability in response to naturally occurring phenolic acids and their synthetic analogues**

Flavonoid metabolites ferulic acid (FA), isoferulic acid (IFA), vanillic acid (VA), isovanillic acid (IVA), caffeic acid (CA), protocatechuic acid (PCA) and 4-hydroxybenzoic acid (4HBA) were screened at 1  $\mu$ M and 10  $\mu$ M for their effect on cell viability of THP-1 cells (**Figure 8. 1-4**) or 20  $\mu$ M for FA and FA-hexyl-ester (FA-Hex-Es) and FA-Propyl ester (FA-Pro-Es) (**Figure 8. 5**). After 24 h of incubation with treatments MTS assay reagent was added to the cells and further incubated for 3 h before reading the cell absorbance. In this assay viable cells are able to provide mitochondrial dehydrogenase to catabolise yellow MTT into purple formazan. The cell survival rate is calculated as the percentage of the purple colour absorbance and normalised to non-treated cells (Cell only). This procedure was further applied to all tested compounds.



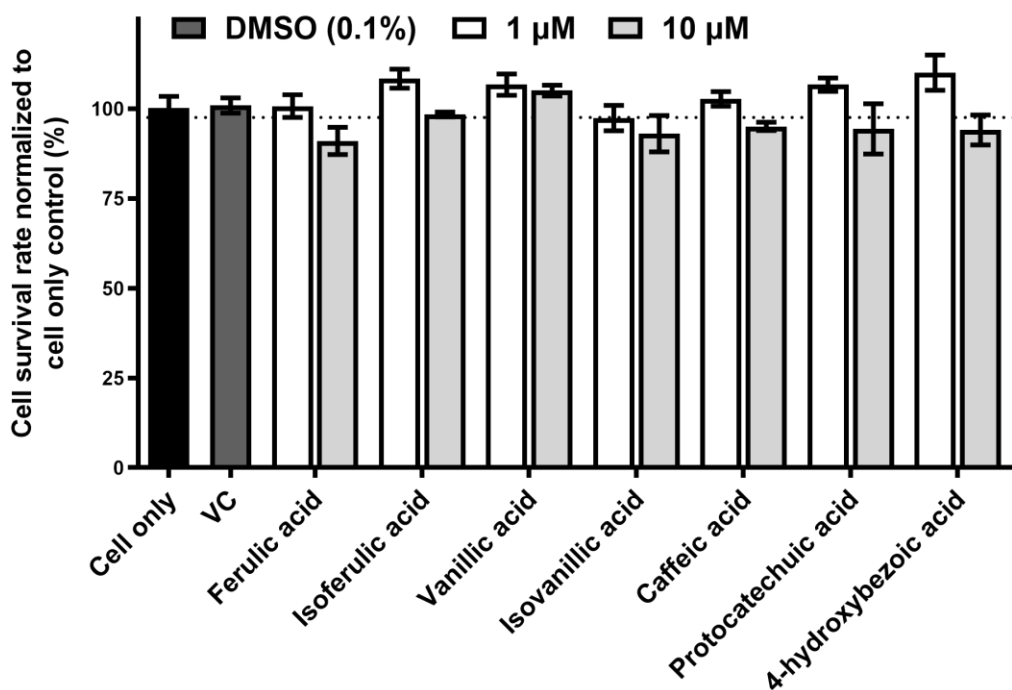


Figure 8. 1 Effect of phenolic acids, flavonoid metabolites on THP-1 cell viability measured by MTS assay.  $1 \times 10^5$  cells/well treated with  $1 \mu\text{M}$  and  $10 \mu\text{M}$  of each compound or 0.1 % DMSO and incubated o/n at  $37^\circ\text{C}$ .  $10 \mu\text{L}$ /well MTS assay reagent was added and returned to incubator for 3h. Columns and error bars represent mean  $\pm$  SEM of 3 technical replicates for each treatment and 6 replicates for DMSO treatments. Significant difference \*  $p < 0.05$  between treatment and non-treatment cells (cell only) analysed by student's t-test.

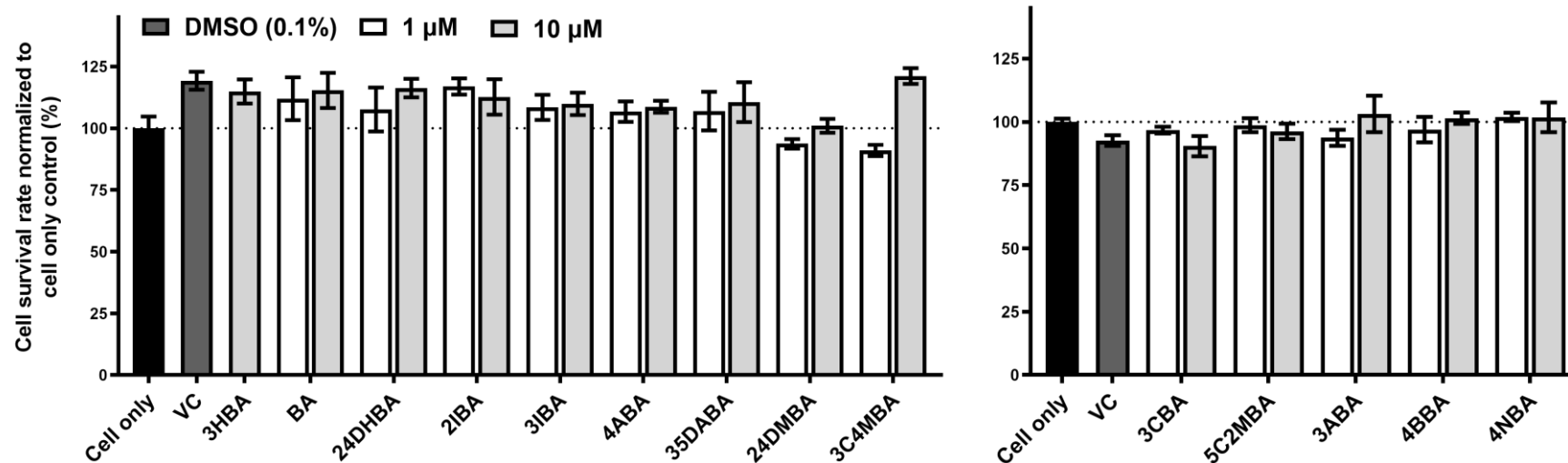


Figure 8. 2 Effect of non-natural phenolic acids on THP-1 cell viability measured with MTS Assay. Cells ( $1 \times 10^5$ /well) treated with  $1 \mu\text{M}$  and  $10 \mu\text{M}$  of each compound or 0.1 % DMSO and incubated o/n at  $37^\circ\text{C}$ .  $10 \mu\text{L}$ /well MTS assay reagent was added and returned to incubator for 3h. Columns and error bars represent mean  $\pm$  SEM of 3 technical replicates for each treatment and 6 replicates for DMSO treatments. Significant difference \*  $p < 0.05$  between treatment and non-treatment cells (cell only) analysed by student's t-test.

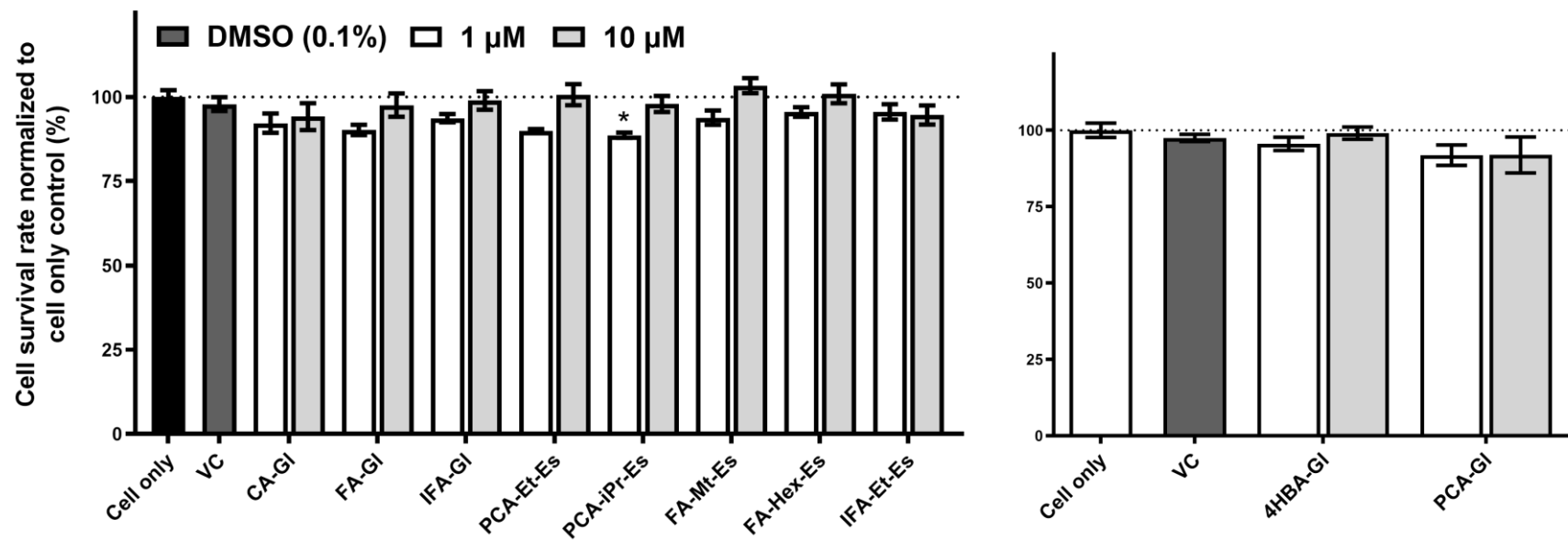


Figure 8.3 Effect of phenolic acids glycine conjugates on THP-1 cell viability measured with MTS Assay. Cells ( $1 \times 10^5$ /well) treated with  $1 \mu\text{M}$  and  $10 \mu\text{M}$  of each compound or 0.1 % DMSO and incubated o/n at  $37^\circ\text{C}$ .  $10 \mu\text{L}$ /well MTS assay reagent was added and returned to incubator for 3h. Columns and error bars represent mean  $\pm$  SEM of 3 technical replicates for each treatment and 6 replicates for DMSO treatments. Significant difference \*  $p < 0.05$  between treatment and non-treatment cells (cell only) analysed by student's t-test.

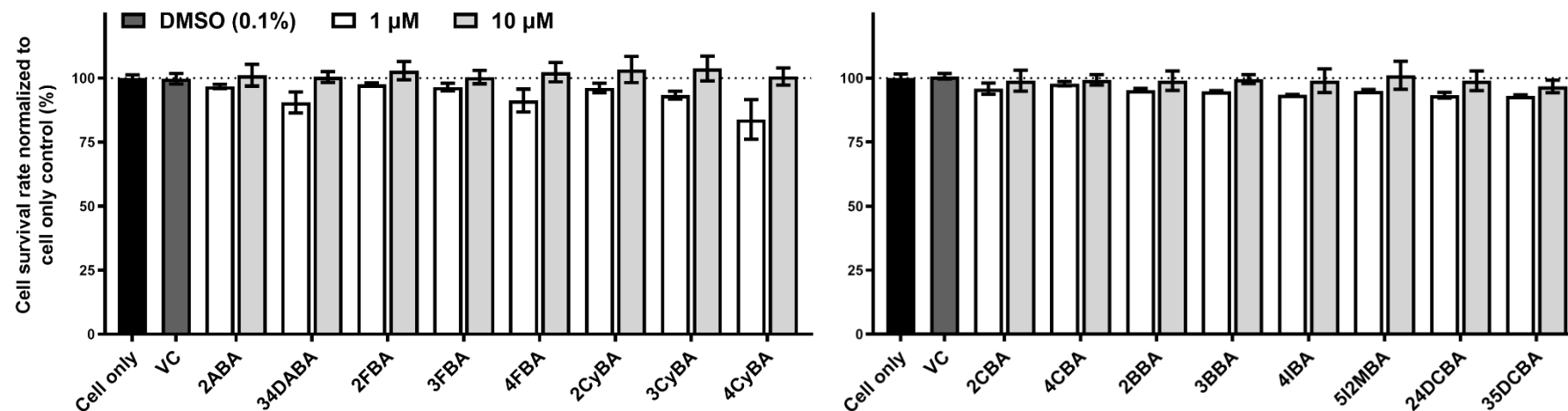


Figure 8. 4 Effect of Halogenated compounds on THP-1 Cell Viability measured with MTS Assay. Cells ( $1 \times 10^5$ /well) treated with  $1 \mu\text{M}$  and  $10 \mu\text{M}$  of each compound or 0.1 % DMSO and incubated o/n at  $37^\circ\text{C}$ .  $10 \mu\text{L}$ /well MTS assay reagent was added and returned to incubator for 3h. Columns and error bars represent mean  $\pm$  SEM of 3 technical replicates for each treatment and 6 replicates for DMSO treatments. Significant difference \*  $p < 0.05$  between treatment and non-treatment cells (cell only) analysed by student's t-test.

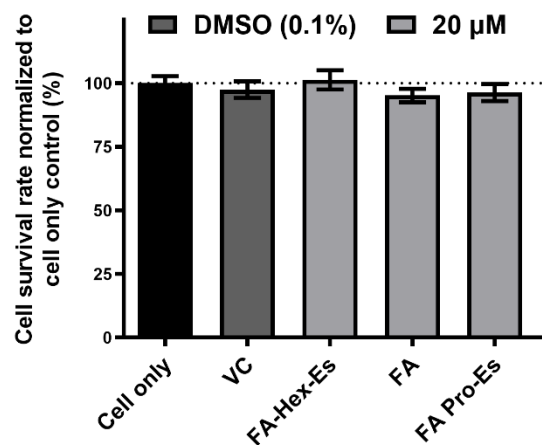


Figure 8. 5 Effect of 20  $\mu\text{M}$  treatment on THP-1 Cell Viability measured with MTS Assay. Cells ( $1 \times 10^5$ /well) treated with 20  $\mu\text{M}$  of each compound or 0.1 % DMSO and incubated o/n at 37°C. 10  $\mu\text{L}$ /well MTS assay reagent was added and returned to incubator for 3h. Columns and error bars represent mean  $\pm$  SEM of 3 technical replicates for each treatment and 6 replicates for DMSO treatments. Significant difference \*  $p < 0.05$  between treatment and non-treatment cells (cell only) analysed by student's t-test.

## **Appendix III: Method Optimization**

### **8.3.1 Optimization for Chapter 3**

#### **8.3.1.1 Comparing 96-well with 24- and 48-well plate for LPS-induced TNF- $\alpha$ secretion in THP-1**

For a high-throughput screening, the use of 96-well plate was compared to 24-well and 48-well plate to test the reproducibility for a more rapid and efficient screening method. Briefly 250  $\mu$ L cells ( $10^6$  cells/mL) were pipetted into a 96-well plate and 500  $\mu$ L into 24- and 48-well plate with a final density of  $0.25 \times 10^6$  and  $0.5 \times 10^6$  cells/well, and pre-incubated with 0.1% DMSO prior treatment with 0.1 ng/mL LPS for 3 h. On each plate eight wells were pre-incubated with 0.1% DMSO, four wells with DMSO alone to provide a negative control, four wells to provide a vehicle control (VC, DMSO+LPS); four wells left untreated as basal control and four wells for LPS treatment alone. TNF- $\alpha$  secretion was measured by ELISA. Results displayed in **Figure 8. 6** shows that TNF- $\alpha$  is absent in basal control and the level for 0.1% DMSO alone is the same, implying that DMSO alone have no effect on TNF- $\alpha$  secretion in THP-1 cells. The level of TNF- $\alpha$  secretion for VC in all three plates were lower than LPS yet not significant (analysed by t-test). When comparing three plates, the LPS and VC level in 24-well plate seemed more consistent and smaller error bars. Therefore, 24-well plate was carried forward.

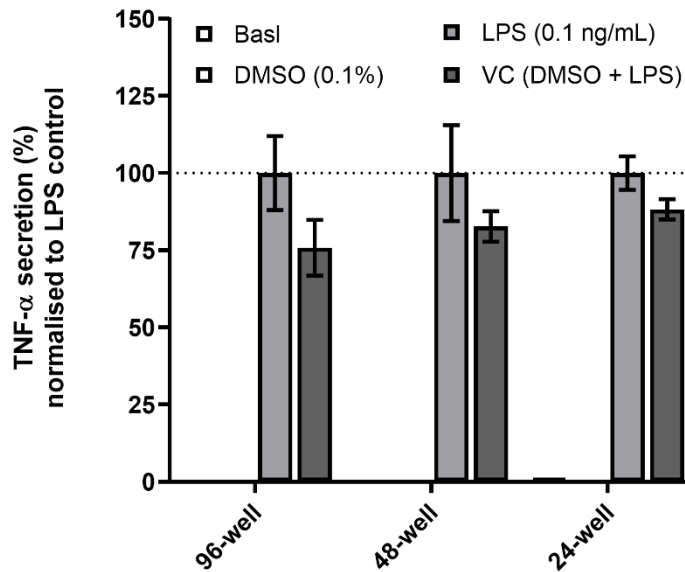


Figure 8. 6 Effect of cell volume and density on LPS-induced TNF- $\alpha$  secretion in THP-1 cells. Cells were seeded in 96-well plate ( $0.25 \times 10^6$  cells/well, in 0.25 mL volume) and in 24- and 48-well plate ( $0.5 \times 10^6$  cells/well (in 0.5 mL volume) and pre-treated with 0.1% DMSO for 30 min prior to adding LPS (0.1 ng/mL) for 3h incubation. TNF- $\alpha$  secretion was measured by ELISA. Data expressed as percentage of LPS treatment for each plate, mean  $\pm$  SEM, n=4, a single experiment with four technical replicates. No significant difference between LPS and VC by students t-test.

### 8.3.1.2 THP-1 Macrophage Optimisation: LPS Kinetics

In order to evaluate the optimal concentration of LPS for TNF- $\alpha$  secretion in PMA-differentiated THP-1 macrophages, the following concentrations were assessed: 1, 10, 100 ng/mL. **Figure 8. 7** indicates a concentration-dependent response in THP-1 macrophages at 1 and 3 h. 1 ng/mL LPS for 3 h was selected as a suitable concentration and time-point for further experiments.

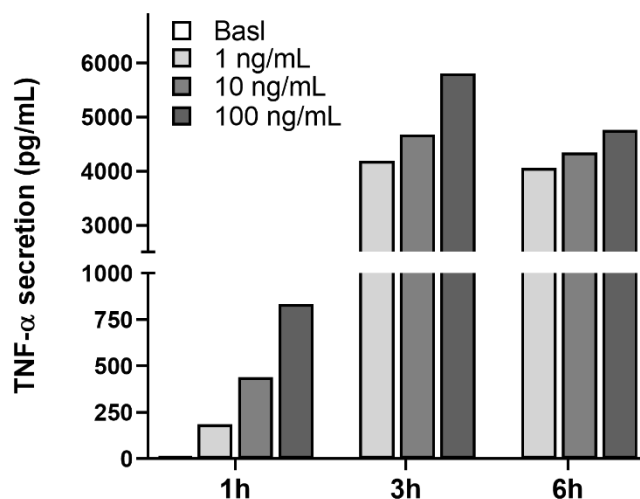


Figure 8. 7 LPS kinetic of THP-1 macrophages. THP-1 cells resuspended in differentiation media (RPMI complete media containing 200 nM PMA). Cells (2 mL/well) were seeded in 12-wells-plate ( $5 \times 10^5$  cell/well) and left to differentiate for 72h at 37°C. Then, cells were washed twice with DPBS and 1 mL/well fresh RPMI complete media was added. Treatment of LPS (1 ng/mL, 10 ng/mL and 100 ng/mL) were added and incubated for 1h, 3h and 6h at 37°C. Supernatants were taken to analyse the TNF- $\alpha$  secretion level by ELISA. Basal is non-treated THP-1 Macrophages. Columns represent a single biological experiment.

### 8.3.1.3 THP-1 Macrophage: Co-incubation of EPA & DHA with LPS

THP-1 were differentiated into macrophages in 12-well plates as described in methods. Macrophages were co-incubated for 3h with LPS (1 ng/mL) and EPA, DHA (at 10  $\mu$ M, 25  $\mu$ M or 50  $\mu$ M), or a mixture of EPA+DHA. Assay was provided with a vehicle control (VC) (0.1% DMSO) and a positive control, 10  $\mu$ M SB 203580. Results displayed on **Figure 8. 8** shows positive control inhibits TNF- $\alpha$  secretion and VC is similar to LPS treatment. However, no effect of EPA, DHA or EPA+DHA at any tested concentration on TNF- $\alpha$  secretion when co-incubated with LPS THP-1 complete media.



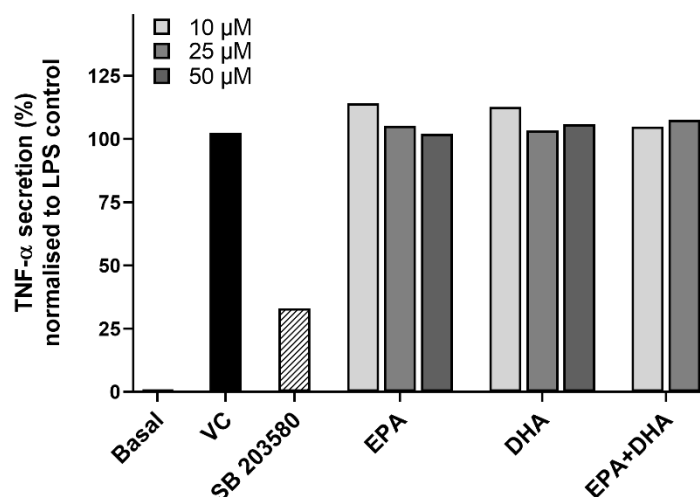


Figure 8. 8 in RPMI complete media co-incubation of LPS with DHA, EPA and EPA&DHA did not inhibit TNF- $\alpha$  secretion from THP-1 macrophages. Differentiated cells were washed twice with DPBS and 1 mL/well fresh RPMI complete media was added. Cells were co-incubated with 1 ng/mL LPS and 10, 25, 50  $\mu$ M EPA or DHA and EPA+DHA, for 3h. As vehicle control (VC) 0.1% DMSO was included and as positive control 10  $\mu$ M SB203580 was used. TNF- $\alpha$  secretion measured by ELISA. Basal is non-treated THP-1 macrophages. n=1.

#### 8.3.1.4 Western blotting Optimisation: The optimal buffer for immunoblot antibody staining

For Westernblot assay, p38 MAPK phosphorylation was induced with LPS in THP-1 for 1h and sample preparation, separation of proteins and transfer into membrane were performed as per methods in chapter 2. The primary antibody staining of immunoblot membranes with P-p38, p38,  $\beta$ -tubulin (1:500) or  $\beta$ -actin (1:2000) were performed in TBST containing 5% milk or 5% BSA. primary antibody for 2h at room temperature on a rotor shaker. Then stained with secondary antibody as per methods in chapter 2. Result on **Figure 8. 9** indicate that primary antibody staining in 5% BSA compared to 5% milk increases the detection of the protein. Therefore, all further Western blot primary antibody staining performed in 5% BSA.

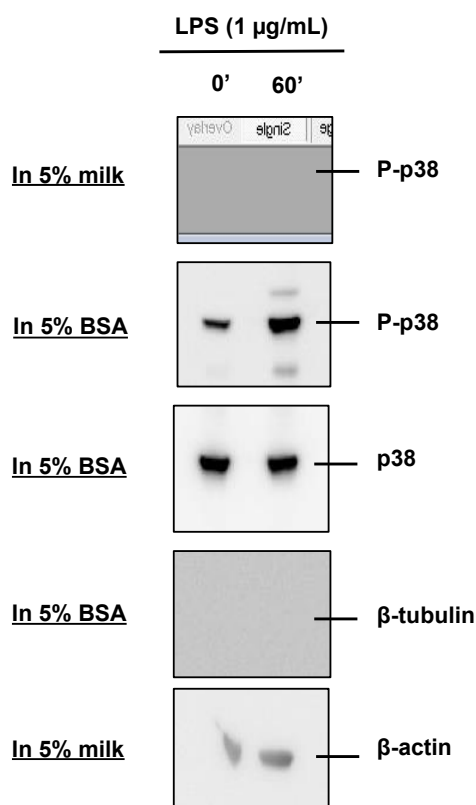


Figure 8. 9 The optimal buffer for immunoblot antibody staining. Immunoblot membrane stained with primary antibody (rabbit mA) against phospho-p38 MAPK, p38 MAPK, β-Tubulin (1:500), and mouse β-actin (1:2000) in blocking buffer (5% milk in TBST) or with 5% BSA in TBST. Then, stained with HRP-conjugated goat anti-rabbit or anti-mouse as secondary antibody. HRP-substrate ECL-chemiluminescence was used (1min) to detected protein by Image Quant 4000 instrument.

### 8.3.1.5 Optimization of NQO1 Enzymatic Activity Assay

NQO1 enzymatic activity assay protocol was optimised for THP-1 cells ( $3 \times 10^4$  cells/well, in 96-well plate). The initial protocol <sup>424</sup> suggests reading plate absorbance immediately after adding reaction buffer where standards (std's) sample concentration is between 15.6-1000 µM/mL. For the, initial test THP-1 ( $3 \times 10^4$  cells/well) was seeded in 96-well plate and treated with 30 µM DMF or left untreated for basal control as described in method chapter. Sample standards were between 15.6-1000 µM/mL. Results (not included) showed a far lower sample absorbance of THP-1 cells (basal and DMF) in comparison to the lowest std absorbance. Next, the experiment

was repeated with lower std's concentration (7.8-500  $\mu\text{M}/\text{mL}$ ) and samples with higher cells density ( $1 \times 10^5$ , and  $2 \times 10^5$  cells/well). However, increasing cell concentration did not increase the sample absorbance dramatically (data not included) and still outside of std's absorbance range. Further, to find the optimal reading time range, standards with lower concentrations (0.5-30  $\mu\text{M}/\text{mL}$ ) and samples with seeding density of  $1 \times 10^5$  cells/well were assessed. And the absorbance was read at different time points to find the optimal reading time range. Results displayed on **Figure 8. 10** shows that the enzymatic activity or recombinant NQO1 standards saturates at absorbance  $\sim 3.5$ . The max concentration is lower than 100  $\mu\text{M}$ . The standards at conc. of 0.5-30  $\mu\text{M}/\text{mL}$  gave a reliable reading time between 3-13 min. And cells seeding density of  $1 \times 10^5$  cells/mL was optimal for reliable fold change between basal and DMF treatment.

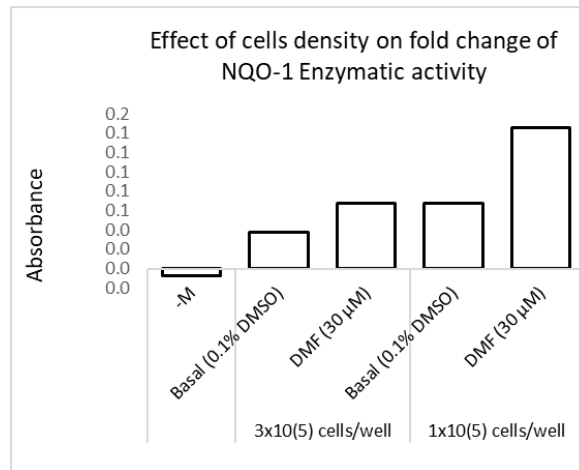
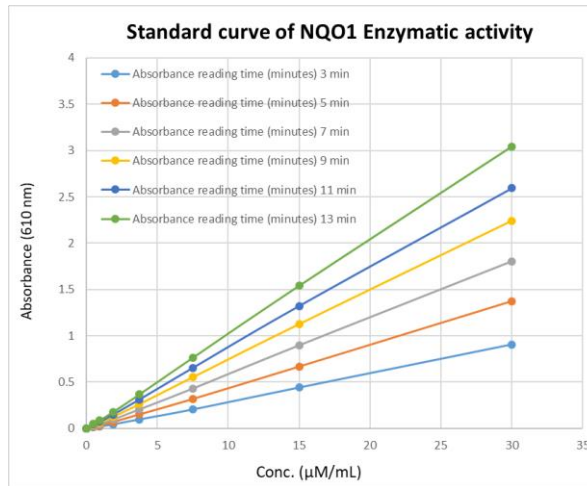
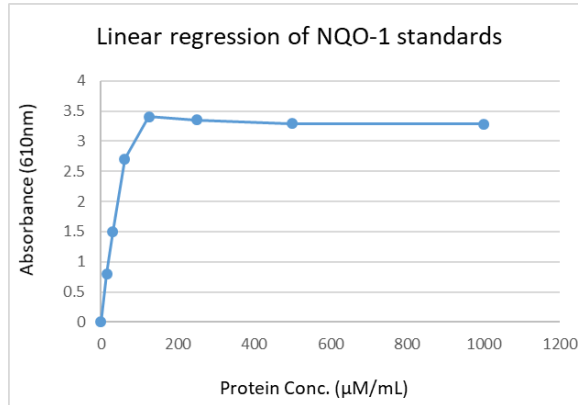


Figure 8. 10 Optimisation of standard curve, kinetic of standard curve, and cell density of NQO1 enzymatic activity assay for THP-1 cells.

### **8.3.1.6 The kinetics of HO-1 and NQO1 mRNA induction in response to FA-Hex-Es and DMF in THP-1**

#### **8.3.1.6.1 Optimisation of HO-1 & NQO1 gene expression kinetic**

Previously in the O'Connell lab, flavonoids have been found to increase HO-1 gene expression and the maximum effect was at 8h<sup>440</sup>. In the current study, firstly, the kinetics of Ferulic acid hexyl ester (**FA-Hex-Es**) on HO-1 and NQO1 gene was investigated at both 4h and 8h. The assay was provided with a positive control, Dimethyl fumarate (**DMF**) and the flavonoid quercetin (**Que**), both for their known effect on increasing HO-1 and NQO1 expression. And 0.1% DMSO was included as basal control for having no effect. Results shown in **Figure 8. 11** indicated that NQO1 and HO-1 gene expression was increased in response to DMF, Que and FA-Hex-Es compared to basal level and the expression was highest at 4h for the latter two respectively. This time point was taken forward for further experiments.

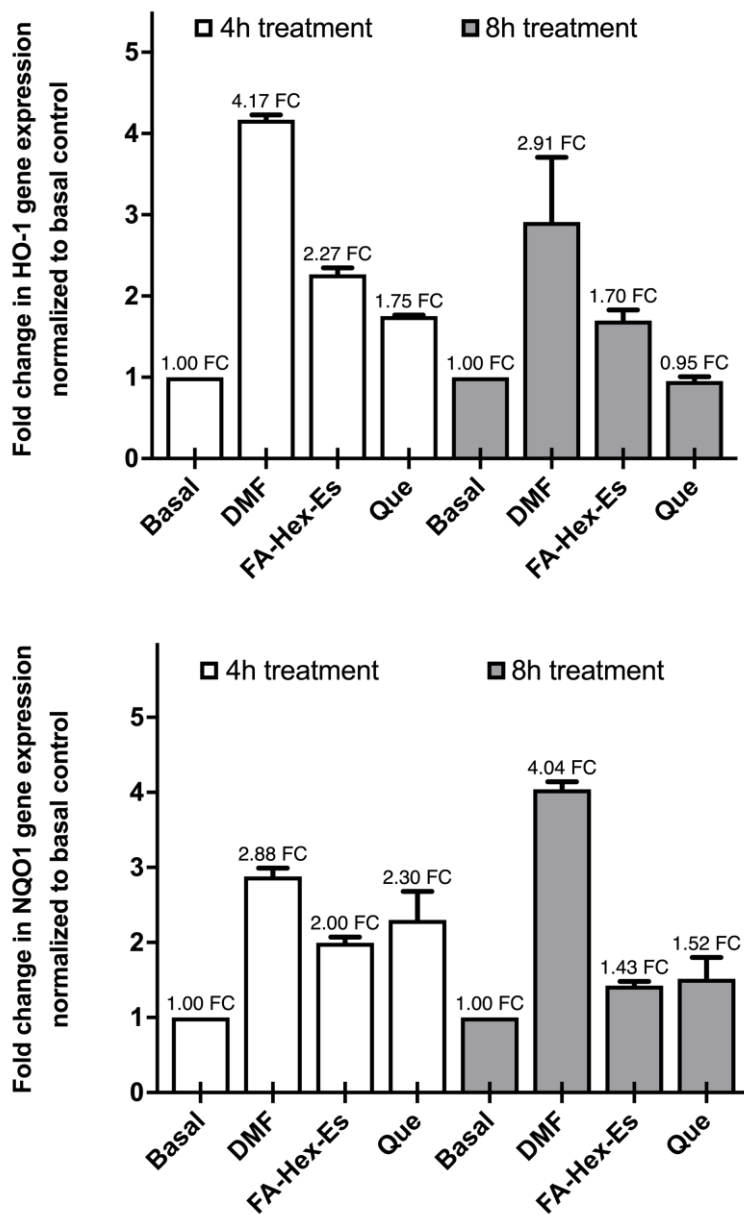


Figure 8. 11 Optimal time point of HO-1 and NQO1 messenger RNA in THP-1 cells for the positive control DMF and Quercetin (Nrf2 inducer) and FA-Hex-Es. THP-1 cells ( $1 \times 10^6$  cells/well) treated with 20  $\mu$ M Ferulic acid- hexyl ester (FA-Hex-Es) and Quercetin (Que), or 0.1% DMSO (basal control) and 30  $\mu$ M Dimethyl fumarate (DMF, as positive control) for 4h and 8h. HO-1 and NQO1 mRNA expression were measured by RT-qPCR. mRNA values were expressed as fold change (relative to GAPDH) normalised to basal control. Mean  $\pm$  SEM, n=2 technical replicates from a single experiment.

### 8.3.1.7 RT-qPCR Melting Curve Analysis of TNF- $\alpha$ , HO-1, NQO1

Example of Optimal melting curves for human TNF- $\alpha$ , HO-1, NQO1 and GAPDH.

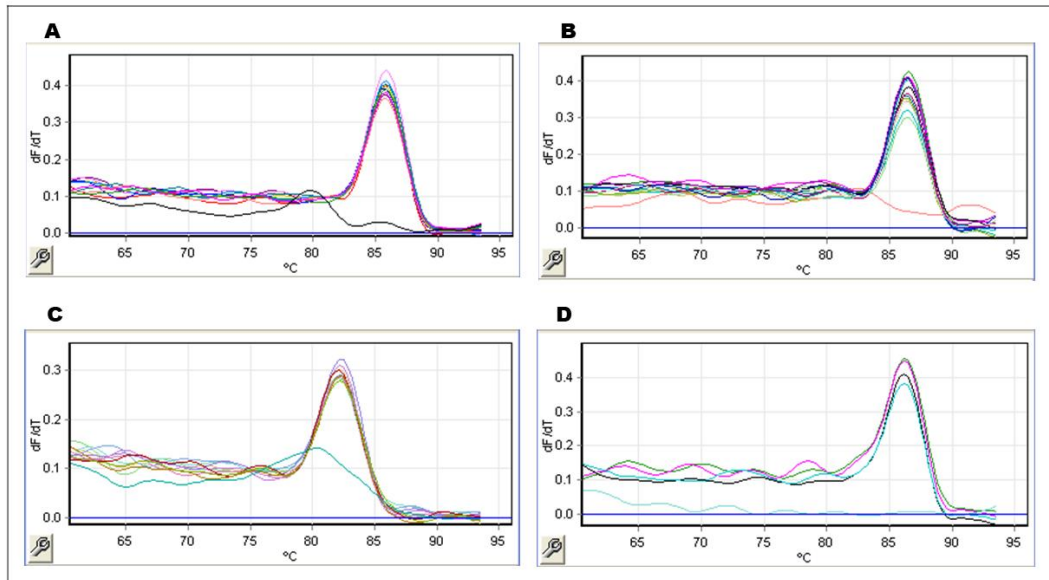


Figure 8. 12 Validation of specificity of qPCR amplification for human A) GAPDH, B) TNF- $\alpha$ , C) HO-1, D) NQO1. Melt curve analysis of RT-qPCR amplification following 40 cycles of denaturation. qPCR was performed with 48 ng cDNA derived from basal (unstimulated) THP-1, and cells incubated with 20  $\mu$ M of each compound for 2h TNF- $\alpha$  and 4h HO-1 & NQO1.

## 8.3.2 Optimization for Chapter 4

### 8.3.2.1 Kinetics of IL-6 Gene Expression in LPS-Induced BV2

The optimal incubation time of BV2 with LPS stimulation for IL-6 gene expression was investigated for 2, 4, 6 and 8 hours according to methods as described in methods chapter. The fold change of IL-6 gene expression was highest at 4 hours as seen from **Figure 8. 13** and this time point was taken forward for duration of BV2 exposure to LPS.

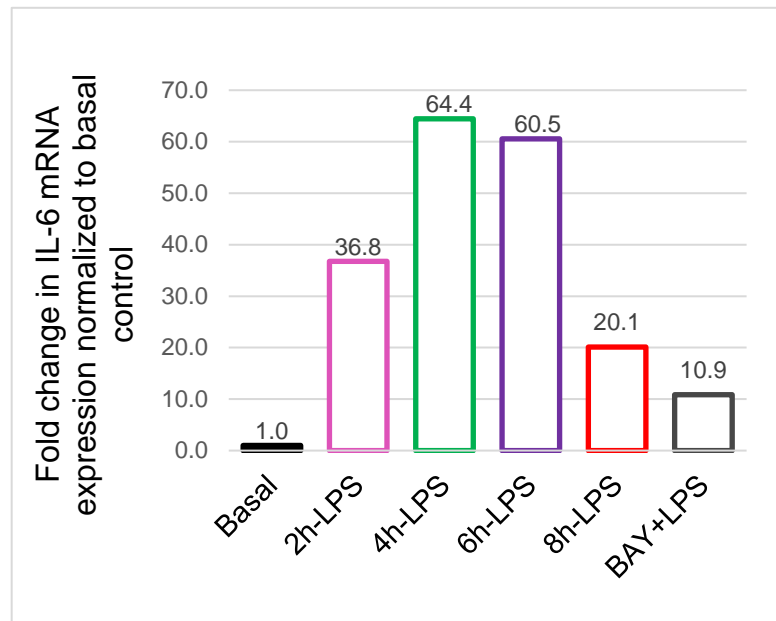


Figure 8. 13 Kinetics of IL-6 gene expression. BV2 cells ( $1 \times 10^5$  cells/well) in 2 mL o/n incubated. Next day 1 mL media removed, and cells treated with 10 ng/mL LPS for 2h, 4h, 6h, and 8h or LPS with or + 0.1  $\mu$ M BAY 11-7082 (BAY) as positive control for 8h or non-treated cells. mRNA expression was measured by RT-qPCR and the values were expressed as fold change (relative to GAPDH) normalised to basal control. Columns represent one biological experiment.



### **8.3.2.2 Optimisation of RT-qPCR Template Concentration for BV2 GAPDH and IL-6 Gene Expression**

Optimal cDNA concentration for RT-qPCR was established for GAPDH and IL-6 genes from BV2. Briefly, two days after splitting, BV2 cells were counted and 2 mL  $5 \times 10^4$  cells/mL were added to a 6 well plate ( $1 \times 10^5$  cells/well). Next day 1 mL media was removed, and cells pre-treated for 30 minutes prior to stimulation with LPS (10 ng/mL final conc.) for 6h. Cell lysis, RNA isolation and cDNA synthesis were performed according to standard protocol as described in methods. Real time qPCR was performed with 12 ng, 24 ng and 48 ng cDNA and with 10  $\mu$ M primers (forward + reverse). Results displayed on **Figure 8. 14** indicate a better amplification with 48 ng cDNA. However, primer-dimer formation as a result of low template cDNA or high concentration of primers can be seen from all tested cDNA templates. This can be clearly seen on the melting curve of samples with 12 and 24 ng cDNA compared to 48 ng cDNA. The amplicon with primer-dimer formation has a lower melting temperature which for GAPDH primers is between 80-85 °C and for IL-6 primers this is between 73-80°C. On the display with 12 ng cDNA template the dominant peak is the one for primer dimers. While on the display with 24 ng cDNA, formation of a peak for the GAPDH amplicon (85-93 °C) and IL-6 amplicon (80-85° C) can be seen. Moreover, the primer-dimer peak on the display with 24 ng cDNA gets smaller for all samples of GAPDH but NTC (blue line) confirming the formation of primer-dimers due to excessive primers and no cDNA template. While IL-6 still shows a very sharp peak for NTC, basal control and BAY (purple, blue and yellow respectively) and a real peak for IL-6 amplicon for LPS and VC samples (green lines). At display with 48 ng cDNA all samples for GAPDH (except NTC, blue line) form a unified big peak of gene GAPDH amplicon and a small peak in NTC indicating primer dimer formation only in this control due to lack of template. However, on the display for IL-6 with 48 ng cDNA a sharp peak for LPS VC can be seen, while BAY (red line) has a small peak for template and a shoulder for primer-dimers, and basal still

show a clear peak for primer-dimers as NTC and a little shoulder for IL-6 amplicon, indicating further optimisation of primer concentration is needed.

### **8.3.2.3 Optimisation of Murine GAPDH and IL-6 primer sets Concentration**

Optimal concentration for murine GAPDH and IL-6 primers were established. In afore mentioned optimisation experiment 10  $\mu$ M primers (forward + reverse) was used and melting temperature indicated primer dimer formation. Here 500 nM primer concentration was compared to 250 nM by using 48 ng cDNA. And further experiment revealed that 250 nM for GAPDH and 150 nM for IL-6 found to be optimal to use with 50 ng template cDNA from BV2 (**Figure 8. 15**).

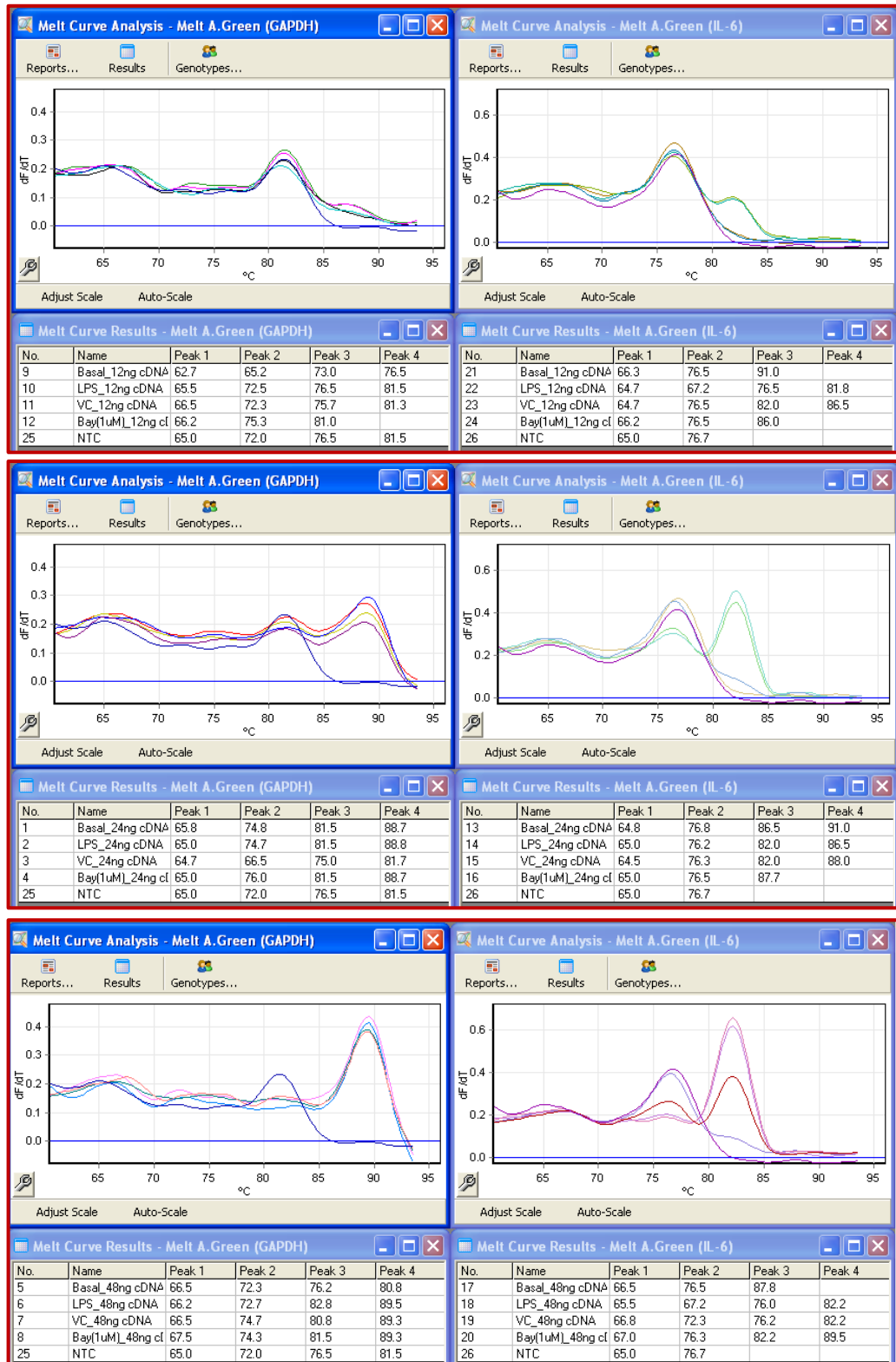


Figure 8. 14 Melting temperature ( $T_m$ ) of BV2 cDNA with three different template concentrations: 12 ng cDNA (upper panel) 24 ng cDNA (middle panel) and 48 ng cDNA (lower panel) amplified with 10  $\mu$ M GAPDH and 10  $\mu$ M IL-6 primer sets.

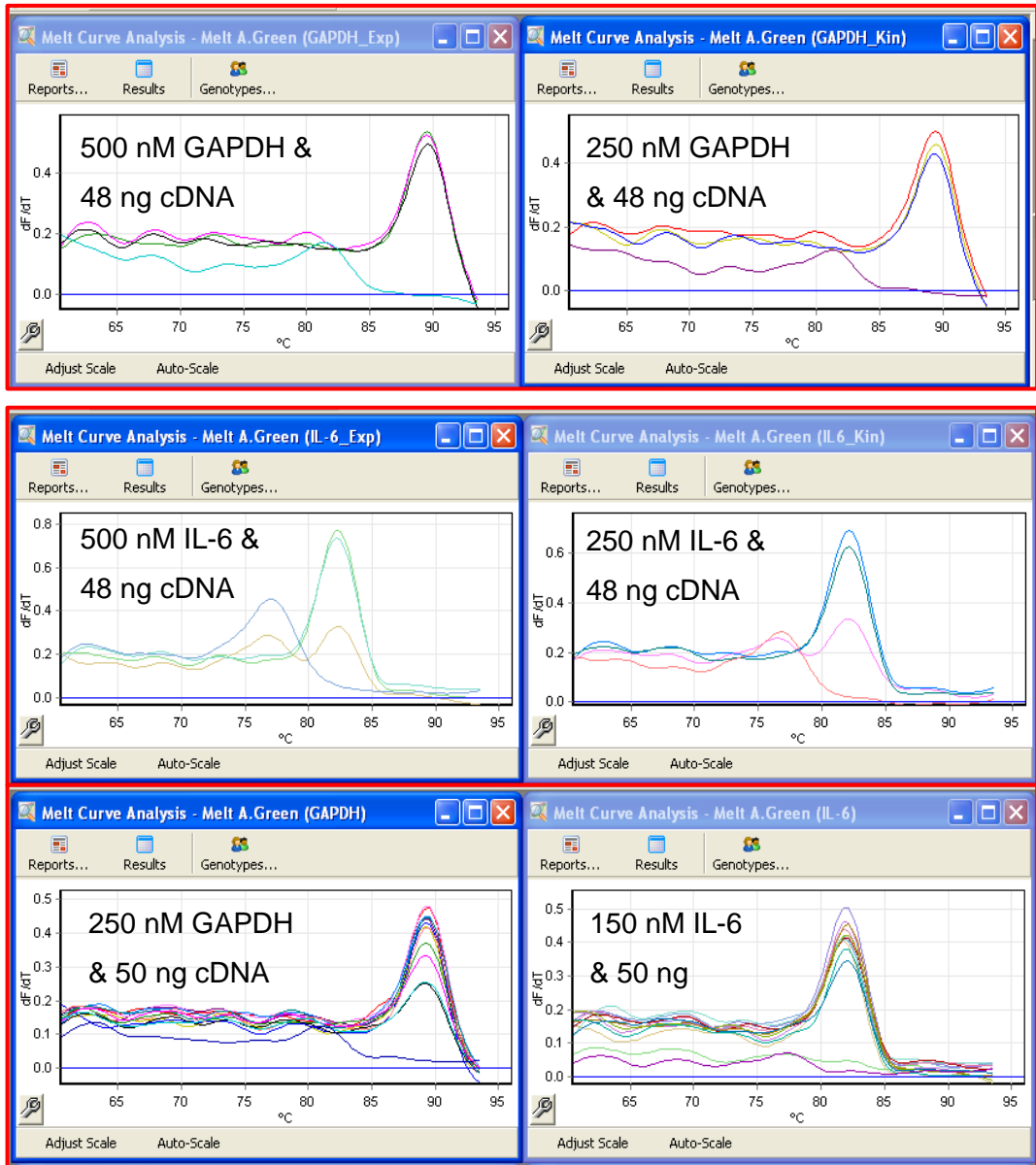


Figure 8. 15 Melting Temperature of Murine GAPDH and IL-6 template and primer pairs. 48 ng cDNA template (upper and middle panel) or 50 ng cDNA template (lower panel) used in combination of 150, 250, 500 nM.

#### **8.3.2.4 LPS Kinetics of BV2 c-Jun/c-Fos phosphorylation in Serum-Free Media**

Non-phospho c-Jun and c-Fos protein expression in BV2 cells were elevated in response to 1 µg/mL LPS treatment (**Chapter 4. Figure 4.11**) in BV2 complete media (DMEM/F12 media supplemented with P/S and 10% FBS). To see if serum-free media has any differential effect on BV2 c-Jun and c-Fos protein levels, a further experiment was performed with similar conditions as in section 4.3.11 with following exceptions: BV2 complete media was replaced with serum-free media and cells were further incubated for 4h or 24h prior treatment with 1 µg/mL LPS. Protein expression was assessed by western blot assay as described in chapter 2. Results shown in Figure 8. 16 show that serum starvation did not alter the effect of LPS on non-phospho c-Jun and c-Fos expression. Therefore, media with serum was taken forward to test effect of potent compounds on c-Jun and c-Fos phosphorylation level in BV2 cells.

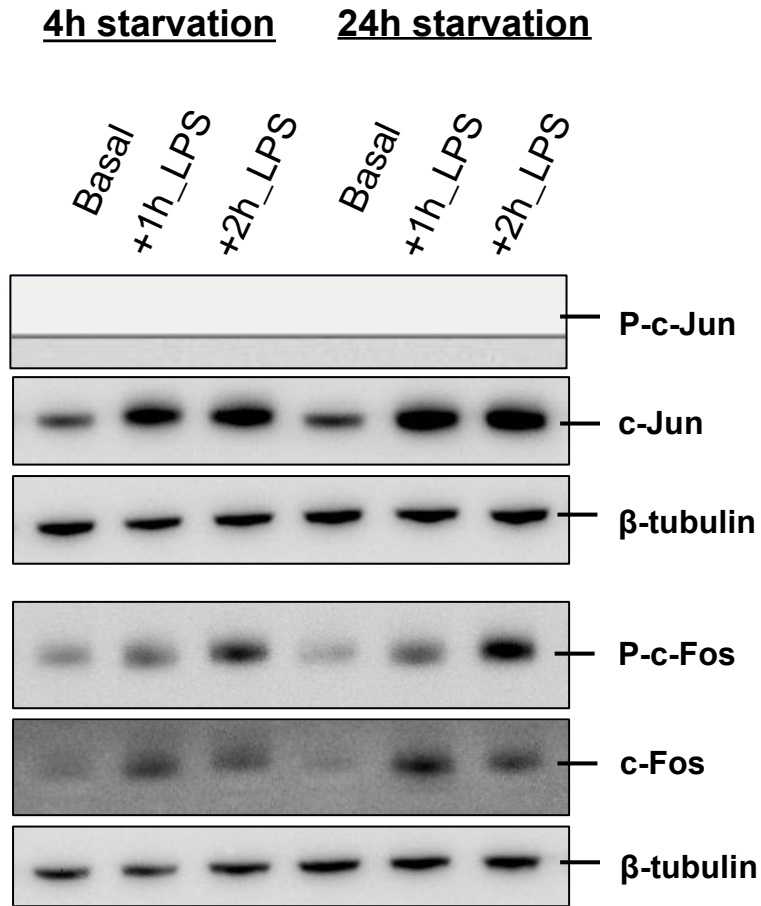
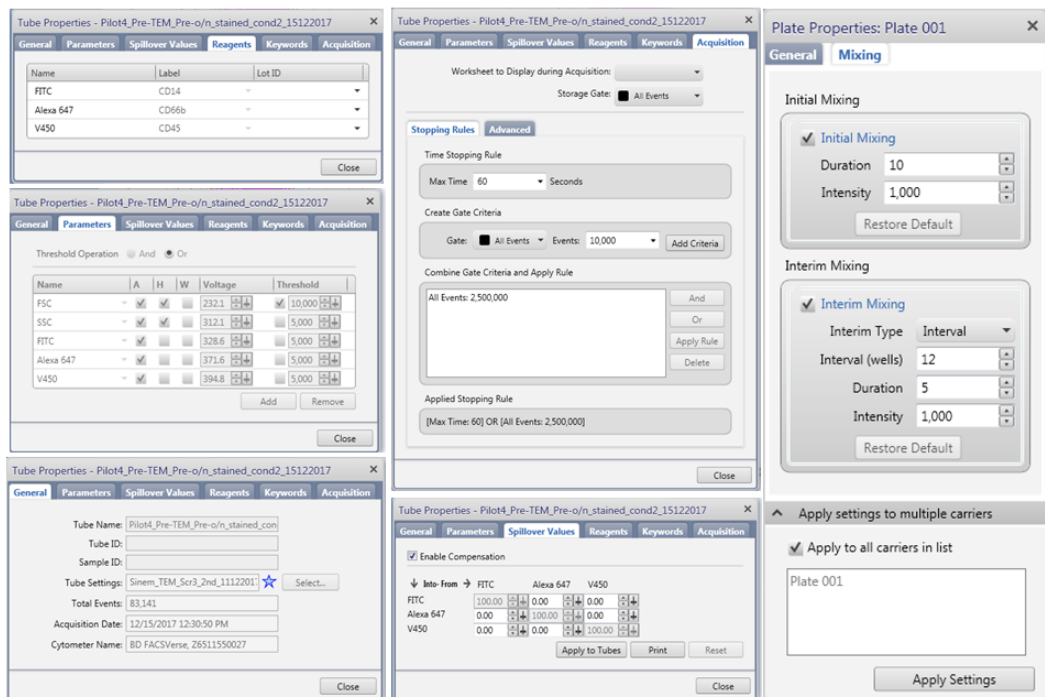


Figure 8. 16 Serum starvation did not alter the effect of LPS on non-phospho c-Jun and c-Fos. BV2 cells ( $2 \times 10^5$  cells/well) o/n incubated prior to stimulation with  $10 \mu\text{g/mL}$  LPS for stated time points. Protein expression was measured by western blot from whole cell lysates. Approximately  $30 \mu\text{g}$  protein per samples loaded and  $\beta$ -Tubulin expression used as protein loading control.

## 8.3.3 Optimization for Chapter 5

### 8.3.3.1 Transendothelial Migration Flow Cytometry Settings

Flow cytometry analysis of transendothelial migration leukocytes were set up as shown in here below panels.



### 8.3.3.2 Gating Strategy of Transendothelial Migration Flow Cytometry

Prior to each screening experiment of transendothelial migration assay, a gating strategy was established for flow cytometry (Figure 8. 17). Before analysing transendothelial migration of leukocytes, both forward- (FSC-A) and side-scatter (SSC-A) were adjusted to

have an optimal separation of death cells (left-side corner) and viable cells (intense dots in the middle of panel). Then another pre-transendothelial migration sample stained specific antibody against biomarkers for viable cells with CD45 (all leukocytes), CD14 (monocytes) and CD66b (neutrophils) to separate cell population into neutrophils, monocytes, and lymphocytes.

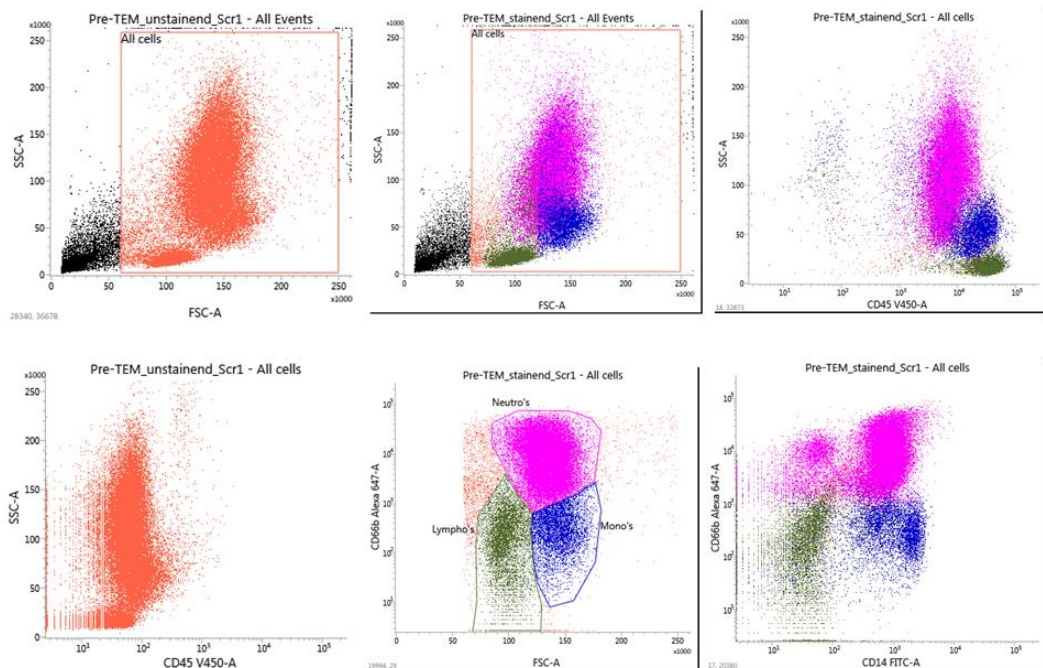


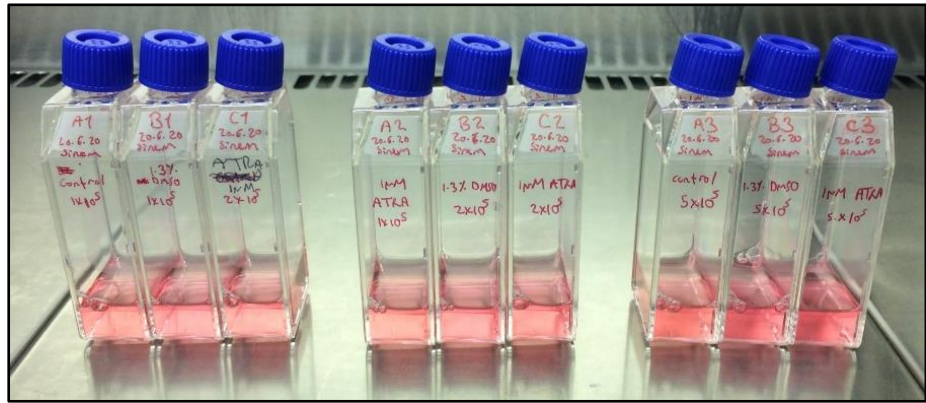
Figure 8. 17 Overview of transendothelial migration flow cytometry gating strategy. Flow cytometry was adjusted for both forward- (FSC-A) and side-scatter (SSC-A) to have an optimal separation of death cells (left-side corner) and viable cells (intense dots in the middle of panel) for non-stained cells (Pre-transendothelial migration). Separation of viable leukocytes into population of neutrophils, monocytes and lymphocytes was performed by a pre-transendothelial migration stained sample with V450-CD45 (all leukocytes), Alexa 647-CD66b (neutrophils) and FITC-CD14 (monocytes).



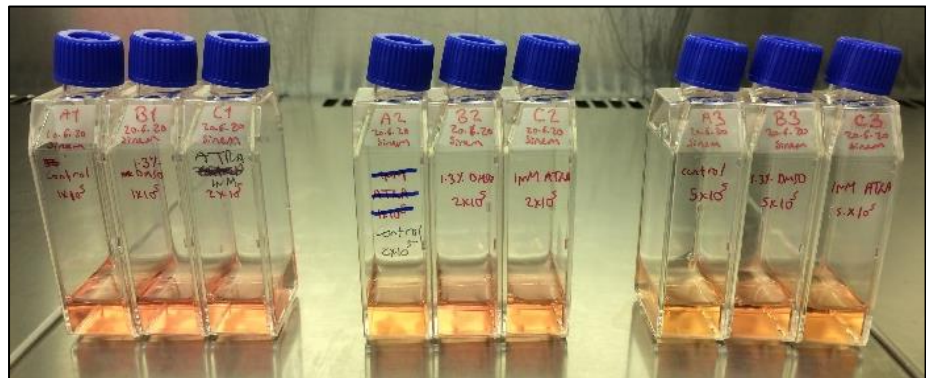
### **8.3.3.3 Cell Growth and Differentiation of HL-60 in diff-media with DMSO and ATRA**

HL-60 cell differentiation into neutrophil like cells by 1.3% DMSO and 1  $\mu$ M ATRA was monitored for 6 days (**Figure 8. 18**). The media colour change was assumed to be corresponding to cell growth. The more growth, the more acidic media become and the colour change from pink to pale yellow. When differentiated, the cell growth slows down and so the change in colour. Even after six days of incubation, the colour of cells media treated with 1.3% DMSO did not change in flasks with lowest ( $1 \times 10^5$  cells/mL) and medium ( $2 \times 10^5$  cells/mL) cell density, indicating differentiation and stopping cell division. While after six days, cell treated with 1  $\mu$ M ATRA stay almost the same as day 2 in flask with only the lowest cell density, suggesting a reliable differentiation condition. The colour of diff-media with DMSO was most stable over the course of 6 days while a little change in diff-media with ATRA.

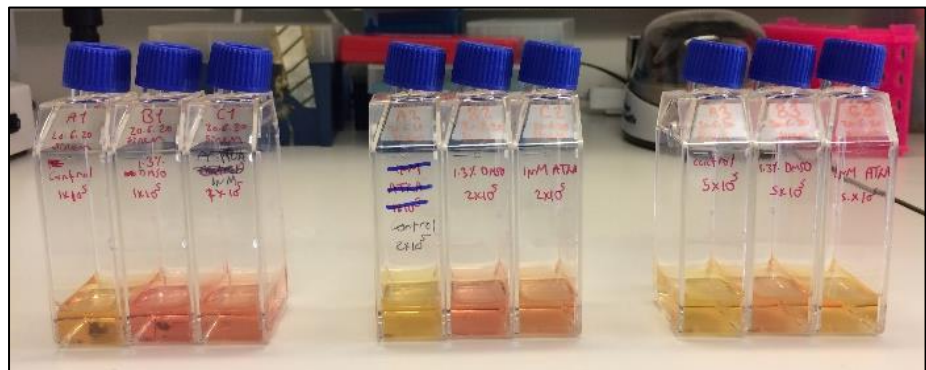
Day 0



Day 1



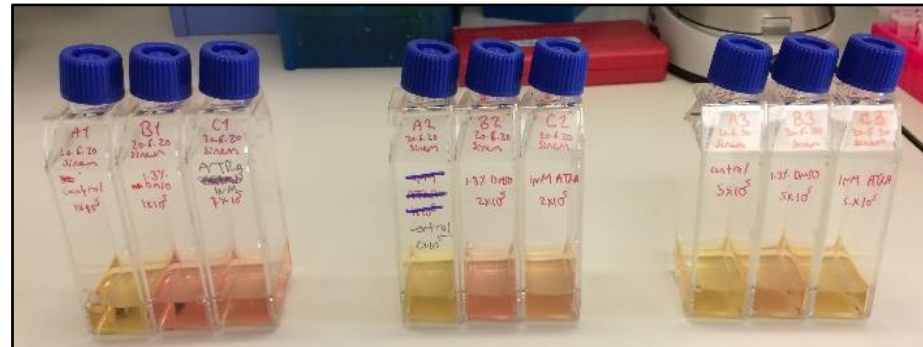
Day 2



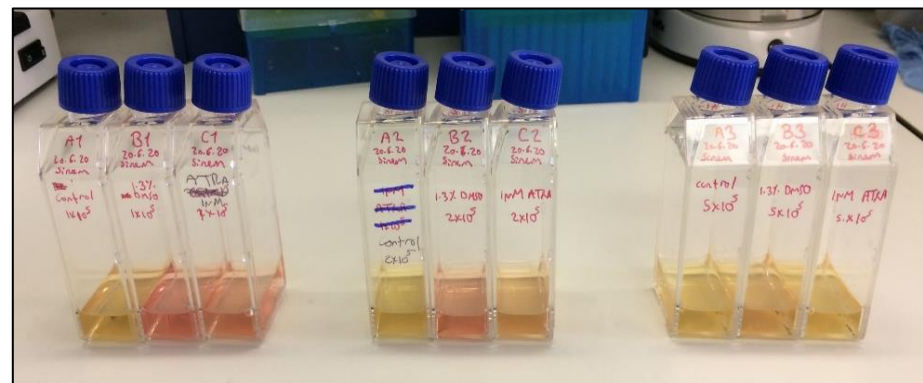
Day 3



Day 4



Day 5



Day 6

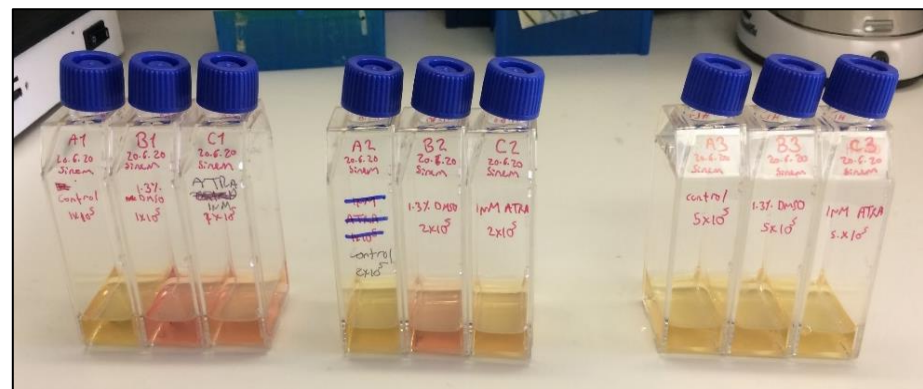
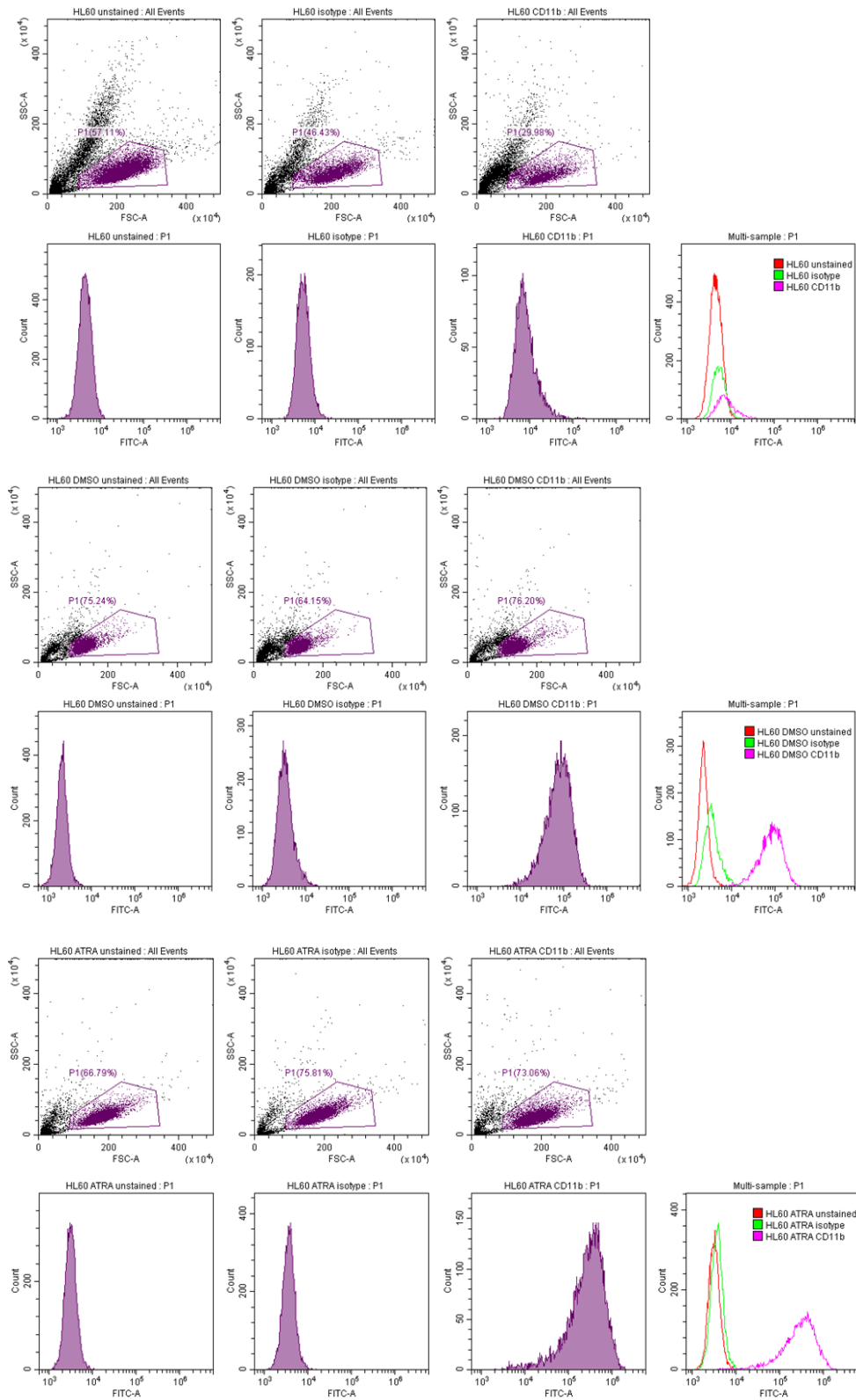


Figure 8. 18 HL-60 growth and differentiation by DMSO and ATRA versus control. Cell were grown in T25 flasks with 10 mL RPMI complete media (control, non-diff media) (A); media with 1.3% DMSO (B) or media with 1  $\mu$ M ATRA (C) with initial seeding density of  $1 \times 10^5$  cells/mL (1),  $2 \times 10^5$  cells/mL (2), and  $5 \times 10^5$  cells/mL (3). Daily pictures taken for the change in media colour to monitor the growth and differentiation.

### 8.3.3.4 Cell growth and Differentiation of HL-60 in T25



### 8.3.3.5 Chemotaxis Effect of Halogenated and Non-halogenated Compounds on THP-1

Table 8.1 Treatment effect of halogenated and non-halogenated phenolic acids at 1  $\mu$ M on THP-1 chemotaxis in response to MCP-1 (0.3 nM).

Treatment	Average change from VC (% $\pm$ SEM)	P value
34DABA	↓ 11.2 $\pm$ 8.5	0.8904
2ABA	↓ 16.2 $\pm$ 10.1	0.6110
2FBA	↓ 16.7 $\pm$ 6.6	0.5796
3FBA	↓ 17.5 $\pm$ 7.7	0.5353
4FBA	↓ 17.2 $\pm$ 5.3	0.5491
2CyBA	↓ 15.9 $\pm$ 9.8	0.6314
3CyBA	↓ 22.1 $\pm$ 9.0	0.2934
4CyBA	↓ 14.7 $\pm$ 6.2	0.2934
2CBA	↓ 16.8 $\pm$ 3.8	0.6181
4CBA	↓ 16.5 $\pm$ 7.2	0.6320
2BBA	↓ 20.8 $\pm$ 8.9	0.3959
3BBA	↓ 19.7 $\pm$ 5.4	0.4517
4IBA	↓ 19.6 $\pm$ 10.9	0.4564
5I2MBA	↓ 14.6 $\pm$ 11.5	0.7466
24DCBA	↓ 22.7 $\pm$ 9.7	0.3071
35DCBA	↓ 25.7 $\pm$ 3.4	0.1970

Treatment added to THP-1 ( $24 \times 10^4$  cells/well) at final concentration of 1  $\mu$ M for 30 min prior to adding 0.3 nM MCP-1 chemokine and further incubation for 4h. **VC** (vehicle control, 0.001% DMSO), **34DABA** (3,4-diaminobenzoic acid), **2ABA** (2-aminobenzoic acid), **2FBA** (2-fluorobenzoic acid), **3FBA** (3-fluorobenzoic acid), **4FBA** (4-fluorobenzoic acid), **2CyBA** (2-cyanoobenzoic acid), **3CyBA** (3-cyanoobenzoic acid), **4CyBA** (4-cyanoobenzoic acid), **2CBA** (2-chlorobenzoic acid), **4CBA** (4-chlorobenzoic acid), **2BBA** (2-bromobenzoic acid), **3BBA** (3-bromobenzoic acid), **4IBA** (3-iodobenzoic acid), **5I2MBA** (5-iodo-2-methoxybenzoic acid), **24DCBA** (2,4-dichlorobenzoic acid), **35DCBA** (3,5-dichlorobenzoic acid). Data represent mean and  $\pm$  SEM of four independent biological experiments, each in two technical replicates. Significance set up  $p > 0.05$  (One-way ANOVA with post hoc Dunnett's test comparing treatments with VC).

Table 8.2 List of PA used in transendothelial migration model with LogP values.

<b>Compound</b>	<b>LogP Values</b>
3-Iodobenzoic acid (3IBA)	2.9
2-Iodobenzoic acid (2IBA)	2.9
4-Bromobenzoic acid (4BBA)	2.8
3-Chlorobenzoic acid (3CBA)	2.7
3-Chloro-4-methoxybenzoic acid (3C4MBA)	2.0
5-Chloro-2-methoxybenzoic acid (5C2MBA)	2.0
4-Nitrobenzoic acid (4NBA)	1.9
Benzoic acid (BA)	1.9
3-Hydroxy-4-methoxycinnamic acid, Isoferulic acid (IFA)	1.7
4-Hydroxybenzoic acid (4HBA)	1.6
2,4-Dimethoxybenzoic acid (24DMBA)	1.6
2,4-Dihydroxybenzoic acid (24DHBA)	1.6
3-Hydroxybenzoic acid (3HBA)	1.5
trans-4-Hydroxy-3-methoxycinnamic acid, Ferulic acid (FA)	1.5
4-Hydroxy-3-methoxybenzoic acid (VA)	1.4
3-Hydroxy-4-methoxybenzoic acid (IVA)	1.2
3,4-Dihydroxycinnamic acid (CA)	1.1
3,4-Dihydroxybenzoic acid (PCA)	0.9
4-Aminobenzoic acid, para-aminobenzoic acid (4ABA)	0.8
3-Aminobenzoic acid (3ABA)	0.7
3,5-Diaminobenzoic acid, (35DABA)	-0.2